tecnología
Glosas de innovacion aplicadas a la pyme

Edición Especial
Noviembre 2021
Special Issue_November 2021
ISSN: 2254 – 4143

# "KALASALINGAM GLOBAL CONFERENCE KGC-2019. INTERNATIONAL CONFERENCE ON SUSTAINABLE DEVELOPMENT"

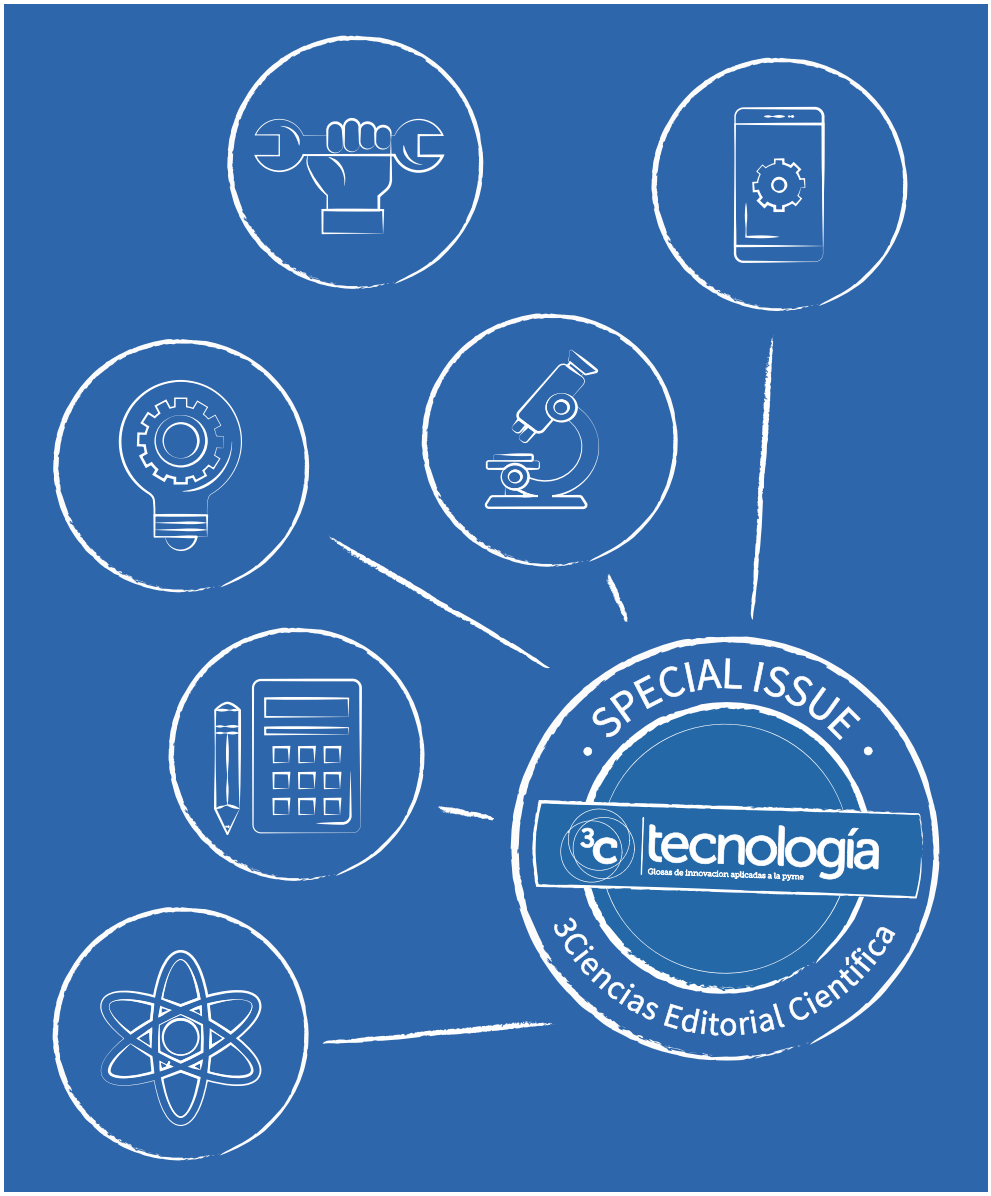

**3C Tecnología. Glosas de innovación aplicadas a la pyme.**

Edición Especial 39-2. Noviembre 2021. *Special Issue 39-2. November 2021.*

Tirada nacional e internacional. *National and internacional circulation.*

Artículos revisados por el método de evaluación de pares de doble ciego.
*Articles reviewed by the double blind peer evaluation method.*

**"Kalasalingam Global Conference KGC-2019.
International Conference on Sustainable Development".**

ISSN: 2254 – 4143
N.º de Depósito Legal: A 268 – 2012
DOI: https://doi.org/10.17993/3ctecno.2021.specialissue8

Edita:
Área de Innovación y Desarrollo, S.L.
Avda. Juan Gil Albert, 1, Alcoy, Alicante (España)
Tel: 965030572
info@3ciencias.com _ www.3ciencias.com



https://doi.org/10.17993/3ctecno.2021.specialissue8

https://doi.org/10.17993/3ctecno.2021.specialissue8

# CONSEJO EDITORIAL EDITORIAL BOARD




https://doi.org/10.17993/3ctecno.2021.specialissue8

# POLÍTICA EDITORIAL

## OBJETIVO EDITORIAL

La Editorial científica 3Ciencias pretende transmitir a la sociedad ideas y proyectos innovadores, plasmados, o bien en artículos originales sometidos a revisión por expertos, o bien en los libros publicados con la más alta calidad científica y técnica.

## COBERTURA TEMÁTICA

3C Tecnología es una revista de carácter científico-social en la que se difunden trabajos originales que abarcan la Arquitectura y los diferentes campos de la Ingeniería, como puede ser Ingeniería Mecánica, Industrial, Informática, Eléctrica, Agronómica, Naval, Física, Química, Civil, Electrónica, Forestal, Aeronáutica y de las Telecomunicaciones.

## NUESTRO PÚBLICO

- Personal investigador.
- Doctorandos.
- Profesores de universidad.
- Oficinas de transferencia de resultados de investigación (OTRI).
- Empresas que desarrollan labor investigadora y quieran publicar alguno de sus estudios.


https://doi.org/10.17993/3ctecno.2021.specialissue8

# AIMS AND SCOPE

## PUBLISHING GOAL

3Ciencias wants to transmit to society innovative projects and ideas. This goal is reached thought the publication of original articles which are subdue to peer review or thorough the publication of scientific books.

## TEMATIC COVERAGE

3C Tecnología is a scientific-social journal in which original works that cover Architecture and the different fields of Engineering are disseminated, such as Mechanical, Industrial, Computer, Electrical, Agronomic, Naval, Physics, Chemistry, Civil, Electronics, Forestry, Aeronautics and Telecommunications.

## OUR TARGET

- Research staff.
- PhD students.
- Professors.
- Research Results Transfer Office.
- Companies that develop research and want to publish some of their works.


https://doi.org/10.17993/3ctecno.2021.specialissue8

# NORMAS DE PUBLICACIÓN

3C Tecnología es una revista arbitrada que utiliza el sistema de revisión por pares de doble ciego (*double-blind peer review*), donde expertos externos en la materia sobre la que trata un trabajo lo evalúan, siempre manteniendo el anonimato, tanto de los autores como de los revisores. La revista sigue las normas de publicación de la APA (American Psychological Association) para su indización en las principales bases de datos internacionales.

Cada número de la revista se edita en versión electrónica (e-ISSN: 2254 – 4143), identificándose cada trabajo con su respectivo código DOI (Digital Object Identifier System).

## PRESENTACIÓN TRABAJOS

Los artículos se presentarán en tipo de letra Baskerville, cuerpo 11, justificados y sin tabuladores. Han de tener formato Word. La extensión será de no más de 6.000 palabras de texto, incluidas referencias.

Los trabajos deben ser enviados exclusivamente por plataforma de gestión de manuscritos OJS:

https://ojs.3ciencias.com/

Toda la información, así como las plantillas a las que deben ceñirse los trabajos se encuentran en:

https://www.3ciencias.com/revista/informacion-para-autores/

https://www.3ciencias.com/normas-de-publicacion/plantillas/


https://doi.org/10.17993/3ctecno.2021.specialissue8

# SUBMISSION GUIDELINES

3C Tecnología is an arbitrated journal that uses the double-blind peer review system, where external experts in the field on which a paper deals evaluate it, always maintaining the anonymity of both the authors and of the reviewers. The journal follows the standards of publication of the APA (American Psychological Association) for indexing in the main international databases.

Each issue of the journal is published in electronic version (e-ISSN: 2254 – 4143), each work being identified with its respective DOI (Digital Object Identifier System) code.

## PRESENTATION WORK

The papers will be presented in Baskerville typeface, body 11, justified and without tabs. They must have Word format. The extension will be no more than 6.000 words of text, including references. Papers must be submitted exclusively by OJS manuscript management platform:

https://ojs.3ciencias.com/

All the information, as well as the templates to which the works must adhere, can be found at:

https://www.3ciencias.com/en/journals/information-for-authors/

https://www.3ciencias.com/en/regulations/templates/


https://doi.org/10.17993/3ctecno.2021.specialissue8

## ESTRUCTURA

Los trabajos originales tenderán a respetar la siguiente estructura: introducción, métodos, resultados, discusión/conclusiones, notas, agradecimientos y referencias bibliográficas.
Es obligatoria la inclusión de referencias, mientras que notas y agradecimientos son opcionales. Se valorará la correcta citación conforme a la 7.ª edición de las normas APA.

## RESPONSABILIDADES ÉTICAS

No se acepta material previamente publicado (deben ser trabajos inéditos). En la lista de autores firmantes deben figurar única y exclusivamente aquellas personas que hayan contribuido intelectualmente (autoría), con un máximo de 4 autores por trabajo. No se aceptan artículos que no cusmplan estrictamente las normas.

## INFORMACIÓN ESTADÍSTICA SOBRE TASAS DE ACEPTACIÓN E INTERNACIONALIZACIÓN

- Número de trabajos aceptados publicados: 40.
- Nivel de aceptación de manuscritos en este número: 68,9%.
- Nivel de rechazo de manuscritos: 31,1%.
- Internacionalización de autores: 2 países (India y Reino Unido).

Normas de publicación: https://www.3ciencias.com/normas-de-publicacion/instrucciones/


https://doi.org/10.17993/3ctecno.2021.specialissue8

## STRUCTURE

The original works will tend to respect the following structure: introduction, methods, results, discussion/conclusions, notes, acknowledgments and bibliographical references. The inclusion of references is mandatory, while notes and acknowledgments are optional. The correct citation will be assessed according to the 7th edition of the APA standards.

## ETHICAL RESPONSIBILITIES

Previously published material is not accepted (they must be unpublished works). The list of signatory authors should include only and exclusively those who have contributed intellectually (authorship), with a maximum of 4 authors per work. Articles that do not strictly comply with the standards are not accepted.

## STATISTICAL INFORMATION ON ACCEPTANCE AND INTERNATIONALIZATION FEES

- Number of accepted papers published: 40.
- Level of acceptance of manuscripts in this number: 68,9%.
- Level of rejection of manuscripts: 31,1%.
- Internationalization of authors: 2 countries (India and United Kingdom).

Guidelines for authors: https://www.3ciencias.com/en/regulations/instructions/


https://doi.org/10.17993/3ctecno.2021.specialissue8

# INDEXACIONES INDEXATIONS



https://doi.org/10.17993/3ctecno.2021.specialissue8

# INDEXACIONES INDEXATIONS



https://doi.org/10.17993/3ctecno.2021.specialissue8

# /SUMARIO/
# /SUMMARY/


https://doi.org/10.17993/3ctecno.2021.specialissue8

https://doi.org/10.17993/3ctecno.2021.specialissue8

https://doi.org/10.17993/3ctecno.2021.specialissue8

https://doi.org/10.17993/3ctecno.2021.specialissue8

https://doi.org/10.17993/3ctecno.2021.specialissue8

https://doi.org/10.17993/3ctecno.2021.specialissue8

# /01/


https://doi.org/10.17993/3ctecno.2021.specialissue8

# GARBAGE MONITORING SYSTEM USING GSM

**Pandiaraj Kadarkarai**
Assistant professor, Department of Electronics and Communication Engineering.
Kalasalingam Academy of Research and Education, Krishnan koil, Tamilnadu, (India).
E-mail: pandiaraj@klu.ac.in
ORCID: https://orcid.org/0000-0001-9610-2172

**Sivakumar Pothiraj**
Professor, Department of Electronics and Communication Engineering.
Kalasalingam Academy of Research and Education, Krishnan koil, Tamilnadu, (India).
E-mail: siva@klu.ac.in
ORCID: https://orcid.org/0000-0003-1328-8093

**Nandhini Venkatesakumaran**
Department of Electronics and Communication Engineering.
Kalasalingam Academy of Research and Education, Krishnan koil, Tamilnadu, (India).
E-mail: nandhinikumaran09@gmail.com
ORCID: https://orcid.org/0000-0001-6509-8334

**Parkavi Seenivasan**
Department of Electronics and Communication Engineering.
Kalasalingam Academy of Research and Education, Krishnan koil, Tamilnadu, (India).
E-mail: parkavi030599@gmail.com
ORCID: https://orcid.org/0000-0002-2054-166X

**Recepción:** 16/10/2019 **Aceptación:** 28/09/2020 **Publicación:** 30/11/2021

**Citación sugerida:**
Kadarkarai, P., Pothiraj, S., Venkatesakumaran, N., y Seenivasan, P. (2021). Garbage monitoring system using GSM. *3C Tecnología. Glosas de innovación aplicadas a la pyme, Edición Especial*, (noviembre, 2021), 21-31. https://doi.org/10.17993/3ctecno.2021.specialissue8.21-31

## ABSTRACT

All over the world waste management is a major problem. Many times, we see that the dustbin placed at public places are overloaded. It creates unhygienic environment for the people. To avoid such things, we have implemented a project known as "Garbage monitoring system using GSM". These dustbins are supplied with low price embedded device that helps in tracking the amount of garbage in the bin. A unique ID is provided for each garbage can which helps to identify the location and the status of the bin. These details will be sent to the concern authorities, with the help of message an immediate action can be made to clean the garbage in the dustbin. Garbage monitoring system is a new idea of implementation which makes a normal dustbin smart using ultrasonic sensors for garbage level detection, display and sending message to the concern department person updating the status of the bin using GSM modem.

## KEYWORDS

Arduino board, Ultrasonic sensor, GSM.


https://doi.org/10.17993/3ctecno.2021.specialissue8.21-31

# 1. INTRODUCTION

In order to preserve the surroundings from all the rubbish that is spread over the world which causes some harmful diseases in the surroundings, due to the accumulation of the municipal solid waste it leads to environmental pollution. A proper maintenance of waste is necessary for economical and effective removal of municipal solid waste. We tend to introduce this idea of Garbage monitoring system using GSM. People are depositing their waste within the garbage can. We are fitting ultrasonic sensor, at the highest of garbage can. Currently the ultrasonic sensor can sense the rubbish level (Jain & Bagherwal, 2017). If garbage amount increases, shortly it'll reach the edge level. As shortly as the threshold value is attained, automatically alert will be sent using GSM module to the registered range, intimating that the rubbish value has reach the extent of about 5cm nearby ultrasonic sensor.

The garbage cans are filled, and the data is sent to the concerned authority for the further process. We used the GSM for the real time information. It is the main part of the communication system which has less price, good performance and which can be implemented easily. If any of the person is making an attempt to deposit their waste within the garbage can, even though the threshold value crosses the range then the LED will glow. This method helps to reduce amount of time used, fuel, and money. There will be lots of rural places which can be benefitted from this technique in future.

# 2. MATERIALS AND METHODS

## 2.1. EXISTING METHOD

Garbage has to be collected manually and periodically whether the dustbin is full or Not.

Drawbacks of the present method

- Less effective
- More time consumption
- Expenditure will be high
- Filthy atmosphere


https://doi.org/10.17993/3ctecno.2021.specialissue8.21-31

- It creates bad odor and causes health problems.

## 2.2. PROPOSED METHOD

The embedded system is widely used in many areas, but the work done by this system will differ from place to place. The project explained here shows one of the uses of microcontroller with GSM and ultrasonic sensor. There is no proper indication of garbage level so the collections of waste in many areas are delayed which causes rotten smell and spread many diseases.

In this paper the "garbage monitoring system using GSM" is introduced. Here the garbage can place in remote areas are monitored through the sensor placed in the bin. To check the status of the dustbin, ultrasonic sensor is used. As, it reaches the threshold level the indication will be sent through GSM which is received by the android mobile which contains the location of the dustbin.

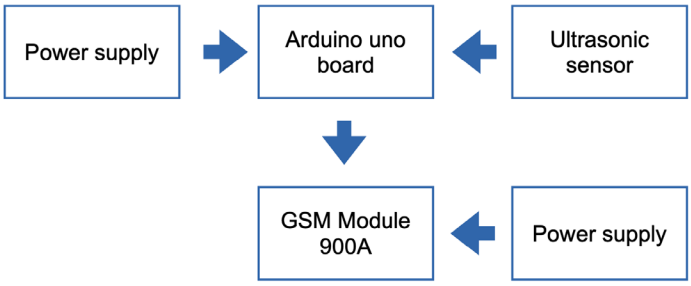


**Figure 1.** Garbage monitoring system using GSM (Block Diagram).
**Source:** own elaboration.

WORKING

The device consists of ultrasonic sensor, the Arduino Uno microcontroller, and the GSM module. Here we are going to discuss about the block diagram of the garbage monitoring system.

### A. HC-SR04 ULTRASONIC SENSOR

To determine the distance of an object, the ultrasonic sensor (HC-SR04) is used. It offers excellent non-contact range from 2 cm to 400 cm or 1" to 13 feet and it detects with high accuracy and stable readings, the status of the waste in the bin is detected with the help of


https://doi.org/10.17993/3ctecno.2021.specialissue8.21-31

this sensor and continues checking of garbage level takes place (Kumar *et al.*, 2017). The readings will be sent to Arduino which acts as system controller.

### B. ARDUINO UNO

The Arduino UNO is supported with microchip ATmega328P microcontroller and it is an open-source microcontroller board (Mirchandani *et al.*, 2017; Dugdhe *et al.*, 2016). The board is provided with sets of digital and analog input/output pins that may be interfaced with several alternative circuits and expansion boards.

The board has fourteen Digital pins, six Analog pins, and programmable with the Integrated Development environment which helps to program the device according to the need. In this project the Arduino board acts as the connector between the sensor and the GSM. The data which is provided by ultrasonic sensor is processed in the Arduino board and the command is sent to GSM.

The red LED which is connected to the Arduino board, as the garbage reaches certain level the LED will glow.

### C. GSM

GSM (Global System for Mobile Communication) is a digital cellular technology used for transmission of mobile voice and data services which operates at the 850MHz, 900MHz, 1800MHz and 1900MHz frequency bands. In this project GSM is used to send the message to the particular number after getting command from the Arduino board (Reddy *et al.*, 2017; Thakker & Narayanamoorthi, 2015). The message is sent as an indication to the authorized number with the address and status of the bin.


https://doi.org/10.17993/3ctecno.2021.specialissue8.21-31

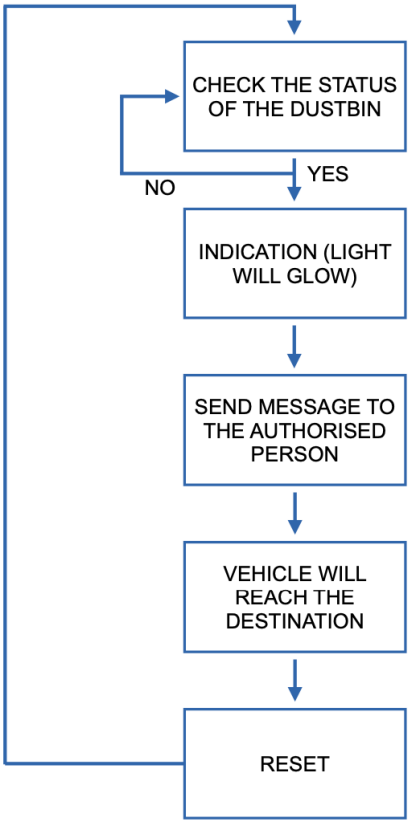


**Figure 2.** Flow chart.
**Source:** own elaboration.

As the flow chart represent the flow of working of the project, the status of the dustbin is checked continuously if the condition becomes true then the process goes to next level otherwise it continues with its checking process. When the condition is true the indication process starts, the LED which is present in the device glow and the message is sent to the authorized person with the provided information the vehicle will reach the destination. After the collection of the garbage the device will get reset.

## 3. RESULTS

In many areas, we can observe the dustbin has been filled. It is very unhygienic, and it will create many diseases to the people in and around the world so, we have introduced a new automated device called "GARBAGE MONITORING SYSTEM USING GSM". This device helps to clean the dustbin in time. To sense the level of the dustbin ultrasonic sensor


https://doi.org/10.17993/3ctecno.2021.specialissue8.21-31

is used (ie) (distance<5cm) and the signal will be sent to the Arduino. Thereby, the signal will be sent to the GSM and the signal from GSM will be sent to the authorized person. In addition to the message, the LED will be glow until the dustbin is cleaned. This device can reduce the time consumption and transportation charge. After this device is implemented, the human interaction will be reduced.

**Figure 3.** Dustbin is not filled.
**Source:** own elaboration.

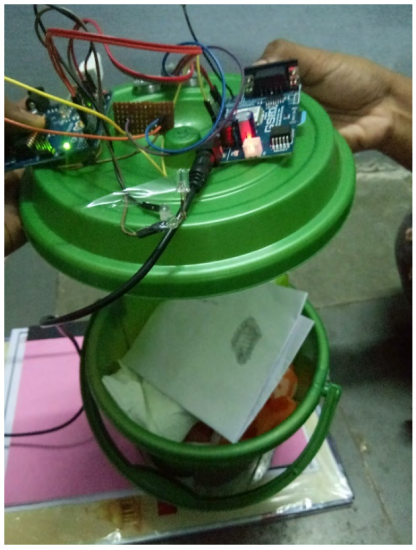

**Figure 4.** The Dustbin is about to fill.
**Source:** own elaboration.


https://doi.org/10.17993/3ctecno.2021.specialissue8.21-31

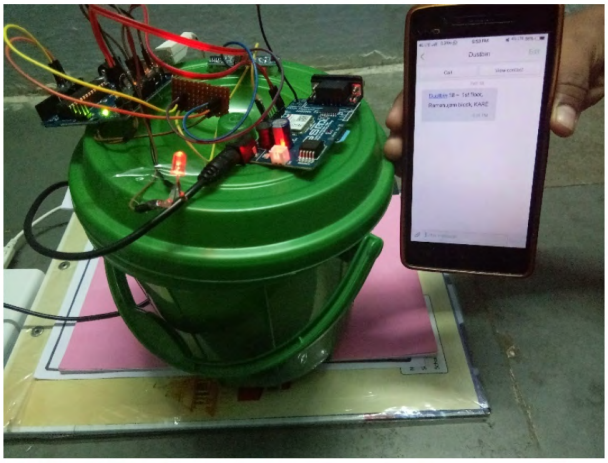

**Figure 5.** Output (Message received).
**Source:** own elaboration.

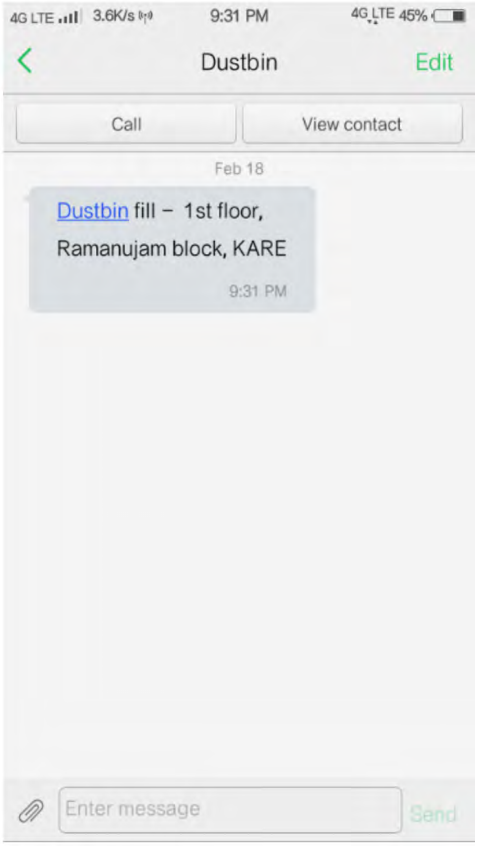


**Figure 6.** Message received.
**Source:** own elaboration.


https://doi.org/10.17993/3ctecno.2021.specialissue8.21-31

## 4. CONCLUSIONS

For correct maintenance and correct observation of the waste, an Arduino based wise alert system is devised. This method averts their regular cleanup of the garbage can by sending caution messages to the particular number periodically and it helps in the cleaning process in real time so this process can be considered as an outstanding performance for the surroundings. In this process it diminishes the number of human resources needed. Thus, the process of cleaning becomes faster compare to the manual process.

## REFERENCES

**Dugdhe, S., Shelar, P., Jire, S., & Apte, A.** (2016). Efficient waste collection system. In *International Conference on Internet of Things and Applications (IOTA)*, pp. 143-147. https://doi.org/10.1109/IOTA.2016.7562711

**Jain, A., & Bagherwal, R.** (2017). Design and Implementation of a Smart Solid Waste Monitoring and Collection System Based on Internet of Things. In *8th International Conference on Computing, Communication and Networking Technologies (ICCCNT)*, pp. 1-5. https://doi.org/10.1109/ICCCNT.2017.8204165

**Joshi, J., Reddy, J., Reddy, P., Agarwal, A., Agarwal, R., Bagga, A., & Bhargava, A.** (2016). Cloud computing based smart garbage monitoring system. In *3rd International Conference on Electronic Design (ICED)*, pp. 70-75. https://doi.org/10.1109/ICED.2016.7804609

**Kumar, B. R. S., Varalakshmi, N., Lokeshwari, S. S., Rohit, K., Manjunath & Sahana, D. N.** (2017). Eco-friendly IOT based waste segregation and management. In *International Conference on Electrical, Electronics, Communication, Computer, and Optimization Techniques (ICEECCOT)*, pp. 297-299. https://doi.org/10.1109/ICEECCOT.2017.8284686

**Kumar, N. S., Vuayalakshmi, B., Prarthana, R. J., & Shankar, A.** (2016). IOT based smart garbage alert system using Arduino UNO. In *IEEE Region 10 Conference (TENCON)*, pp. 1028-1034. https://doi.org/10.1109/TENCON.2016.7848162

**Kumar, S. V., Kumaran, T. S., Kumar, A. K., & Mathapati, M.** (2017). Smart garbage monitoring and clearance system using internet of things. In *IEEE International Conference on Smart Technologies and Management for Computing, Communication, Controls, Energy and Materials (ICSTM)*, pp. 184-189. https://doi.org/10.1109/ICSTM.2017.8089148

**Longhi, S., Marzioni, D., Alidori, E., Di Buo, G., Prist, M., Grisostomi, M., & Pirro, M.** (2012). Solid Waste Management Architecture Using Wireless Sensor Network Technology. In *5th International Conference on New Technologies, Mobility and Security (NTMS)*, pp. 1-5. https://doi.org/10.1109/NTMS.2012.6208764

**Mirchandani, S., Wadhwa, S., Wadhwa, P., & Joseph, R.** (2017). IoT enabled dustbins. In *International Conference on Big Data, IoT and Data Science (BID)*, pp. 73-76. https://doi.org/10.1109/BID.2017.8336576

**Reddy, P. S. N., Naik, R. N., Kumar, A. A., & Kishor, S. N.** (2017). Wireless dust bin monitoring and alert system using Arduino. In *Second International Conference on Electrical, Computer and Communication Technologies (ICECCT)*, pp. 1-5. https://doi.org/10.1109/ICECCT.2017.8117960

**Thakker, S., & Narayanamoorthi, R.** (2015). Smart and wireless waste management. In *International Conference on Innovations in Information, Embedded and Communication Systems (ICIIECS)*, pp. 1-4. https://doi.org/10.1109/ICIIECS.2015.7193141

https://doi.org/10.17993/3ctecno.2021.specialissue8.21-31

# /02/


https://doi.org/10.17993/3ctecno.2021.specialissue8

# AUTOMATIC WATERING SYSTEM USING ARDUINO

**P. Naveen**
Master of Engineering (M.E). Assistant professor, Electronics and Communication Engineering, Kalasalingam Academy of Research and Education. Madurai, (India).
E-mail: naveenamp88@gmail.com
ORCID: https://orcid.org/0000-0002-5202-2557

**R. Adapala**
Student, Electronics and Communication Engineering, Kalasalingam Academy of Research and Education. Madurai, (India).
E-mail: rohanadapala07@gmail.com
ORCID: https://orcid.org/0000-0001-5212-2710

**A. Sreekanth**
Student, Electronics and Communication Engineering, Kalasalingam Academy of Research and Education. Madurai, (India).
E-mail: sriikanth124@gmail.com
ORCID: https://orcid.org/0000-0001-7978-2671

**B. Rakesh**
Student, Electronics and Communication Engineering, Kalasalingam Academy of Research and Education. Madurai, (India).
E-mail: binnyrake@gmail.com
ORCID: https://orcid.org/0000-0003-3532-9511

**Recepción:** 16/10/2019 **Aceptación:** 11/09/2020 **Publicación:** 30/11/2021

**Citación sugerida:**
Naveen, P., Adapala, R., Sreekanth, A., y Rakesh, B. (2021). Automatic watering system using Arduino. *3C Tecnología. Glosas de innovación aplicadas a la pyme, Edición Especial,* (noviembre, 2021), 33-39. https://doi.org/10.17993/3ctecno.2021.specialissue8.33-39

## ABSTRACT

The growing needs of man and the increasing population of earth causes the scarcity of water. This greatly affects the plants, and the requirement water management is high. Water use has been growing globally at more than twice the rate of population increases in the last century, and an increasing number of regions are reaching the limit at which water services can be sustainably delivered, especially in arid regions. In the present scenario the conventional methods of watering, like flood mode and sprinkler, is not that much effective and is responsible for water wastage. Improper watering systems create breeding areas for disease spreading organisms. Hence, the way watering pants must be smart, and this is achieved by watering plants depending on the necessity of plants and the moisture level of water. This project deals with an automated plant watering system that senses the moisture content of the soil thus determining the necessity of pumping water with the collected data. Also determines the minimum amount of water required to maintain the balance between the soil defensible water and environment parameters.

## KEYWORDS

Arduino, Soil moisture sensor, Power supply, Relay.


https://doi.org/10.17993/3ctecno.2021.specialissue8.33-39

# 1. INTRODUCTION

At the present scenario, in the era of innovation where the technology is growing in terms of electrical and other new technologies, the life of people must be uncomplicated and more favorable and there is a need for lot of self-working system that are able to replace or bring down man's effort in their daily tasks. We propose a similar system called automatic self-plant watering system, which is basically a framework of monitoring planting and agriculture opportunities that uses sensors to detect the soil moisture content with a microcontroller and Arduino .Since asymmetrical watering results in plant efficient elements loss in the soil and may even results in spoil of the plants, Finding the method to find weather the watering is necessary or not and to give what we have to water the plants is foremost. Due to social process and inadequacy of place people started growing plants in an unfit windowsill location. It is very essential to use the water assets and a system is mandatory, to manage this task without man's existence. Machine-controlled watering system estimates and processes the existing plant and then materials required along with the amount of water quantity needed by that plant, dropping the amount of water to let the plants be water efficient.

# 2. MATERIALS AND METHOD

**Materials:**

Arduino, soil moisture sensor, power supply, relay, water motor.

**Method:**

The method of flowing water all by itself and monitoring the same in a display to let the user know about it is the second major task we need to solve. When the Arduino gets level 1 as input the user gets a display word of it and the first level of watering is done to maintain the water moisture level required to match the water. It has a system that can deliver a heavy load to pump the water. The opposite work happens when the logic-low is received.

We use a moisture detector that uses a sensing element in it to find the amount of moisture present in the soil and is connected to an external micro controller like an AVR or Arduino. The Arduino is connected to a computer to load a program to save the obtained results and


https://doi.org/10.17993/3ctecno.2021.specialissue8.33-39

give the output to a display and to control the amount of water flow. Also, we use a moisture sensor to find the amount of watering required for further flow of plant to be healthy.

## 3. RESULTS

The result of the project declares that, if the soil moisture is low then moisture sensor sends signal as level 1 to Arduino and it passes signal to relay which switches the power to the motor pump and provides water to the plant. If soil moisture is high, then the sensor send signal as level 0 and Arduino will not pass any signal to relay.

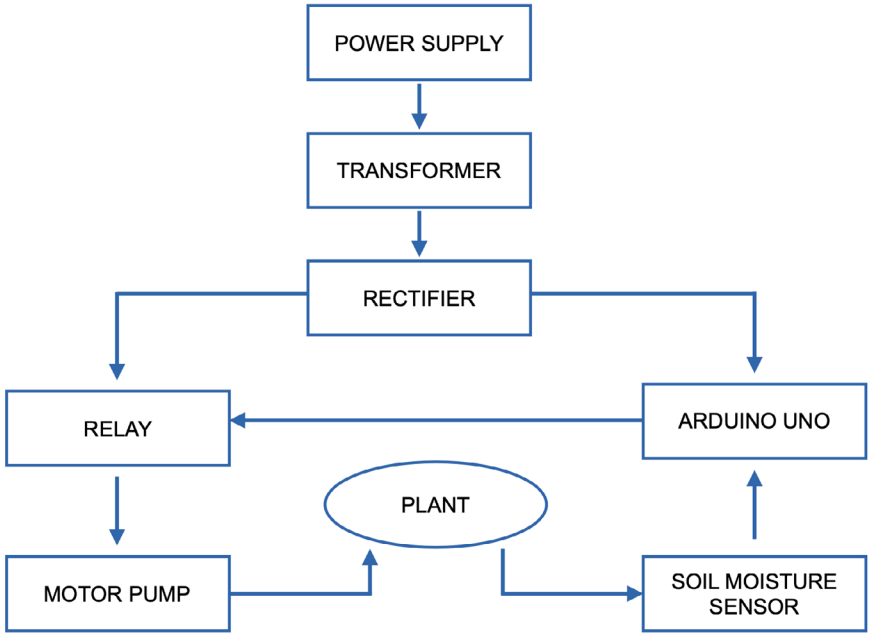


**Figure 1.** Block diagram.
**Source:** own elaboration.

## 4. CONCLUSIONS

The proposed system provides a vague output and cannot be dependent completely as all the plants are not having the same requirements for its watering needs. Some plants can be survived with less amount of water and withstand drought conditions. Monitoring a watering system based on the soil moisture level is not much efficient but provides a temporary solution to solve the problem. The development of the project must be further


https://doi.org/10.17993/3ctecno.2021.specialissue8.33-39

done depending on the amount of water required for the specific plant. Automatic irrigation systems improve water use and Reduce water wastage. This project can Contribute to socio-economic development. It has a quick response and is computer user friendly. The primary use of this program is farmers and Gardeners do not have enough time for their watering, they do not miss crops or plants. This project is also an application for farmers wasting water unknowingly during irrigation. The main purpose of this smart project is, it is very innovative, user friendly, less time consuming, and more efficient than the existing system.

## REFERENCES

**Beckwith, R., Teibel, D., & Bowen, P.** (2004). Report from the Field: Results from an Agricultural Wireless Sensor Network. *Proceedings of the 29th Annual IEEE International Conference on Local Computer Networks (LCN'04)*. http://profesores.elo.utfsm.cl/~agv/research/interno06/papers/AgricultureWSN.pdf

**Fu, Q., Xing, Z., & Ma, Y.** (2004). Applying Multivariate Auto Regression Model to Forecast the Water Requirement of Well Irrigation Rice in Sanjiang Plain. N*ature and Science, 2*(2), 8-14. http://www.sciencepub.net/nature/0202/02fu.pdf

**Kim, Y., & Evans, R. G.** (2009). Software design for wireless sensor-based site-specific irrigation. *Computers and Electronics in Agriculture, 66*(2), 159-165. https://doi.org/10.1016/j.compag.2009.01.007

**Kim, Y., Evans, R. G., & Iversen, W. M.** (2008). Remote Sensing and Control of an Irrigation System Using a Distributed Wireless Sensor Network. *IEEE Transactions on Instrumentation and Measurement, 57*(7), 1379-1387. https://doi.org/10.1109/TIM.2008.917198

**Li, F., Wang, B., Huang, Y., Teng, Y., & Cai, T.** (2011). Study on the Management System of Farmland Intelligent Irrigation. In Li, D., Liu, Y., & Chen, Y. (eds.) *Computer and Computing Technologies in Agriculture IV.* CCTA 2010. IFIP Advances in Information and Communication Technology, vol. 345. Springer, Berlin, Heidelberg. https://doi.org/10.1007/978-3-642-18336-2_83


https://doi.org/10.17993/3ctecno.2021.specialissue8.33-39

**Morais, R., Valente, A., & Serodio, C.** (2005). *A Wireless Sensor Network for Smart Irrigation and Environmental Monitoring: A Position Article.* Data Acquisition Station for Agriculture. https://www.researchgate.net/publication/229000796_A_wireless_sensor_network_for_smart_irrigation_and_environmental_monitoring_A_position_article

**Putjaikal, N., Phusae, S., Chen-im, A., Phunchongharn, P., & Akkarajitsakul, K.** (2016). A Control System in an Intelligent Farming by using Arduino Technology. In *Fifth ICT International Student Project Conference (ICT-ISPC)*. http://smartfasal.in/wp/wp-content/uploads/2019/09/A-control-system-in-an-intelligent-farming-by-using-arduino-technology.pdf

**Rehman, A.-U., & Shaikh, Z. A.** (2008). Towards Design of Context Aware Sensor Grid Framework for Agriculture. *Proceedings of World Academy of Science, Engineering and Technology.* https://www.researchgate.net/publication/236960807_Towards_design_of_context-aware_sensor_grid_framework_for_agriculture

**Wang, N., Zhang, N., & Wang, M.** (2006). Wireless sensors in agriculture and food industry—Recent development and future perspective. *Computers and Electronics in Agriculture, 50*(1), 1-14. https://doi.org/10.1016/j.compag.2005.09.003

https://doi.org/10.17993/3ctecno.2021.specialissue8.33-39

# /03/


https://doi.org/10.17993/3ctecno.2021.specialissue8

# LOW-COST NON-INVASIVE SMART BED SYSTEM USING MEDICAL DEVICES EMBEDDED WITH IOT

**M. Sakthimohan**
Assistant Professor, ECE, Kalasalingam Academy of Research and Education, Anand Nagar, Krishnankoil, (India).
E-mail: sakthimohan.m@klu.ac.in
ORCID: https://orcid.org/0000-0002-8151-4745

**G. Elizabeth Rani**
Assistant Professor, CSE, Kalasalingam Academy of Research and Education, Anand Nagar, Krishnankoil, (India).
E-mail: g.elizabeth@klu.ac.in
ORCID: https://orcid.org/0000-0002-4513-2109

**J. Deny**
Assistant Professor, ECE, Kalasalingam Academy of Research and Education, Anand Nagar, Krishnankoil, (India).
E-mail: j.deny@klu.ac.in
ORCID: https://orcid.org/0000-0001-6515-3575

**S. N. Susmitha**
Student, ECE, Kalasalingam Academy of Research and Education, Anand Nagar, Krishnankoil, (India).
E-mail: sushmashahnaz20@gmail.com
ORCID: https://orcid.org/0000-0002-9251-4789

**S. Sobiya**
tudent, ECE, Kalasalingam Academy of Research and Education, Anand Nagar, Krishnankoil, (India).
E-mail: sobiyasanthanam@gmail.com
ORCID: https://orcid.org/0000-0002-7851-4459

**Recepción:** 16/10/2019 **Aceptación:** 28/09/2020 **Publicación:** 30/11/2021

**Citación sugerida:**
Sakthimohan, M., Rani, G. E., Deny, J., Susmitha, S. N., y Sobiya, S. (2021). Low-cost non-invasive smart bed system using medical devices embedded with IoT. *3C Tecnología. Glosas de innovación aplicadas a la pyme, Edición Especial*, (noviembre, 2021), 41-51. https://doi.org/10.17993/3ctecno.2021.specialissue8.41-51

## ABSTRACT

Now a days, advances in information and communication technology have prompted the rise of internet of things (IOT). In the modern era, the usage of IOT technologies brings the physician and doctor to monitor the health condition of the patient even in remote and rural areas can be examined and consulted by doctors worldwide where the database of the patient is uploaded in sub-server and sends to government website using android technology .In this paper, different kinds of sensor modules and controller are used to monitor the health parameter of patient includes heart rate, temperature, pulse rate respectively and the measured parameter can be transmitted to the microcontroller sequentially. From the measured value blood oxygen level, carbon dioxide level, hemoglobin, stress, and glucose level flow can be derived, the main aim of the project is to access the individual health condition of the patient by the doctor anywhere in the world. The death rate because of these kind of simple health problems will be reduced and the convenience for treatment time alert is invented, the remote health monitoring system with the help of internet of things (IOT) which has the portable features.

## KEYWORDS

Sensors, Micro-Controller, Wi-Fi module, IOT, NON-Invasive method.


https://doi.org/10.17993/3ctecno.2021.specialissue8.41-51

# 1. INTRODUCTION

Health monitoring plays a key role in our day-to-day life based on this criterion; it is technically called as tele-medicine. Which will clearly focus on the patients' health monitoring system by forming an instrument with various type of sensors and equipment's which will receive and sends the data to the database in the mode of wireless communication to the desired professional who wants to monitor the patient, the key idea is to concentrate on metabolic disorder called diabetes (Jin *et al.*, 2017). Where regular checking of blood glucose is needed keeping this concept, we have planned to design a device which can monitor the patient's health regularly to have a clear record on the patient's status of health. Based on the types of diabetes namely diabetes I and diabetes II where both are chronic diseases which affects the way your body regulate the blood sugar. The clinical records are studied as normal level (<100 mg/dl), prediabetes (100-125 mg/dl), diabetes (>126 mg/dl) and death (>700 mg/dl) so according to this data's this project is designed based on the above listed values as the triggering peaks when it is recorded. This project aims for design and authenticate the system that automatically informs the relative personnel about their healthiness of an elderly person, if the person's pulse rate, temperature and other related parameters drops below or rise beyond a threshold level. So, the main moto of this work is making wireless and to make that as remote access. These techniques are referred in the domain of bioinstrumentation, computer, and telecommunication (Quaiyum *et al.*, 2017).

# 2. MATERIALS AND METHODS

The main goal is to design an instrument which is fitted to the patient as a wearable which is also portable, technically it is named as tele-health care device this device is for mainly monitoring the health regularly based on the records doctors can discuss the patient's health and recommend them for further medication steps. If the patient is discharged after treatment and located in a remote location it is easy for them to monitor the health by their doctor without physical presence (Sakthimohan & Deny, 2021). Main sensors in this device constitutes near infra-red ray, which is used to attain the absorption co-efficient from the blood to achieve the glucose level. So that it becomes the non-invasive method of glucose monitoring system. Where near infra-red ray method plays a major role in it (Yu *et al.*, 2017). Optimum insulin dosage should be monitored because of the abrupt changes in


https://doi.org/10.17993/3ctecno.2021.specialissue8.41-51

blood glucose levels so for this kind of fluctuations are monitored by using this instrument. The calibrated values are of approximates the near and far recordings by mean square values, so that the design constitutes all the values by the physical attributes and processes the data's according to the user defines functions (Sakthimohan & Deny, 2020a). Therefore, the devices involved according to this proposed design is Arduino mega board, pulse sensor, temperature sensor, respiratory sensor and fingerprint sensor as an input device, Whereas the output devices are LCD, Wi-Fi module and some smart devices like computer or smart phones. The statistical analysis of this paper is to increase the benefit by 20% of the total population. In depth study about what sensors to be used for this non-invasive blood glucose monitoring system is carried out by evaluating the individual process taken by each sensor (Martinez, 2002). Pulse sensor which will find the bpm and stores the value, next the temperature sensor and the respiratory sensor will check the patients thermal and blood pressure rate indirectly by using mathematical model in code, whereas the fingerprint sensor calculates the absorption coefficient of blood glucose level, by cumulating all the obtained. Values the blood glucose level (Sakthimohan & Deny, 2020b).

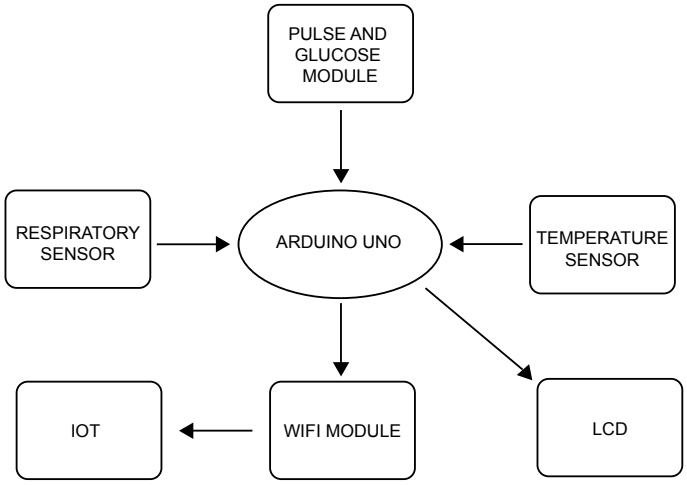


**Figure 1.** Block Diagram.
**Source:** own elaboration.

Figure 1 describes the last part in this system is IOT database implementation method which follows the data framing method to indicate the past and present inputs and the average values are determined by the slope which gives the parameter's Range of glucose and stress.


https://doi.org/10.17993/3ctecno.2021.specialissue8.41-51

### 2.1. INPUTS & OUTPUTS BY ANALYZING THE PHYSICAL PARAMETERS

The system design is framed by three sectors micro-controller, sensors and actuators and communication device. Micro-controller used here is Arduino mega board, where the input ports are connected with sensors and actuators like pulse sensor, temperature sensor, respiratory sensor and fingerprint sensor (Raikham *et al.*, 2018). The output ports are connected with Wi-Fi module, LCD display and smart phone.

### 2.2. NON-INVASIVE HEALTH MONITORING

Comparing to other health monitoring system our proposed Non-Invasive help us to monitor health with the help of sensor (Sakthimohan *et al.*, 2020). In existing system, we need to take blood of human beings after that measurement to be taken but our proposed system no need to take much more risk in humans. Our sensor predicts the health of human beings (Harbouche *et al.*, 2017).

## 3. DESIGN SPECIFICATION

The description of the block diagram consists of two major components. Heartbeat sensor and temperature sensor which constitutes a couple of parameters which incorporates the trigger values based on the modes classified as babies, children, and adults where the average values for these three categories are 72, 90 and 120 respectively. Whenever there is bradycardia (low heartbeat level) or tachycardia (higher heartbeat level) the system responds to it and calls the function which will alert (or) records the value as per the unit beats per minutes (bpm) similarly the system also responds to temperature level by getting the amount of body temperature corresponding to maximum peak le (36-37.8c).

Respiratory criteria are also concerned in this process.


https://doi.org/10.17993/3ctecno.2021.specialissue8.41-51

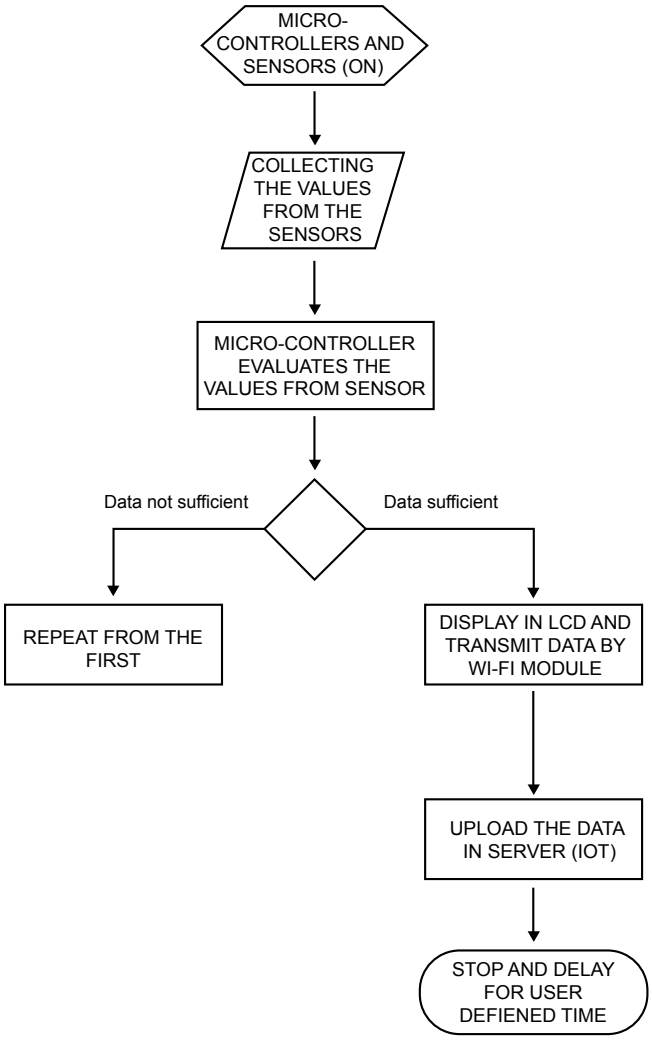


**Figure 2.** Flow Chart.
**Source:** own elaboration.

Figure 2 shows that Micro controller (Arduino mega board) is connected with sensors and other communication devices where pulse sensor, temperature sensor, respiratory sensor and fingerprint sensor are the input devices to the micro-controller the physical quantities like heat, pressure and radiation gets the values of each parameters and gives them to the Arduino mega board , which processes the given data and indicated the blood glucose level the final process after the inputs is to calibrate the level of inputs and display them in the output section where we use LCD (16*2) for on-board indication of results and for remote access using Wi-Fi module we integrate it with the IOT platform which sends the data's


https://doi.org/10.17993/3ctecno.2021.specialissue8.41-51

to the devices like smart phones (or) computers. So, this system works on the basis of data recording and analysis of peak values which gives the output data to the corresponding devices.

# 4. RESULTS AND DISCUSSION

Table 1 describes using the components which makes the combinational work of calculating the blood carbon dioxide, oxygen, stress level, infra-red ray absorption coefficient factor and temperature the calculation are made, and the results are uploaded to the database using the IOT platform, so that previously the range of values are made to be recorded, like low, medium and high. Whereas the monitoring system triggers output to be displayed in the interface by wireless data transfer using wi-fi module. Where various parameters like blood glucose level, blood oxygen level, and temperature and pulse rate are tabulated according to the various ranges attained from the patient. So, these values are uploaded to the processor in order to check the low, normal and high-risk level.

**Table 1.** Results.

| Parameters | Case 1: (Low) | Case 2: (Normal) | Case 3: (High) |
|---|---|---|---|
| Blood Glucose Level | 62mg/dl | 120mg/dl | 232mg/dl |
| Blood Oxygen Level | 89% <O2 | 92% O2 | 100% >CO2 |
| Temperature | 92 | 98.4 | 102 |
| Pulse Rate | 72(bpm) | 90(bpm) | 120(bpm) |

**Source:** own elaboration.

## 4.1. FUTURE SCOPE

Using these ideas from the project in the fore coming days further enhancement can be done by the following ideas.

- To implement remote viral fever recording system.
- To reduce size and optimize the code which will minimize the processing time.
- Also, to use this device for industrial and commercial purpose
- To introduce more parameters and alerting system.


https://doi.org/10.17993/3ctecno.2021.specialissue8.41-51

## 5. CONCLUSIONS

Our proposed work helps human beings in measuring health monitor systems. Using Respiratory and Temperature sensor by sensing the human's health was monitored. The components which make the combinational work of calculating the blood carbon dioxide, oxygen, stress level, infra-red ray absorption coefficient factor and temperature the calculations are made and the results are uploaded to the database using the IOT platform, so that previously the range of values are made to be recorded, like low, medium and high. Whereas the monitoring system triggers output to be displayed in the interface by wireless data transfer using Wi-Fi module. Without taking blood from human being can monitor glucose, blood oxygen level. Our proposed device helps human beings in multiple manner.

## REFERENCES

**Harbouche, A., Noureddine, D., Mohammed, E., Ben-Othman, J., & Kobbane, A.** (2017). Model driven flexible design of a wireless body sensor network for health monitoring. *Computer Networks, 129*(5), 548-571. http://thesis.univ-biskra.dz/3844/3/Article%20Elsevier%20-HARBOUCHE%20Ahmed.pdf

**Jarchi, D., Salvi, D., Velardo, C., Mahdi, A., Tarassenko, L., & Clifton, D. A.** (2018). Estimation of HRV and SpO2 from Wrist-Worn Commercial Sensors for Clinical Settings. In *2018 IEEE 15th International Conference on Wearable and Implantable Body Sensor Networks (BSN)*, pp. 144-147. https://doi.org/10.1109/BSN.2018.8329679

**Jin, H., Tao, X., Dong, S., Qin, Y., Yu, L., Luo, J., & Deen, M. J.** (2017). Flexible surface acoustic wave respiration sensor for monitoring obstructive sleep apnea syndrome. *Journal of Micromechanics and Microengineering, 27*(11), 1–7. https://iopscience.iop.org/article/10.1088/1361-6439/aa8ae0/meta

**Kraitl, J., Klinger, D., Fricke, D., Timm, U., & Ewald, H.** (2013). Non-invasive Measurement of Blood Components. In Mukhopadhyay, S., Jayasundera, K., & Fuchs, A. (eds) *Advancement in Sensing Technology. Smart Sensors, Measurement and Instrumentation,* vol 1. Springer, Berlin, Heidelberg. https://doi.org/10.1007/978-3-642-32180-1_14

**Martinez, L.** (2002). A Non-Invasive Spectral Reflectance Method for Mapping Blood Oxygen Saturation in Wounds. *Applied Imagery Pattern Recognition Workshop, 2002.* Proceedings, pp. 112-116. https://doi.org/10.1109/AIPR.2002.1182263

**Pak, J. G., & Park, K. H.** (2012). Advanced Pulse Oximetry System for Remote Monitoring and Management. *BioMed Research International, Article ID 930582*. https://doi.org/10.1155/2012/930582

**Quaiyum, F., Ren, L., Nahar, S., Foroughian, F., & Fathy, A.** (2017). Development of a reconfigurable low cost multi-mode radar system for contactless vital signs detection. In *2017 IEEE MTT-S International Microwave Symposium (IMS),* 1245-1247. https://www.semanticscholar.org/paper/Development-of-a-reconfigurable-low-cost-multi-mode-Quaiyum-Ren/85cc3bbc04eda1d434e382216fa83aada2b2dcd4

**Raikham, P., Kumar, R., Shah, R. K., Hazarika, M., & Sonkar, R. K.** (2018). Non-invasive blood components measurement using optical sensor system interface. In *2018 3rd International Conference on Microwave and Photonics (ICMAP)*, pp. 1-2. https://doi.org/10.1109/ICMAP.2018.8354638

**Reedy, A. K., Boby, G., Mohan, M. N., & Kumar, J. V.** (2011). A Novel Method for the Measurement of Oxygen Saturation in Arterial Blood. In *2011 IEEE International Instrumentation and Measurement Technology Conference*, pp. 1-5. https://doi.org/10.1109/IMTC.2011.5944066

**Sakthimohan, M., & Deny, J.** (2020a). An Enhanced 8x8 Vedic Multiplier Design by Applying Urdhva-Tiryakbhyam Sutra. *International Journal of Advanced Science and Technology, 29*(05), 3348 - 3358. http://sersc.org/journals/index.php/IJAST/article/view/12015

**Sakthimohan, M., & Deny, J.** (2020b). An Optimistic Design of 16-Tap FIR Filter with Radix-4 Booth Multiplier Using Improved Booth Recoding Algorithm. *Microprocessors and Microsystems*, 103453. https://doi.org/10.1016/j.micpro.2020.103453

**Sakthimohan, M., & Deny, J.** (2021). An Efficient Design of 8 * 8 Wallace Tree Multiplier Using 2 and 3-Bit Adders. In Shakya, S., Balas, V. E., Haoxiang, W., Baig, Z. (eds)

*Proceedings of International Conference on Sustainable Expert Systems. Lecture Notes in Networks and Systems*, vol. 176. Springer, Singapore. https://doi.org/10.1007/978-981-33-4355-9_3

**Sakthimohan, M., Deny, J., Rani, G. E., Mahendran, J., Ahmed, J. A. J., & Azeem, M.** (2020). IOT based shrewd agronomy method. *Materials Today: Proceedings.* https://doi.org/10.1016/j.matpr.2020.11.096

**Yang, D., Zhu, J., & Zhu, P.** (2015). SpO2 and Heart Rate Measurement with Wearable Watch Based on PPG. In *2015 IET International Conference on Biomedical Image and Signal Processing (ICBISP 2015),* 2015, pp. 1-5. https://doi.org/10.1049/cp.2015.0784

**Yu, C., Xu, W., Zhang, N., & Yu, C.** (2017). Non-invasive smart health monitoring system based on optical fiber interferometers. In *2017 16th International Conference on Optical Communications and Networks (ICOCN),* pp. 1-3. https://doi.org/10.1109/ICOCN.2017.8121526.

**Zonios, G., Bykowski, J., & Kollias, N.** (2001). Skin Melanin, Hemoglobin, and Light Scattering Properties can be Quantitatively Assessed In Vivo Using Diffuse Reflectance Spectroscopy. *Journal Of Investigative Dermatology, 117*(6), 1452-1457. https://doi.org/10.1046/j.0022-202x.2001.01577.x

https://doi.org/10.17993/3ctecno.2021.specialissue8.41-51

/04/


https://doi.org/10.17993/3ctecno.2021.specialissue8

# HIGH PERFORMANCE NETWORK INTRUSION DETECTION ENGINE

**K. S. Dhanalakshmi**
Assistant professor III, Department of ECE, School of Electronics and Electrical Technology.
Kalasalingam Academy of Research and Education, Anand Nagar.
Krishnankoil, Virudhunagar District, (India).
E-mail: k.s.dhanalakshmi@klu.ac.in
ORCID: https://orcid.org/0000-0001-6285-3656

**S. Sorna Bala**
Student, Electronics and Communication Engineering.
Kalasalingam Academy of Research and Education. Madurai, (India).
E-mail: balaabi2608@gmail.com
ORCID: https://orcid.org/0000-0003-0112-493X

**M. Subha**
Student, Electronics and Communication Engineering.
Kalasalingam Academy of Research and Education. Madurai, (India).
E-mail: subhamuthuraj1998@gmail.com
ORCID: https://orcid.org/0000-0002-7945-451X

**R. Subharisha**
Student, Electronics and Communication Engineering.
Kalasalingam Academy of Research and Education. Madurai, (India).
E-mail: subharisha29@gmail.com
ORCID: https://orcid.org/0000-0002-5374-8800

**Recepción:** 16/10/2019 **Aceptación:** 28/09/2020 **Publicación:** 30/11/2021

**Citación sugerida:**
Dhanalakshmi, K. S., Sorna, S., Subha, M., y Subharisha, R. (2021). High performance network intrusion detection engine. *3C Tecnología. Glosas de innovación aplicadas a la pyme, Edición Especial,* (noviembre, 2021), 53-69. https://doi.org/10.17993/3ctecno.2021.specialissue8.53-69

## ABSTRACT

Security administration plays a significant role in network management tasks. The intrusion detection systems are designed to shield the provision, confidentiality and integrity of vital network information systems. The system we have planned to design can scan, classify and monitor the network traffic in real time while not affecting network throughput. Since most of the business intrusion detection systems are at usually expensive or abundant costly and that they tend to represent a major resource demand in themselves, for tiny networks, use of such IDS isn't possible. Thus, principally open supply IDS are being employed. IDS are one in everything about preeminent tried and dependable advances to watch the approaching and active system traffic to spot unapproved utilization and no right treatment of PC frameworks arrange. NIDS are normally incapable to execute whole system bundles, which winds up in fragmented investigations and in this way considerable postponements in fast and high-load conditions. HIDSs can watch malevolent networks and multiple actions happening isolated the endangered host. An HIDS stays located next to the tip purpose of an electronic network that has anti-threat applications like spyware detection, firewalls and antivirus software system plans, which give access to outdoor backgrounds like the Web.

## KEYWORDS

Intrusion detection system, Network Security, Network Intrusion Detection System, Intrusion Detection Expert System.


https://doi.org/10.17993/3ctecno.2021.specialissue8.53-69

# 1. INTRODUCTION

In this project we've the world design of SOC box in addition as many strategies accustomed take a look at its accuracy and performance.

Security could be a noteworthy worry in every aspect of our reality. New systems and instrumentation are conceived to affirm protection. Notwithstanding, PC systems still face a few dangers. There are normally three phases to accomplishing security in processing framework systems: interference, location and amendment. Interference is attractive to recognition and redress, anyway it is beyond the realm of imagination to expect to stop 100 percent of assaults. In addition, identification methods give extra right leads in recognizing malignant aggressors than redress procedures.

Redress methods are embraced to shield PC frameworks. Together with aversion, they effectively work to dam interruptions, however, it will still battle a thriving intrusion. All the same variety of thriving attacks can be controlled exploitations, various effective assaults can be controlled utilizing counteractive action procedures if an assault is recognized at the between time phases of bar frameworks. This is regularly intense, because of some independent assaults will overcome the anticipation framework. It's a matter of a framework being assaulted, traded off, and therefore breaking down. Here we require a between time stage like the discovery stage, that should be certain all through interruptions.

Accordingly, the discovery approach is most well-gotten a kick out of the chance to constrict system cost and fill inside the hole among revision and avoidance components. Snort could be a tool for tiny, gentle utilized network. Snort is beneficial when it is not cost efficient to deploy NIDS. Snort includes a real time alerting capability. Snort will be designed for long periods of your time while not requiring observance or body maintenance, and might so evenly utilized as an integral a part of most network security infrastructures. Accuracy and False Negative Rate (FNR) & False Positive Rate (FPR) are accustomed compare performance of algorithmic rule. Accuracy is used for mensuration the share of failure and proper detection similarly as the range of false alarms generated from IDS. FNR could be a proportion of samples that are according as traditional. FPR could be a proportion of set to give traditional instances that is incorrectly classified.


https://doi.org/10.17993/3ctecno.2021.specialissue8.53-69

This section offers a short review of the prevailing analysis work associated with intrusion detection system. From Big Data Analytics for Network Intrusion Detection paper, we tend to came to understand that this analogy network flows, logs and system events for intrusion detection by Wang and Jones (2018), in this projected system, the big data analysis will correlate multiple information sources into coherent read, determined suspicious activities and eventually accomplish economical intrusion detection. Wei Wa Nge conferred a Light Weight Intrusion Detection in laptop Networks. In this paper, the intrusion detection in big data environment needs for light weight models that are ready to accomplish real time performance throughput detection. It improves the potency of information process in intrusion detection. In this work we projected three strategies of information abstraction particularly, ideal extraction, attribute choice and attribute abstraction.

Roesch (1999) conferred a Snort Light Weight Intrusion Detection for Network. In this paper, Roesch (1999) had realized the various applications wherever the snort can be terribly helpful as a component of an integrated network security infrastructure. Snort was designed to fulfil the necessity of a prototypic lightweight network intrusion detection system. Lee and Huang (2013) given a Pattern Matching Scheme with High Throughput Performance and Low Memory Requirements. Serving and detection of malicious attacks against networks was mentioned in this paper (Lee & Huang, 2013). The pattern-matching architecture with high throughput performance and low memory requirements.

Armstrong, Korah, and Salivahanan (2018) presented an Efficient String Matching FPGA for Speed Up Network Intrusion Detection. In this paper, the authors had discussed about the efficiency of IDS using FPGA that designed by string- matching system. The proposed system can maintain throughput of 19.2 Gbps with performance in terms of Performance Efficiency Metric (PEM). In this paper Armstrong *et al.* (2018) discussed about the emerging new artificial intelligence technique which can be used in the real-life problems. They have also made an approach for user behavior modelling and presented the display results from the preliminary testing needed for their project. Zhang *et al.* (2001) presented a Hide: A Hierarchical Network IDS. In this paper, Zhang *et al.* (2001), described about the architecture of their system i.e., Hierarchical Network Intrusion Detection System. They had also briefed the contents about statistical pre-processing techniques and components.


https://doi.org/10.17993/3ctecno.2021.specialissue8.53-69

Jyothi, Addepalli and Karri (2018) presented a DPFEE: a High Performance Scalable Pre-Processor for Network Security Systems. In this paper, the authors, had discussed about the Deep Packet Field Extraction Engine (DPFEE) for application layer field extraction to software. It also Provides software acceleration for field extraction and operates at their maximum efficiency. Sadhasivan and Balasubramanian (2017) presented a Novel LWCSO-PKM Based Feature Automation and Classification of Attack Types in SCADA Network. In this paper the authors had explained about the Linear Weighted CSK Optimization (LWCSO) algorithm which is used to achieve better performance than the existing classification techniques and Intrusion Detection System algorithms (Sadhasivan & Balasubramanian, 2017a). This also helped a lot for our project in detecting Intrusions that more often affects the network systems.

## 2. LITERATURE SURVEY

An Intrusion Detection System (IDS) is a device or software application that monitors a networks or systems for malicious activity or policy violations. Any malicious activity or violations are typically reported either to an administrator or collected centrally using a security information and event management (SIEM) system (Roesch, 1999). In the past years, there are no techniques available for the detection of Intrusion occurring in a system or engine since 1984 (Lee & Huang, 2013). Between 1984 and 1986, Dorothy and Denning and Peter Neuman researched and developed the primary model of the Intrusion Detection System. This image was named as Intrusion Detection Expert System (IDES). This ady was at first rule primarily based expert system trained to discovered the malicious activity (Armstrong *et al.*, 2018).

In 2017, under the title "Big Data Analytics for Network Intrusion Detection" Randy Jones bought a conclusion for the problem of investigating the progressive of strategies techniques in network intrusion detection. His conclusion is that cleaning and querying information with incomplete creaky records (Zhang *et al.*, 2001). In 2016, Martin Roesch (1999) has revealed a paper on the title "SNORT- Light-weight Intrusion Detection for Networks". Within the paper he designed Snort to fulfill the necessities of a prototypic light-weight network intrusion detection system that may be an answer for the matter of finding


https://doi.org/10.17993/3ctecno.2021.specialissue8.53-69

totally different applications wherever it is terribly helpful as a component of an integrated network security infrastructure.

For the purpose of achieving high throughput performance and low memory requirements by helping and detecting malicious attacks against networks by Lee and Huang (2013).

## 3. BLOCK DIAGRAM

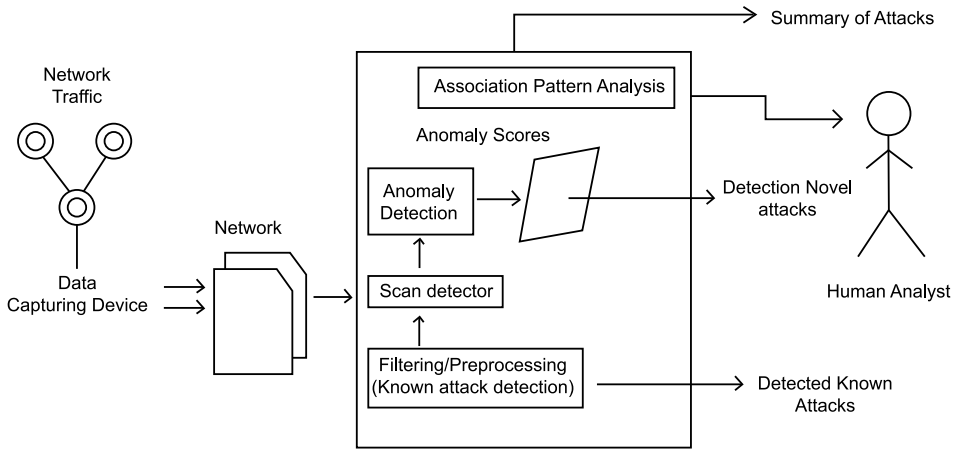


**Figure 1.** Block Diagram of Intrusion Detection Systems.
**Source:** own elaboration.

Anomaly detection is needed to scan the attackers which will intrude the network. It is needed because nowadays the network traffic was very high which is having many possibilities of assaulting the data's which are valuable. Hence the network intrusion system is very important for analyzing the attackers such as Harmful viruses etc. The above diagram Figure 1 explains the IDS system which will works to safeguard the data's present in the network.

## 4. DESCRIPTION

We begin by providing a general summary of the system, followed by the presentation of the design wherever we tend to detail every part. The proposed system of our work is explained here with the steps involved in the Intrusion Detection System to safeguard the Data. The Steps involved are Preprocessing, DOS analysis with respective classification and clustering methods.


https://doi.org/10.17993/3ctecno.2021.specialissue8.53-69

## 4.1. PRE-PROCESSING

Pre-processing may be a data mining technique that involves remodeling raw information into a comprehensible format. Real world information is commonly incomplete, inconsistent, or lacking in sure behaviors or trends and is probably going to contain several errors. Pre-processing may be a verified methodology of partitioning such problems. Pre-processing prepares raw information for any processing. The normal data pre-processing methodology is reacting because it starts with data that's assumed prepared for analysis and there's no feedback and impact for the manner of data assortment. The information inconsistency between data sets is that the main issue for pre-processing.

The Major task of pre-processing are:

- Data Cleaning: may be a method of fill in missing values, smoothing the noisy data, establish or take away outliers and resolve inconsistencies.
- Data Integration: Integration of multiple data bases, data cubes or files.
- Data Transformation: is a task of data standardization and aggregation.
- Data Reduction: Data reduction is that the method of reduced illustrations in volume however produces the identical or similar analytical results.
- Data Discretization: It may be a part of data reduction however with explicit importance, particularly for numerical information.
- Segmentation: may be a method dividing the market of potential customers into totally different teams and segments on the idea of sure characteristics. Segmentation suggests that to divide the market place into components, or segments that are determinable, accessible and profitable and have a growth potential.
- Feature extraction: may be a transformation of the computer file into a group of options that are distinctive properties of input pattern that helps in differentiating between the classes of input pattern. It's the method of etymologizing new options from the initial features so as to scale back price of feature mensuration, increase classifier potency, and permit higher classification accuracy. Remodeling the computer file into the set of options is named feature extraction. If the feature


https://doi.org/10.17993/3ctecno.2021.specialissue8.53-69

extractors are rigorously chosen it's expected that the feature set can perform the required task victimization the reduced illustration rather than full size input. Feature extraction refers to extraction of linguistic item from the documents to produce a sample distribution of their content. This can be the method by that a brand-new set of discriminative options is obtained from those accessible new set of features. This can be a method of reducing information by measure of sure or options. These options are employed in a classifier. Once the information is simply too massive to be processed, the information is remodeled into a reduced illustration set of options. The methods of choosing a set of variables that's to be employed in the development of the feature vector. It's spatiality reduction method, wherever associate degree initial set of raw variables is reduced to lot of manageable teams for process. Classification of intrusions is based on:

- Location.
- Functionality.
- Deployment approach.
- Detection mechanism.

## 4.2. DENIAL OF SERVICE (DOS)

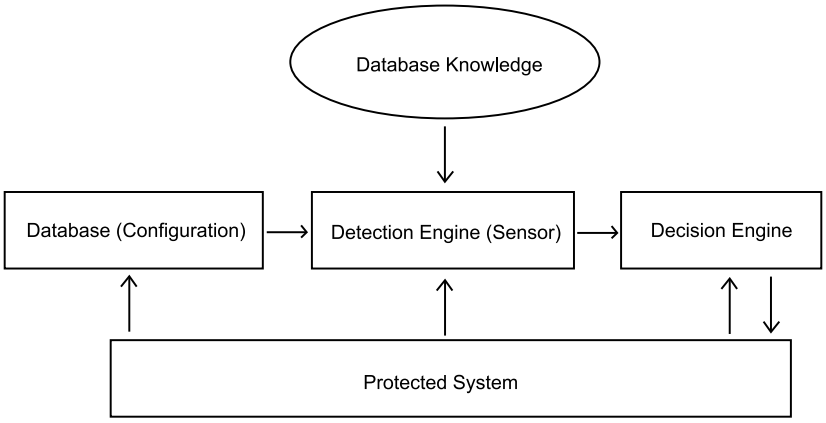


**Figure 2.** Denial of Service.
**Source:** own elaboration.

The above Figure 2 describes a DOS attack. It's associate degree attack within which the attacker floods a computing or memory resource with false request so it is unable to function


https://doi.org/10.17993/3ctecno.2021.specialissue8.53-69

as the legitimate request and therefore denying users access to the service. Probing is an attack with the goal of gaining the configuration of the target machine or network.

User to Route (U2R): These attacks have the goal of gaining body access to the machine within which the attacker encompasses a user level access.

Remote to Local (R2L): R2L is an attack within which the user sends packet to a machine over web which the user doesn't have access to so as to show the vulnerabilities and exploit privileges which a neighborhood user would wear a pc. Performance Analysis: It is a measure of the success or failure of a project using various parameters. It helps in developing a positive culture of project management that yields excellent results.

A good program performance typically needs: proper management of stack holders, Performance Analysis may be method of examination actual project value and schedule performance to the performance activity baseline for the aim of analyzing this standing of a project. Intrusion Detection System: An intrusion detection system (IDS) is utilized to make security experts mindful to bundles coming and takeoff a checked system. IDSs are ordinarily acclimated smell out system bundles, in this manner giving an OK comprehension of what's very occurring on the system. An IDS depends on either equipment or code, any place approaching and cordial individuals and additionally system traffic are tuned in to, and can possibly notice and report any evidence of assaults.

The common activities of IDS code will be named pursues:

- Monitoring whole or potentially fractional packets.
- Detecting suspicious exercises.
- Recording required occasions and making refreshes the system manager.

The specialized IDS mechanism is predicted on however, wherever and what it detects, together with obligatory necessities. In particular, IDSs should be bolstered flexible and ascendible system parts to oblige the powerful increment in the present system situations. They should give simple give direct administration and operational systems and ventures as opposed to confusing basic undertakings, and that they should give simple ID components. Intrusion Detection System (IDSs) can be classified into 3 types: a Network-Based Intrusion Detection System (NIDS) and a Host-Based Intrusion Detection System


https://doi.org/10.17993/3ctecno.2021.specialissue8.53-69

(HIDS), and a Hybrid-Based Intrusion Detection System (hybrid IDS) associate an HIDS detects malicious activities on a one personal computer whereas an NIDS distinguishes interruption by recognition numerous hosts and looking at system traffic. IDS technologies like HIDS, NIDS are used along to correlate information from every device and create choices consistent with what these IDSs monitors.

IDS are classified into 3 primary sorts: network-based, host-based and hybrid. Network-based IDSs: Network-based IDSs (NIDSs) have become a vital element of an associate organization's security solution. Associate NIDS is equipped for location a wide fluctuate of noxious and undesirable assaults happening in an application, system and transport layers, together with unforeseen administrations bolstered on various applications. Moreover, NIDSs can find and screen system traffic and secure PC frameworks from system based dangers while not arrange approach infringement.

NIDS are normally incapable to execute whole system bundles, which winds up in fragmented investigations and in this way considerable postponements in fast and high-load conditions.

It is currently normal to check NIDSs in rapid frameworks with massive accounts of information, however they're not able amend pernicious exercises and dangers. NIDS are effective and helpful in dominant malevolent activity and intimidations underneath environments wherever traffic is consistently upward. NIDSs are additionally divided into software or hardware-based. It's conjointly ascertained software-based NIDSs still need improvement for a network with a high capacity of high-speed knowledge, however they're helpful for little networks. However, one in all foremost robust and common ASCII text file NIDS is Snort. Host-based IDSs: Host-based IDSs (HIDSs are authorized to viewed alleged occasions occurring in home-grown host machines.

HIDS are adaptable because of their installation over servers, workstations and notebooks, as compared to NIDS. Additionally, HIDSs can watch malevolent networks and multiple actions happening isolated the endangered host. An HIDS stays located next to the tip purpose of an electronic network that has anti-threat applications like spyware detection, firewalls and antivirus software system plans, which give access to outdoor backgrounds like the Web. It's going to battle with present security policies of firewalls and operational


https://doi.org/10.17993/3ctecno.2021.specialissue8.53-69

schemes. It cannot simply investigate intrusion trials on several CPUs. It will be terribly troublesome to keep-up in massive networks with totally diverse operative systems and arrangements.

It will be restricted by assailants once the system is negotiated. Hybrid-based IDSs: In around things, HIDSs and NIDSs could incapable to accomplish the necessities aimed at intrusion detection as a result of somebody sort of IDS has each essential merits and faults. Consequently, a mix of an HIDS and a NIDS is thought as a Hybrid IDSs. Snort Summary: Snort is handy freed from price besides is stratified between the highest systems obtainable todays through the simplest options. It's discharged as an ASCII text file NIDS supported a rule-based IDS, that provisions data in text files, such text files will be changed by a text editor. Rules remain classified into categories wherever the principles that belong towards every class are hold on as information in isolated files; such records are then combined to the main configuration folder. The information is seized in standings supported on delineated rules, that are browse at the data configuring of the Snort.

Snort part roles: A Snort-based NIDSs incorporates the subsequent of the resulting foremost components:

- Packet Decoder.
- Pre-processors
- Detection Engine.
- Work and Alerting System and
- Output Modules.

Snort will drop few packets as a result of it runs in real time if the maneuver is in NIDS method with significant and high-volume traffic flow. This system employments the Snort instruction to sight the intrusion action to remain bestowed within the information packet. The Snort rule can read the chains which need to be matched against all packets.


https://doi.org/10.17993/3ctecno.2021.specialissue8.53-69

# 5. EXPERIMENTAL RESULTS AND DISCUSSION

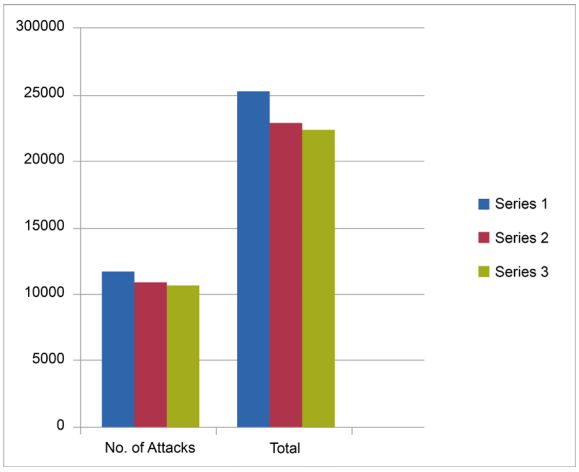


**Figure 3.** Graph representing no. of attacks and total datas.
**Source:** own elaboration.

The above Figure 3 shows the graph representing number of attacks and total datas. The graph is plotted between the number of attacks and total. The blue colour represents the number of attacks and the total of the first normal record. The red colour represents the number of attacks and the total of the second normal record. The green colour represents the number of attacks and the total of the third normal record.

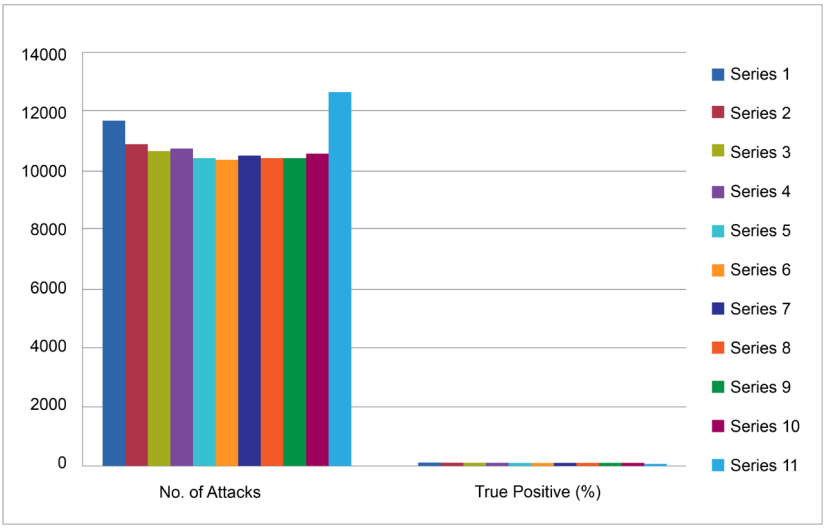


**Figure 4.** Graph representing no. of attacks and true positive %.
**Source:** own elaboration.

The above Figure 4 represents the graph of number of attacks and true positive


https://doi.org/10.17993/3ctecno.2021.specialissue8.53-69

percentage. The graph is plotted against number of attacks to true negative percentage of the intrusion. The colour variations show the corresponding attack and its true negative percentage.

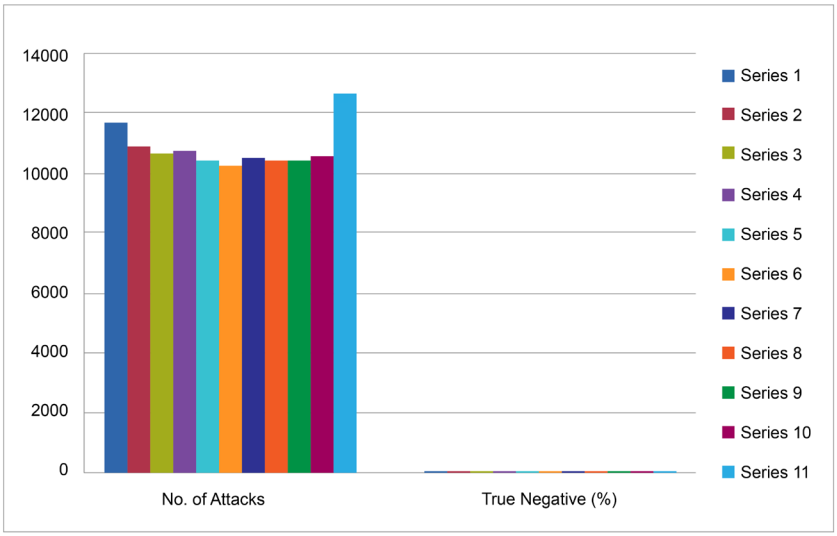


**Figure 5.** Graph representing no. of attacks and True negative %.
**Source:** own elaboration.

The above Figure 5 represents the graph of number of attacks and true negative percentage. The graph is plotted against number of attacks to true positive percentage of the intrusion. The colour variations show the corresponding attack and its true positive percentage.

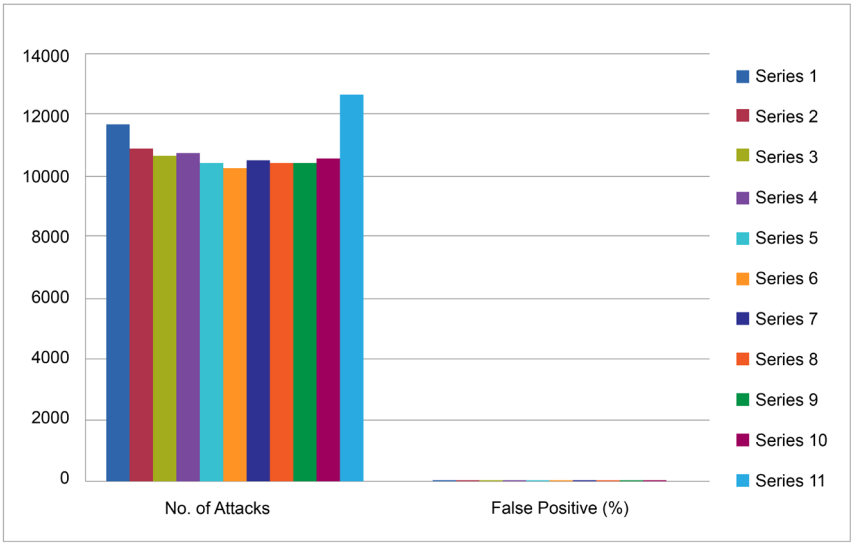


**Figure 6.** Graph representing no. of attacks and False positive %.
**Source:** own elaboration.


https://doi.org/10.17993/3ctecno.2021.specialissue8.53-69

The above Figure 6 represents the graph of number of attacks and false positive percentage. The graph is plotted against number of attacks to false positive percentage of the intrusion. The colour variations show the corresponding attack and its false positive percentage.

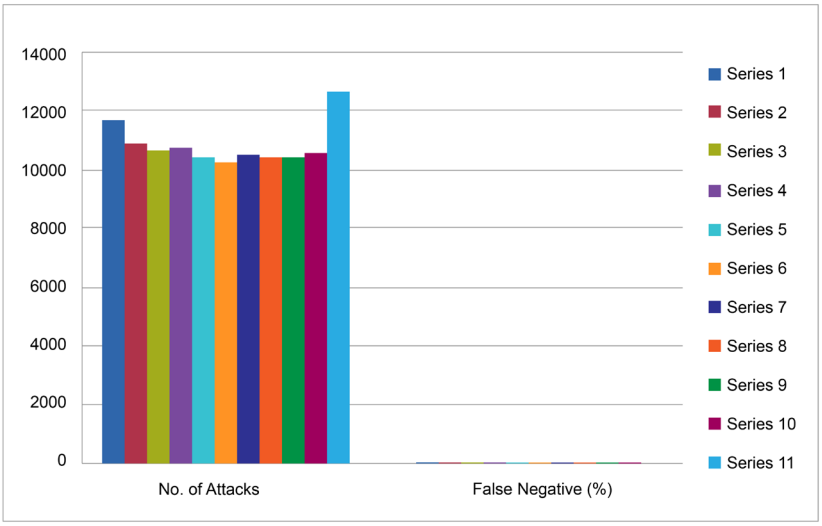


**Figure 7.** Graph representing no. of attacks and false negative %.
**Source:** own elaboration.

The above Figure 7 represents the graph of number of attacks and false negative percentage. The graph is plotted against number of attacks to false negative percentage of the intrusion. The colour variations show the corresponding attack and its false negative percentage.

## 6. CONCLUSIONS

We have considered a most recent dataset KDD set for detailed analysis keeping in view its increasing demand in the research community. Various shortcomings of the dataset have been studied and outlined. Solutions to counter such issues, has also been provided. We tried to solve such issues through experiment. We also re-label the dataset with the labeling information provided by Canadian Institute of Cyber security. Moreover, we have also seen a major issue of class imbalance has been reduced by such class relabeling. As a future work the dataset can be class wise resampled to generate two or more training and testing samples set separately to be used by research community. Snort was designed to fulfill the wants of a prototypal a light weight network intrusion detection system, it became a tiny


https://doi.org/10.17993/3ctecno.2021.specialissue8.53-69

low, flexible and extremely capable system that's in use round the world on each giant and tiny network.

## ACKNOWLEDGEMENT

We thank the Department of Electronics and Communication Engineering, School of Electronics and Electrical Technology of Kalasalingam Academy of Research and Education, Tamil Nadu, India for permitting to use the computational facilities available in Centre for Research in Signal Processing and VLSI Design which was setup with the support of the Department of Science and Technology (DST), New Delhi under FIST Program.

## REFERENCES

**Armstrong, J., Korah, R., & Salivahanan, S.** (2018). Efficient String Matching FPGA for speed up Network Intrusion Detection. *Applied Mathematic & Information Sciences, 12*(2), 397-404. http://www.naturalspublishing.com/files/published/u40jti0ukf6096.pdf

**Dhanalakshmi, K. S., & Kannapiran, B.** (2017). Analysis of KDD CUP Dataset Using Multi-Agent Methodology with Effective Fuzzy Based Intrusion Detection System. *Journal of Applied Security Research, 12*(3), 424-439. https://doi.org/10.1080/19361610.2017.1315760

**Jyothi, V., Addepalli, S. K., & Karri, R.** (2018). DPFEE: A high performance scalable pre- processor for network security systems. *IEEE Transactions on Multi-Scale Computing Systems, 4*(1), 55-68. https://ieeexplore.ieee.org/document/8078262

**Kabiri, P., & Ghorbani, A. A.** (2005). Research on intrusion detection and response: A survey. *IJ Network Security, 1*(2), 84-102. https://www.researchgate.net/publication/45681663_Research_on_Intrusion_Detection_and_Response_A_Survey

**Lee, T.-H., & Huang, N.-L.** (2013). A pattern-matching scheme with high throughput performance and low memory requirement. In *IEEE/ACM Transactions on Networking*


https://doi.org/10.17993/3ctecno.2021.specialissue8.53-69

*(TON), 21*(4), 1104-1116. https://cial.csie.ncku.edu.tw/presentation/group_pdf/(TON)%20A%20Pattern-Matching%20Scheme%20With%20H.pdf

**Roesch, M.** (1999). Snort-Lightweight intrusion detection for network. *Proceedings of the 13th System Administration Conference.* Seattle: USENIX Association. Vol. 238. https://www.semanticscholar.org/paper/Snort%3A-Lightweight-Intrusion-Detection-for-Networks-Roesch/363d109c3f00026f9ef904dd8cc3c935ee463b65

**Sadhasivan, D. K., & Balasubramanian, K.** (2017a). A fusion of multiagent functionalities for effective intrusion detection system. *Security and Communication Networks. Article ID 6216078*. https://doi.org/10.1155/2017/6216078

**Sadhasivan, D. K., & Balasubramanian, K.** (2017b). A novel LWCSO-PKM-based feature optimization and classification of attack types in SCADA network. *Arabian Journal for Science and Engineering, 42*(8), 3435-3449. https://doi.org/10.1007/s13369-017-2524-0

**Wang, L., & Jones, R.** (2018). Big Data Analytics of Network Traffic and Attacks. In *IEEE National Aerospace and Electronics Conference (NAECON)*, pp. 117-123. https://ieeexplore.ieee.org/document/8556802

**Wang, W., Liu, J., Pitsilis, G., & Zhang, X.** (2018). Abstracting massive data for lightweight intrusion detection in computer networks. *Information Sciences, 433-434,* 417-430. https://www.semanticscholar.org/paper/Abstracting-massive-data-for-lightweight-intrusion-Wang-Liu/6ee2cffa04c7ab2121c52734bf5238113ec6f9e0

**Zhang, Z., Li, J., Manikopoulos, C. N., Jorgenson, J., & Ucles, J.** (2001). HIDE: a hierarchical network intrusion detection system using statistical preprocessing and neural network classification. *Proceedings of the IEEE Workshop on Information Assurance and Security.* http://citeseerx.ist.psu.edu/viewdoc/download?doi=10.1.1.67.857&rep=rep1&type=pdf


https://doi.org/10.17993/3ctecno.2021.specialissue8.53-69

https://doi.org/10.17993/3ctecno.2021.specialissue8.53-69

# /05/


https://doi.org/10.17993/3ctecno.2021.specialissue8

# A NON-INTRUSIVE METHOD FOR DRIVER DROWSINESS DETECTION USING FACIAL LANDMARKS

**Sivakumar Pothiraj**
Professor, ECE Department, Kalasalingam Academy of Research and Education (Deemed to be University). Krishnankoil, (India).
E-mail: siva@klu.ac.in
ORCID: https://orcid.org/0000-0003-1328-8093

**Rampranav Vadlamani**
Student, ECE Department, Kalasalingam Academy of Research and Education (Deemed to be University). Krishnankoil, (India).
E-mail: vrampranav9@gmail.com
ORCID: https://orcid.org/0000-0001-9270-6884

**Bonthu Pavan Kumar Reddy**
Student, ECE Department, Kalasalingam Academy of Research and Education (Deemed to be University). Krishnankoil, (India).
E-mail: vrampranav9@gmail.com
ORCID: https://orcid.org/0000-0003-1718-040X

**Recepción:** 16/10/2019 **Aceptación:** 14/10/2020 **Publicación:** 30/11/2021

**Citación sugerida:**
Pothiraj, S., Vadlamani, R., y Reddy, B. P. K. (2021). A non-intrusive method for driver drowsiness detection using facial landmarks. *3C Tecnología. Glosas de innovación aplicadas a la pyme, Edición Especial*, (noviembre, 2021), 71-85. https://doi.org/10.17993/3ctecno.2021.specialissue8.71-85

## ABSTRACT

Driver weariness is one of the real reasons behind accidents. Recognizing the sleepiness of the driver is one of the best methods for estimating driver weariness. The motivation behind this paper is to build up a drowsiness detection system that works by monitoring the eye movement of the driver and alerting the driver by producing an alarm or vibration when the person is found drowsy. This paper shows a non-intrusive model for the fatigue detection dependent on processing video streams of an individual's face. The proposed model is not quite the same as meddlesome techniques dependent on natural methodology (Electroencephalogram, Electrooculogram and some sensors), which require gadgets explicitly. Unlike traditional image processing techniques, we use computer vision and machine learning technique to display a prototypal adaptation of a real-time system with individual feedback to monitor and identify when the driver may be sleepy directly from a web camera. The drowsiness detection model depends on face alignment and then evaluation of the Eye Aspect Ratio (EAR) which uses Histogram of oriented gradient (HOG) features combined with Support Vector Machine (SVM) classifier for blink detection. Utilizing such a system, it is conceivable to alarm the client of the threat of nodding off, so that enough actions can be made, diminishing the risk of human mistake and avoiding accidents.

## KEYWORDS

Non-Intrusive Method, Facial Landmarks, Support Vector Machine, Eye Aspect Ratio (EAR).


https://doi.org/10.17993/3ctecno.2021.specialissue8.71-85

# 1. INTRODUCTION

Drowsiness is an automatic human physical movement. Since tiredness can be specifically identified with the human fixation and liveliness, drowsiness identification has been connected in fields like in human behaviour investigation, fatigue detection, readiness level estimation and so on. When the driver experiences drowsiness state, he starts losing the control and he might be suddenly deviated from the road and may hit an obstacle or another car. Driver weariness is one of the critical factors in many auto collisions. Safe driving is a noteworthy worry of social orders everywhere throughout the world. A huge number of individuals are seriously harmed because of drivers nodding off at the wheels every year. According to the poll conducted by the National Sleep Foundation's Sleep, 60% of people have fallen sleepy while driving. However, many people cannot tell whether they are about to fall asleep or not. 30% of car crashes have been brought about by drowsiness alone.

The signs of the driver drowsiness are:

- Hard to focus, frequent blinking.
- Continuous Yawning
- Daydreaming; wandering/disconnected thoughts
- Difficulty in keeping his head up
- Might be feeling of restless.

Various techniques have been proposed for fatigue/drowsiness detection. These techniques are based on Image Processing, Electroencephalograph, Electrooculogram, Electrocardiogram, and artificial neural network. The image processing-based techniques are divided into three categories. These categories are matching of a template technique, detecting of an eye blink, the technique based on yawning, identifying the pose of the head. The techniques to measure drowsiness are classified into two types.

- Intrusive Techniques.
- Non- Intrusive Techniques.

Intrusive techniques require the use of some explicit gadgets which always require some measuring gadgets to be in contact with human body which causes some sort of disturbance to the person so these are often referred to as contact type method (Electroencephalogram,


https://doi.org/10.17993/3ctecno.2021.specialissue8.71-85

Electrooculogram), whereas in Nonintrusive techniques there is no need of such devices which require contact and it requires high-quality cameras for capturing images or monitoring the video stream, it is also known as contactless method.

In this paper, we propose a system for drowsiness detection which uses computer vision techniques which uses a machine learning library. Object recognition, tracking is a standout amongst the most created research spaces in the field of image processing and computer vision. It is used in several useful applications in all the available domains like video-stream analysis, industrial automation, internet of things, robotics, security and surveillance, and in many more applications. The similar idea is used to detect the human body to identify eye, mouth, arms and recognizing its shape and movement, making a diagnosis and deriving human behavior. There are many algorithms for blink detection which are trained on a wild dataset.

In the proposed system, we monitor the driver continuously and intimate the driver about the drowsiness when the specified conditions are met. We use facial landmarks technique which identifies the face region. The algorithm behind the facial landmarks is the Histogram of oriented gradients combined with support vector machine classifier. The detector we use is a pre-trained model trained on HELEN dataset. A threshold value of eye aspect ratio will be kept. The person is monitored continuously, and the eye aspect ratio is evaluated each time and compared with the threshold value to decide whether the state of the eye is open or not. It will be implemented using OpenCV in Python.

## 2. RELATED WORKS

Yan *et al.* (2016) proposed a model for real-time drowsiness detection depending on PERCLOS evaluation and grayscale image processing to identify whether the driver is sleepy or not. Their algorithm was comprised of three steps. First, it identifies the position of the face of the driver and converts them into grey-scale images, and then the position of eyes is localized using a small template. Secondly, the data obtained in the first step is used to establish a drowsiness model and at last, depending on the individual drowsiness model the developed system monitors the driver's state without interruption. Once the driver is found to have sleepiness state, an alarm is produced to alert the driver.


https://doi.org/10.17993/3ctecno.2021.specialissue8.71-85

Leo and Sankar (2015) used Haar based cascade classifier for identification of eyes and the Histogram oriented gradients with Support vector machines for the detection of blink. When the eye blinks were detected the PERCLOS value for the eyes was calculated. If the computed value is beyond six seconds, it classifies the person as drowsy. First, the driver's face is monitored through a camera and then Viola and Jones's method was used to identifying the face of the driver. Once the face is identified the Haar features are extracted and then the blink detection algorithm is used to determine the blink in the video stream and then the PERCLOS is evaluated.

According to Amin and Rahmati (2011), the developed system acquires the images in a sequence and given as input in the first step. The system follows 4 steps: Detection of the face, extraction of facial components, tracking of facial components and detection of drowsiness. In that system, the background subtraction method is used to detect the face region in the image and this step is repeated until the face region is obtained accurately. The facial components like eyes, eyebrows and mouth region are extracted. The method used in the second step is Horizontal projection and template matching. The results obtained in the third step is matched with the reference template for tracking. Using the reference template, the person can be identified as feeling sleepy or not.

## 3. METHODOLOGY

This paper presents an algorithm to precisely estimate the position of eyes using facial landmarks in a computationally efficient way. Our proposed model has 4 phases.

- Monitoring for the face in a video stream.
- Applying Facial Landmarks.
- Evaluating the eye aspect ratio (EAR).
- Drowsiness detection.

Unlike some traditional image processing techniques for extracting eye regions or to detect blinks, which typically involves the following processes:

(1) Face Detection (2) Eye Localization (3) Localizing the white eye region (4) Identifying whether the white region disappears for a certain time which indicates the blink of an eye


https://doi.org/10.17993/3ctecno.2021.specialissue8.71-85

(5) Evaluate some parameters related to detect the state of an eye(open or close). Using these methods, the output can be achieved but the result may vary when there is a head movement, or any facial expression variation is noticed.

Our goal is to detect the eyes using a shape prediction technique. The machine learning library 'dlib' has the facial landmark detector which has been trained based on HELEN dataset. The algorithm behind this detector is the combination of Histogram of oriented gradients (HOG) and Support Vector Machines classifier.

A. Histogram of oriented gradients

The functions we use from dlib library has been trained based on the HOG algorithm. HOG is a feature descriptor which is a portrayal of an image that simplifies the image by removing unnecessary information and extracting useful information The feature vector generated by the algorithms is given into an image classification algorithm like Support Vector Machine (SVM) to generate accurate outcomes.

In the HOG feature descriptor, the directions of gradients distribution are used as features. Gradients values are mapped to 0-255. Pixels with large negative change will be black, pixels with large positive change will be white, and pixels with little or no change will be gray.

B. Facial Landmarks

Dlib is a landmark's facial detector with pretrained models. It has two types of models. They are

- 5-point landmark detector.
- 68-point landmark detector.


https://doi.org/10.17993/3ctecno.2021.specialissue8.71-85


**Figure 1.** 5-point detector.
**Source:** own elaboration.

The 5-point detector localizes:

- 2 points for the left eye.
- 2 points for the right eye.
- 1 point on the nose.

Whereas the 68-point detector localizes regions along the eyes, eyebrows, nose, mouth and jawline.


**Figure 2.** 68-point detector.
**Source:** own elaboration.

In terms of speed, the 5-point detector is 8-10% faster than the 68-point detector and it also consumes 10 times less memory. So, the 5-point detector is fast and the most appropriate use of 5-point detector is the face alignment.

But for our proposed work since we need to compute eye aspect ratio, if we use 5-point detector we cannot evaluate the eye aspect ratio as there were no vertical points for eye


https://doi.org/10.17993/3ctecno.2021.specialissue8.71-85

region so we are using the 68 point detector where we have six points per eye and the eye aspect ratio can be computed easily to produces the accurate results.

C. Computing Eye Aspect Ratio

The Eye Aspect Ratio is an estimate of the eye-opening state. If the computed Eye Aspect Ratio value is lower than a threshold value, we could tell that the person's eyes are closed. The indexes of the eyes are taken into consideration to compute the eye aspect ratio value.

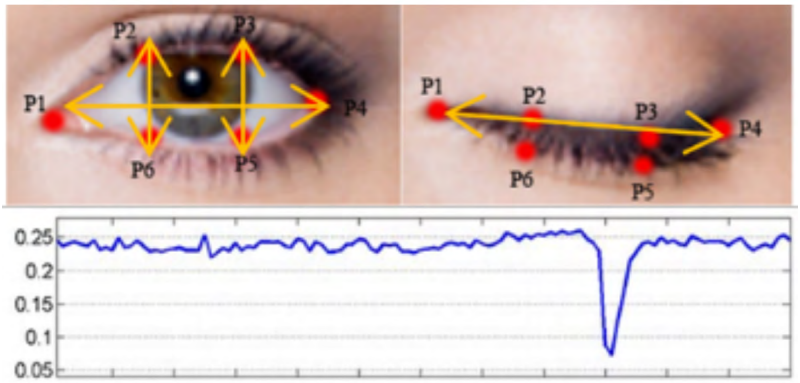


**Figure 3.** Eye aspect Ratio.
**Source:** own elaboration.

The numerator of the EAR equation calculates the distance between the vertical eye landmarks while the denominator calculates the distance between horizontal eye landmarks. When the eye is detected open the EAR value is almost constant and when the eye is closed (blink) the EAR suddenly drops to zero.

$$\mathrm{EAR} = \frac{\|p_2 - p_6\| + \|p_3 - p_5\|}{2\|p_1 - p_4\|}$$

We can use this simple equation to avoid image processing techniques and the blinking detection simply depends on the ratio of vertical and horizontal eye landmark distances. We use SciPy package to compute the Euclidean distance between eye facial landmarks We also include play sound library so that a suitable alert can be produced when the EAR value is below a threshold value.


https://doi.org/10.17993/3ctecno.2021.specialissue8.71-85

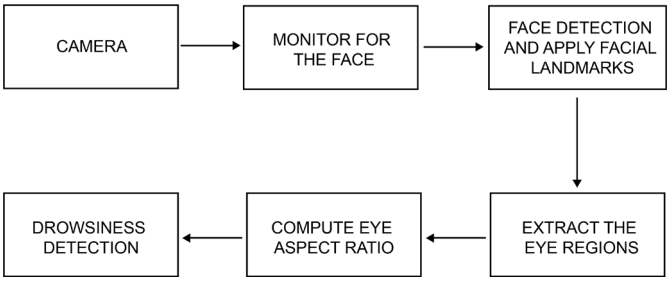


**Figure 4.** Block Diagram of Drowsiness detection system.
**Source:** own elaboration.

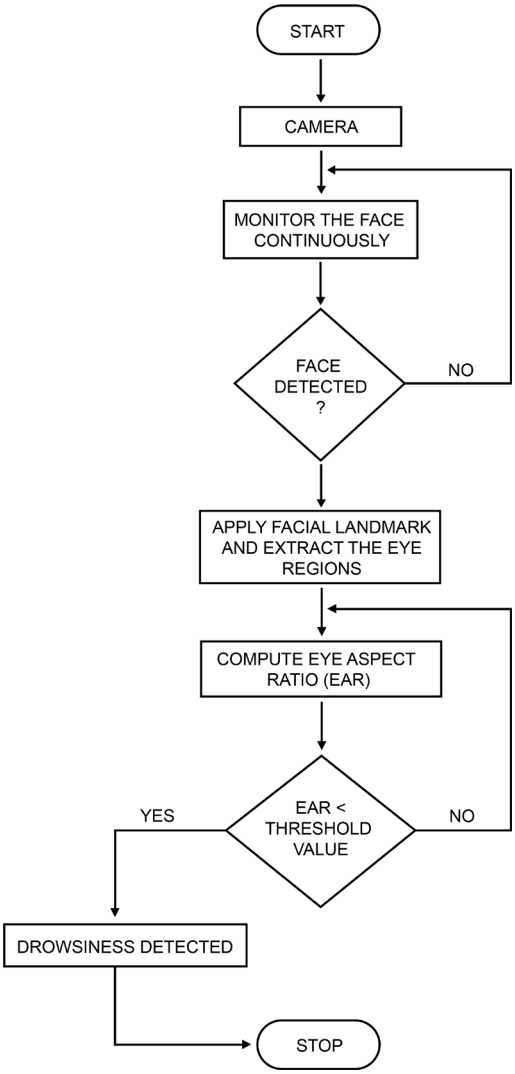


**Figure 5.** Flowchart of our system.
**Source:** own elaboration.


https://doi.org/10.17993/3ctecno.2021.specialissue8.71-85

# 4. RESULTS

The face of the driver was monitored continuously, and the landmarks were applied when the face was found. Even if there is a tilt in the head movement the detector was able to identify the eye regions if the face was in the scope of the camera. Once the eye regions are obtained the eye aspect ratio is evaluated. The threshold we kept is 0.28 as it would be more approximate value for almost 70% of the people. And when the eye aspect ratio computed was found to be below the threshold value then an alarm was produced. And if the EAR value is above the threshold value then the EAR would be continuously monitored until we turn off the device. We observed that the CNN based detector works well for non-frontal faces at odd angles where HOG based detector struggles.

Unfortunately, CNN based detector is computationally heavy and is not suitable for real-time video now. We use HOG detector as it is highly efficient and there is no need of detecting any faces at odd angles. When the face is detected the facial landmarks will be applied and eye regions will be extracted and to make it visible, we applied draw Contour method. The indexes of the eye are sent to the eye aspect ratio method and computed for each eye and prints the average value. The output shows the EAR value obtained.

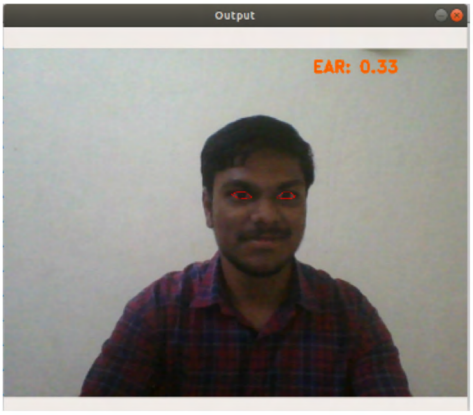


**Figure 6.** EAR Output.
**Source:** own elaboration.


https://doi.org/10.17993/3ctecno.2021.specialissue8.71-85


**Figure 7.** Drowsiness Detected.
**Source:** own elaboration.

```
EAR =  0.1515151515151515
Drowsiness Detected
EAR =  0.19637411189775061
Drowsiness Detected
EAR =  0.2505931158125547
Drowsiness Detected
EAR =  0.2781769974983058
Drowsiness Detected
```

**Figure 8.** EAR Values.
**Source:** own elaboration.

When the eye aspect ratio computed is below the threshold value i.e. 0.28 and it lasts for 40 consecutive frames then drowsiness will be detected, and this process will be repeated continuously.

## 5. CONCLUSIONS

In this paper, a non-intrusive method for drowsiness detection was implemented using detector from dlib library and OpenCV in Python. The predictor we used is a 68-landmark predictor. The person will be monitored continuously and when detected the landmarks will be applied and EAR value is evaluated and then compared that with the threshold value. The proposed approach uses Eye Aspect Ratio and Eye Closure Ratio with adaptive thresholding to detect driver's drowsiness in real-time. This is useful in situations when the drivers are used to arduous workload and drive unceasingly for long distances. The system,


https://doi.org/10.17993/3ctecno.2021.specialissue8.71-85

if integrated, can reduce the number of fatalities and harms that happen regularly due to these drowsy states of the drivers.

The developed system works well under the daylight conditions and in any resolutions. If the device should be used under dark conditions as well, then we can implement the system using night vision cameras. This makes the system suitable to work in any conditions.

## ACKNOWLEDGEMENT

Authors want to express their gratitude to ECE Department at Kalasalingam Academy of Research and Education for allowing them to utilize the computing facilities in DST-FIST sponsored VLSI Research Laboratory.

## REFERENCES

**Amin, M., & Rahmati, M.** (2011). Driver drowsiness detection using face expression recognition. *IEEE International Conference on Signal and Image Processing Applications (ICSIPA), 12*(3), 337–341. https://doi.org/10.1109/ICSIPA.2011.6144162

**Anjali, K. U., Thampi, A. K., Vijayaraman, A., Francis, M. F., Jeffy, N., & Rajan, B. K.** (2016). Real-Time Nonintrusive Monitoring and Detection of Eye Blinking in view of Accident Prevention due to Drowsiness. In *International Conference on Circuit, Power and Computing Technologies (ICCPCT),* 102-104. https://doi.org/10.1109/ICCPCT.2016.7530224

**Divjak, M., & Bischof, H.** (2009). Eye Blink Based Fatigue Detection for Prevention of Computer Vision Syndrome. In *MVA2009 IAPR Conference on Machine Vision Applications,* 350–353.

**Ghods, V., Sohrabi, M. K., & Joulaeian, M.** (2017). Accurate Detection of Human Face Position in the Environmental Images using Gabor Wavelet Transformations. *Computing Conference,* 633–637. https://doi.org/10.1109/SAI.2017.8252162

**Goyal, K., Agarwal, K., & Kumar, R.** (2017). Face detection and tracking: Using OpenCV. In *International conference of Electronics, Communication and Aerospace Technology (ICECA)*. https://doi.org/10.1109/ICECA.2017.8203730

**Kazem, V., & Sullivan, J.** (2014). One-millisecond face alignment with an ensemble of regression trees. In *IEEE Computer Society Conference on Computer Vision and Pattern Recognition*, 1867–1874.

**Leo, P., & Sankar, D.** (2015). Detection of drowsiness based on HOG features and SVM classifiers. *Proceedings of the 2015 IEEE International Conference on Research in Computational Intelligence and Communication Networks (ICRCICN)*. https://doi.org/10.1109/ICRCICN.2015.7434232

**Mingxing, J., Hengyuan, X., & Fei, W.** (2012). Research on Driver's Face Detection and Position Method Based on Image Processing. In *24th Chinese Control and Decision Conference (CCDC)*, 196–202. https://doi.org/10.1109/CCDC.2012.6244315

**Owayjan1, M., Achkar, R., & Iskandar, M.** (2016). Face Detection with Expression Recognition using Artificial Neural Networks. In *3rd Middle East Conference on Biomedical Engineering (MECBME)*. https://doi.org/10.1109/MECBME.2016.7745421

**Pedregosa, F., Varoquaux, G., Gramfort, A., Michel, V., Thirion, B., Grisel, O., Blondel, M., Prettenhofer, P., Weiss, R., Dubourg, V., Vanderplas, J., Passos, A., Cournapeau, D., brucher, M., Perrot, M., & Duchesnay, É.** (2011). Scikit-learn: Machine learning in Python. *Journal of Machine Learning Research, 12*, 2826-2830. https://www.jmlr.org/papers/volume12/pedregosa11a/pedregosa11a.pdf

**Salehian, S., & Far, B.** (2007). Embedded Real-Time Blink Detection System for Driver Fatigue Monitoring. In *27th International Conference on Software Engineering and Knowledge Engineering*. https://doi.org/10.18293/SEKE2015-249

**Wazwaz, A. A., Herbawi, A. O., Teeti, M. J., & Hmeed, S. Y.** (2018). Raspberry Pi and Computers-Based Face Detection and Recognition System. In *4th International Conference on Computer and Technology Applications (ICCTA)*, 171–174. https://doi.org/10.1109/CATA.2018.8398677

**Yan, J.-J., Kuo, H.-H., Lin, Y.-F., & Liao, T.-L.** (2016). Real-Time Driver Drowsiness Detection System Based on PERCLOS and Grayscale Image Processing. *Proceedings of the 2016 International Symposium on Computer, Consumer and Control (IS3C)*, pp. 243-246. https://doi.org/10.1109/is3c.2016.72

https://doi.org/10.17993/3ctecno.2021.specialissue8.71-85

# /06/


https://doi.org/10.17993/3ctecno.2021.specialissue8

# ARDUINO BASED WIRELESS SENSOR NETWORK SYSTEMS FOR AGRICULTURE

**Kalpana Murugan**
Department of Electronics and Communication Engineering, School of Electronics and Electrical Technology, Kalasalingam Academy of Research and Education, Krishnankoil, Virudhunagar (Dt), (India).
E-mail: drmkalpanaece@gmail.com
ORCID: https://orcid.org/0000-0002-5121-0468

**R. Alaguselvi**
Department of Electronics and Communication Engineering, School of Electronics and Electrical Technology, Kalasalingam Academy of Research and Education, Krishnankoil, Virudhunagar (Dt), (India).
E-mail: alaguselvir3@gmail.com
ORCID: https://orcid.org/0000-0002-7909-549X

**Recepción:** 16/10/2019 **Aceptación:** 11/09/2020 **Publicación:** 30/11/2021

**Citación sugerida:**
Murugan, K., y Alaguselvi, R. (2021). Arduino based wireless sensor network systems for agriculture. *3C Tecnología. Glosas de innovación aplicadas a la pyme, Edición Especial,* (noviembre, 2021), 87-97. https://doi.org/10.17993/3ctecno.2021.specialissue8.87-97

## ABSTRACT

Now a day's agriculture is the most important significant role in the society for the last few decades. Farmers mainly depend upon the agriculture for their daily lively hood. Main aim of this work is to measure the various parameters of agriculture are soil moisture, temperature, humidity and gas. This work proposes a Smart TMHG Measurement System, to measure the values of Temperature, Moisture, Humidity and Gas. Initially soil moisture sensor, humidity sensors, gas sensor and water pump which is connected to arduino. These measured values are displayed in Liquid Crystal Display (LCD). After detecting soil moisture and Humidity level, dc pump will be on or off based on the measured value. Arduino module control the ON or OFF the motor pump using an embedded c program. This information will be send to the user with the help of Wireless Sensor Network (WSN) for taking remedial action. Smart TMHG Measurement System will make farmers to increase the crop for better yield and make them economically benefit. Smart TMHG Measurement System used to measure the parameters of soil moisture, temperature, humidity and gas in remote location by using wireless sensor network which will help the community of farmer on service based, to reduce the cost, rather than the other sources.

## KEYWORDS

Wireless Sensor Network, Soil moisture, Humidity, Temperature, Gas, Arduino Board, LCD display.


https://doi.org/10.17993/3ctecno.2021.specialissue8.87-97

# 1. INTRODUCTION

Water shortage is one of the major problems in world. Many different methods are incorporated for conservation of water. Water is essential for each and every field of crop, every human being, plants, animals etc., in an agriculture water place a vital role for yield crops. For cropping yield excess of water is given to the field, Wastage of water is a major problem in agriculture. So, a number of techniques are available to save or to control the wastage of water. Wireless sensor network (WSN) is a small, inexpensive, low power and distributed devices which are capable of local processing and wireless communications are used for various applications like environmental monitoring, habitat monitoring, seismic detection, health care, Industrial monitoring, home automation etc.

Ditch Irrigation is the old methodology, where ditches are dug out by us and seedlings are planted in horizontal manner aligned pattern. Water is made to move to different canals via siphon tubes. These are mainly used in olden days. The water can be saved by using this method. Water is given near the roots itself then the roots can observe the water how much it needed. Instead of allowing water around the tree or crops up to certain distance. Through this methodology water can be saved effectively.

It is a very tough process and also labor is more involved and investment will be high for laboring purpose. In this process the field is cut into the multiple steps and supported by keeping of walls while the plain areas are used for plantation and the idea is that the water runs down each step watering each column. If the user is in travelling, then this type of automatic irrigation method is helpful for sending water to the land automatically and stops sending water when the crop is not needed.

The work of Kim, Evans and Iversen (2008) represents real time monitoring and control of variable rate irrigation controller. The sensor nodes measure environmental parameter and transmit data to base station where base station process data through a user-friendly decision making program and all data commands send to irrigation control station.

Nandurkar, Thool and Thool (2014) represents the design of smart sprinkler system using mesh capable WSN for monitoring and control of field irrigation system. This system provides accuracy by controlling the soil moisture level between the thresholds. Sensor


https://doi.org/10.17993/3ctecno.2021.specialissue8.87-97

nodes send data to base station every time the timer variable overflows. Base station has an actuator interface to control solenoid valve using Graphical User Interface (GUI). Rinnovando group (Rgroup) is working with agriculture experts that concentrate on monitoring microclimate in tomato greenhouse proposed in Mancuso and Bustaffa (2006). The main goal of monitoring is to measure when the crop is on risk of developing and the farmer treat the field with fertilizer only when needed.

Thilagavathi (2013) proposed a WSN based system that provides online system to control and maintain the farm remotely by logging into a farming website. Cameras used to capture live videos of the farm. By using these videos, the user able to see the real condition of the farm and control the farm remotely from any part of the world.

Kodali and Muraleedhar (2015) represents the overall history of spices as black pepper, cardamom and clove in different states where these spices are cultivated and exporters of spices and the problem faced by farming community related to pest and irrigation. Indigenous design and development of Wireless Sensor and Actuator Network (WSAN) is proposed in Shaikh *et al.* (2010).

For better control of irrigation process in third world countries like Pakistan, it is necessary to develop cost effective hardware system. They design system using three components as sensor node to sense data, Actuator node for switching on/off of the connected actuator devices and sink nod for gathering data for decision- making.

Singh, Chyan and Sebastian (2010) represents the design of a system which takes soil samples when an event triggered with an outside event such as rain event. The system has variable sampling rates with interface to soil sensors and rain gauge. Wireless soil sensor network monitor an event of rain and soil moisture content. Such system consists of rain detection module and sensory module.

Martinelli *et al.* (2009) represents the use of WSN that provide real time data collected by sensor node. Each node collect data concerned with the voltage of the battery, internal voltage and current provided by solar panel and the temperature of the microcontroller to perform real time monitoring of the network stated. After measured data, the sensor board is switches off and RF sends the collected data over radio channel to sink node. Design of


https://doi.org/10.17993/3ctecno.2021.specialissue8.87-97

water saving irrigation control system based on WSN which is the combination of fuzzy logic and neural network. Fuzzy logic is a mathematic model and neural network that has self-learning ability to adapt changing environment. Fuzzy neural network is an integrated set of fuzzy logic reasoning ability and powerful self-learning ability of neural network. Sensor nodes measure soil moisture, temperature, humidity, light intensity and through LAN or WAN data transmitted to gateway node to upper machine and irrigation control system control electromagnetic valve to precision irrigation according to real time feedback information collected by measuring data.

## 2. RELATED WORK

Rani and Kamalesh (2014) represents the design of distributed control system of indoor wireless temperature and humidity to improve the overall performance of the system to detect change in the temperature and humidity. Design of an adaptive irrigation controller using WSN for monitoring the soil moisture status and controlling the irrigation program schedule is proposed in Shaikh *et al.* (2010).

Singh *et al.* (2010) proposes tree topology and cluster based multi-hop routing algorithm to reduce energy consumption while data transmission of nodes uses WSN for monitor and collect crop water requirements such as temperature, humidity, soil moisture and irrigation volume to build the machine learning model and data aggregation.

Design of an automated irrigation system using WSN including soil moisture sensor, air temperature sensor and air humidity sensor in order to collect environmental data and controlling the irrigation system is proposed in Ameer *et al.* (2015). By using smart phone, the irrigation system uses values to turn on/off the solenoid valve.

Wan (2012) analyses the use of Programmable System-On-Chip (PSoC) technology as a part of WSN to monitor and control various greenhouse parameter. The author discuss the problem faced by management server as like data, congestion and intercommunication between nodes. WSN based applications used with a specific protocol and system on chip-based hardware with programmable radio (Yao *et al.*, 2010). It combines sensors and actuators in a WSN for successful deployment of WSN for Precision Agriculture. To charge electrical devices, it used solar photovoltaic and rechargeable batteries.


https://doi.org/10.17993/3ctecno.2021.specialissue8.87-97

Zhang and Chang (2011) present the implementation of GPRS communication as a gateway between WSN and internet. Artificial immune systems connected to the internet by using GPRS. Various data transmission approaches are used to implement closed loop Irrigation system within Precision Agriculture. Closed loop irrigation system is used to apply correct amount of water in correct place at right time and save the natural resources.

In the work of Zhang and Chang (2011) the system is modeled in outdoor environment using Tiny OS based IRIS motes to measure the moisture level of the paddy field. Moisture sensors measure the soil moisture level. The system sets a threshold value; if the voltage exceeds that threshold then it represents the driest soil. This system has better visualization and monitoring GUI. In order to overcome all the above drawbacks, Smart TMHG measurement system is proposed.

# 3. MATERIALS AND METHODS

## 3.1. SMART TMHG MEASUREMENT SYSTEM

Smart TMHG Measurement System is mainly used to measures the values of Temperature, Moisture, Humidity and Gas. These measured values are displayed in LCD display. Initially soil moisture and Humidity sensors are dip in to the soil, which is connected to arduino. Measuring all the values, it will be displayed in the LCD. After detecting soil moisture and Humidity level condition, dc pump will be on or off. This information will be send to the user with the help of WSN for taking remedial action. To switch ON or OFF the motor pump an embedded c program in the arduino module is used. Main objective of this proposed method is that to help the community of people on service based to reduce the cost rather than the other sources.


https://doi.org/10.17993/3ctecno.2021.specialissue8.87-97

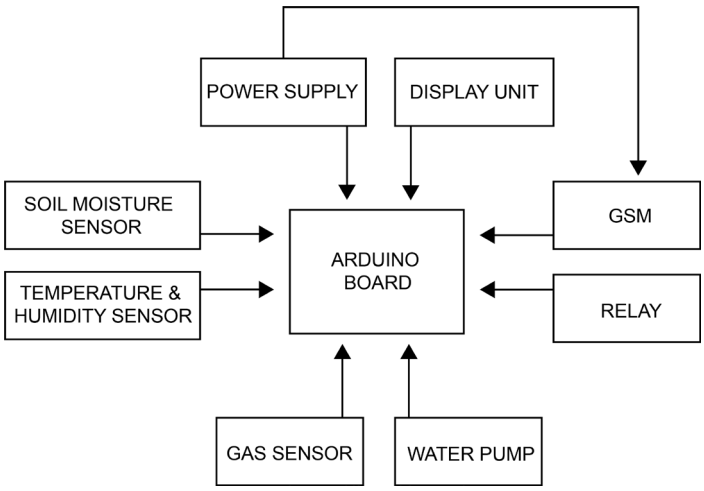


**Figure 1.** Block Diagram.
**Source:** own elaboration.

Plant sample is fixed with an individual soil moisture sensor. Each plant sample demands different moisture conditions. The Arduino module is used to read the analog input values from the four sensors placed in the samples. The pumps are switched off under normal conditions and are programmed to operate only when the soil moisture goes below certain threshold levels which are specific to the plant. The Arduino interface controls the working of the pumps which continue to irrigate the fields till the moisture levels exceed the upper threshold value. Simultaneously, the status of the active pump is indicated in the mobile phone of the user. This is entirely controlled by the Node MCU module. The automatic refresh feature of this module helps in continuous updating of all the three pumps on the mobile phone screen.

## 4. RESULTS

SMART TMHG MEASUREMENT SYSTEM is implemented in real time. Soil Moisture, Humidity, Temperature and gas measured by using an aurdino board. The main aim of the project is that measuring the parameters and knowing the farmer that how much amount should be present in the atmosphere. Wireless Sensor network is used to implement this work. The measured values are displayed in the LCD display. Output of Real Time Implementation as shown in Figure 2.


https://doi.org/10.17993/3ctecno.2021.specialissue8.87-97

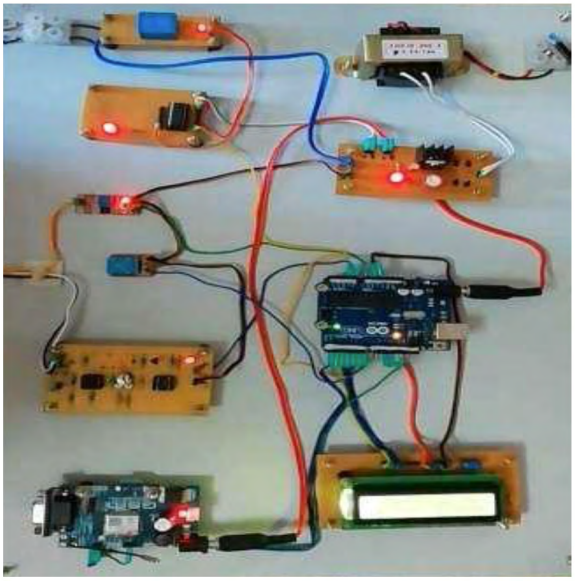

**Figure 2.** Output for Arduino Based Agriculture.
**Source:** own elaboration.

## 5. CONCLUSIONS

This work proposes a Smart TMHG Measurement System to measure the various parameters of agriculture field like soil moisture, temperature, humidity and gas. These measured values are displayed in LCD. After detecting the soil moisture and Humidity level, dc pump will be on or off based on the measured value. Arduino module control the ON or OFF the motor pump using an embedded c program. The pumps are switched off under normal conditions, when the soil moisture goes below certain threshold levels the pump goes ON, it was programmed in arduino module. The Arduino interface controls the working of the pumps which continue to irrigate the fields till the moisture levels exceed the upper threshold value. This information sent to the user with the help of WSN for taking remedial action. The Smart TMHG Measurement System will make farmers to increase the crop for better yield and make them economically (90%) benefit in remote location by using WSN.


https://doi.org/10.17993/3ctecno.2021.specialissue8.87-97

## ACKNOWLEDGEMENT

We would like to thank International Research Center of Kalasalingam Academy of Research and Education for providing financial assistance under the scheme of University Research Fellowship(URF) and we also thank the Department of Electronics and Communication Engineering of Kalasalingam Academy of Research and Education, India for permitting to use the computational facilities available in Signal Processing and VLSI Design which was setup with the support of the Department of Science and Technology (DST).

## REFERENCES

**Ameer, S., Chaubey, S. S., Joseph, M., Rajasekhar, P., Abhinav, S., & Ravikiran, R.** (2015). Notice of Retraction Automatic irrigation system through a solar power. In *International Conference on Electrical, Electronics, Signals, Communication and Optimization*, pp. 1-5, IEEE. https://doi.org/10.1109/EESCO.2015.7254015

**Fazackerley, S., & Lawrence, R.** (2010). Reducing turfgrass water consumption using sensor nodes and an adaptive irrigation controller. In *IEEE Sensors Applications Symposium*, pp. 90-94, IEEE. https://doi.org/10.1109/SAS.2010.5439386

**Kaewmard, N., & Saiyod, S.** (2014). Sensor data collection and irrigation control on vegetable crop using smart phone and wireless sensor networks for smart farm. In *IEEE Conference on Wireless Sensors,* pp. 106-112, IEEE. https://doi.org/10.1109/ICWISE.2014.7042670

**Kim, Y., Evans, R. G., & Iversen, W. M.** (2008). Remote sensing and control of an irrigation system using a distributed wireless sensor network. *IEEE transactions on instrumentation and measurement, 57*(7), 1379-1387. https://doi.org/10.1109/TIM.2008.917198

**Kodali, R. K., & Muraleedhar, A.** (2015). WSN in spice cultivation. In *International Conference on Green Computing and Internet of Things*, pp. 1173-1177, IEEE. https://doi.org/10.1109/ICGCIoT.2015.7380640

**Mancuso, M., & Bustaffa, F.** (2006). A wireless sensors network for monitoring environmental variables in a tomato greenhouse. In *IEEE International Workshop on Factory Communication Systems*, Vol. 10.

**Martinelli, M., Ioriatti, L., Viani, F., Benedetti, M., & Massa, A.** (2009). A WSN-based solution for precision farm purposes. *IEEE International Geoscience and Remote Sensing Symposium, 5,* V-469. https://doi.org/10.1109/IGARSS.2009.5417630

**Mat, I., Kassim, M. R. M., & Harun, A. N.** (2014). Precision irrigation performance measurement using wireless sensor network. In Sixth International Conference on Ubiquitous and Future Networks, pp. 154-157, IEEE. https://doi.org/10.1109/ICUFN.2014.6876771

**Nandurkar, S. R., Thool, V. R., & Thool, R. C.** (2014). Design and development of precision agriculture system using wireless sensor network. In *First International Conference on Automation, Control, Energy and Systems,* pp. 1-6, IEEE. https://doi.org/10.1109/TENCON.2015.7372834

**Peng, X., & Liu, G.** (2012). Intelligent water-saving irrigation system based on fuzzy control and wireless sensor network. In *Fourth International Conference on Digital Home,* pp. 252-256, IEEE. https://doi.org/10.1109/ICDH.2012.13

**Rani, M. U., & Kamalesh, S.** (2014). Web based service to monitor automatic irrigation system for the agriculture field using sensors. In *International Conference on Advances in Electrical Engineering,* pp. 1-5, IEEE. https://doi.org/10.1109/ICAEE.2014.6838569

**Shaikh, Z. A., Yousuf, H., Nawaz, F., Kirmani, M., & Kiran, S.** (2010). Crop irrigation control using wireless sensor and actuator network (WSAN). In *International Conference on Information and Emerging Technologies,* pp. 1-5, IEEE. https://doi.org/10.1109/ICIET.2010.5625669

**Singh, A., Chyan, L. S., & Sebastian, P.** (2010). Sensor integration in a Wireless Sensor Network system for environmental monitoring system. In *International Conference on Intelligent and Advanced Systems,* pp. 1-5, IEEE. https://doi.org/10.1109/ICIAS.2010.5716114

**Thilagavathi, G.** (2013). Online farming based on embedded systems and wireless sensor networks. In *International Conference on Computation of Power, Energy, Information and Communication*, pp. 71-74, IEEE. https://doi.org/10.1109/ICCPEIC.2013.6778501

**Wan, S.** (2012). Research on the Model for Crop Water Requirements in Wireless Sensor Networks. In *International Conference on Management of e-Commerce and e-Government*, pp. 234-237. IEEE. https://doi.org/10.1109/ICMeCG.2012.77

**Yao, Z., Lou, G., Zeng, X., & Zhao, Q.** (2010). Research and development precision irrigation control system in agricultural. *International Conference on Computer and Communication Technologies in Agriculture Engineering, 3*, 117-120. https://doi.org/10.1109/CCTAE.2010.5544390

**Zhang, X., & Chang, B.** (2011). Research of temperature and humidity monitoring system based on WSN and fuzzy control. In *International Conference on Electronics and Optoelectronics, 4*, V4-300. https://doi.org/10.1109/ICEOE.2011.6013489


https://doi.org/10.17993/3ctecno.2021.specialissue8.87-97

/07/


https://doi.org/10.17993/3ctecno.2021.specialissue8

# AIR POLLUTION ALERT SYSTEM USING IOT WITH GPRS

**Kalpana Murugan**
Department of Electronics and Communication Engineering,
Kalasalingam Academy of Research and Education, Krishnankoil, Virudhunagar (Dt), (India).
E-mail: drmkalpanaece@gmail.com
ORCID: https://orcid.org/0000-0002-5121-0468

**S. Murugeswari**
Department of Electronics and Communication Engineering,
Kalasalingam Academy of Research and Education, Krishnankoil, Virudhunagar (Dt), (India).
E-mail: sudha.murugeswari@gmail.com
ORCID: https://orcid.org/0000-0002-5240-4360

**Vaishnavi Parlapalli**
Department of Electronics and Communication Engineering,
Kalasalingam Academy of Research and Education, Krishnankoil, Virudhunagar (Dt), (India).
E-mail: vaishnavi31198@gmail.com
ORCID: https://orcid.org/0000-0003-1012-1618

**Cherukuri Mohana Teja**
Department of Electronics and Communication Engineering,
Kalasalingam Academy of Research and Education, Krishnankoil, Virudhunagar (Dt), (India).
E-mail: cherukuriteja77@gmail.com
ORCID: https://orcid.org/0000-0001-6541-6179

**Karasala Triveni**
Department of Electronics and Communication Engineering,
Kalasalingam Academy of Research and Education,Krishnankoil, Virudhunagar (Dt), (India).
E-mail: triveni1898@gmail.com
ORCID: https://orcid.org/0000-0001-5015-7063

**Recepción:** 25/10/2019 **Aceptación:** 07/08/2020 **Publicación:** 30/11/2021

**Citación sugerida:**
Murugan, K., Murugeswari, S., Parlapalli, V., Teja, C. M., y Triveni, K. (2021). Air pollution alert system using IoT with GPRS. *3C Tecnología. Glosas de innovación aplicadas a la pyme, Edición Especial,* (noviembre, 2021), 99-111. https://doi.org/10.17993/3ctecno.2021.specialissue8.99-111

## ABSTRACT

The air pollution is considered as the major problem which is caused due to the increase of the vehicles. To reduce the air pollution, many countries has explained different technologies like Zigbee based monitoring system which is used to measure the quality of an air. In this project a Wireless Inspection and Notification System (WINS) is proposed through the concept of Internet of Things (IoT). By implementing the system, it is possible to identify the harmful gases that present in the environment. In this WINS system, it uses GPRS based technology as a low cost and smart wireless communication method is adopted to collect and transmit the information about the harmful gases. The collected information will be stored for future purposes. To detect the environment pollution, proposed system uses different gas sensors i.e., CO sensor, MQ135 gas sensor and LM35 temperature sensor which is used to detect the pollution that present in the environment.

## KEYWORDS

Air pollution, WINS, IoT, Wi-Fi module, CO sensor, MQ135 sensor, LM35 temperature sensor.


https://doi.org/10.17993/3ctecno.2021.specialissue8.99-111

# 1. INTRODUCTION

IoT is a system which is related to all types of devices such as electronic, mechanical, some objects and all other living organisms. It helps in transferring data without any human support. It is generally used where network connectivity comes into the picture. It allows devices to exchange data between any two objects with minimum human interaction. With the help of IoT based technology scientists have developed new security challenges and ensuring security to IoT based products is given as major priority. Also, IoT induces faith within users so they believe that the IoT based systems do not have any weakness (vulnerability). In case if these products are secured properly there is a chance of potential breach.

GPRS (General Packet Radio Service) is a TTL based module. The type of GPRS used is SIM900. The frequency range available in India for GPRS module is between 900- 1900 Mhz. In other countries like U.S it can be used below 900 i.e., 850 Mhz. The proposed system works with a power supply of 5v. Also, this system provided with an inbuilt rectifier that reduces the input voltage of any value to its required number of volts.

Air pollution occurs when the large amount of biological and gaseous substances is exposed to atmosphere. This results the emergence of several new diseases and sometimes it leads to death of living organisms. Not only living beings but also it causes damage to food crops and may even damage environment. Main reasons behind all these activities are excessive use of gas emitting machinery. This problem is mainly observed in metropolitan cities like Chennai, Bangalore etc., this problem even leads to change in climate condition in an untimely manner. The main remedy to eradicate air pollution is by utilizing natural power supplies like solar energy, wind energy and tidal energy instead of these harmful machineries.

In Now-a-days air pollution is the major problem of every country. Due to this air pollution many people are facing different health issues. The rate of health issues has been growing faster in many areas which contain developing industrialization. It also may be due to the increase of number of vehicles which releases harmful gases. In this system the quality of air will be monitored, and it provides the output in threshold values. The proposed system uses three different sensors such as MQ135, MQ7. LM35 sensor is added in this system to


https://doi.org/10.17993/3ctecno.2021.specialissue8.99-111

show the amount of temperature and humidity. These sensors are used to identify different types of gases like CO2, CO, and Benzene. When these gases are detected by the sensors, the gases values are measured, and the threshold values of the gases are displayed on the LCD. When the threshold value is beyond the particular level, it provides buzzing sound by the buzzer that present in the system. This proposed system can be installed anywhere but mostly in industries and houses, where gases are mostly to be found.

In this IoT project it uses Arduino UNO, CO sensor, MQ135 gas sensor and LM35 temperature sensor, which is used to monitor the pollution level. This system uses GPRS module to monitor the air pollution from any place using PC or mobile. In SECTION-II, related literature survey was discussed. In SECTION-III, has been discussed along with its proposed method. In SECTION-IV, the results have analyzed and discussed. Finally, this paper is concluded with a Conclusion in the SECTION-V.

## 2. RELATED WORK

Mansour *et al.* (2014) explains about a set of gas sensors that are developed on stacks and infrastructure of a ZigBee and central server will support both short-term real time incident management and a long-term strategic management. It is a low data rate and low power wireless communication technology. Low-cost air-quality monitoring nodes consist of gas sensors with Wi-Fi module (Parmar, Lakhani, & Chattopadhyay, 2017; Xiaojun, Xianpeng, & Peng, 2015). It evaluates concentration of gases like CO, CO2, SO2 using sensors. The monitoring system has highly complex equipment technology and unstable operation. A wireless multi-gas sensing system is capable to identify the concentration of harmful elements like CO, CO2 and CH2O. A mobile app is developed to show data related to the concentration of gases when it is too high. The hardware sharing technique is used to reduce the hardware cost (Huang *et al.*, 2018).

Papers of Phala, Kumar, and Hancke (2016) and Kumar and Jasuja (2017), uses set of sensors to take the measurements of air present in the environment. The wireless network transmits the information to the base station. Gas concentration values are plotted on the Graphical User Interface (GUI). Low-cost air pollution sensors used to monitor air pollution at spatio temporal resolution. Sensor calibration must be effective to improve


https://doi.org/10.17993/3ctecno.2021.specialissue8.99-111

the data quality. Data quality of sensors is used to maintain the reliability (Maag, Zhou, & Thiele, 2018).

Recurrent air quality predictor is used to monitor the air quality. It provides one-hour prediction model which is used to monitor the current values of air pollution and to predict the air quality (Gu, Qiao, & Lin, 2018).

Papers of Cataliotti *et al.* (2014) and Devahema *et al.* (2018) contain different kinds of data sources received from open IoT platform and gives access to users. This work majorly deals with the different types of data classification and mobile crowd sensing management. It gives all possible methods for meeting different kinds of security challenges and vulnerabilities.

In the work of Sarjerao and Prakasarao (2018) and Shah and Mishra (2016), helps to monitor the quality of various parameters such as CO, CO2, temperature, humidity, and air pressure. IoT plays a major role in this model. IoT is integrated with cloud computing for better management of different data sources, and it is designed with low power and low-cost arm based minicomputer Raspberry pi. The main aim of this project is to identify pollutants in water with the help of IoT. Ultraviolent light sensor is used along with a 2 in one temperature and PH sensor. With the help of these sensors the purity of water, surrounding temperature, turbidity as well as acid and base levels of the water can be monitored. This data is transferred through cloud (Jamil *et al.*, 2015; Guanochanga *et al.*, 2018).

In this model a circuit is designed in such a way that it always keeps an eye on the amount of solid and gaseous wastes emitted by vehicles, industries, and others etc., Sensors are used to determine the level of co and co2 emitted and to determine humidity levels. Normal and abnormal values are recorded and transmitted to the user through IoT (Saha *et al.*, 2017).

In the study of Huang *et al.* (2018) a wireless gas monitoring mechanism is designed which can detect the 3 fixed toxic gases i.e., CO, CO2 and CH2O. The detected data can be monitored by the user with the help of an android app. Through this app the levels of these gases are known and when they exceeded a particular limit the user gets notified and the required precautionary measures were also sending to the user. Here instead of Wi-Fi, Bluetooth module is used which consumes low power. Also, the power consumption data


https://doi.org/10.17993/3ctecno.2021.specialissue8.99-111

is also transferred to the user to know the amount of power consumed along the sensor adjustment values.

In the works of Yang *et al.* (2017) and Benammar *et al.* (2018) provide an effective algorithm in which the pollution monitor is done by taking two different areas are considered i.e., a 2-D space like footpath and a 3-D space like a room inside a building. Sensors are used to determine the level of toxic impurities, when hardware is implemented and based on results the precautionary measures was taken. This is highly accurate method and consumes low power to a great extent, but only drawback is that the design of algorithm is a time taking process.

Marques, Ferreira, and Pitarma (2019) and Ahmed, Banu, and Paul (2017) discuss about SHE management system. SHE means Safety, Health and Environment management system. SHE is designed based on ZigBee wireless sensor network. It mainly focuses on Industrial sites. It contains a sensing network, router network and a monitoring network. It can measure various parameters and gas concentration. Any gas exceeding a particular limit this system warns the user and inform to take immediate precautionary measures.

# 3. MATERIALS AND METHODS

## 3.1. WIRELESS INSPECTION AND NOTIFICATION (WINS) THROUGH IOT

This project proposes Wireless Inspection and Notification System (WINS) through the concept of internet of things (IoT) as shown in Figure 1. By implementing the system, it is possible to identify the harmful gases that present in the environment. In this system, it uses GPRS based technology as a low cost and smart wireless communication method is adopted to collect and transmit the information about the harmful gases. WINS systems monitor the pollution and update it to web server so that the user can monitor anywhere through internet. The collected information will be stored for future purposes.


https://doi.org/10.17993/3ctecno.2021.specialissue8.99-111

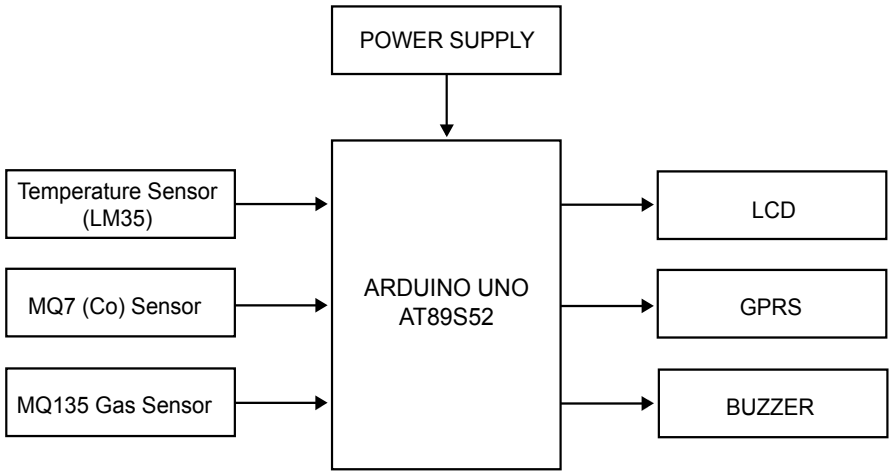


**Figure 1.** Block Diagram.
**Source:** own elaboration.

The main concept of this system is to identify the gas with the use of MQ135 and MQ6 gas sensors. The MQ135 sensor can sense NH3, NOx, Alcohol, Benzene, Smoke, and CO2. When the components are connected in an Arduino, it will sense all gases and it provides the gaseous level in PPM (Parts per Million). The output of the gas level is converted with respect to PPM, uses a library function of MQ135 and MQ7 gas sensor. The air quality safe level is 350PPM. If the value of air quality level exceeds 1000PPM, it leads to sleepiness, headache, and stuffy air. If the value increases beyond 2000PPM it leads to increased heart rate and other diseases. If the value is less than 1000PPM, then the LCD and Web page will display "Fresh air". When the value will be more than 1000PPM, then Buzzer will give beep sound and the LCD display shown the air level like "Poor Air, and the web page screen like Open Windows". When the gas level is increases above 2000PPM the buzzer will keep giving beep sound and it gives alert message in smart phone through GPS Module. The LCD and Web page will display "Harmful Air, go to Fresh Air".

**Temperature sensor (LM35):**

The LM35 series are precision integrated circuit. This sensor is used to detect the amount of temperature that present in the surroundings. It provides the output in centigrade, and it displays the output on LCD.


https://doi.org/10.17993/3ctecno.2021.specialissue8.99-111

**MQ7(CO):**

It is a sensor which is used to detect the harmful gases like CO and CO2 and provides the output values on LCD.

**MQ135 Gas sensor:**

The MQ135 sensor can sense NH3, Alcohol, Benzene, Smoke, CO2. When these components are connected to Arduino then it will sense all gases and it provides the gaseous level in PPM.

**Arduino Uno At89s52:**

Arduino board is used to boot the program from ROM memory, and it will wait for the sensor data. And it converts an analog data to the digital using ADC converter. If the sensor data is beyond the critical value alert a message will be send to the IOT web page.

**LCD:**

It is electrically modulated optical device that uses the light modulating properties of liquid crystal. It is used to display the threshold values of harmful gases like co2 and co. it also indicates gases values in PPM.

**GPRS:**

GPRS provides data rates of 56 – 144K bits/second and has a moderate speed data transform. This system is an integrated part of GSM network switching sub system. This component is used for long distance communication. With the use of this component the user can be able to monitor the gases values from longer distances with the use of web page.

**BUZZER:**

Buzzer is an audio signaling device. It is used to provide the alert message like buzzing or beeping sound when the harmful gases are emitted in the atmosphere.


https://doi.org/10.17993/3ctecno.2021.specialissue8.99-111

# 4. RESULTS

Hardware implementation of an air pollution monitoring system output as shown in Figure 2. The above figure shows the result that it contains the level of CO2 and shows the temperature value. Whenever the sensors used in the system, it is used to detect the gases that present in the atmosphere. If there is a gas, proposed method gives an alarm sound with the help of buzzer. This alarm sound will be considered as an alert message to take the preventive measures.

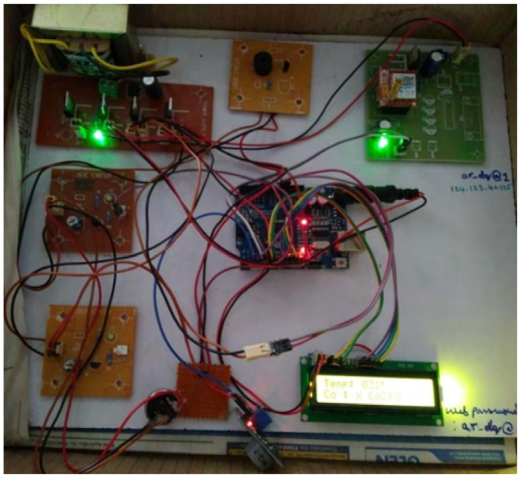

**Figure 2.** Output of Air Pollution Monitoring System.
**Source:** own elaboration.

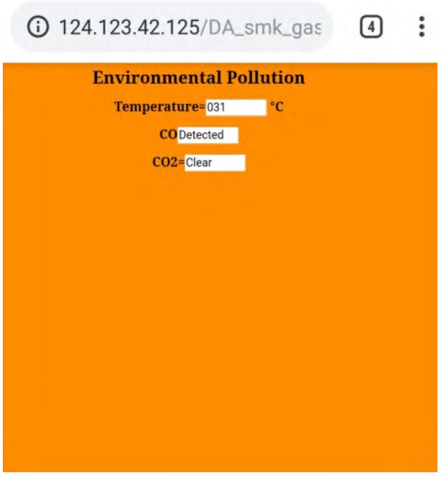


**Figure 3.** Result of webpage.
**Source:** own elaboration.


https://doi.org/10.17993/3ctecno.2021.specialissue8.99-111

In this project GPRS module is used. Figure 3. shows that the temperature value and the status of the gas has been displayed using web page.

## 5. CONCLUSIONS

This work proposed Wireless Inspection and Notification (Wins) through IOT. It is used to monitor the air pollution using Arduino UNO board and GPRS module using IoT technology. This technology is used to monitor the quality of an air. Here MQ7 and MQ135 sensors used to sense the various types of dangerous gases. GPRS module is used to monitor the gas concentration from longer distances, and it connects entire process to internet. LCD (Liquid Crystal Display) is used to display the gaseous values. By using of buzzer, the user can get the alert message. This alert message is used to take the preventive measures by the user. This proposed system will be useful for society.

## ACKNOWLEDGEMENT

We would like to thank International Research Center of Kalasalingam Academy of Research and Education for providing financial assistance under the scheme of University Research Fellowship(URF) and we also thank the Department of Electronics and Communication Engineering of Kalasalingam Academy of Research and Education, India for permitting to use the computational facilities available in Signal Processing and VLSI Design which was setup with the support of the Department of Science and Technology (DST).

## REFERENCES

**Ahmed, M. M., Banu, S., & Paul, B.** (2017). Real-time air quality monitoring system for Bangladesh's perspective based on Internet of Things. In *2017 3rd International Conference on Electrical Information and Communication Technology (EICT)* (pp. 1-5). IEEE. https://www.semanticscholar.org/paper/Real-time-air-quality-monitoring-system-for-based-Ahmed-Banu/520860de7d1f77d12480151d198945fe25bb678d

**Benammar, M., Abdaoui, A., Ahmad, S. H., Touati, F., & Kadri, A.** (2018). A modular IoT platform for real-time indoor air quality monitoring. *Sensors, 18*(2), 581. https://doi.org/10.3390/s18020581


https://doi.org/10.17993/3ctecno.2021.specialissue8.99-111

**Cataliotti, A., Cipriani, G., Cosentino, V., Di Cara, D., Di Dio, V., Guaiana, S., Panzavecchia, N., & Tinè, G.** (2014). A prototypal architecture of a IEEE 21451 network for smart grid applications based on power line communications. *IEEE Sensors Journal, 15*(5), 2460-2467. https://ieeexplore.ieee.org/document/6849478

**Devahema, P. V., Vamsi, S. S., Garg, A., Anand, A., & Gupta, D. R.** (2018). IoT Based Air Pollution Monitoring System. *Journal of Network Communications and Emerging Technologies (JNCET), 8*(4), 100-103. https://www.jncet.org/Manuscripts/Volume-8/Issue-4/Vol-8-issue-4-M-23.pdf

**Gu, K., Qiao, J., & Lin, W.** (2018). Recurrent air quality predictor based on meteorology- and pollution-related factors. *IEEE Transactions on Industrial Informatics, 14*(9), 3946-3955. https://ieeexplore.ieee.org/document/8259327

**Guanochanga, B., Cachipuendo, R., Fuertes, W., Salvador, S., Benítez, D. S., Toulkeridis, T., Torres, J., Tapia, F., & Meneses, F.** (2018). Real-time air pollution monitoring systems using wireless sensor networks connected in a cloud-computing, wrapped up web services. In *Proceedings of the future technologies conference* (pp. 171-184). Springer, Cham. https://www.semanticscholar.org/paper/Real-Time-Air-Pollution-Monitoring-Systems-Using-in-Guanochanga-Cachipuendo/0fa7f310ef4ace2d1e7e6470bdd3c64983fe10a8

**Huang, C. M., Liu, Y. J., Hsieh, Y. J., Lai, W. L., Juan, C. Y., Chen, S. Y., Yang, C. C., & Wu, C. M.** (2018). A multi-gas sensing system for air quality monitoring. In *2018 IEEE International Conference on Applied System Invention (ICASI)* (pp. 834-837). IEEE. https://ieeexplore.ieee.org/document/8394393

**Huang, C. M., Liu, Y. J., Hsieh, Y. J., Lai, W. L., Juan, C. Y., Chen, S. Y., ... & Wu, C. M.** (2018). A multi-gas sensing system for air quality monitoring. In *2018 IEEE International Conference on Applied System Invention (ICASI)* (pp. 834-837). IEEE.

**Jamil, M. S., Jamil, M. A., Mazhar, A., Ikram, A., Ahmed, A., & Munawar, U.** (2015). Smart environment monitoring system by employing wireless sensor networks on vehicles for pollution free smart cities. *Procedia Engineering, 107*, 480-484. https://doi.org/10.1016/j.proeng.2015.06.106


https://doi.org/10.17993/3ctecno.2021.specialissue8.99-111

**Kumar, S., & Jasuja, A.** (2017). Air quality monitoring system based on IoT using Raspberry Pi. In *2017 International Conference on Computing, Communication and Automation (ICCCA)* (pp. 1341-1346). IEEE. https://www.semanticscholar.org/paper/Air-quality-monitoring-system-based-on-IoT-using-Pi-Kumar-Jasuja/78a0ea3f112ee0ddcd9baeb6cddeceffaa18157f

**Maag, B., Zhou, Z., & Thiele, L.** (2018). A survey on sensor calibration in air pollution monitoring deployments. *IEEE Internet of Things Journal, 5*(6), 4857-4870. https://ieeexplore.ieee.org/abstract/document/8405565

**Mansour, S., Nasser, N., Karim, L., & Ali, A.** (2014). Wireless sensor network-based air quality monitoring system. In *2014 International Conference on Computing, Networking and Communications (ICNC)* (pp. 545-550). IEEE. https://www.semanticscholar.org/paper/Wireless-Sensor-Network-based-air-quality-system-Mansour-Nasser/2c78e3e28b85345a5f32a1f1819bcae8e75dc99b

**Marques, G., Ferreira, C. R., & Pitarma, R.** (2019). Indoor air quality assessment using a CO 2 monitoring system based on internet of things. *Journal of medical systems, 43*(3), 1-10. https://doi.org/10.1007/s10916-019-1184-x

**Parmar, G., Lakhani, S., & Chattopadhyay, M. K.** (2017). An IoT based low cost air pollution monitoring system. In *2017 International Conference on Recent Innovations in Signal processing and Embedded Systems (RISE)* (pp. 524-528). IEEE. https://www.semanticscholar.org/paper/An-IoT-based-low-cost-air-pollution-monitoring-Parmar-Lakhani/172a48db2a15ce2b73ce62e99811efc067f20672

**Phala, K. S. E., Kumar, A., & Hancke, G. P.** (2016). Air quality monitoring system based on ISO/IEC/IEEE 21451 standards. *IEEE Sensors Journal, 16*(12), 5037-5045. https://ieeexplore.ieee.org/document/7456204

**Saha, H. N., Auddy, S., Chatterjee, A., Pal, S., Sarkar, S., Singh, R., Singh, A. K., Sharan, P., Banerjee, S., Sarkar, R., & Maity, A.** (2017). IoT solutions for smart cities. In *8th Annual Industrial Automation and Electromechanical Engineering Conference (IEMECON)*. https://ieeexplore.ieee.org/document/8079565


https://doi.org/10.17993/3ctecno.2021.specialissue8.99-111

**Sarjerao, B. S., & Prakasarao, A.** (2018). A low cost smart pollution measurement system using rest api and esp32. In *2018 3rd International Conference for Convergence in Technology (I2CT)* (pp. 1-5). IEEE. https://ieeexplore.ieee.org/document/8529500

**Shah, J., & Mishra, B.** (2016). IoT enabled environmental monitoring system for smart cities. In *2016 international conference on internet of things and applications (IOTA)* (pp. 383-388). IEEE. https://www.semanticscholar.org/paper/IoT-enabled-environmental-monitoring-system-for-Shah-Mishra/b4ff3a0490d5de57ecc8acb3ae951e49c8fcb50e

**Xiaojun, C., Xianpeng, L., & Peng, X.** (2015). IOT-based air pollution monitoring and forecasting system. In *2015 international conference on computer and computational sciences (ICCCS)* (pp. 257-260). IEEE. https://www.semanticscholar.org/paper/IOT-based-air-pollution-monitoring-and-forecasting-Xiaojun-Xianpeng/508b2d446d0864ee4cefc01c0a008c5c995251ab

**Yang, Y., Zheng, Z., Bian, K., Song, L., & Han, Z.** (2017). Real-time profiling of fine-grained air quality index distribution using UAV sensing. *IEEE Internet of Things Journal, 5*(1), 186-198. https://ieeexplore.ieee.org/document/8119942


https://doi.org/10.17993/3ctecno.2021.specialissue8.99-111

/08/


https://doi.org/10.17993/3ctecno.2021.specialissue8

# OPTIMIZATION OF MULTIPLIER IN REVERSIBLE LOGIC

**N. Bhuvaneswary**
Assistant Professor, Department of ECE, Kalasalingam Academy of Research And Education, Anand Nagar. Krishnankoil,Virudhunagar District, (India).
E-mail: bhuvaneswary.n@klu.ac.in
ORCID: https://orcid.org/0000-0001-6400-6602

**Adhi Lakshmi**
Associate Professor, Department of ECE, Kalasalingam Academy of Research And Education, Anand Nagar. Krishnankoil,Virudhunagar District, (India).
E-mail: lakshmi@klu.ac.in
ORCID: https://orcid.org/0000-0002-6744-7048

**Recepción:** 25/10/2019 **Aceptación:** 30/09/2020 **Publicación:** 30/11/2021

**Citación sugerida:**
Bhuvaneswary, N., y Lakshmi, A. (2021). Optimization of multiplier in reversible logic. *3C Tecnología. Glosas de innovación aplicadas a la pyme, Edición Especial,* (noviembre, 2021), 113-123. https://doi.org/10.17993/3ctecno.2021.specialissue8.113-123

## ABSTRACT

Reversible logic is leading area in power consumption. Based on its application, its emerging trend in power consumption. In ideal situations, reversible circuit yield nil power. Different methods of multiplier optimized in this paper. Like quantum computers, multipliers required to develop computational units. In the paper, two different methods of multiplier developed with very large bit width. Based on partial products hierarchical method is developed. Another method is Karatsuba's algorithm developed based on divide and conquers method. Finally, we compare the results of both two methods. The projected reversible multipliers are enhanced in terms of quantum cost, number of constant inputs, number of garbage outputs and complexity in hardware. In nanotechnology applications this multiplier can be used to construct complex system.

## KEYWORDS

Karatsuba's algorithm, Hierarchical method, FFT, Reversible gates.


https://doi.org/10.17993/3ctecno.2021.specialissue8.113-123

# 1. INTRODUCTION

One of the foremost issues in VLSI design is reducing power. In early days, due to information loss irreversible logic leads to power dissipation (Zhirnov *et al.*, 2003). When one bit information lost, it leads to dissipate at least KTln2 joules of energy, where K=1.380650 x 10-23 m2kg-2K-1 (joules Kelvin-1) is the Boltzmann's constant and T is the temperature (Zhirnov *et al.*, 2003). Reversible logic blocks do not lose information because it has internally zero power dissipation. To eliminate KTln2 joules of energy dissipation, circuit must be developed with reversible logic gates.

In the subsequent, based on the reversible logic multipliers are synthesized. Initially multipliers synthesized based on Toffoli circuit (Karatsuba & Ofman, 1963; Islam *et al.*, 2009). Also, multiplier can be synthesized based on different reversible gates. In addition to that, multipliers have been proposed with large bit-width.

This paper proposes a multiplier in reversible logic with large bit-width. Two methods are projected, the foremost method is hierarchical method and another one is Karatsuba method applied to the application of FFT.

Respite of the paper systematized as follows. Reversible logic gates ideas and necessity described in Segment II. In Segment III, basics of reversible functions and circuits are discussed. Segment IV provides algorithm of proposed work. Segment V provides the design of Hierarchical and Karatsuba method. Segment VI determines the conclusion.

# 2. REVERSIBLE LOGIC GATES

In segment II, basic reversible logic gates are described which is being used in the design. Figure 1 displays a 3*3 Toffoli gate. The input path is I (A, B and C) and the output path is O (P, Q, and R). The outputs of the gate are well defined by P=A, Q=B, R=AB$\oplus$C.


https://doi.org/10.17993/3ctecno.2021.specialissue8.113-123

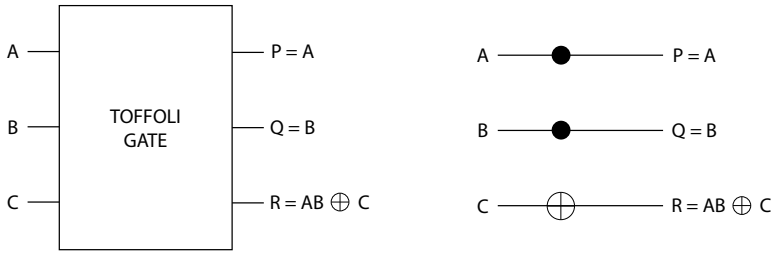


**Figure 1.** Toffoli Gate.
**Source:** own elaboration.

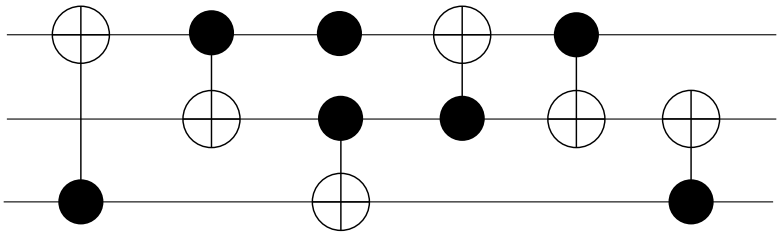

**Figure 2.** Toffoli circuit.
**Source:** own elaboration.

Figure 2 shows a Toffoli circuit with 6 gates, quantum cost value 10, cost of transistor 56 and 3 circuit lines respectively. Black circle ● is denoted as control lines and the cross line ⊕ denoted as target lines.

## 3. BASICS OF REVERSIBLE LOGIC

**Demarcation 1:** A reversible function $f : \mathbb{B}^n \rightarrow \mathbb{B}^m$ is defined as if (1) its amount of outputs is same as the amount of inputs and (2) it plots every input design to a distinctive output.

Reversible function is required to be embed in irreversible to reduce data loss, which requires circuit lines to produce constant inputs and garbage outputs. The least count of circuit lines is added, and it determined by number of existences of the most numerous output pattern (Toffoli, 1980). Reversible functions realized based on restrictions as if fan-out and feedback are not indorsed (Wille & Drechsler, 2009).


https://doi.org/10.17993/3ctecno.2021.specialissue8.113-123

**Demarcation 2:** Inputs in reversible circuit G $X = \{x_i \mid 1 \le i \le n\}$ determined by reversible gates gi cascaded, i.e. $G = \prod_{i=1}^{d} g_i$ gi where the number of gate denoted as d. In general, different reversible gates are there. In which most used gate is Toffoli because it is universal, multiple gate control.

**Demarcation 3:** Let the domain function denoted as $X := \{x_i \mid 1 \le i \le n\}$. g(C; t) is the form of universal multiple control Toffoli gate, where $C = \{x_{ji} \mid 1 \le i \le k\} \subset X$ control lines set denoted as X and with t 62 C the target line denoted as t = xl. The target line is inverted when control lines set assigned as one, that is., When control line is empty the input vector of the gate has been charted to $\prod_{i=1}^{l-1} x_i . x_l \oplus 1, \prod_{i=l+1}^{n} x_i$, then the target is inverted. In the subsequent, Toffoli gates are referred as multiple control gate. Toffoli gate also called as Not gate when it has zero control lines.

# 4. PROPOSED REVERSIBLE MULTIPLIER

## 4.1. HIERARCHICAL METHOD

In this segment, multiplier synthesized based on hierarchical method by means of controlled increasers. To calculate partial products, multiply two factors $a = \sum_{i=0}^{n-1} a_i \cdot 2^i$ and $b = \sum_{i=0}^{n-1} b_i \cdot 2^i$ then add the products together, i.e. $a \cdot b = \sum_{i=0}^{n-1} (a_i \cdot \sum_{i=0}^{n-1} b_j \cdot 2^j) \cdot 2^i$. When the bit ai assigned as one then the particular bit of bj multiplied by particular rule of 2 is additional to the product. This can be apprehended by controlled functions. Therefore, by using hierarchical method number of multiple n-bit apprehends multiplier by distinct n-bit controlled increasers. The factors of multiple bit multiplication are $a = \prod_{i=0}^{n-1} a_i$ and $b = \prod_{i=0}^{n-1} b_i$ as well as the product $c = \prod_{i=0}^{2 \cdot n-1} c_i$ here, the i-th controlled increaser is controlled by ai. It conditionally adds the value of b to $\prod_{j=i}^{n-1+i} c_i$ i.e. to the n bits of the product c beginning from the i-th bit. To modify the j-th bit of the product, lower bit does not consider until the j-th controlled increaser. Therefore, by a bit shifter, we can realize the controlled increasers without considering lower bits. The n + i-th position of the product carries carry, which further not used and, thus, carries zero.


https://doi.org/10.17993/3ctecno.2021.specialissue8.113-123

```
1  for i = 0  to  n - 1
2  {
3                 T_{j=i}^{n+i} c_i   +=a_i   T_{i=0}^{n-1} b_i
4  }
```

**Example 1:** Consider a 3-bit factors based on hierarchical a = a2a1a0 and b = b2b1b0 along with the product c = 5c4c3c 2c1c0. To realize this kind of multiplication we required 3 controlled increasers. a0 is control the initial controlled increaser. In addition to that it temporarily added 2nd factor b to last 3 LSB of product c2c1c0. Carry writes over to third MSB bit c3. a1 is control the 2nd controlled increaser. In addition to that it temporarily added 2nd factor b with product c, i.e. to c3c2c1. Carry writes over to second MSB bit c4. a2 controls the 3rd controlled increaser. In addition to that it temporarily added 2nd factor b with product c, i.e. to c4c3c2. Carry writes over to MSB bit c5.

## 4.2. KARATSUBA METHOD

In this segment Karatsuba's algorithm, based multiplier designed with divide and conquer method. Based on this method multiplication realized by multiplying two factors with smaller bit-width and additionally perform some less expensive operations. Consider an n-bit multiplication with m = 2.k, Both multiple factors (example. $a = \sum_{i=0}^{2\cdot k-1} a_i \cdot 2^i$ are split as an upper part $\overline{a} := \sum_{i=k}^{2\cdot k-1} a_i \cdot 2^{i-k}$ and a lower part $\underline{a} := \sum_{i=0}^{k-1} a_i \cdot 2^i$ such that $a = \overline{a} \cdot 2^k + \underline{a}$. With this demonstration the subsequent equations are:

$$
\begin{aligned}
a \cdot b &= \left(\overline{a} \cdot 2^k + \underline{a}\right) \cdot \left(\overline{b} \cdot 2^k + \underline{b}\right) \\
&= \overline{a} \cdot \overline{b} \cdot 2^{2 \cdot k} + (\underline{a} \cdot \overline{b} + \overline{a} \cdot \underline{b}) \cdot 2^k + \underline{a} \cdot \underline{b} \\
&= \overline{a} \cdot \overline{b} \cdot 2^{2 \cdot k} + (\underline{a} \cdot \overline{b} + \overline{a} \cdot \underline{b} + \overline{a} \cdot \overline{b} + \underline{a} \cdot \underline{b} - \overline{a} \cdot \overline{b} - \underline{a} \cdot \underline{b}) \cdot 2^k + \underline{a} \cdot \underline{b} \\
&= \overline{a} \cdot \overline{b} \cdot 2^{2 \cdot k} + (\underline{a} \cdot (\underline{b} + \overline{b}) + \overline{a} \cdot (\underline{b} + \overline{b}) - \overline{a} \cdot \overline{b} - \underline{a} \cdot \underline{b}) \cdot 2^k + \underline{a} \cdot \underline{b} \\
&= \overline{a} \cdot \overline{b} \cdot 2^{2 \cdot k} + ((\underline{a} + \overline{a}) \cdot (\underline{b} + \overline{b}) - \overline{a} \cdot \overline{b} - \underline{a} \cdot \underline{b}) \cdot 2^k + \underline{a} \cdot \underline{b}
\end{aligned}
$$

These expressions indicate that 3 k-bit multiplications, bit shits and subtractions realized from a (2.k)-bit multiplication. In addition to that, circuit lines are necessary for reversible logic. For small bit width Karatsuba method is not applicable, the variable turning Point


https://doi.org/10.17993/3ctecno.2021.specialissue8.113-123

signifies the bit-width lower. The Karatsuba method-based multiplication is used afar the turning Point.

**Example 2:**

Let us deliberate eight-bit Karatsuba multiplication and turning point t = 6. The turning point t is less than 8 bit and even the conditional lines 1 and 4 does not hold and computed K as four (line 7). Then, in line eight, new variables d, e, f are initialized which leads to 20 garbage lines i.e 4.4+4 = 20. Then, the 2 minor multiplications c= c7c6c5c4c3c2c1c0 =a3a2a1a0 _ b3b2b1b0 = $\underline{a} \cdot \underline{b}$ (line 9) and $\overline{c} = \overline{a} \cdot \overline{b}$ (line 10) are performed, respectively. In previous segment, same method realized using hierarchical method. Then, the result of the multiplications directly consigned to the product of the bits. To modify the product of the sums this result must be used that calculated next. These sums are d=d4d3d2d1d0= a7a6a5a4+a3a2a1a0 = $\overline{a} + \underline{a}$ (line 11) and $e = \overline{b} + \underline{b}$ (line 12). To perform this operation, copy the 1st sum to the target until it uninitialized and increase the function by adding 2nd sum. To get the 3rd sub product, result of this 1st and 2nd sums are multiplied h = d.e (line 13).

1 if ( n < *turningPoint*)
2 c = $MULT_H$ (*a*,*b*)
3
4 if ( n % 2 = 1)
5 init $a_n, b_n, c_{2 \cdot n+1}$ with 0
6
7 $k := \lfloor \frac{n}{2} \rfloor$
8 init $d, e$ ($k$ + 1 bits), $f$ (2 · $k$ + 2 bits ) with 0
9 $\overline{c} = MULT_K (\overline{a}, \overline{b})$
10 $\underline{c} = MULT_K (\underline{a}, \underline{b})$
11 $d = \overline{a} + \underline{a}$
12 $e = \overline{b} + \underline{b}$
13 $h = MULT_K (d, e)$
14 $h -= \overline{c}$
15 $h -= \underline{c}$
16 $\top_{i=k}^{3 \cdot k + 3} c_i \mathrel{+}= h$

Multiplication performed by the hierarchical approach when turning point is greater than the bit.


https://doi.org/10.17993/3ctecno.2021.specialissue8.113-123

# 5. DESIGN OF REVERSIBLE MULTIPLIER

## 5.1. HIERARCHICAL METHOD

For example, we have to multiply the two binary values i.e. 0000000000001011 and 0000000010000001 representing with 16bits. The simulated waveform for this example is done using reversible logic; the result for this multiplication is 00000000000000000000010110001011.

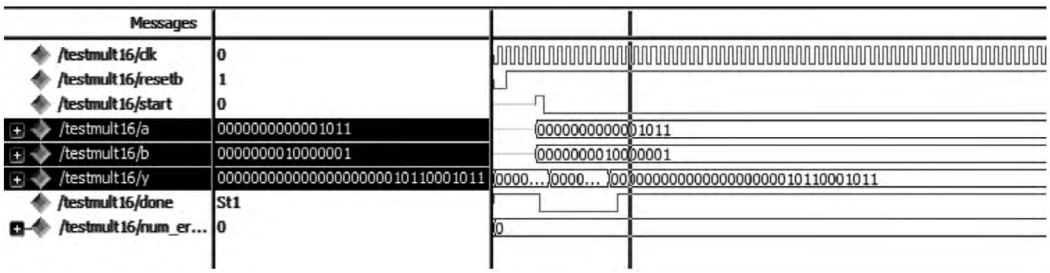


## 5.2. KARATSUBA METHOD

For example, the same values can be multiplied using karatsuba method representing with 16bits.

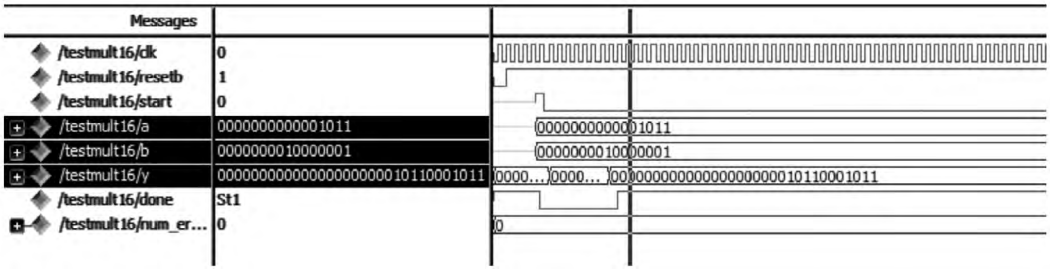


# 6. CONCLUSIONS

This paper proposes a multiplier with very large bit-width using reversible logic. The Hierarchical method only applicable for small bit-width but the Karatsuba method applicable for large bit-width. The results are compared using synthesized result of device


https://doi.org/10.17993/3ctecno.2021.specialissue8.113-123

utilization of the two methods. The Karatsuba method is better than the Hierarchical method because the device utilization was more in the case of Hierarchical method that is mention in Table 1. The projected reversible multipliers are enhanced in terms of quantum cost, number of constant inputs, number of garbage outputs and complexity in hardware. In nanotechnology applications this multiplier can be used to construct complex system.

This result is taken by 16bit multiplication of two binary values 0000000000001011 and 0000000010000001.

**Table 1.** Comparison of proposed systems.

| | NO. OF FLIP FLOPS | NO. OF 4INPUT LUTS | NO. OF IOBS |
|---|---|---|---|
| Hierarchical method | 81 | 122 | 68 |
| Karatsuba method | 36 | 72 | 64 |

**Source:** own elaboration.

## REFERENCES

**Bennett, C. H.** (1973). Logical reversibility of computation. *IBM Journal of Research and Development, 17*(6), 525-532. https://doi.org/10.1147/rd.176.0525

**Desoete, B., & De Vos, A.** (2002). A reversible carry-look-ahead adder using control gates. *Integration-the VLSI journal, 33*(1-2), 89–104. https://biblio.ugent.be/publication/160416

**Fazel, K., Thornton, M. A., & Rice, J. E.** (2007). ESOP-based Toffoli gate cascade generation. In *2007 IEEE Pacific Rim Conference on Communications, Computers and Signal Processing*, pp. 206-209. https://ieeexplore.ieee.org/document/4313212

**Gupta, P., Agrawal, A., & Jha, N. K.** (2006). An algorithm for synthesis of reversible logic circuits. *IEEE Transactions on Computer-Aided Design of Integrated Circuits and Systems, 25*(11), 2317–2330. https://ieeexplore.ieee.org/document/1715418


https://doi.org/10.17993/3ctecno.2021.specialissue8.113-123

**Haghparast, M., Jassbi, S. J., Navi, K., & Hashemipour, O.** (2008). Design of a novel reversible multiplier circuit using HNG gate in nanotechnology. *World Applied Sciences Journal, 3*(6), 974–978. https://www.idosi.org/wasj/wasj3(6)/19.pdf

**Islam, M. S., Rahman, M. M., Begum, Z., & Hafiz, M. Z.** (2009). Low cost quantum realization of reversible multiplier circuit. *Information Technology Journal, 8*(2), 208–213. https://scialert.net/abstract/?doi=itj.2009.208.213

**Karatsuba, A., & Ofman, Y.** (1963). Multiplication of many-digital numbers by automatic computers. *Doklady Akad. Nauk SSSR, 145*(2), 293-294. http://www.mathnet.ru/php/archive.phtml?wshow=paper&jrnid=dan&paperid=26729&option_lang=eng

**Landauer, R.** (1961). Irreversibility and heat generation in the computing process. *IBM Journal of Research and Development, 5*(3), 183-191. https://doi.org/10.1147/rd.53.0183

**Maslov, D., & Dueck, G. W.** (2004). Reversible cascades with minimal garbage. *Computer-Aided Design of Integrated Circuits and Systems, 23*(11), 1497–1509. https://ieeexplore.ieee.org/document/1350877

**Miller, D. M., Maslov, D., & Dueck, G. W.** (2003). A transformation based algorithm for reversible logic synthesis. *Proceedings 2003. Design Automation Conference* (IEEE Cat. No. 03CH37451), pp. 318-323. http://web.cecs.pdx.edu/~mperkows/temp/March17/dac.pdf

**Nielsen, M. A., & Chuang, I. L.** (2000). *Quantum Computation and Quantum Information.* Cambridge University Press. http://mmrc.amss.cas.cn/tlb/201702/W020170224608149940643.pdf

**Shende, V. V., Prasad, A. K., Markov, I. L., & Hayes, J. P.** (2003). Synthesis of reversible logic circuits. *IEEE Transactions on Computer-Aided Design of Integrated Circuits and Systems, 22*(6), 710–722. https://ieeexplore.ieee.org/document/1201583

**Shor, P. W.** (1994). Algorithms for quantum computation: discrete logarithms and factoring. *Proceedings 35th Annual Symposium on Foundations of Computer Science*, pp. 124-134. https://ieeexplore.ieee.org/document/365700

**Thapliyal, H., & Srinivas, M. B.** (2006). Novel reversible multiplier architecture using reversible TSG gate. In *International Conference on Computer Systems and Applications*, pp. 100–103. https://ieeexplore.ieee.org/document/1618339

**Toffoli, T.** (1980). Reversible computing. In Bakker, J. W. de., and Leeuwen, J. van (eds.) *Automata, Languages and Programming.* Springer.

**Vandersypen, L., Steffen, M., Breyta, G., Yannoni, C. S., Sherwood, M. H., & Chuang, I. L.** (2001). Experimental realization of Shor's quantum factoring algorithm using nuclear magnetic resonance. *Nature, 414,* 883–887. https://doi.org/10.1038/414883a

**Wille, R., & Drechsler, R.** (2009). BDD-based synthesis of reversible logic for large functions. In *46th ACM/IEEE Design Automation Conference*, pp. 270–275. https://ieeexplore.ieee.org/document/5227151

**Zhirnov, V. V., Cavin, R. K., Hutchby, J. A., & Bourianoff, G. I.** (2003). Limits to binary logic switch scaling – a gedanken model. *Proceedings of the IEEE, 91*(11), 1934–1939. https://ieeexplore.ieee.org/document/1240081


https://doi.org/10.17993/3ctecno.2021.specialissue8.113-123

/09/


https://doi.org/10.17993/3ctecno.2021.specialissue8

# HYBRID CLASSIFIER FOR BRAIN ABNORMALITY DETECTION IN BRAIN MRI

**Adhi Lakshmi**
Associate Professor, Electronics and Communication Engineering, Kalasalingam Academy of Research and Education, Tamilnadu, (India).
E-mail: lakshmi@klu.ac.in
ORCID: http://orcid.org/0000-0002-6744-7048

**Thangadurai Arivoli**
Professor/Principal, Electronics and Communication Engineering, Vicram College of Engineering, Tamilnadu, (India).
E-mail: t.arivoli@gmail.com
ORCID: http://orcid.org/0000-0003-1612-1029

**M. Pallikonda Rajasekaran**
Professor/ Director of Controller of Examination,Electronics and communication EngineeringKalasalingam Academy Of Research and Education, Tamilnadu, (India).
E-mail: m.p.raja80@gmail.com
ORCID: https://orcid.org/0000-0001-6942-4512

**N. Bhuvaneshwary**
Assistant professor, Electronics and Communication Engineering, Kalasalingam Academy of Research and Education, Krishnankoil, Tamilnadu, (India).
E-mail: bhuvaneswary.n@klu.ac.in
ORCID: http://orcid.org/0000-0001-6400-6602

**S. Sathya**
PG student,Eectronics and Communication Engineering, Kalasalingam Academy Of Research and Education, Krishnanloil, Tamilnadu, (India).
E-mail: ssathya08nov@gmail.com
ORCID: https://orcid.org/0000-0002-1440-663X

**Recepción:** 25/10/2019 **Aceptación:** 20/10/2020 **Publicación:** 30/11/2021

**Citación sugerida:**
Lakshmi, A., Arivoli, T., Rajasekaran, M., Bhuvaneshwary, N., y Sathya, S. (2021). Hybrid classifier for brain abnormality detection in brain MRI. *3C Tecnología. Glosas de innovación aplicadas a la pyme, Edición Especial,* (noviembre, 2021), 125-153. https://doi.org/10.17993/3ctecno.2021.specialissue8.125-153

## ABSTRACT

Brain abnormality detection is very essential now a days. Brain abnormality includes both massive abnormal growth of cells called tumour and blood lump in a veins or artery. If The abnormalities are detected at the earlier stages it would help to save life. The symptoms for the abnormalities are same and vary with patient aging and severity of the abnormality. The algorithm which works for tumor can not be used for the detection of abnormality caused in blood lumps of veins and artery. Normally the tumor is the massive growth of the cell and the features can be extracted and applied for the classifier to identify the severity of the abnormality. But the detection of abnormality caused in vein or artery due to blood lumps are very difficult to identify and feature extraction is also difficult. A sophisticated algorithm should be used for identifying the blood lumps. This paper deals with hybrid classifier (SVM and ANFIS) for detecting the abnormalities such as tumour as well as stroke. Till now separate algorithms are used for detecting tumour or stroke from brain MR image. In our proposed work it is possible to identify stroke or tumour with same algorithm by using different hybrid classifiers. The proposed system helps the physicians to diagnose human brain stroke. Accuracy of 0.999, sensitivity 0.38, specificity 0.86, PPV 0.91, NPV 0.99 is obtained by ANFIS classifier. Three quantitative events to calculate brain tumor of average segmentation results: Similarity Index (SI), Overlap fraction (OF), and Extra Fraction (EF) is 0.776194, 0.775198, 0.222213 is obtained by SVM classifier.

## KEYWORDS

SVM, ANFIS, Brain Stroke, Tumour.


https://doi.org/10.17993/3ctecno.2021.specialissue8.125-153

# 1. INTRODUCTION

## Brain Stroke

Stroke otherwise called as "Brain Attack" that happens in the brain rather than the heart. A stroke or "brain assault" occurs:

- Due to blood lump in a veins or artery.
- Due to blood vein breakage, interfering with blood stream to a region of the brain.

As it happens, brain cells start to expire. When brain cells die during a stroke, functions such as speech, movement and memory guarded by that part of the brain are vanished. The lost of function depends on the location of the stroke and on its severity i.e., the amount of brain cell loss. Several persons get well entirely from fewer severe strokes, while other strokes can be considered life threatening. Opposite treatments are required for both strokes namely ischemic stroke and hemorrhagic stroke.

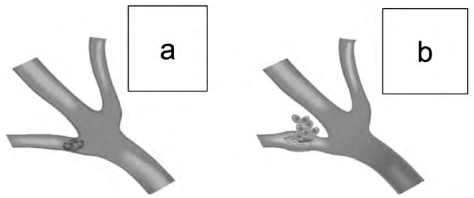


**Figure 1.** Brain Attack. a) Ischemic, b) Hemorrhagic Stroke.
**Suorce:** own elaboration.

## Brain Tumour

A tumour is unusual tissue that develops by unrestrained cell splitting up. Healing methods vary depending on the following factors such as tumour type, size, location, age and medical health of the person. Curing method may be therapeutic or attention on discharging indications.


**Figure 2.** MRI Brain Tumours.
**Suorce:** own elaboration.


https://doi.org/10.17993/3ctecno.2021.specialissue8.125-153

Primary brain tumours may be benign (non-cancerous) or malignant (cancerous). A benign brain tumour develops gradually and malignant brain tumour grows rapidly, has unequal boundaries, and spreads to close by brain areas. Sometimes they are called brain cancer. Whether a brain tumour is benign, malignant are potentially life-threatening. Grade means the way tumour cells look under the microscope and is a suggestion of aggressiveness. If the tumours are detected at near the beginning stage there is the opportunity of saving the life.

Cerebrovascular accident (CVA) is a damage caused because of functionality of brain due to lack of flow of blood (Adams *et al.*, 2005). This smash up is due to either ischemic or hemorrhage. Blockage of blood in blood vessels inside the brain is known as Ischemic stroke. Ischemicstroke results in about 80% deaths caused by all strokes. Bleeding of blood in blood vessels inside the brain is called Hemorrhagic stroke (Udupa & Samarasekera, 1996). In any case, the damaged area of the brain cannot function in a normal way. When brain cells expire, the tasks controlled by the region of the brain are vanished.

Kharat and Kulkarni (2012) presented the classification of brain tumors using neural networks. Due to complexity and variance, the MR image classification was a difficult task. Generally two neural network techniques were used.

The taken out features are categorized using Multi Layer Perceptron (MLP) (Amutha & Rajagopalan, 2013). Feature lessening is expertise by grade of the features using Information gain. Multilayer Perceptron (MLP) is used to categorize the extracted features.

Mid line of brain helps in measuring the brain's amount of equilibrium. Here, the brain's amount of equilibrium was determined using MLS technique (Dzialowski *et al.*, 2012). It can detect early identification of ischemic stroke to improvise effectiveness and correctness of medical practice.

Hema and Bhavani (2013) suggested SVM, K-NN, ANN and decision tree classification with accuracy of 98%, 97%, 96% and 92%. This system helped the physicians for enhanced detect of human brain stroke, for advance action. The brain area affected by abrasion can be accurately detached from the brain image. It improves the exactness in recognition of ischemic stroke.


https://doi.org/10.17993/3ctecno.2021.specialissue8.125-153

An improved watershed image segmentation technique was existing by Bala (2012). Watershed Transformation based an edge detection algorithm was used for image segmentation and makes use of gradient operators in mathematical morphology. But the drawback is over segmentation. To avoid over segmentation, Prewitt's edge detection operator with noise removal techniques and image enhancement wereestablished and the trouble of over segmentation was also reduced.

Mahmoud-Ghoneim *et al.* (2003) developed in intensity-based analysis. Features of different types can be calculated for texture analysis, such as co-occurrence matrix.

Udupa and Samarasekera (1996) presented the purpose fuzzy connectedness procedure has been applied. The grades of work have 0.750, 0.706, and 0.107 SI, OF, and EF respectively. Our proposed work has higher performance than the work by Udupa and Samarasekera (1996).

From the literature survey it was understood that fully automated system to detect stroke or tumour will assist the doctor very much. Till now separate algorithms are used for detecting tumour or stroke from brain MR image. In our proposed work it is possible to identify stroke or tumour with same algorithm by using different hybrid classifiers.

## 2. MATERIALS AND METHODS

The main objective is to detect the presence of Brain Abnormalities in MRI by Hybrid (SVM and ANFIS) classifiers. The Brain Abnormalities such as stroke and tumor images are classified by Image Intensity Threshold Level. After the classification, images are preprocessed. After preprocessing, the features are extracted and the Hybrid classifiers are used to segmentation and detection of Brain Abnormalities and also performance analysis if performed.


https://doi.org/10.17993/3ctecno.2021.specialissue8.125-153

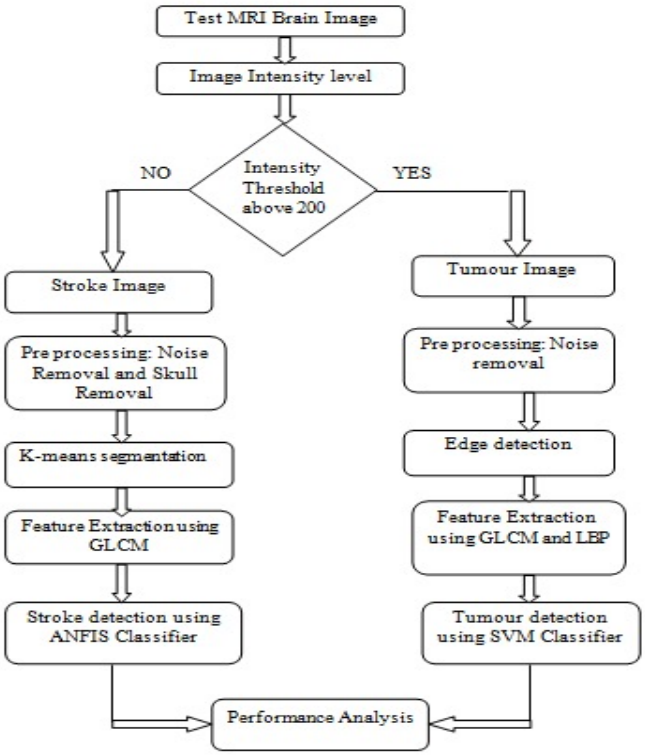


**Figure 3.** Proposed Data flow diagram.
**Suorce:** own elaboration.

## 2.1. PROPOSED METHOD FOR IDENTIFYING TUMOUR

If the tested MRI image intensity level is above 200, it will detect tumour otherwise to detect stroke as shown in the block diagram in Figure 4 the following steps will be carried in tumor segmentation:

- Pre-processing-Noise removal using Anisotropic filter.
- Canny Edge detection.
- Feature Extraction using GLCM matrix and LBP.
- Tumor detection using SVM classifier.


https://doi.org/10.17993/3ctecno.2021.specialissue8.125-153

### 2.1.1. PRE-PROCESSING-NOISE REMOVAL USING ANISOTROPIC FILTER

It is necessary to reduce image noise exclusive of removing noteworthy elements of the image content such as edges, lines or other elements those are significant for the understanding of the image.

The dataset of numerous diverse images of the brain tumour have studied and through testing threshold appropriate for those images are identified. Then, for same intensity ranges in all the images, the maximum and the smallest intensities are restricted to the range [0,255]. Then anisotropic diffusion is defined as,

$$\frac{\partial I}{\partial t} = div(c(x,y,t)\nabla I) = \nabla c \bullet \nabla I + c(x,y,t)\Delta I \tag{1}$$

where $\Delta$ means the Laplacian, $\nabla$ signifies the gradient, div (…) is the divergence operator and c(x,y,t) is the diffusion coefficient. C(x,y,t) organizes the degree of diffusion and is regularly preferred as a the image gradient so as to conserve boundaries in the image.

Pietro Perona and Jitendra Malik lead the way the knowledge of anisotropic diffusion in 1990 and projected two functions for the diffusion coefficient:

$$c(\|\nabla I\|) = e^{-(\|\nabla I\|/K)^2} \tag{2}$$

$$c(\|\nabla I\|) = \frac{1}{1+(\frac{\|\nabla I\|}{K})^2} \tag{3}$$

Where K manages the sensitivity to boundaries. The noise removed brain MR image byanisotropic filtering is shown in Figure 4.


https://doi.org/10.17993/3ctecno.2021.specialissue8.125-153

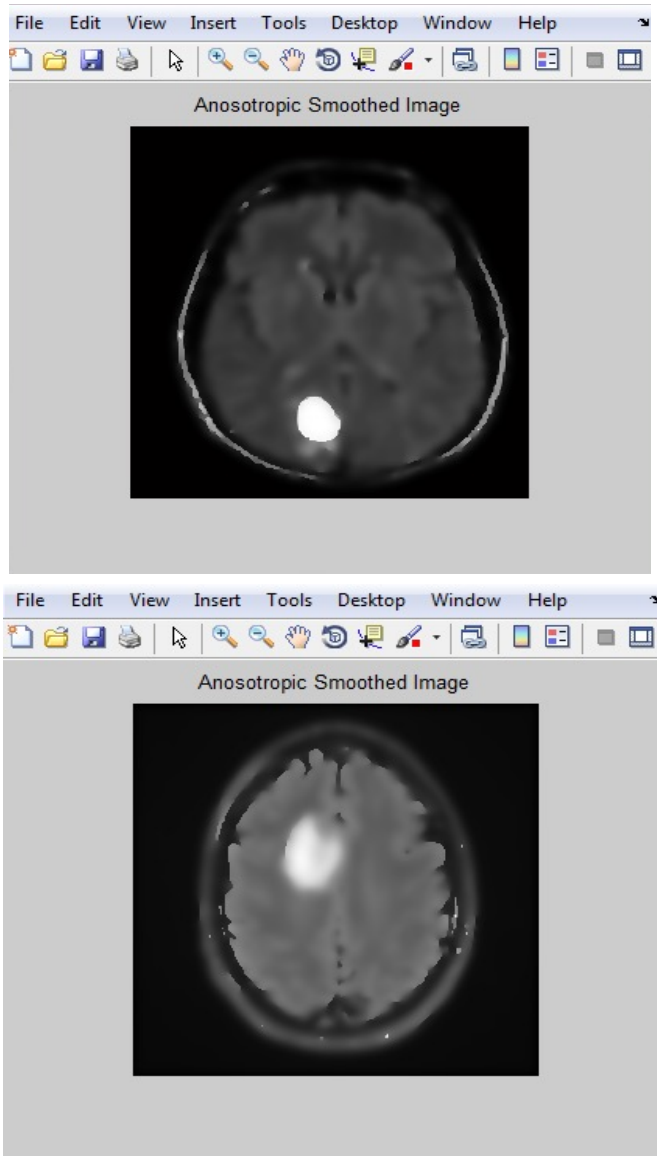


**Figure 4**. Noise Removed brain MR image using Anisotropic filter.
**Suorce**: own elaboration.

The noise filtered image, the intensity gradient of the image is found out. This is done by applying pair of convolution mask along the x and y directions. Then gradient strength and direction is found out using the formula.

$$G = \sqrt{G_x^{\,2} + G_y^{\,2}} \quad \theta = \arctan\left(\frac{G_y}{G_x}\right) \tag{4}$$


https://doi.org/10.17993/3ctecno.2021.specialissue8.125-153

The direction was rounded off to any possible angle values namely (0, 45, 90 and 135). By doing this operation pixel which belongs to edges of theimage will be maintained and the pixel which are not belong to edges of the image are removed. Canny provides two thresholds namely upper and lower. If the pixel gradient is larger than upper threshold value, that pixel is established as edge. If the pixel gradient is lesser than the lower threshold value, then it is discarded. The Canny Edge detected brain MRI is shown in Figure 5.

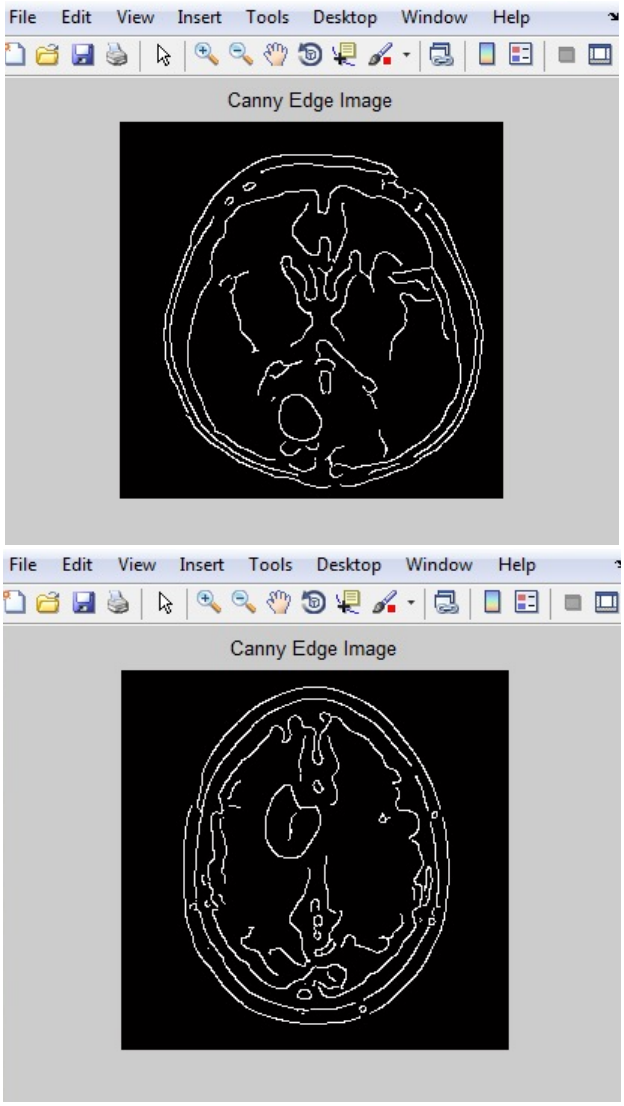


**Figure 5.** Canny Edge Detection.
**Suorce:** own elaboration.


https://doi.org/10.17993/3ctecno.2021.specialissue8.125-153

### 2.1.2 FEATURE EXTRACTION USING GLCM MATRIX AND LBP

The replicating pattern of local dissimilarity in image intensity is called consistency. This technique can be in consistency studies co-occurrence matrix. The information of pixel strength was expected from image that can be done using co-occurrence matrix. This pattern will compare by excellent consistency than by common consistency. The gray level co-occurrence matrix (GLCM) technique is a method of removing second order values stability elements. Though, the performance of a certain GLCM based on aspect, on top of the position the consistency characteristics; hinge on on the amount of gray levels applied. The subsequent representations are: mean value of P is represented as μ. were the means and standard deviations of Px and Py are denoted as μx, μy, σx and σy. The size of the occurrence matrix is represented as G. At this time the sum of rows and columns of co-occurrence matrix is identical. The subsequent GLCM characteristics are used in our study attempt: angular second moment, contrast, entropy, and correlation, sum of squares, variation entropy, inverse distinction moment, inertia, cluster importance, cluster shade, energy, homogeneity, distinction and diversity in variance. They are clear in following Equations.

1) Angular second moment (ASM):

$$ASM = \sum_{i-0}^{G-1} \sum_{j-0}^{G-1} \{p(i,j)\}^2 \tag{5}$$

ASM is a determined similarity of the image. A standardized image will enclose simply some gray intensities, GLCM provides simply a rare except comparatively elevated ideals of P (i, j).

2) Contrast:

$$Contrast = \sum_{n-0}^{G-1} n^2 \left\{ \sum_{i-1}^{G} \sum_{j-1}^{G} p(i,j) \right\}, |i-j| = n \tag{6}$$

It is determined for the limited deviation in an image.


https://doi.org/10.17993/3ctecno.2021.specialissue8.125-153

3) Inverse distinction moment (IDM):

$$IDM = \sum_{i-0}^{G-1} \sum_{j-0}^{G-1} \frac{1}{1+(i-j)^2} p(i,j) \tag{7}$$

IDM as well as inclined with the similarity of the image.

4) Entropy:

$$Entropy = -\sum_{i-0}^{G-1} \sum_{j-0}^{G-1} p(i,j) \times \log p(i,j) \tag{8}$$

It assesses the disarray or density of an image.

5) Correlation:

$$Correlation = \sum_{i-0}^{G-1} \sum_{j-0}^{G-1} \frac{\{(i \times j) \times p(i,j) + (\mu_x \times \mu_y)\}}{\sigma_x \times \sigma_y} \tag{9}$$

It is calculated for gray level linear reliance

6) Sum of squares, variance:

$$\text{var} = \sum_{i-0}^{G-1} \sum_{j-0}^{G-1} (i-\mu)^2 p(i,j) \tag{10}$$

It is calculated for gray level dissimilarities at an assured distance, d.

7) Variation entropy:

$$D_{Ent} = -\sum_{i-0}^{G-1} p_{(x+y)}(i) \log(p_{x+y}(i)) \tag{11}$$

Variation entropy is an evaluate, of histogram satisfied and rational rate among two images.


https://doi.org/10.17993/3ctecno.2021.specialissue8.125-153

8) Inertia:

$$Inertia = \sum_{i-0}^{G-1} \sum_{j-0}^{G-1} (i-j)^2 \times p(i,j) \tag{12}$$

The inertia specifies the portion of gray scales in the image.

9) Cluster shade:

$$Shade = \sum_{i-0}^{G-1} \sum_{j-0}^{G-1} \left\{ i + j - \mu_x - \mu_y \right\}^3 \times p(i,j) \tag{13}$$

The image is not symmetric while darkness is elevated.

10) Cluster prominence:

$$\Pr om = \sum_{i-0}^{G-1} \sum_{j-0}^{G-1} \left\{ i + j - \mu_x - \mu_y \right\}^4 \times p(i,j) \tag{14}$$

Cluster Prominence specifies the image is not symmetric while prominences are elevated.

11) Energy:

$$Energy = \sum_{i-0}^{G-1} \sum_{j-0}^{G-1} p(i,j)^2 \tag{15}$$

The energy of a surface explains the evenness of the surface. Energy is one for a stable image.

12) Homogeneity:

$$Homogenity = \sum_{i-0}^{G-1} \sum_{j-0}^{G-1} \frac{p(i,j)}{1+|i-j|} \tag{16}$$

Homogeneity proceeds a worth that events the nearness of the allocation of essentials in the GLCM to the GLCM slanting. It is 1 for a slanting GLCM. A standardized image will effect in a co-occurrence matrix with a mixture of elevated and short P [i, j]'s. A varied image will effect in an even extend of P [i, j]'s.


https://doi.org/10.17993/3ctecno.2021.specialissue8.125-153

13) Distinction:

$$Distinction = \sum_{i-0}^{G-1} \sum_{j-0}^{G-1} |i - j| \times p(i, j) \tag{17}$$

It is determined to find constancy between two groups.

14) Diversity in variance:

$$\text{var} = \sum_{i-0}^{G-1} \sum_{j-0}^{G-1} (i - \mu)^2 \times p(i, j) \tag{18}$$

It is the summation of divergence among greatness of the middle pixel and its locality. The GLCM feature is tabulated in Figure 6.

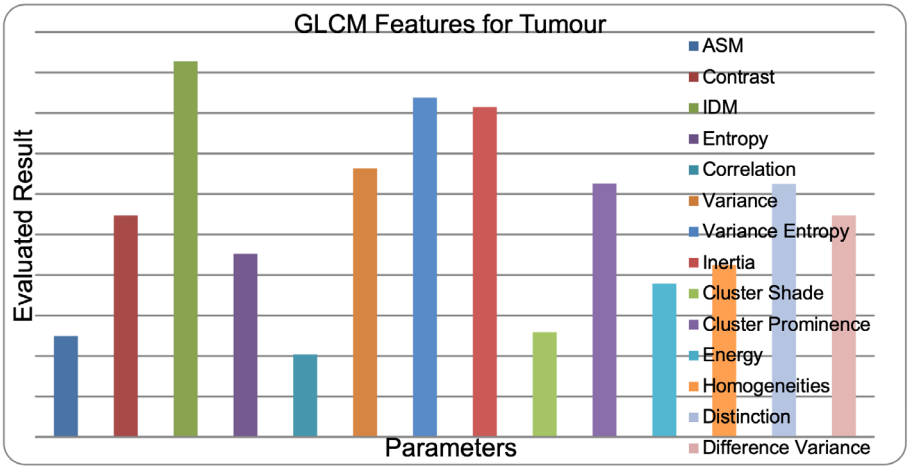


**Figure 6.** GLCM Features performance for Tumour.
**Suorce:** own elaboration.

Local Binary Patterns: the LBP feature vector is fashioned in the following manner:

- The inspected space is segregated into chambers (e.g. 16x16 pixels for each chamber).
- For every pixel in a chamber, evaluate the pixel to each one of its 8 neighbors (on its left-top, left-middle, left-bottom, right-top, etc.) either in clockwise or counter-clockwise.


https://doi.org/10.17993/3ctecno.2021.specialissue8.125-153

- If the middle pixel's value is superior to the nearby value then replace with "1". If not, replace with "0". Thus 8-digit binary number (which is generally changed to decimal).
- Histogram is computed over the cell (i.e., arrangement of pixels are lesser or larger than the midpoint) and feature vector of the box is obtained.
- The feature vector can be trained using the Support Vector Machine (SVM) and ANFIS to classify images.

### 2.1.3 TUMOR DETECTION USING SVM CLASSIFIER

SVM fundamentally tries to split the given data into decision plane. Decision plane is a hyper plane which splits the data into two classes. Training points obtained by the feature vectors are the supporting vector which describes the hyper plane. The training data x contains of n data trials each of m dimensions and fitting to class y, is expressed as:

$$(x_1, y_1)...(x_i, y_i)...(x_n, y_n), x\xi R^m, y\xi\{+1,-1\} \quad (19)$$

**Table 1**. GLCM Matrixfor Tumor Results.

| PARAMETERS | RESULTS |
|---|---|
| ASM | 2.49 |
| Contrast | 5.47 |
| IDM | 9.28 |
| Entropy | 4.52 |
| Correlation | 2.04 |
| Variance | 6.63 |
| Variance Entropy | 8.38 |
| Inertia | 8.15 |
| Cluster Shade | 2.59 |


https://doi.org/10.17993/3ctecno.2021.specialissue8.125-153

| | |
|---|---|
| Cluster Prominence | 6.26 |
| Energy | 3.79 |
| Homogeneities | 4.25 |
| Distinction | 6.25 |
| Difference Variance | 5.47 |

**Source:** own elaboration.

SVM assigns data (xi ,y) into an infinitedimensional hyper plane (xi ,y) by using Gaussian kernel function and describes its rule decision as sign (f(x)). The discriminant function f(x) produces the optimal hyper plane decision border by using weight vector w* and bias b*.

$$f(x) = w^{*}\phi(x) + b^{*} \tag{20}$$

The optimal values of w* and b are assessed by explaining the following optimization problem.

$$\min_{w,\xi}\{\frac{1}{2}w^{2} + C\sum_{i=1}^{n}\xi_{i}\}; y_{i}(w.\phi(x_{i}) + b)) \geq 1 - \xi_{i}, \xi_{i} \geq 0 \tag{21}$$

where, C is regularization constraint, which lastly produces optimum level for weight vector w* and bias b*. Figure 7 represents the malignant brain tumour identified image by using SVM classifier.

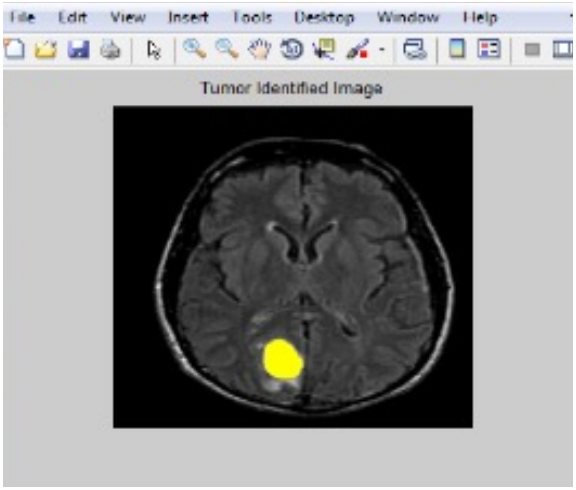



https://doi.org/10.17993/3ctecno.2021.specialissue8.125-153

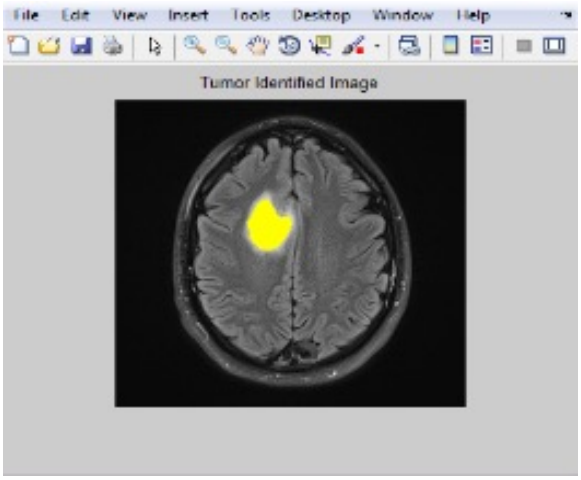


**Figure 7.** Tumour Identified Image.
**Suorce:** own elaboration.

## 2.2. PROPOSED FOR IDENTIFYING STROKE

If the tested MRI image intensity level is below 200, it will detect stroke otherwise to detect tumour. The following steps will be carried in stroke segmentation as shown in Figure 4. All process are same except the classifier.

- Noise and skull removal in pre processing.
- K-means segmentation.
- Feature Extraction using GLCM.
- Stroke detection using ANFIS classifier.

### 2.2.1. PRE-PROCESSING-NOISE AND SKULL REMOVAL

The same preprocessing steps of brain tumor MRI is carried over here The noisy image removed from noise and skull is shown in Figure 8.


https://doi.org/10.17993/3ctecno.2021.specialissue8.125-153

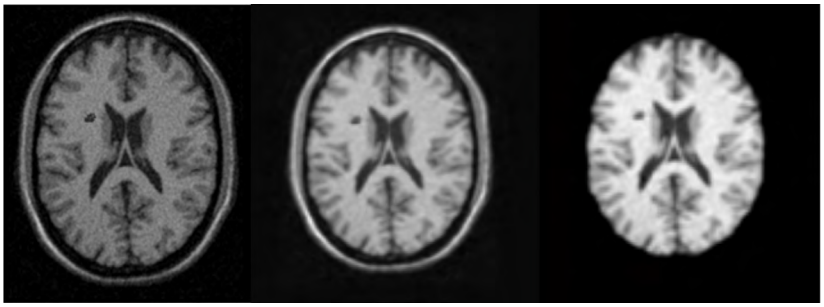

**Figure 8.** (a) Noise affected image. (b) noise removed image. (c) Skull removed image.
**Suorce:** own elaboration.

### 2.2.2 K-MEANS SEGMENTATION

K-means clustering targets to divide n interpretations into k clusters in which each reflection belongs to the cluster with the near mean, helping as a model of the cluster.

The subsequent steps of K-means:The total number of clusters k with primary cluster centroid was chosennvi=1,2,…k (22)

Separation of the input statistics points into k clusters with allocating everystatistics element xj to the neighbouring cluster centroid vi by nominated distance extent. Euclidean distance equation was given as,

$$d_{ij} = \left\| X_j - v_i \right\| \tag{23}$$

Where X = {x1, x2, . . .xn} is the input data set.

Cluster transfer matrix Ui calculated which is the separation of the data points with the binary bias value of the jth data point to the ith cluster such that U = |ui, j| and u i, j in {0,1}for all i, j

$$\sum_{i-1}^{k} u_{ij} = 1 for all j and 0 < \sum_{j-1}^{n} u_{ij} < n \quad for \quad all \quad 1 \tag{24}$$

Centroid is rearranged using the membership values by


https://doi.org/10.17993/3ctecno.2021.specialissue8.125-153

$$v_i = \frac{\sum_{j-1}^{n} u_{ij} X_j}{\sum_{ij-1}^{n} u_{ij}} \quad for \quad all \quad i \tag{25}$$

The iteration will be carried over by step 2, until there is no change in the centroid of the cluster from the previous iteration. The k-means clustering process improves the sum-of-squared-error-based objective function Jw(u, v) then

$$J_W(u,v) = \sum_{i-1}^{n} \sum_{j-1}^{n} \left\| X_j - v_i \right\|^2 \tag{26}$$

The projected method K-means clustering is exact hopeful algorithm for clustering formation from Ischemic stroke MR image. To test our projected technique a Magnetic Resonance Imaging (MRI) image of human brain was taken. The k-mean segmented image is given in the Figure 9.

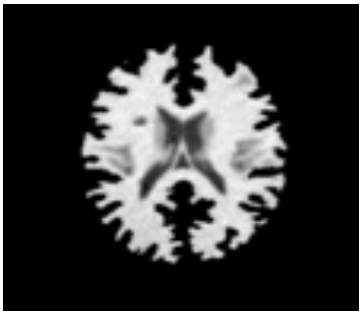

**Figure 9**. k-means clustering image.
**Suorce:** own elaboration.

### 2.2.3 FEATURE EXTRACTION USING GLCM

The feature extraction is carried as in brain tumour MRI. The features are tabulated in Table 2. In Figure 10 GLCM features analysis of stroke graph is provided.


https://doi.org/10.17993/3ctecno.2021.specialissue8.125-153

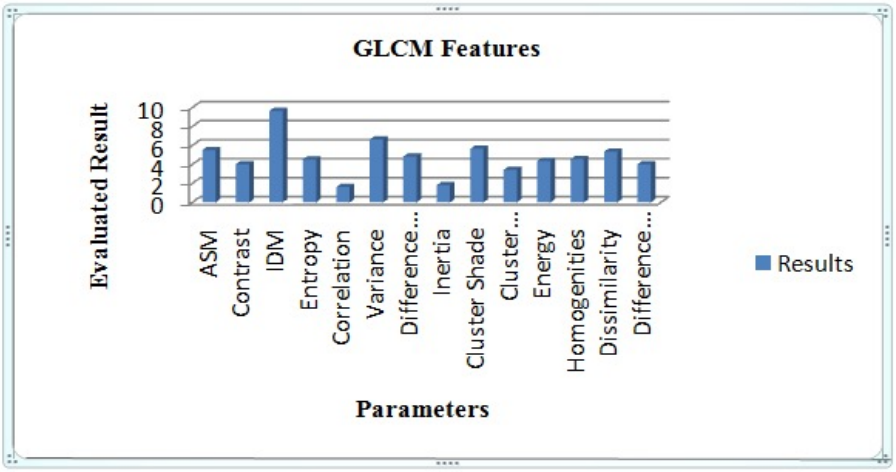


**Figure 10.** GLCM Features performance for stroke.
**Suorce:** own elaboration

**Table 2.** GLCM Matrix for Stroke Results.

| PARAMETERS | RESULTS |
|---|---|
| ASM | 5.51 |
| Contrast | 4.02 |
| IDM | 9.63 |
| Entropy | 4.52 |
| Correlation | 1.62 |
| Variance | 6.63 |
| Variance Entropy | 4.83 |
| Inertia | 1.81 |
| Cluster Shade | 5.64 |
| Cluster Prominence | 3.43 |
| Energy | 4.35 |
| Homogeneities | 4.55 |
| Distinction | 5.33 |
| Difference Variance | 4.02 |

**Suorce:** own elaboration.


https://doi.org/10.17993/3ctecno.2021.specialissue8.125-153

Stroke detection using ANFIS classifier

It uses hybrid knowledge technique that proposes ANFIS to build an input-output plotting model. In the simulation, the ANFIS architecture uses IF THEN rules.

ANFIS Architecture

Assume - two inputs X and Y and one output Z

Rule 1: If x is A1 and y is B1,

then f1=p1x+q1y+r1 (27)

Rule 2:If x is A2 and y is B2,

then f2 = p2x + q2y +r2 (28)

Layer 1

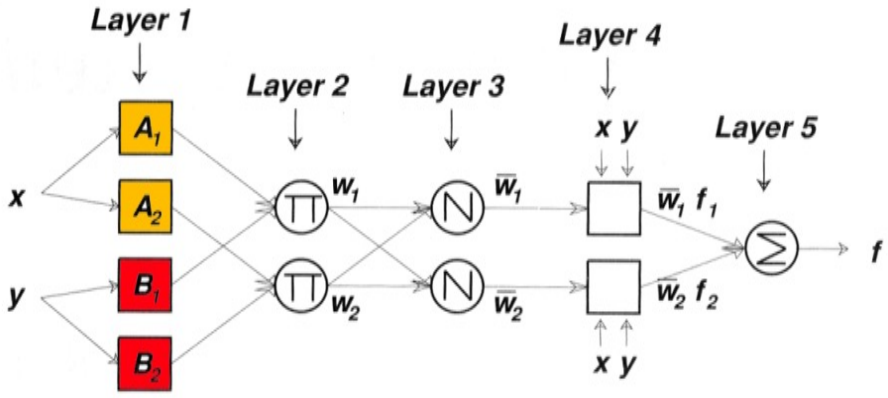


**Figure 11**. Layer Architecture of ANFIS.
**Suorce:** own elaboration.

Every node i in this layer is an adaptive node with a node function, O1,i = mAi (x), for I = 1,2, or O1,i = mBi-2 (y), for I = 3,4 (29)


https://doi.org/10.17993/3ctecno.2021.specialissue8.125-153

Layer 2

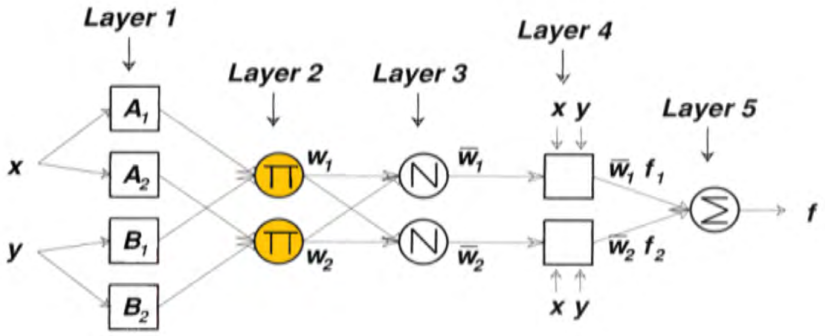


**Figure 12.** 2nd layer Architecture of ANFIS.
**Suorce:** own elaboration.

Every node i in 2nd layer is a fixed node labeled ∏, whose yield is the multiplication of all the incoming signals:

$$O2,i = Wi = \min\{mAi\,(x)\,,\, mBi\,(y)\},\ i = 1,2 \tag{30}$$

Each node output characterizes the firing asset of an instruction.

Layer 3

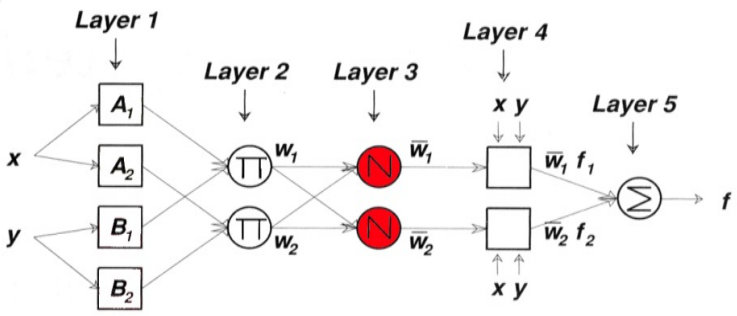


**Figure 13.** 3rd layer Architecture of ANFIS.
**Suorce:** own elaboration.

Every node in 3rd layer is a fixed node labeled N.

$$O3,i = Wi = Wi\ /(W1+W2)\ ,\ i = 1,2 \tag{31}$$


https://doi.org/10.17993/3ctecno.2021.specialissue8.125-153

The ith node estimates the proportion of the ith instruction's firing asset to the sum of all rules'firingstregths.

Layer 4

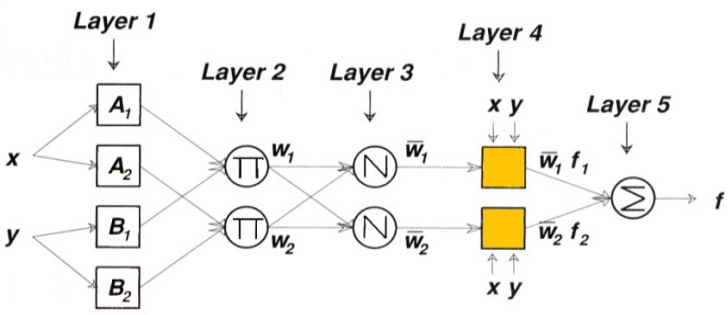


**Figure 14-15.** 4th layer Architecture of ANFIS.
**Suorce:** own elaboration.

Every node i in this layer is an adaptive node with a node function,

$$O_{4,i} = \bar{w}_i f_i = \bar{w}_i (p_i x + q_i y + r_i) \ldots \text{Consequent parameters.} \quad (32)$$

Layer 5

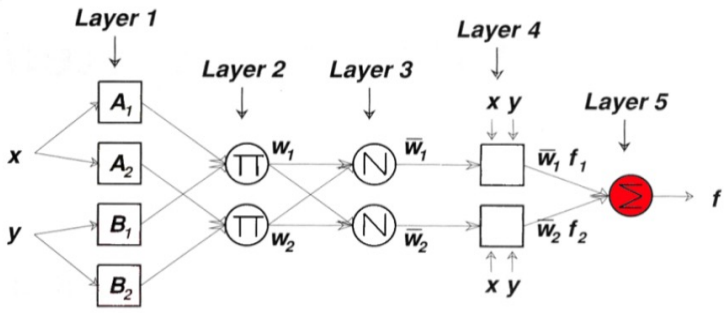


**Figure 15.** 5th layer Architecture of ANFIS.
**Suorce:** own elaboration.

The nodes in this layer is a stable node labeled S, used to calculate the complete yield as the summation of all received signals.

$$O_{5,1} = \sum_i \bar{w}_i f_i. \quad (33)$$

By using ANFIS classifier, stroke can be detected and is shown in Figure 16.


https://doi.org/10.17993/3ctecno.2021.specialissue8.125-153

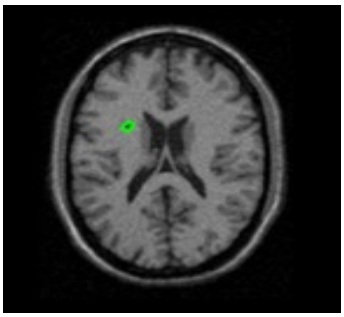

**Figure 16.** Stroke Identified Image.
**Suorce:** own elaboration.

# 3. RESULTS

## 3.1. PERFORMANCE ANALYSIS FOR STROKE USING ANFIS CLASSIFIER

The classifier namely ANFIS had established to ischemic brain and normal brain. The performance of the classifier in provisions of sensitivity, specificity and accuracy was estimated. The performances are tabulated in Table 3. The accuracy obtained in 0.99 using ANFIS classifier.

Human brain stroke can be diagnose using this proposed system. Accuracy of 0.998428 isobtained by ANFIS classifier. In Figure 17 performance analysis graph is given using ANFIS classifier.

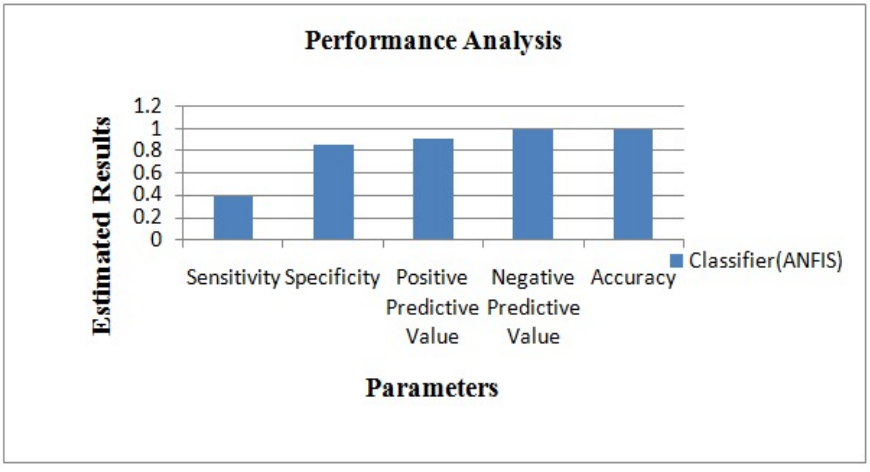


**Figure 17.** Performance Evaluation Graph in Stroke.
**Suorce:** own elaboration


https://doi.org/10.17993/3ctecno.2021.specialissue8.125-153

## 3.2. PERFORMANCE ANALYSIS OF TUMOUR

The SVM Classifiers had established to classify benign brain tumour and malignant brain tumour. The performance of the classifiers in provisions of similarity index, overlap fraction and Extra fraction was estimated.

Three quantitative events to calculate in the region of the segmentation result are Similarity Index (SI), Overlap fraction (OF), and Extra Fraction (EF).

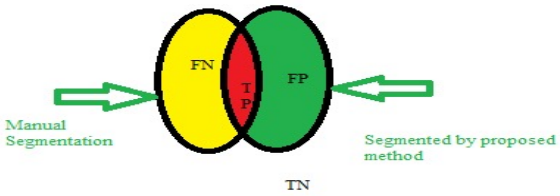


**Figure 18.** Comparison between the various performance parameter by proposed segmented regions and manual segmentation.
**Suorce:** own elaboration.

Figure 18 shows that TP is the amount of true-positive pixels identified by manual segmentation and proposed method, FP is the amount of false-positive pixels noticed by manual segmentation and proposed method, and FN is the amount of false-negative pixels comparative to the tumourarea with manual segmentation but it is not identified by the proposed method.

$$\text{Overlap Fraction} = \frac{TP}{TP + FN} \tag{34}$$

$$\text{Extra Fraction (EF)} = \frac{FP}{TP + FN} \tag{35}$$

$$\text{Similarity Index} = \frac{2 \times TP}{2 \times TP + FP + FN} \tag{36}$$

In a worthy segmentation Similarity Index (SI), Overlap Fraction (OF) which are achieved by equations (36), (34) should be high and Extra fraction (EF) obtained by equation (35)


https://doi.org/10.17993/3ctecno.2021.specialissue8.125-153

should be low. The performances are tabulated in Table 3. In Figure 17 performance analysis graphs are given.

**Table 3.** Segmentation.

| PARAMETERS | SIMILARITY INDEX (SI) | OVERLAP FRACTION (OF) | EXTRA FRACTION (EF) |
|---|---|---|---|
| Tumour Image set 1 | 0.785531 | 0.783523 | 0.211364 |
| Tumour Image set 2 | 0.766866 | 0.766866 | 0.233134 |
| Average | 0.776198 | 0.775194 | 0.222249 |

**Suorce:** own elaboration.

## 4. DISCUSSION

Our projected method is executed in MATLAB. The projected method has been tried on dataset of real brain MR images containing of normal and tumor brain images. Hybrid classifier for detecting abnormalities in brain has been proposed. The abnormality may be stroke or brain tumour. Separate algorithm will be used for detecting brain tumour and stroke. In the projected method, the abnormality region is segmented and it is treated as test image. Based on the intensity level of the abnormalities, either it will detect stroke or tumour. If the threshold value is less than 200 then it will be considered as stroke brain MRI. Then pre-processing and skull removal of image is carried out. After which the segmentation is passed out by using K-means algorithm. Then from the segmented result, features are extracted using GLCM matrix in order to train the ANFIS classifier and performance analysis is carried out. If the threshold value is above 200 then it will be considered as tumour brain MRI. Then pre-processing and edge detection of image is carried out by using anisotropic filter and canny edge detections method. After which the segmentation is passed out by K-means algorithm. Features are extracted using GLCM matrix and LBP in order to train the SVM classifier and performance analysis is carried out in terms of Similarity Index (SI), Overlap Fraction (OF), and Extra Fraction (EF).


https://doi.org/10.17993/3ctecno.2021.specialissue8.125-153

## 5. CONCLUSIONS

The proposal of image segmentation and classification appears to be an interesting task, as the medical images are exposed to noise. In particular anisotropic filter based image de-noising scheme proves to be an efficient method for noise removal. Computer aided detection system helps in detecting ischemic stroke and malignant brain tumor has been developed. This system detects to generate accurate quantitative results. The proposed system helps the physicians to diagnose human brain stroke. Accuracy of 0.999, sensitivity 0.38, specificity 0.86, PPV 0.91, NPV 0.99 is obtained by ANFIS classifier. Three quantitative events to calculate brain tumor of average segmentation results: Similarity Index (SI), Overlap fraction (OF), and Extra Fraction (EF) is 0.776194, 0.775198, 0.222213 is obtained by SVM classifier. It usually aided to progress the accuracy in detection of malignant brain tumor.

## ACKNOWLEDGEMENT

We would like to thank our institution Kalasalingam Academy of Research and Education for support.

## REFERENCES

**Adams, H., Adams, R., Zoppo, G. del, & Goldstein, L. B.** (2005). Guidelines for the early management of patients with ischemicstroke, guidelines update, a scientific statement from the Stroke Council of the American Heart Association/ American Stroke Association. *Stroke, 36*(2), 916–921. https://doi.org/10.1161/01.STR.0000163257.66207.2d

**Amutha, C., & Rajagopalan, S. P.** (2013). Brain stroke classification based on MultiLayer Perceptron using Watershed segmentation. *Journal of Theoretical and Applied Information Technology, 56*(2), 410-416. https://www.researchgate.net/publication/285940599_Brain_stroke_classification_based_on_multi-layer_perceptron_using_watershed_segmentation_and_gabor_filter


https://doi.org/10.17993/3ctecno.2021.specialissue8.125-153

**Bala, A.** (2012). An Improved Watershed Image Segmentation Technique using MATLAB. *International Journal of Scientific & Engineering Research, 3*(6), 5-8. https://www.ijser.org/researchpaper/an-improved-watershed-image-segmentation-technique-using-matlab.pdf

**Bian, W., Hess, C. P., Chang, S. M., Nelson, S. J., & Lupo, J. M.** (2013). Computer-aided detection of radiation-induced cerebral micro bleeds on susceptibility-weighted MR images. *NeuroImage: Clinical, 2*, 282–290. https://pubmed.ncbi.nlm.nih.gov/24179783/

**Dzialowski, I., Hill, M. D., Coutts, S. B., Demchuk, A. M., Kent, D. M., Wunderlich, O., & von Kummer, R.** (2012). Extent of Early Ischemic Changes on Computed Tomography (CT) Before Thrombolysis Prognostic, Value of the Alberta Stroke Program Early CT Score in ECASS II. *Stroke, 37*(4),973-978. https://doi.org/10.1161/01.STR.0000206215.62441.56

**Ford, A. L., An, H., Vo, K. D., Lin, W., & Lee, J.-M.** (2012). Defining the Ischemic penumbra using hyper active neuroimaging: driving quantitative Ischemic Thresholds. *Translational Stroke Research, 3*(2), 198-204. https://pubmed.ncbi.nlm.nih.gov/24323775/

**Grady, L.** (2006). Random Walks for Image Segmentation. *IEEE Transactionson Pattern Analysis and Machine Intelligence, 28*(11), 1768–1783. https://ieeexplore.ieee.org/document/1704833

**Grady, L., & Schwartz, E. L.** (2006). Isoperimetric Graph Partitioning for Image Segmentation. *IEEE Transactionson Pattern Analysis and Machine Intelligence, 28*(3), 469–475. https://ieeexplore.ieee.org/document/1580491

**Hema, N., & Bhavani, R.** (2013). Computer aided detection of ischemic stroke using segmentation and texture features. *Measurement,* (46), 1865-1874. https://www.infona.pl/resource/bwmeta1.element.elsevier-6cea82e0-3e95-37c1-81e7-b48eb7905e72

**Kharat, K. D., & Kulkarni, P. P.** (2012). Brain Tumor Classification Using Neural Network Based Methods. *International Journal of Computer Science and Informatics*


https://doi.org/10.17993/3ctecno.2021.specialissue8.125-153

*ISSN (PRINT)*, *1*(4), 2231–5292. https://www.interscience.in/cgi/viewcontent.cgi?article=1075&context=ijcsi

**Mahmoud-Ghoneim, D., Toussaint, G., Constans, J.-M., & Certaines, J. D. de.** (2003). Three dimensional texture analysis in MRI: a preliminary evaluation in gliomas. *Magnetic Resonance Imaging, 21*(9), 983-987. https://doi.org/10.1016/S0730-725X(03)00201-7

**Rekik, I., Allassonnière, S., Carpenter, T. K., & Wardlaw, J. M.** (2012). Medical image analysis methods in MR/CT-imaged acute-subacute ischemic stroke lesion: Segmentation, prediction and insights into dynamic evolution simulation models. *NeuroImage: Clinical, 1*(1), 164–178. https://doi.org/10.1016/j.nicl.2012.10.003

**Runchey, S., & McGee, S.** (2010). Does This Patient Have a Hemorrhagic Stroke?. JAMA: *the journal of the American Medical Association, 303*(22), 2280-2286. https://doi.org/10.1001/jama.2010.754

**Shi, J., & Malik, J.** (2000). Normalized Cuts and Image Segmentation. *IEEE Transactionsonpatternanalysis and machine intelligence, 22*(8), 888-905. https://ieeexplore.ieee.org/document/868688

**Thom, T., Haase, N., Rosamond, W., Howard, V. J., Rumsfeld, J., Manolio, T., Zheng, Z.-J., Flegal, K., O'Donnell, C., Kittner, S., Lloyd-Jones, D., Goff, D. D., Hong, J., Adams, R., Friday, G., Furie, K., Gorelick, P., Kissela, B., Marler, J., … & Wolf, P.** (2006). Heartdisease and stroke statistics update: a report from the American Heart Association Statistics Committee and Stroke Statistics Subcommittee. *Circulation, 113*(6), 85–151. https://pubmed.ncbi.nlm.nih.gov/16407573/

**Toni, D., Iweins, F., von Kummer, R., Busse, O., Bogousslavsky, J., Falcou, A. E., Lesaffre, E., & Lenzi, G. L.** (2006). Identification of lacunar in farcts before thrombolysis in the ECASS 1 study. *Neurology, 54*(2),684–688. https://pubmed.ncbi.nlm.nih.gov/10680804/


https://doi.org/10.17993/3ctecno.2021.specialissue8.125-153

**Udupa, J., & Samarasekera, S.** (1996). Fuzzy Connectedness and Object Definition: Theory, Algorithms, and Applications in Image Segmentation. *CVGIP Graph. Model. Image Process., 58,* 246-261. https://www.semanticscholar.org/paper/Fuzzy-Connectedness-and-Object-Definition%3A-Theory%2C-Udupa-Samarasekera/4a3e9fcfc88d53cdf0b7633fbc914f98d1e92225

**Von Kummer, R.** (2005). The impact of CT on acute stroke treatment. In P. Lyden (ed.), *Thrombolytic Therapy for Stroke.* Humana Press, pp. 249–278.


https://doi.org/10.17993/3ctecno.2021.specialissue8.125-153

# /10/


https://doi.org/10.17993/3ctecno.2021.specialissue8

# A STUDY ON QUEUING ISSUE IN TACTICALL ENVIRONMENT

**S. Radha**
Research Scholar, Department of Mathematics, Kalasalingam Academy of Research and Education, Krishnankovil, (India).
E-mail: kradhai87@gmail.com
ORCID: https://orcid.org/0000-0003-0507-2794

**S. Maragathasundari**
Associate Professor, Department of Mathematics, Kalasalingam Academy of Research and Education, Krishnankovil, (India).
E-mail: maragatham01@gmail.com
ORCID: https://orcid.org/0000-0003-1210-6411

**P. Manikandan**
Assistant Professor, Department of Electronics and Communication Engineering, Kalasalingam Academy of Research and Education, Krishnankovil, (India).
E-mail: maanip85@gmail.com.
ORCID: https://orcid.org/0000-0002-5737-0235

**Recepción:** 25/10/2019 **Aceptación:** 29/09/2020 **Publicación:** 30/11/2021

**Citación sugerida:**
Radha, S., Maragathasundari, S., y Manikandan, P. (2021). A study on queuing issue in tacticall environment. *3C Tecnología. Glosas de innovación aplicadas a la pyme, Edición Especial*, (noviembre, 2021), 155-177. https://doi.org/10.17993/3ctecno.2021.specialissue8.155-177

## ABSTRACT

TactiCall MCI empowers direct correspondence from the individual mariner to central command. It encourages the proficient and quick trade of information and voice all through the whole system, using the best accessible data transmission paying little respect to the strategic condition. TactiCall MCI's stage independency will enable you to keep up your inheritance hardware while streamlining your operational effectiveness through, for example, specially appointed directing. TactiCall MCI will keep you associated with your very own powers, joint powers and partners while ideally abusing the accessible limit and improving your situational mindfulness and operational proficiency. This study represents the fact of Queuing issue consisting of different aspects like stages of service, service interruption , maintenance work and revamp process in TACTI CALL environment. This problem is well analyzed by means of supplementary variable method of Queuing approach. As a result we derive all the Queue performance measures of the above queuing issue. Numerical illustration and the graphical representation elaborate the explanation of the result at the end for the TactiCall environment queuing issue.

## KEYWORDS

Service, Long vacation, Reneging, Short vacation, Service interruption, Repair, Delay.


https://doi.org/10.17993/3ctecno.2021.specialissue8.155-177

# 1. INTRODUCTION

TactiCall MCI the executives interface utilizes a customer/server based HMI that is gotten to by verified T-MCI administrators utilizing standard HTTPS. T-MCI the executives administrators utilize this interface to control the switch and transmission frameworks. The administration HMI is actualized as a major aspect of the item and consequently requires no incorporation exertion. T-MCI likewise gives an immediate checking and control interface to applications (machine-to-machine). One of the essential employments of this interface is for T-MCI to give correspondence framework status data to applications on a sub-second reason for stream control purposes. This recreates the customary communication where an application is associated straightforwardly to the radio however without the burdens related with such stove channeling. T-MCI gives broad system checking data abilities by means of both the administration and application interfaces.

Artino, Folga, and Swan (2006) depicted another hypoxia worldview that consolidated the ROBD with strategic flight triggers. Majumdar (2005) gave the measurable estimation and calculation of correspondence parameters utilized in planning and advancing laser correspondence frameworks that were dependable under every single climate condition. Echols (2004) created specialized gauges that would take into account accomplishments of interoperability between worldwide strategic correspondence systems.

Chatterjee and Pal (1993) gave a diagram of the exceptional highlights and future patterns in satellite correspondence. Misra, Misra, and Tripathi (2013) talked about the progression of various applications viewpoint present and future in satellite correspondence. Erkan and Uzun (2004) depicted the essential highlights and client administrations of TASMUS and with the help of concurrent voice and information capacities, TASMUS intended to shape versatile, survivable, adaptable and secure system to help all the present and future correspondence prerequisites of the strategic leaders. Holmström, Rajamäki, and Hult (2011) accomplished the part hazards among administrators and correspondence channels; better directing and need capacities; considering security and interruption chances and including particularity.

Burkholder-Allen *et al.* (2009) displayed the Boutulism Questionnaire, which would help with the screening of setbacks, gave instructive and indicative signs to clinician and the


https://doi.org/10.17993/3ctecno.2021.specialissue8.155-177

lay open, and made a layer of insurance for the social insurance framework. Suri *et al.* (2009) saw from a few strategic systems administration tests and shows the exercises gained from organization of the Mockets middleware to help strategic correspondences. Crainic (1988) surveys the fundamental issues with respect to the strategic arranging of cargo rail transportation and the important models tending to these issues. Maragathasundari and Sowmiyah (2015) made an investigation M/G/1 Queuing System with expanded excursion, administration interference; defer time and stages in fix. Strategic arranging models for inventory network the board analyzed by Swaminathan and Tayur (2003). Maragathasundari, Srinivasan, and Ranjitham (2014) researched clump landing queuing framework with two phases of administration.

## 1.1. TACTICALL MCI

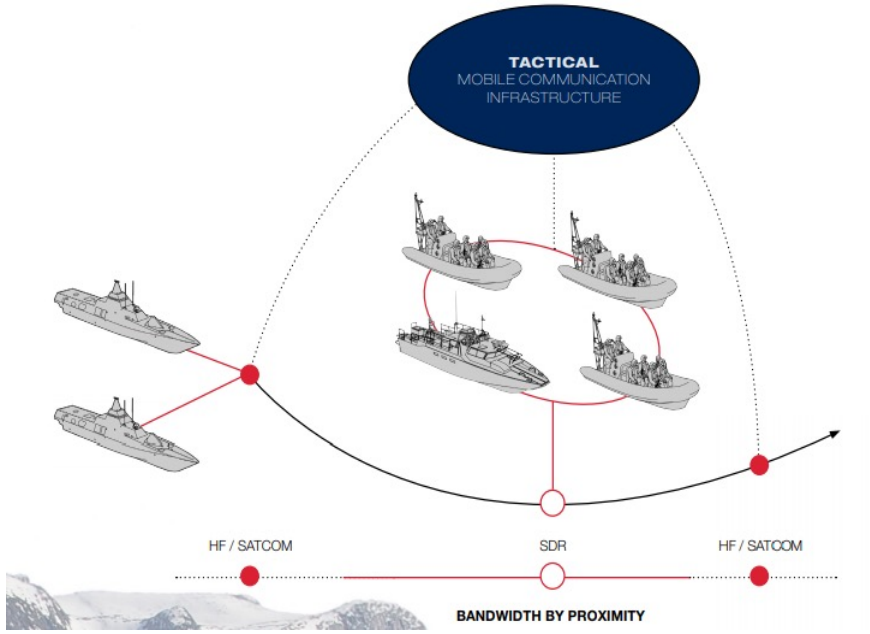


**Graphic 1.** Tactical Mobile Communication Infrastructure.
**Source:** own elaboration.

TactiCall MCI is worked to help your operational necessities, keeping you associated with your system by conveying a hearty and secure voice and information correspondence arrangement. TactiCall MCI is a QoS - and asset mindful strategic switch that oversees


https://doi.org/10.17993/3ctecno.2021.specialissue8.155-177

access to correspondence administrations (for example given by radios) for mixed media applications and arranged gadgets. TactiCall MCI's measured and versatile plan underpins inheritance joining in light of future development.

Utilize accessible heritage hardware, coordinate with IP systems administration and downplay relocation cost. Well-ordered delicate and equipment redesigns dependent on operational needs. Future-verification through simple well-ordered updates and extra usefulness Job based login. Evacuating stovepipes by presenting use of shared correspondence assets dependent on strategic conditions and current transmission prerequisites. Limit accumulation through organized data transfer capacity determination. Remote and adaptable administration of whole system through IP technology. Enhanced heartiness utilizing dynamic directing. Consistent incorporation of heterogeneous systems.

From the next section onwards various factors like service rendered in the tacticall, different types of maintenance works, kinds of interruptions, delay in getting into the repair process and how the repair is carried out are explained in detail.

## 1.2. AD-HOC ROUTING

TactiCall MCI automatically chooses the highest possible bandwidth at all times – guaranteeing the best communication path available.

*1) Operational Ad-Hoc routing.*

*2) Maximizing network performance.*

*3) Automatically optimizing bandwidth selection.*

*4) Enabling seamless data traffic.*

TactiCall MCI can be given as a virtual machine and facilitated on existing figuring equipment – implying that no new equipment is required. TactiCall MCI will guarantee stepwise incorporation and updates as per operational and mechanical prerequisites. TactiCall MCI programming coordinated into effectively existing equipment guarantees a cost productive and future-confirmation arrangement that consolidates existing in-administration gear.


https://doi.org/10.17993/3ctecno.2021.specialissue8.155-177

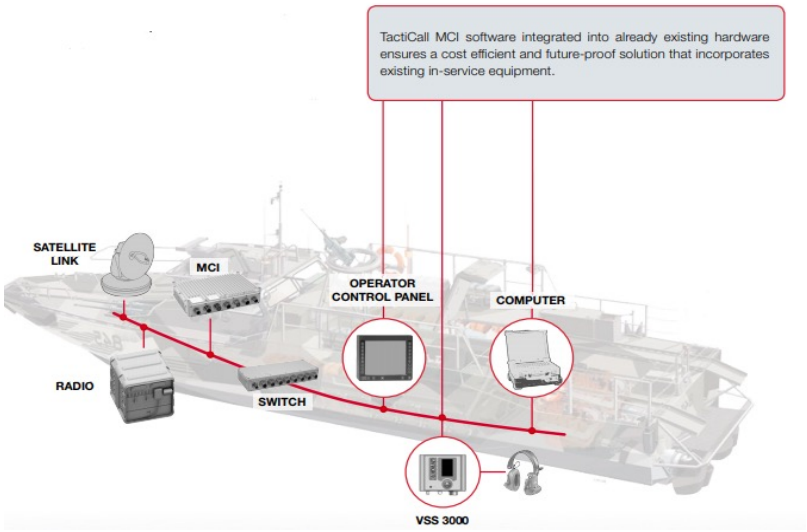


**Graphic 2.** Tactical MCI software integrate.
**Source:** own elaboration.

## 1.3. SHORT VACATION (MINIMAL MAINTENANCE WORK)

Proactive MCI maintenance on the other hand, focuses on identifying and solving problems before they materialize.

**During Short Vacation Types:**

*1) Proactive Maintenance by the Engineer.*

*2) Cleaning Process.*

*3) First Line Service.*

One kind of protection upkeep is ordinarily performed by the designer who has been sent to a server in light of issue. While the designer is at the tacticall server, the person in question will complete deterrent upkeep trying to avert future issues. Architects for the most part will check the best 10 realized deficiency conditions .Fault testing can be a to a great extent manual procedure requiring a decent arrangement of time, anyway it's positively superior to no deterrent support by any means. Another way to deal with proactive support may be increasingly appealing to associations that desire to improve proficiency while bringing down operational expenses.


https://doi.org/10.17993/3ctecno.2021.specialissue8.155-177

## 1.4. DURING LONG VACATION (MAXIMAL MAINTENANCE WORK)

*1) Second line Maintenance / Hardware testing.*

*2) Software testing.*

***SECONDARY MAINTENANCE***

This alludes to work which just tacticall MCI seller's support faculty can do, for example, taking care of hardware breakdowns, parts trades, gear upkeep, and so forth. Experts adopt a proactive strategy to second Line Hardware Maintenance which incorporates the diagnosing of issues and the substitution of breaking down outer parts. By playing out various preventive support visits every year, they discover potential issues before the segment disappointment. Specialists supplant consumable parts, clean, grease up, adjust, and test the majority of the segments to guarantee appropriate usefulness. Experts are prepared to chip away at brands.

***SOFTWARE TESTING***

Designer needs to execute the accompanying Test Cases for maritime correspondence server created by the product engineer. And still, after all that it gathers more opportunity for correspondence server the mariners will become irritated and look for some other close-by exchange server. Consequently reneging happens.

## 1.5. SERVER BREAKDOWN

Normally, when we state a server is down, what we mean is that the program that is intended to react to demands from the system isn't doing as such. That is our Tacticall can't most likely react for the mariners in the proper time. There are various reasons that could occur, and every one of them requires an alternate arrangement. Here are a few models:

The ability to the MCI framework it keeps running on was cut. There are numerous reasons this could occur, including however not constrained to individuals pulling the wrong attachment while doing support, cleaning, and so forth. All things considered, you need to reestablish control.


https://doi.org/10.17993/3ctecno.2021.specialissue8.155-177

The system association quit working. This could be a direct result of a physical link that got unplugged, or in light of the fact that some bit of system hardware fizzled. System gear can overheat. In some cases there are unobtrusive bugs in the product it runs that lone appear from time to time, and the system gear should be restarted. Now and again, some absolutely random framework utilizing a similar system can go haywire and flood the system with a lot of traffic, which could back off everything else and some of the time considerably trigger issues in the product or setup that aren't generally taken note.

The PC is associated with power and the system, however for reasons unknown it isn't quite. Perhaps the power was cut before, and the PC isn't designed to walk out on when the power is reestablished.

The PC is on; however the working framework isn't running. Generally this implies the working framework slammed, in which case the main thing you can do is more often than not to restart the machine, or that the working framework never stacked when the machine fueled up, which likely methods there is some kind of problem with the plate it is put away on.

## 1.6. REPAIR STAGE 1

*1) The simplest solution is often the best*

For instance, does the MCI server have control, or did somebody accidentally unplug the power rope? In the event that the machine clearly has control, however there doesn't appear to be any system availability, verify whether the Ethernet or fiber link has been unintentionally unplugged.

a) If basic troubleshooting doesn't work:

Since we've checked the majority of our links and other fringe gadgets, endeavor to ping the gadget from inside the LANLuckily, the ping order is general, so this ought to be clear paying little respect to the stage being used. In the event that the mariner can ping the server from inside the LAN, take a stab at pinging the server from outside of the LAN. Doing this will go far in deciding whether the issue is at the steering and exchanging level, as opposed


https://doi.org/10.17993/3ctecno.2021.specialissue8.155-177

to at the server level. Additionally, if our Web server is virtualized, take a stab at pinging the IP address of the physical machine itself. This will assist us with furthering segregate the issue. In the event that we can't ping the server by any stretch of the imagination, and we've certainly checked the system association, it's an ideal opportunity to go further.

b) Delay: Nope, the Web server is still down:

We've checked the peripheral cables. The sailors've attempted to ping the box, and still don't have network access to the server. Fortunately you have basically disengaged the issue to either the physical machine or the working framework. Presently we understood that the whole programming arrangement .After finishing the real fix work, the server will go for the optional phase of fix that is to refreshing the working framework. That being said it accumulates more opportunity for correspondence server the mariners will become upset and scan for some other close-by substitute server. Consequently reneging happens.

### 1.7. STAGE 2

Updates for working frameworks are discharging every now and again. Remaining over these updates can be motivating. This is the reason we use modernized fix the executives instruments and have checking set up to alarm us when a framework is obsolete. In the event that we are refreshing our server physically (or not under any condition), we may miss significant security refreshes. Programmers regularly filter for defenselessly frameworks inside hours of an issue being uncovered. So quick reaction is vital. After this whole programming upgrade, the mariner can use the tacticall MCI uninterruptedly.

## 2. METHODOLOGY OF SOLVING THE ABOVE TACTI CALL ENVIRONEMTAL QUEUING ISSUE

The above characterized Queuing issue is disentangled by using the supplementary variable technique. For every one of the organization time, remain by server escape time and fix time valuable variables are used. Unwavering state line gauge dispersal and the different execution measure are settled. Numeral outline legitimizes the model and the graphical depiction gives a sensible picture about the decisions to be taken before the startup of the organization. To deteriorate the issue of clog in the TACTI CALL make benefits, an


https://doi.org/10.17993/3ctecno.2021.specialissue8.155-177

obvious endorsement is rendered toward the end, by strategies for looking at the numerical results and graphical examination of the model.

## 2.1. STEPS INVOLVED IN THE USAGE OF SUPPLEMENTARY VARIABLE METHOD

First we frame the governing equations for the queuing problem involved in tacticall environment in section by using the parameters like service rendered, short vacation, long vacation, system break down, delay in getting into repair process and stages of repair process.

As a second step, we process out the initial boundary conditions of the problem defined.

Next by the usage of various supplementary variables, we derive the probability generating function of the queue size of the tacticall queuing problem. In continuation, length of the queue, number of customers (works to be carried out) in the system, waiting time of the customers in the queue as well as in the system are derived.

All those derivations are justified by means of numerical illustration and graphical portrayal. Based on that, investigation have been made in the numerical study and the analysis is carried out in the analysis report. Having a deep study on the analysis, one can get the idea of minimizing the service interruption in the tacticall environment or to avoid in getting into break down of the system. Moreover system maintenance work is required whether for shorter duration or longer duration could be predicted. This study helps to carry out the various factors in tacticall issue in an accurate manner. This leads to the length of the queue to be minimal in the system. Utilization factor would be made to a maximal. Tacticall system works to a maximal level.

## 2.2. GOVERNING EQUATIONS OF THE MODEL

By means of birth and death process of Queuing study, we first frame the governing equations of the tacticall issue:

$$\frac{d}{dx}M_n(x) + (\lambda + \mu(x) + \beta)M_n(x) = \lambda \sum_{j=1}^{n} d_j M_{n-j}(x). \quad (1)$$

$$\frac{d}{dx}M_0(x) + (\lambda + \mu(x) + \beta)M_0(x) = 0\ . \quad (2)$$


https://doi.org/10.17993/3ctecno.2021.specialissue8.155-177

$$\frac{d}{dx}V_n^{(L)}(x) + (\lambda + \mu_L(x))V_n^{(L)}(x) = \lambda \sum_{j=1}^{n} d_j V_{n-j}^{(L)}(x). \quad (3)$$

$$\frac{d}{dx}V_0^{(L)}(x) + (\lambda + \mu_L(x))V_0^{(L)}(x) = 0\,. \quad (4)$$

$$\frac{d}{dx}V_n^{(S)}(x) + (\lambda + \mu_S(x))V_n^{(S)}(x) = \lambda \sum_{j=1}^{n} d_j V_{n-j}^{(S)}(x). \quad (5)$$

$$\frac{d}{dx}V_0^{(S)}(x) + (\lambda + \mu_S(x))V_0^{(S)}(x) = 0. \quad (6)$$

$$\frac{d}{dx}R_n^{(1)}(x) + \left(\lambda + \mu_r^{(1)}(x)\right)R_n^{(1)}(x) = \lambda \sum_{j=1}^{n} d_j R_{n-j}^{(1)}(x). \quad (7)$$

$$\frac{d}{dx}R_0^{(1)}(x) + \left(\lambda + \mu_r^{(1)}(x)\right)R_0^{(1)}(x) = 0. \quad (8)$$

$$\frac{d}{dx}D_n(x) + (\lambda + \eta(x) + \xi)D_n(x) = \lambda \sum_{j=1}^{n} d_j D_{n-j}(x) + \xi D_{n+1} \quad (9)$$

$$\frac{d}{dx}D_0(x) + (\lambda + \eta(x) + \xi)D_0(x) = 0. \quad (10)$$

$$\frac{d}{dx}R_n^{(2)}(x) + \left(\lambda + \mu_r^{(2)}(x)\right)R_n^{(2)}(x) = \lambda \sum_{j=1}^{n} d_j R_{n-j}^{(2)}(x). \quad (11)$$

$$\frac{d}{dx}R_0^{(2)}(x) + \left(\lambda + \mu_r^{(2)}(x)\right)R_0^{(2)}(x) = 0. \quad (12)$$

$$\lambda Q = \int_0^\infty M_0(x)\mu(x)dx + \int_0^\infty V_0^{(L)}(x)\mu_L(x)dx + \int_0^\infty V_0^{(S)}(x)\mu_S(x)dx + \int_0^\infty R_0^{(2)}(x)\,\mu_r^{(2)}(x)dx. \quad (13)$$

## 2.3. BOUNDARY CONDITIONS

The following boundary conditions are used to solve the above equations:

$$M_n(0) = \int_0^\infty M_{n+1}(x)\mu(x)dx + \int_0^\infty V_{n+1}^{(L)}(x)\mu_L(x)dx + \int_0^\infty V_{n+1}^{(S)}(x)\mu_S(x)dx + \int_0^\infty R_{n+1}^{(2)}(x)\mu_r^{(2)}(x)dx. \quad (14)$$

$$V_n^{(L)}(0) = a\int_0^\infty M_n(x)\mu(x)dx. \quad (15)$$

$$V_n^{(S)}(0) = b\int_0^\infty M_n(x)\mu(x)dx. \quad (16)$$

$$R_n^{(1)}(0) = \beta\int_0^\infty M_n(x). \quad (17)$$

$$D_n(0) = \int_0^\infty R_n^{(1)}(x)\mu_r^{(1)}(x)dx. \quad (18)$$

$$R_n^{(2)}(0) = \int_0^\infty D_n(x)\eta(x)dx. \quad (19)$$


https://doi.org/10.17993/3ctecno.2021.specialissue8.155-177

## 2.4. DISTRIBUTION OF THE LINE LENGTH

Solving of equations from (1) - (12), multiply (1) by $z^n$ and sum over n from 1 to ∞ and add it to (2) resulting the following equation:

$$\frac{d}{dx}M(x,z) + (\lambda - \lambda D(z) + \mu(x) + \beta)M(x,z) = 0. \tag{20}$$

Similarly,

$$\frac{d}{dx}V^{(L)}(x,z) + (\lambda - \lambda D(z) + \mu_L(x))V^{(L)}(x,z) = 0. \tag{21}$$

$$\frac{d}{dx}V^{(S)}(x,z) + (\lambda - \lambda D(z) + \mu_S(x))V^{(S)}(x,z) = 0. \tag{22}$$

$$\frac{d}{dx}R^{(1)}(x,z) + \left(\lambda - \lambda D(z) + \mu_r^{(1)}(x)\right)R^{(1)}(x,z) = 0. \tag{23}$$

$$\frac{d}{dx}D(x,z) + \left(\lambda - \lambda D(z) + \xi - \frac{\xi}{z}\right)D(x,z) = 0. \tag{24}$$

$$\frac{d}{dx}R^{(2)}(x,z) + \left(\lambda - \lambda D(z) + \mu_r^{(2)}(x)\right)R^{(2)}(x,z) = 0. \tag{25}$$

Applying the same for boundary conditions: Solving of equations from (1) - (12), multiply (1) by $z^n$ and sum over n from 1 to ∞ and add it to (2) resulting the following equation:

Applying the same for boundary conditions:

$$zM(0,z) = \int_0^\infty M(x,z)\mu(x)dx + \int_0^\infty V^{(L)}(x,z)\mu_L(x)dx + \int_0^\infty V^{(S)}(x,z)\mu_S(x)dx + \int_0^\infty R^{(2)}(x,z)\mu_r^{(2)}(x) + \lambda(D(z) - 1)Q. \tag{26}$$

$$V^{(L)}(0,z) = a\int_0^\infty M(x,z)\,\mu(x)dx. \tag{27}$$

$$V^{(S)}(0,z) = b\int_0^\infty M(x,z)\,\mu(x)dx. \tag{28}$$

$$R^{(1)}(0,z) = \beta z M(z). \tag{29}$$

$$D(0,z) = \int_0^\infty R^{(1)}(x,z)\mu_r^{(1)}(x)dx. \tag{30}$$

$$R^{(2)}(0,z) = \int_0^\infty D(x,z)\eta(x)dx. \tag{31}$$

Now Integrating (20) from 0 to, it gives

$$M(x,z) = M(0,z)e^{-(\lambda-\lambda D(z))-\int_0^\infty \mu(t)dt} \tag{32}$$


https://doi.org/10.17993/3ctecno.2021.specialissue8.155-177

Integrating the above by parts, we get

$$M(x,z) = M(0,z)\left[\frac{1-\bar{E}(a_1)}{a_1}\right], a_1 = \lambda - \lambda D(z) + \beta \tag{33}$$

Where $\bar{E}(a_1) = \int_0^\infty e^{-(\lambda-\lambda D(z)+\beta)} dE(x)$ is the Laplace Stieltje's transform of the service time. Again multiplying (32) by μ(x) and integrating, we get

$$\int_0^\infty M(x,z)\,\mu(x)dx = M(0,z)\overline{E_1}(a_1) \tag{34}$$

Similarly

$$V^{(L)}(z) = V^{(L)}(0,z)\left[\frac{1-\overline{E_2}(a_2)}{a_2}\right], a_2 = \lambda - \lambda D(z) = aM(0,z)\overline{E_1}(a_1)\left[\frac{1-\overline{E_2}(a_2)}{a_2}\right] \tag{35}$$

$$\int_0^\infty V^{(L)}(x,z)\,\mu_L(x)dx = V^{(L)}(0,z)\overline{E_2}(a_2) \quad = aM(0,z)\overline{E_1}(a_1)\overline{E_2}(a_2). \tag{36}$$

$$V^{(S)}(z) = V^{(S)}(0,z)\left[\frac{1-\overline{E_3}(a_2)}{a_2}\right] \quad = bM(0,z)\overline{E_1}(a_1)\left[\frac{1-\overline{E_3}(a_2)}{a_2}\right]. \tag{37}$$

$$\int_0^\infty V^{(S)}(x,z)\,\mu_S(x)dx = bM(0,z)\overline{E_1}(a_1)\overline{E_3}(a_2). \tag{38}$$

$$R^{(1)}(z) = R^{(1)}(0,z)\left[\frac{1-\overline{E_4}(a_2)}{a_2}\right] = \beta z M(0,z)\left[\frac{1-\overline{E_1}(a_1)}{a_1}\right]\left[\frac{1-\overline{E_4}(a_2)}{a_2}\right]. \tag{39}$$

$$\int_0^\infty R^{(1)}(x,z)\mu_r^{(1)}(x)dx = \beta z M(0,z)\left[\frac{1-\overline{E_1}(a_1)}{a_1}\right]\overline{E_4}(a_2). \tag{40}$$

$$D(z) = D(0,z)\left[\frac{1-\overline{E_5}(a_3)}{a_3}\right], \textit{ where } a_3 = \lambda - \lambda D(z) + \xi - \frac{\xi}{z} = \beta z M(0,z)\left[\frac{1-\overline{E_1}(a_1)}{a_1}\right]\overline{E_4}(a_2)\left[\frac{1-\overline{E_5}(a_3)}{a_3}\right]. \tag{41}$$

$$\int_0^\infty D(x,z)\eta(x)dx = \beta z M(0,z)\left[\frac{1-\overline{E_1}(a_1)}{a_1}\right]\overline{E_4}(a_2)\overline{E_5}(a_3) \tag{42}$$

$$R^{(2)}(z) = R^{(2)}(0,z)\left[\frac{1-\overline{E_6}(a_2)}{a_2}\right] \quad = \beta z M(0,z)\left[\frac{1-\overline{E_1}(a_1)}{a_1}\right]\left[\frac{1-\overline{E_6}(a_2)}{a_2}\right]\overline{E_4}(a_2)\overline{E_5}(a_3). \tag{43}$$


https://doi.org/10.17993/3ctecno.2021.specialissue8.155-177

$$\int_0^\infty R^{(2)}(x,z)\mu_r^{(2)}(x)dx = \beta z M(0,z)\left[\frac{1-\overline{E_1}(a_1)}{a_1}\right]\overline{E_6}(a_2)\overline{E_4}(a_2)\overline{E_5}(a_3). \quad (44)$$

Substituting (34), (36), (38), (44) in (26), we get:

$$M(0,z) = \frac{\lambda(D(z)-1)Q}{z-\overline{E_1}(a_1)\left(\overline{E_2}(a_2)+\overline{E_3}(a_2)(a+b)\right)-\beta z\overline{E_6}(a_2)\overline{E_4}(a_2)\overline{E_5}(a_3)\left[\frac{1-\overline{E_1}(a_1)}{a_1}\right]}. \quad (45)$$

Using the above (33), (35), (37), (39) (41) and (43) becomes,

$$M(z) = \frac{\lambda(D(z)-1)Q\left[\frac{1-\overline{E_1}(a_1)}{a_1}\right]}{z-\bar{E}(a_1)\left(\overline{E_2}(a_2)+\overline{E_3}(a_2)(a+b)\right)-\beta z\overline{E_6}(a_2)\overline{E_4}(a_2)\overline{E_5}(a_3)\left[\frac{1-\overline{E_1}(a_1)}{a_1}\right]}. \quad (46)$$

$$V^{(L)}(z) = \frac{-\lambda Qa[1-\overline{E_2}(a_2)]\overline{E_1}(a_1)}{z-\overline{E_1}(a_1)\left(\overline{E_2}(a_2)+\overline{E_3}(a_2)(a+b)\right)-\beta z\overline{E_6}(a_2)\overline{E_4}(a_2)\overline{E_5}(a_3)\left[\frac{1-\overline{E_1}(a_1)}{a_1}\right]}. \quad (47)$$

$$V^{(S)}(z) = \frac{-\lambda Qb\overline{E_1}(a_1)[1-\overline{E_3}(a_2)]}{z-\overline{E_1}(a_1)\left(\overline{E_2}(a_2)+\overline{E_3}(a_2)(a+b)\right)-\beta z\overline{E_6}(a_2)\overline{E_4}(a_2)\overline{E_5}(a_3)\left[\frac{1-\overline{E_1}(a_1)}{a_1}\right]}. \quad (48)$$

$$R^{(1)}(z) = \frac{-\beta z\lambda Q\left[\frac{1-\overline{E_1}(a_1)}{a_1}\right][1-\overline{E_4}(a_2)]}{z-\overline{E_1}(a_1)\left(\overline{E_2}(a_2)+\overline{E_3}(a_2)(a+b)\right)-\beta z\overline{E_6}(a_2)\overline{E_4}(a_2)\overline{E_5}(a_3)\left[\frac{1-\overline{E_1}(a_1)}{a_1}\right]}. \quad (49)$$

$$R^{(2)}(z) = \frac{-\beta z\lambda Q\left[\frac{1-\overline{E_1}(a_1)}{a_1}\right][1-\overline{E_6}(a_2)]\overline{E_4}(a_2)\overline{E_5}(a_3)}{z-\overline{E_1}(a_1)\left(\overline{E_2}(a_2)+\overline{E_3}(a_2)(a+b)\right)-\beta z\overline{E_6}(a_2)\overline{E_4}(a_2)\overline{E_5}(a_3)\left[\frac{1-\overline{E_1}(a_1)}{a_1}\right]}. \quad (50)$$

$$D(z) = \frac{\beta z\lambda Q[D(z)-1]\left[\frac{1-\overline{E_1}(a_1)}{a_1}\right]\overline{E_4}(a_2)\left[\frac{1-\overline{E_5}(a_3)}{a_3}\right]}{z-\overline{E_1}(a_1)\left(\overline{E_2}(a_2)+\overline{E_3}(a_2)(a+b)\right)-\beta z\overline{E_6}(a_2)\overline{E_4}(a_2)\overline{E_5}(a_3)\left[\frac{1-\overline{E_1}(a_1)}{a_1}\right]}. \quad (51)$$

# 3. RESULTS

## 3.1. PROBABILITY GENERATING FUNCTION OF THE QUEUE SIZE

To find the probability making limit of the line gauge paying little mind to the state of the structure. Let $W_q$ (z) be the probability generating function of the queue length no matter what the state of the system is

(i.e) $W_q(z) = M(z) + V^{(L)}(z) + V^{(S)}(z) + R^{(1)}(z) + R^{(2)}(z) + D(z)$


https://doi.org/10.17993/3ctecno.2021.specialissue8.155-177

Then adding:

(46) – (51), we get:

$$W_q(z) = \frac{\begin{array}{c}\lambda(D(z)-1)Q\left[\frac{1-\overline{E_1}(a_1)}{a_1}\right]-\lambda Qa[1-\overline{E_2}(a_2)]\overline{E_1}(a_1)- \\ \lambda Qb\overline{E_1}(a_1)[1-\overline{E_3}(a_2)] \\ -\beta z\lambda Q\left[\frac{1-\overline{E_1}(a_1)}{a_1}\right][1-\overline{E_4}(a_2)]-\beta z\lambda Q\left[\frac{1-\overline{E_1}(a_1)}{a_1}\right] \\ [1-\overline{E_6}(a_2)]\overline{E_4}(a_2)\overline{E_5}(a_3) \\ \beta z\lambda Q[D(z)-1]\left[\frac{1-\overline{E_1}(a_1)}{a_1}\right]\overline{E_4}(a_2)\left[\frac{1-\overline{E_5}(a_3)}{a_3}\right]\end{array}}{\begin{array}{c}z-\overline{E_1}(a_1)\left(\overline{E_2}(a_2)+\overline{E_3}(a_2)(a+b)\right)- \\ \beta z\overline{E_6}(a_2)\overline{E_4}(a_2)\overline{E_5}(a_3) \\ \left[\frac{1-\overline{E_1}(a_1)}{a_1}\right]\end{array}} \quad (52)$$

The idle time $Q$ is determined by using the normalization condition:

$$W_q(1)+Q=1$$

Using L'Hopital's rule, we get:

$$\lim_{z\to 1} W_q(z) = \frac{N'(1)}{D'(1)}$$

Also $Q = \frac{D'(1)}{D'(1)+N'(1)}$

From $Q$, the utilization factor $\rho$ can be determined.

## 3.2. SYSTEM QUEUE EXECUTION PROCEDURES

Let $L_q$ a chance to demonstrate the reliable state typical number of customers in the line.

By then:

$$L_q = \frac{d}{dz}W_q(z)\Big|_{z=1} = \frac{d}{dz}\left\{\frac{N(z)}{D(z)}\right\}\Big|_{z=1}$$

Where $N(z)$ and $D(z)$ are the numerator and denominator of (52).

Since $W_q(z) = \frac{0}{0}$ at $=1$ , we utilize two-fold separation and get:


https://doi.org/10.17993/3ctecno.2021.specialissue8.155-177

$$L_q = \lim_{z\to 1}\frac{d}{dz}W_q(z) = \frac{D'(1)N''(1)-D''(1)N'(1)}{2(D'(1))^2}. \quad (53)$$

Where primes mean subordinates with respect to $z$ and after a course of action of logarithmic enhancement, we get length of the queue $L_q$ closed frame.

$$D'(1) = 1 + 2\lambda(a+b)\overline{E_1}'(\beta) - (a+b)\lambda\big(E(B_2)+E(B_3)\big) - \beta\left(\frac{1-\overline{E_1}(\beta)}{\beta}\right)\big[1-\overline{E_1}'(\beta) + \lambda E(B_4) + E(B_5)(-\lambda+\xi) + \lambda E(B_6)\big]. \quad (54)$$

$$N'(1) = \lambda\left\{\left(\frac{1-\overline{E_1}(\beta)}{\beta}\right) + \left(\frac{1-\overline{E_1}(\beta)}{\beta}\right)\big(\beta E(B_5)\big) + \lambda\big(E(B_3)+E(B_2)\big)\overline{E_1}(\beta)(a+b)\right\}. \quad (55)$$

$$N''(1) = \lambda\left\{\lambda[E(B_2)+E(B_3)]\left[-\lambda\overline{E_1}'(\beta) + \beta\left(\frac{1-\overline{E_1}(\beta)}{\beta}\right)\big(E(B_6)+E(B_4)\big)\right] + \overline{E_1}'(\beta) + \left(\frac{1-\overline{E_1}(\beta)}{\beta}\right)\big(\beta E(B_5)\big) + \overline{E_1}'(\beta) + \overline{E_1}'(\beta)\big(\beta E(B_5)\big) + \left(\frac{1-\overline{E_1}(\beta)}{\beta}\right)[\beta E(B_5) + \lambda\beta E(B_4)E(B_5) + \beta(\lambda-\xi)E(B_5^2)]\right\}$$

$$\left\{\lambda[E(B_2)+E(B_3)]\left[-\lambda\overline{E_1}'(\beta) + \beta\left(\frac{1-\overline{E_1}(\beta)}{\beta}\right)\big(E(B_6)+E(B_4)\big)\right] + \overline{E_1}'(\beta) + \left(\frac{1-\overline{E_1}(\beta)}{\beta}\right)\big(\beta E(B_5)\big) + \overline{E_1}'(\beta) + \overline{E_1}'(\beta)\big(\beta E(B_5)\big) + \left(\frac{1-\overline{E_1}(\beta)}{\beta}\right)[\beta E(B_5) + \lambda\beta E(B_4)E(B_5) + \beta(\lambda-\xi)E(B_5^2)]\right\}. \quad (56)$$

$$D''(1) = -2\lambda^2\overline{E_1}''(\beta)(a+b) + \overline{E_1}'(\beta)(a+b)\lambda^2\big(E(B_2)+E(B_5)\big) + (a+b)\lambda^2\overline{E_1}'(\beta)\big(E(B_2)+E(B_3)\big) - (a+b)\overline{E_1}(\beta)\lambda^2\big(E(B_2^2)+E(B_3^2)\big) - \beta\left[\big(-\overline{E_1}'(\beta)\big) + \left(\frac{1-\overline{E_1}(\beta)}{\beta}\right)\lambda[E(B_4)+E(B_5)+E(B_6)]\right] - \beta[-\overline{E_1}'(\beta) - \overline{E_1}'(\beta)\lambda[E(B_4)+E(B_5)+E(B_6)] + \lambda\overline{E_1}''(\beta)] - \beta\left[-\overline{E_1}'(\beta)\lambda E(B_4) + \left(\frac{1-\overline{E_1}(\beta)}{\beta}\right)\lambda E(B_4) + \left(\frac{1-\overline{E_1}(\beta)}{\beta}\right)[\lambda^2E(B_4^2) + \lambda^2E(B_6)E(B_4) + \lambda E(B_4)E(B_5)(-\lambda+\xi)]\right] - \beta\left[\left(\frac{1-\overline{E_1}(\beta)}{\beta}\right)\lambda E(B_6) - \lambda\overline{E_1}'(\beta)E(B_6) + \left(\frac{1-\overline{E_1}(\beta)}{\beta}\right)[-\lambda^2E(B_4) + \lambda^2E(B_6^2) + \lambda E(B_5)(-\lambda+\xi)]\right] - \beta\left[\left(\frac{1-\overline{E_1}(\beta)}{\beta}\right)E(B_5)(\lambda-\xi) + \left(\frac{1-\overline{E_1}(\beta)}{\beta}\right)[\lambda E(B_4)E(B_5)(\lambda-\xi) + \lambda E(B_6)E(B_5)(\lambda-\xi) + (-\lambda+\xi)^2E(B_5^2)] + \overline{E_1}(\beta)E(B_5)(-\lambda+\xi)\right]. \quad (57)$$


https://doi.org/10.17993/3ctecno.2021.specialissue8.155-177

Substituting for $\mathcal{N}'(1)$, $\mathcal{N}''(1)$, $D'(1)$, $D''(1)$ from (54) – (57) in (53), we obtain $L_q$ in closed form.

Further the mean waiting time of a customer in the queue as well as in the system and the number of customers waiting in the system can be found using Little's formula:

$$W_q = \frac{L_q}{\lambda}\ , W = \frac{L}{\lambda}, L = L_q + \rho$$

## 3.3. NUMERICAL JUSTIFICATION OF THE MODEL

Assume that service time follows exponential distribution in particular and based on this condition, the numerical justification is elaborated below. The values are collected accordingly:

$$\mu = 2.8, \mu_L = 3.6, \mu_S = 4.5, \mu_r^{(1)} = 3.5, \mu_r^{(2)} = 2, \eta = 3, \xi = 2.5, \beta = 3, \xi = 1, a = 0.6, b = 0.4 \overline{E_1}'(\beta) = \frac{-\beta}{(\mu+\beta)^2}, E(B_2) = \frac{1}{\mu_L}, E(B_3) = \frac{1}{\mu_S}, E(B_4) = \frac{1}{\mu_r^{(1)}}, E(B_5) = \frac{1}{\eta}, E(B_6) = \frac{1}{\mu_r^{(2)}}, \overline{E_1}(\beta) = \frac{\mu}{\mu+\beta}, E(B_2^2) = \frac{2}{\mu_L^2}, E(B_5^2) = \frac{2}{\eta^2}, E(B_6^2) = \frac{2}{\left(\mu_r^{(2)}\right)^2}, E(B_4^2) = \frac{2}{\left(\mu_r^{(1)}\right)^2}, E(B_5^2) = \frac{2}{\mu_S^2}$$

**Table 1.** Effect Of Change In ξ : ξ=1,1.2,1.4,1.6,1.8.

| $Q$ | $\rho$ | $Lq$ | $W_q$ | $L$ | $W$ |
|---|---|---|---|---|---|
| 0.4354 | 0.5646 | 3.5076 | 1.1692 | 4.0722 | 1.3574 |
| 0.5516 | 0.4484 | 1.5393 | 0.5131 | 1.9877 | 0.6626 |
| 0.6296 | 0.3704 | 0.9113 | 0.3038 | 1.2817 | 0.4272 |
| 0.6856 | 0.3144 | 0.6175 | 0.2058 | 0.9319 | 0.3106 |
| 0.7277 | 0.2723 | 0.4534 | 0.1511 | 0.7257 | 0.2419 |

**Source:** own elaboration.


https://doi.org/10.17993/3ctecno.2021.specialissue8.155-177

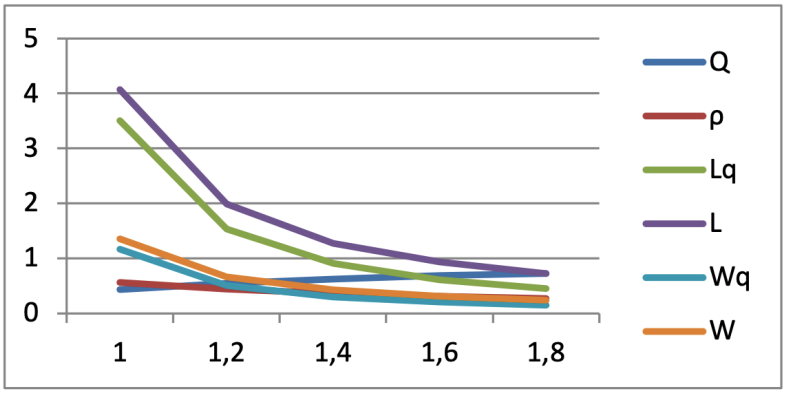


**Graphic 3**. Effect of change in ξ.
**Source:** own elaboration.

**Table 2.** Effect Of Change In a : a=0.5,0.6,0.7,0.8,0.9.

| $Q$ | $\rho$ | $Lq$ | $W_q$ | $L$ | $W$ |
|---|---|---|---|---|---|
| 0.4582 | 0.5418 | 3.0381 | 1.0127 | 3.5799 | 1.1933 |
| 0.4600 | 0.5400 | 2.8510 | 0.9503 | 3.3910 | 1.1303 |
| 0.4615 | 0.5385 | 2.6931 | 0.8971 | 3.2298 | 1.0766 |
| 0.4629 | 0.5371 | 2.5532 | 0.8511 | 3.0903 | 1.0301 |
| 0.4641 | 0.5359 | 2.4327 | 0.8109 | 2.9686 | 0.9895 |

**Source:** own elaboration.

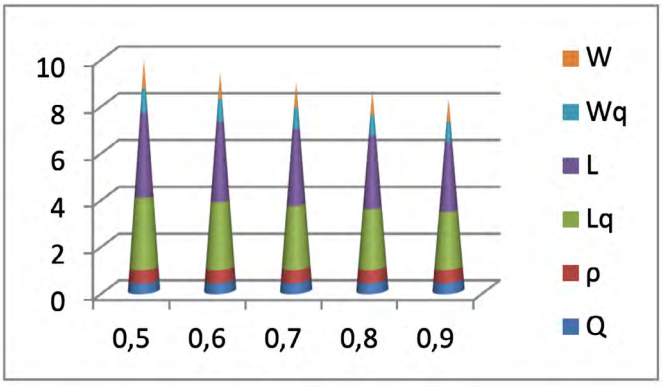


**Graphic 4**. Effect of change in a.
**Source:** own elaboration.


https://doi.org/10.17993/3ctecno.2021.specialissue8.155-177

# 4. DISCUSSIONS

All the values in the table are as expected. In Table 1, probability of considering the concept of reneging takes place. Due to impatience, customers leave the system after joining the queue. This concept is defined as reneging as explained earlier. Hence in this tacticall issue increase in reneging makes the work lessen to be carried out in tacticall problem. Therefore length of the queue gets diminished. Number of customers in the system gets lessen too. This leads to the waiting time of the customers in the queue as well as in the system to get reduced. All these measures are gotten only due to the increase in the reneging concept. This has to be avoided by the way of reducing the time factor of delay process. Hence whenever service interruption occurs, the system has to be introduced into the reneging process immediately. Hence the server can render its service without any delay and it leads to keeps away from Reneging.

Table 2 indicates the concept of increase in getting the probability of long vacation. So maximal maintenance work can be carried out in the system. Hence the increase in probability of long vacation, (the process of maintenance work time) makes the system to run faster than the earlier and hence the performance measures of the system get reduced. Maintenance work is the unavoidable feature in the concept of Queuing problem.

# 5. CONCLUSIONS

In nature of TACTI CALL, Queuing issue comprising of administration, short get-away, long excursion, administration interference, fix process, phases of fix process happen. Here we had an itemized examination on various kinds of excursions and administration break in the framework. What's more, in this lining framework, framework doesn't get onto fix process right away. It concedes a deferral between the administration separate and the procedure of fix. Additionally, here fix process is completed in two phases. Get-away procedure assumes a significant job in this Queuing procedure of correspondence study. The issue is very much explained by advantageous variable strategy and the essential execution measures are determined. Numerical investigation of the application delineates the Queuing approach towards the issue by and large. This introduction acknowledges noticeable work in social occasion units, correspondence structure, and development crossing centers, framework


https://doi.org/10.17993/3ctecno.2021.specialissue8.155-177

planning, etc. Benefits of this queuing procedure is reducing the time for work delay. It helps to give the service to customers at right time.

## 5. ACKNOWLEDGEMENT

We would like to thank our institution Kalasalingam Academy of Research and Education for support.

## REFERENCES

**Artino, A.R., Folga, R.V., & Swan, B.D.** (2006). Mask-on Hypoxia Training For Tactical Jet Aviators: Evaluation of an Alternate Instructional Paradigm. *Avitation Space and Environmental Science, 77*(8), 857-863. https://pubmed.ncbi.nlm.nih.gov/16909882/

**Burkholder-Allen, K., Rega, P., Bork, C., & Budd, C.** (2009). Boutulism Questionnaire: A Tactical Tool For Community Use in a Mass Casualty incident. *Nursing and Health Sciences, 11*(4), 374-377. https://doi.org/10.1111/j.1442-2018.2009.00489.x

**Cerf, V. G., & Cain, E.** (1983). The DOD Internet Architecture model. Elsevier science Publishers, *Computer Networks, North Holland, 7*, 307-318. http://citeseerx.ist.psu.edu/viewdoc/download?doi=10.1.1.88.7505&rep=rep1&type=pdf

**Chatterjee, C.K., & Pal, S.** (1993). Present and Future Trends in Military Satellite Communication System. *Defense Science Journal, 43*(1), 37-42. https://doi.org/10.14429/dsj.43.4208

**Crainic, T.G.** (1988). Rail Tactical Planning: Issues, Models and Tools. In Bianco L., La Bella A. (eds.) Freight Transport Planning and Logistics. *Lecture Notes in Economics and Mathematical Systems, vol 317*. Springer, Berlin, Heidelberg. https://doi.org/10.1007/978-3-662-02551-2_16

**Echols, C. J.** (2004). Developing Standards for interoperability of tactical communication systems. *Journal of Telecommunication and Information Technology, 4*, 3-5.


https://doi.org/10.17993/3ctecno.2021.specialissue8.155-177

**Erkan, E. Ç., & Uzun, S.** (2004). User Services of Tactical Communication in the Digital Stage. *Journal of Telecommunications and Information Technology, 4*, 39-44. https://citeseerx.ist.psu.edu/viewdoc/download?doi=10.1.1.839.3752&rep=rep1&type=pdf

**Holmström, J., Rajamäki, J., & Hult, T.** (2011). The Future Solutions and Technologies of Public Safety Communication. *International Journal of Communication 5*(3), 115-122. http://www.ajeco.fi/pdf/International_Journal_of_Communications_DSiP_20-739.pdf

**Majumdar, A.** (2005). Free-space laser communications in atmospheric channel. *Journal of Optical and Fiber communications Reports, 2*(4), 345-396. https://doi.org/10.1007/s10297-005-0054-0

**Maragathasundari, S., & Sowmiyah, S.** (2015). M/G/1 Queuing System with Extended Vacation, Service Interruption, Delay time and Stages in Repair. *Journal of Computer and Mathematical Science, 6*(7), 363-370. http://compmath-journal.org/dnload/S-Maragathasundari-and-S-Sowmiyah/CMJV06I07P0363.pdf

**Maragathasundari, S., Srinivasan, S., & Ranjitham, A.** (2014). Batch Arrival Queuing System with two stages of service. *International Journal of Mathematical Analysis, 8*(6), 247-258. http://dx.doi.org/10.12988/ijma.2014.411

**Misra, D., Misra, D. K., & Tripathi, S.P.** (2013). Satellite Communication, Advancement, Issues, Challenges and Applications. *International Journal of Advanced Research in Computer and Communication Engineering, 2*(4), 1681-1686. https://www.ijarcce.com/upload/2013/april/11-Misra%20Dinesh%20Kumar%20-%20Satellite%20Communication%20Advancement,%20Issues,%20Challenges%20and%20Applications.pdf

**Scott, C.H., Skelton, O.G., & Rolland, E.** (2000). Tactical and Strategic models for satellite customer Assignment. *Journal of the Operational Research Society, 51*(1), 61-71. https://doi.org/10.1057/palgrave.jors.2600860

**Suri, N., Benyagnu, E., Tortonesi, M., Stefanelli, C., Kovach, J., & Hanna, J.** (2009). Communications middleware for tactical environments: Observations, experiences,

and lessons learned. *IEEE Communications Magazine, 47*(10), 56-63. https://ieeexplore.ieee.org/document/5273809

**Swaminathan, J.M., & Tayur, S.** (2003). Tactical Planning Models for Supply Chain Management. *Supply Chain Management*. https://www.semanticscholar.org/paper/Tactical-Planning-Models-for-Supply-Chain-Swaminathan-Tayur/d7d231221f3c3d06c33d3a5116866d3b7587be33


https://doi.org/10.17993/3ctecno.2021.specialissue8.155-177

https://doi.org/10.17993/3ctecno.2021.specialissue8.155-177

/11/


https://doi.org/10.17993/3ctecno.2021.specialissue8

# QUEUING CONFIGURATION IN SATELLITE COMMUNICATION

**S. Maragathasundari**
Associate professor, Department of Mathematics, Kalasalingam Academy of Research and Education Krishnankoil, (India).
E-mail: maragatham01@gmail.com.
ORCID: https://orcid.org/0000-0003-1210-6411

**G. Ammakkannu**
Associate Professor, Department of Mathematics, Kalasalingam Academy of Research and Education, Krishnankovil, (India).
E-mail: ammakannu1975@gmail.com.
ORCID: https://orcid.org/0000-0002-8789-2093

**P. Manikandan**
Assistant Professor, Department of Electronics and Communication Engineering, Kalasalingam Academy of Research and Education, Krishnankovil, (India).
E-mail: maanip85@gmail.com.
ORCID: https://orcid.org/0000-0002-5737-0235

**Recepción:** 25/10/2019 **Aceptación:** 24/08/2020 **Publicación:** 30/11/2021

**Citación sugerida:**
Maragathasundari, S., Ammakkannu, G., y Manikandan, P. (2021). Queuing configuration in satellite communication. *3C Tecnología. Glosas de innovación aplicadas a la pyme, Edición Especial,* (noviembre, 2021), 179-197. https://doi.org/10.17993/3ctecno.2021.specialissue8.179-197

## ABSTRACT

Satellite correspondence frameworks have been utilized for a considerable length of time to give fixed point and versatile administrations to the business and military markets around the world. The procedure completed in satellite correspondence is changed over as a Queuing issue and the issue is settled by methods for Supplementary variable technique of Queuing. It results in the derivations of the Queue execution proportions of the framework which causes the procedure to recognize the deformities in the process. It likewise gives the thought regarding the uplift of the methods in satellite correspondence systems which prompts a smooth running of the communication in a profitable manner. Numerical outline and Graphical portrayal given toward the end makes an intricate thought regarding the lining procedure occurring in satellite correspondence.

## KEYWORDS

Delay, Compulsory vacation, Reneging, Feedback service.


https://doi.org/10.17993/3ctecno.2021.specialissue8.179-197

# 1. INTRODUCTION

Services incorporate two-way media communications, route, and TV and radio telecom. As in most present-day remote frameworks, satellite correspondences transfer speeds have developed after some time with advanced information rates beginning from kilobits every second (Kbps) to current framework wide limit of more than 100 gigabits for each second (Gbps).

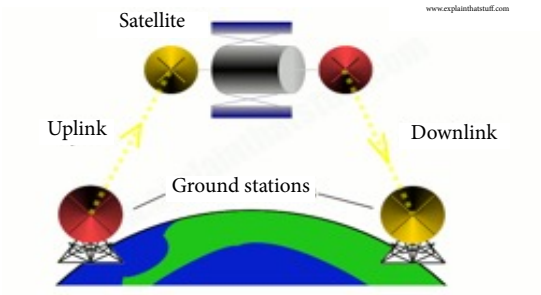


**Graphic 1.** Satellite communication.
**Source:** own elaboration.

There is currently extraordinary improvement in the arrangement of new high throughput satellite broadband arrangements equipped for conveying web, voice, video and other special interchanges administrations. Real administrators and supporters either have propelled or are making arrangements for a wide scope of uses, including purchaser as well as gas and oil, calamity recuperation, aeronautical, oceanic, military and other mission basic prerequisites. For each satellite arrangement, there is a lot bigger arrangement of earthbound based frameworks, or ground stations, extending from satellite control offices to end-client gadgets. The approval, support and investigating of these ground stations regularly requires a mix of indoor and outside testing of various RF and IF subsystems and segments. Lam (1980) studied this paper in general about the models on multilevel diversity coding.

Fantacci and Zoppi (2000) studied the performance of different polling systems used in wireless local networks where the transmission channel exhibits a non-stationary behavior. Yeung and Zhang (1999) discussed about the maximum channel throughput of CSMA approaches unity in the limit of very long queues. Giambene and Kota (2006) suggested a


https://doi.org/10.17993/3ctecno.2021.specialissue8.179-197

work in detail about the interaction of different layers that can be permitted to improve the higher-layer goodput as well as user satisfaction.

Hung, Montpetit, and Kesidis (1998) describes an ATM-based satellite network, focusing on the networking (ATM) aspects of the design. Chang and Lin (1993) studied the performance of VSAT-based satellite wide area networks. Basic geostationary and non-geostationary satellite constellations are considered. Financial success of satellite personal communication systems was examined by Lutz (1998). Louvros, Pylarinos, and Kotsopoulos (2007) investigated a new model which is proposed with a dedicated queue for each transceiver in the cell.

Zaim (2003) calculated a new call and hand-off call blocking probabilities in LEO satellite networks carrying voice calls. Maragathasundari (2015) derived the execution measures for a mass section queuing model of three periods of organization with different journey strategies. Maragathasundari *et al.* (2017) described a non-markovian queuing model of restricted admissibility and service interruption in which entry was taken after a Poisson method. Zhu *et al.* (2012) discussed about the Load Balancing Routing Based on Agent for Polar-orbit LEO satellite networks. Maragathasundari and Karthikeyan (2016) investigated a mass queuing model with short and long escape.

## 1.1. COMMUNICATIONS SATELLITES

Communications satellites are "space mirrors" that can help us bounce radio, TV, Internet data, and other kinds of information from one side of Earth to the other.

## 1.2. UPLINKS AND DOWNLINKS

In the event that you need to send something like a TV communicates from one side of Earth to the next, there are three phases included. To start with, there's, where information is channeled up to the satellite from a ground station on Earth. Next, the satellite procedures the information utilizing various installed transponders (radio recipients, intensifiers, and transmitters). These lift the approaching sign and change their recurrence, so approaching sign don't get mistook for active ones. Various transponders in a similar satellite are utilized to deal with various TV stations carried on various frequencies. At last, there's the downlink, where information is sent down to another ground station somewhere else on


https://doi.org/10.17993/3ctecno.2021.specialissue8.179-197

Earth. Despite the fact that there's generally only a solitary uplink, there might be a large number of downlinks, for instance, if numerous individuals are getting a similar satellite TV signal without a moment's delay. While a correspondences satellite may transfer a sign between one sender and beneficiary (started up into space and withdraw once more, with one uplink and one downlink), satellite communicates commonly include at least one uplink (for at least one TV stations) and different downlinks.

The above communication progression is converted as a Queuing problem. The problems faced in the process are diagnosed and the corresponding performance measures of the Queuing system of the satellite communication are derived. The communication procedure is explained in terms of Queuing parameters as Stages of service, Delay, compulsory vacation, Reneging and feedback service

## 1.3. STAGE 1: DELAY PROCESS

Much like some other correspondences' medium: inertness is the time taken for data to go from the inception to the goal and possibly for the reaction to return.

Dormancy in satellites is particularly progressively evident due to the exceptionally long separations that the sign must go into space and back. The separation voyaged relies upon the area of the satellite and along these lines its circle. There are three primary satellite sorts utilized in satellite correspondences:

1) Geostationary/geosynchronous/GEO: these satellites stay in a generally fixed position in the sky contrasted with a situation on the equator. In this way you don't have to modify your reception apparatus and it is dependably in a known relative position in the sky. These satellites are around 32,786km from the Earth.
2) Low Earth Orbit (LEO): The Iridium satellites are just 781km from the surface there are bunches of them and they cooperate like a flying cell arrange.
3) Medium Earth Orbit (MEO): It has another player financially with O3b circling at 8063km, they will have less satellite, giving lower dormancy than GEO however more limit and less satellites than Iridium.


https://doi.org/10.17993/3ctecno.2021.specialissue8.179-197

## 1.4. COMPULSARY VACATION

On-orbit satellite servicing will elongate the life of some very expensive satellites. Its application areas are very broad where each one has its own importance based on scientific, economic, strategic, and societal benefits. Repair and maintenance of the satellites in space keep a unique and valuable asset operational, essentially improving it beyond its design lifetime or the reliability of its subsystems. It improves overall mission robustness and offers a unique capability to improve risk posture through post-launch operations.

The process of on-orbit satellite is very simple. For the purpose, a service spacecraft is built with robotic arms. The major components here include an advanced spacecraft with a specialized toolkit and robotic arms just like humans for capturing, interacting with, and manipulating a client, software for managing semi-autonomous servicing tasks, and an advanced sensor suite for careful rendezvous and proximity operations. In case when any satellite developing a snag is discovered, the servicing spacecraft is made to approach it, grab it, pull it close, and repair or exchange the faulty part with a toolkit it is carrying. If a satellite runs out of the fuel, similar technology is used to refuel it.

In past, it was not possible to repair all satellites in orbit. It was mandatory to build them accordingly so that they can be serviced. Like for example when all three-rubidium clock of IRNSS 1A satellite failed, then it was pushed to graveyard. The satellite was launched by Indian space and research organization (ISRO) as the first in the queue of India's own regional navigation system, NAVIC. But today the technology has matured and can repair all satellites on orbit. The Servicer designed SSL is compatible with most government and commercial spacecraft that are currently in orbit, even those not designed to be serviced in space.

## 1.5. STAGE 2: (OPTIONAL)

If the satellite is not working properly even after the maintenance done at the compulsory vacation, the satellite may go for an extended optional vacation. Luckily, the propelled apply autonomy installed new satellite overhauling undertakings are planned to lessen the quantity of satellites confronting this sort of inopportune retirement. Overhauling rocket can fix, reposition, and refuel satellites utilizing automated arms, and will in the long run


https://doi.org/10.17993/3ctecno.2021.specialissue8.179-197

have the option to collect satellites altogether in space. Satellite overhauling could wipe out the requirement for governments and organizations to contribute millions — and once in while billions — into structuring, building, and propelling a substitution satellite each time fixes or fuel are required. Overhauling would likewise serve a national security job, the same number of government satellites hand-off basic data that shouldn't be disturbed. The innovation even can possibly enable people to achieve Mars.

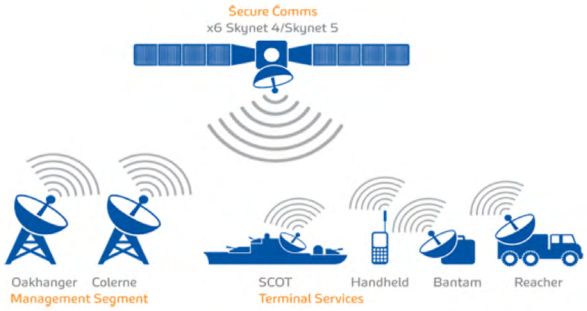


**Graphic 2.** Satellite service.
**Source:** own elaboration.

## 1.6. RENEGING

Likewise, because of restlessness clients may leave the framework subsequent to joining the line. This procedure of reneging happens during mandatory excursion with parameter γ.

The clients/clients are holding up at the less than desirable end to get any sort of valuable data which are to be sent by the transponders at the uplink stations. Be that as it may, the procedure of gathering, might be postponed a ton during the movement of necessary support.

Consequently, the client may become irritated and they are not willing to remain back in the line. Thus, they will look for some other downlink station to show signs of improvement gathering of sign on schedule. Henceforth reneging happens.

## 1.7. FEEDBACK SERVICE

Furthermore, if the client is disappointed with the administration, they can decide on an input administration with likelihood p.


https://doi.org/10.17993/3ctecno.2021.specialissue8.179-197

Criticism administration is essential, if the sign sent by the transponder isn't appropriately gotten by the end clients. Henceforth the undesired or undesirable sign got at the recipient may nourished back again to get the unadulterated type of sign. i.e. signal without clamor. So as to keep away from this sort of loud flag, we have to avert our framework with considerably more proficiency.

So as to give high throughput, the inertness ought to be low. There were a few stages which are recorded underneath, to diminish the input administrations. A large number of these arrangements hazard creating more flotsam and jetsam from impacts, and all future costly and disputable. Another methodology is to forestall space crashes in any case through better traffic control. Today, satellite administrators don't have exact orbital parameters for different satellites that may represent a danger of impact. Just a couple of nations — primarily the United States, and somewhat China, Europe, and Russia — approach exact following information, and that data is stayed quiet, in case it uncovers insights concerning the advanced instrumentation used to assemble it.

Military organizers have since quite a while ago discussed the requirement for "space situational mindfulness", and the military tracks satellites for its very own motivations. But the inexorably jam-packed nature of close earth circles, in addition to the risk presented by crash flotsam and jetsam, has driven numerous to contend that we need comparable following abilities for the regular citizen area. The shabby method to do this is to make a portion of the military information open; the costly way is manufacturing a different, absolutely regular citizen following framework. The parts utilized for the uplink and downlink correspondence ought to be very much prepared with no harms. The gear used for this sort of correspondence ought to be kept up appropriately, with a wide range of approval procedures to give productive sign at the less than desirable end.

## 2. METHODOLOGY OF SOLVING THE ABOVE QUEUING ISSUE

### 2.1. METHODOLOGY

The above queuing issue is solved by supplementary variable technique of queuing theory.


https://doi.org/10.17993/3ctecno.2021.specialissue8.179-197

First, we outline the administering conditions for the lining issue engaged with satellite correspondence concentrate in area 4 by utilizing the boundaries like help rendered, short excursion, long get-away, delay in getting into upkeep work, reneging, input administration and phases of administration. Here help is rendered into two phases which make the framework to work out in a simplicity way.

As a subsequent advance, we process out the underlying limit states of the issue characterized.

Next by the utilization of different advantageous factors, we infer the likelihood creating capacity of the line size of the satellite correspondence lining issue. In continuation, length of the line, number of clients (attempts to be completed) in the framework, holding up time of the clients in the line just as in the framework are inferred.

## 2.2. BENEFITS

All the deductions are defended by methods for numerical outline and graphical depiction. In light of that, examination have been made in the numerical investigation and the investigation is done in the examination report. Having a profound report on the examination, one can get limiting the defer procedure in getting into the excursion method in the Satellite. Additionally, framework support work is required whether for shorter length or longer span could be anticipated. This investigation assists with doing the different components in correspondence issue in an exact way. This prompts the length of the line to be negligible in the framework. Use factor would be made to a maximal. Satellite correspondence framework attempts to a maximal level.

# 3. ASSUMPTIONS UNDER LYING THE MODEL

Customers arrive in groups to the Queuing system (In the process of communication).

Clients arrive in batches to the system modelling supermarkets with mean arrival rate $\lambda > 0$.

$\lambda e_k$ (k = 1 to n) be the first order probability that a batch of $r$ customers arrive at the system.

Here, $0 \leq e_k \leq 1$ and $\sum_{k=1}^{n} e_k = 1$


https://doi.org/10.17993/3ctecno.2021.specialissue8.179-197

For the first stage of service, $S_n^{(1)}(x),\theta_1(x)$ is the conditional probability of completion of completion of first stage of service. The probability distribution function of the first stage of service and its corresponding density function are given by $G_1^*(x)$ and $g_1^*(x)$.Hence

$$\theta_1(x) = \frac{g_1^*(x)}{1 - G_1^*(x)}, \quad g_1^*(x)(s) = \theta_1(s)e^{-\int_0^s \theta_1(x)dx}$$

Similarly for all the other parameters Delay process $(D_n(x))$, Compulsory vacation $(M_n(x))$, Stage 2 process $(S_n^{(2)}(x))$ we have the following functions respectively:

$$\theta_j(x) = \frac{g_j^*(x)}{1-G_j^*(x)}, \quad g_j^*(x)(s) = \theta_j(s)e^{-\int_0^s \theta_j(x)dx}, \text{j} = 2, 3, 4$$

## 4. STEADY STATE CONDITIONS OVERSEEING THE FRAMEWORK

$$\frac{d}{dx}S_n^{(1)}(x) + (\lambda + \theta_1(x))S_n^{(1)}(x) = \lambda \sum_{k=1}^n e_k S_{n-k}^{(1)}(x). \tag{1}$$

$$\frac{d}{dx}S_0^{(1)}(x) + (\lambda + \theta_1(x))S_0^{(1)}(x) = 0. \tag{2}$$

$$\frac{d}{dx}D_n(x) + (\lambda + \theta_2(x))D_n(x) = \lambda \sum_{k=1}^n e_k\, D_{n-k}(x). \tag{3}$$

$$\frac{d}{dx}D_0(x) + (\lambda + \theta_2(x))D_0(x) = 0. \tag{4}$$

$$\frac{d}{dx}M_n(x) + (\lambda + \theta_3(x) + \gamma)M_n(x) = \lambda \sum_{k=1}^n e_k\, M_{n-k}(x) + \gamma M_{n+1}(x). \tag{5}$$

$$\frac{d}{dx}M_0(x) + \big(\lambda + \theta_3(x)\big)M_0(x) = 0. \tag{6}$$

$$\frac{d}{dx}S_n^{(2)}(x) + (\lambda + \theta_4(x))S_n^{(2)}(x) = \lambda \sum_{k=1}^n e_k S_{n-k}^{(2)}(x). \tag{7}$$

$$\frac{d}{dx}S_0^{(2)}(x) + \big(\lambda + \theta_4(x)\big)S_0^{(2)}(x) = 0. \tag{8}$$

$$\lambda Q = (1 - r)\int_0^\infty M_0(x)\theta_3(x)dx + (1 - p)\int_0^\infty S_0^{(2)}(x)\,\theta_4(x)dx. \tag{9}$$

The following boundary conditions are used to solve the above equations.


https://doi.org/10.17993/3ctecno.2021.specialissue8.179-197

$$S_n^{(1)}(0) = (1-r)\int_0^\infty M_{n+1}(x)\,\theta_3(x)dx + p\int_0^\infty S_n^{(2)}(x)\theta_4(x)dx + (1-p)\int_0^\infty S_{n+1}^{(2)}(x)\theta_4(x)dx. \quad (10)$$

$$D_n(0) = \int_0^\infty S_n^{(1)}(x)\,\theta_1(x)dx. \quad (11)$$

$$M_n(0) = q\int_0^\infty D_n(x)\,\theta_2(x)dx. \quad (12)$$

$$S_n^{(2)}(0) = r\int_0^\infty M_n(x)\theta_3(x)dx. \quad (13)$$

## 5. DISTRIBUTION OF THE QUEUE LENGTH AT ANY POINT OF TIME

Multiply (1) by $z^n$ and sum over $n$ from 1 to ∞ and add it to (2) results in the following equation

$$\frac{d}{dx}S_n^{(1)}(x,z) + (\lambda - \lambda E_k(z) + \theta_1(x))S_n^{(1)}(x,z) = 0. \quad (14)$$

$$\frac{d}{dx}D_n(x,z) + (\lambda - \lambda E_k(z) + \theta_2(x))D_n(x,z) = 0. \quad (15)$$

$$\frac{d}{dx}M_n(x,z) + \left(\lambda - \lambda E_k(z) + \gamma - \frac{\gamma}{z} + \theta_3(x)\right)M_n(x,z) = 0. \quad (16)$$

$$\frac{d}{dx}S_n^{(2)}(x,z) + (\lambda - \lambda E_k(z) + \theta_4(x))S_n^{(2)}(x,z) = 0. \quad (17)$$

Similarly,

$$zS_n^{(1)}(0,z) = (1-r)\int_0^\infty M_n(x,z)\theta_3(x)dx + p\int_0^\infty S_n^{(2)}(x,z)\theta_4(x)dx + (1-p)\int_0^\infty S_n^{(2)}(x,z)\theta_4(x)dx + \lambda(E_k(z)-1)Q. \quad (18)$$

$$D_n(0,z) = \int_0^\infty S_n^{(1)}(x,z)\theta_1(x)dx. \quad (19)$$

$$M_n(0,z) = q\int_0^\infty D_n(x,z)\theta_2(x)dx \quad . \quad (20)$$

$$S_n^{(2)}(0,z) = r\int_0^\infty M_n(x,z)\theta_3(x)dx. \quad (21)$$

Now integrating (14) from 0 to x, it gives


https://doi.org/10.17993/3ctecno.2021.specialissue8.179-197

$$S_n^{(1)}(x,z) = S_n^{(1)}(0,z)e^{-(\lambda-\lambda E_k(z))-\int_0^x \theta_1(t)dt.} \tag{22}$$

Integrating the above by parts,

$$S_n^{(1)}(z) = S_n^{(1)}(0,z)\left(\frac{1-G_1^*(w)}{w}\right), w = \lambda - \lambda E_k(z). \tag{23}$$

Where $G_1^*(w) = \int_0^\infty e^{-(\lambda-\lambda E_k(z))x} dG_1(x)$ is the Laplace Stieltje's transform of the service time.

Again multiply (22) by $\theta_1(x)$ and integrating,

$$\int_0^\infty S_n^{(1)}(x,z)\theta_1(x)dx = S_n^{(1)}(0,z)G_1^*(w) \ . \tag{24}$$

Similarly, from the other parameters, we have

$$D_n(z) = D_n(0,z)\left(\frac{1-G_2^*(w)}{w}\right). \tag{25}$$

$$\int_0^\infty D_n(x,z)\theta_2(x)dx = S_n^{(1)}(0,z)G_1^*(w)G_2^*(w). \tag{26}$$

$$M_n(z) = M_n(0,z)\left(\frac{1-G_3^*(k)}{k}\right), k = \lambda - \lambda E_k(z) + \gamma - \frac{\gamma}{z}$$

$$= qS_n^{(1)}(0,z)G_1^*(w)G_2^*(w)\left(\frac{1-G_3^*(k)}{k}\right). \tag{27}$$

$$\int_0^\infty M_n(x,z)\theta_3(x)dx = qS_n^{(1)}(0,z)G_1^*(w)G_2^*(w)G_3^*(k) \tag{28}$$

$$S_n^{(2)}(z) = S_n^{(2)}(0,z)\frac{\left(1-{G_4}^*(w)\right)}{w}.$$

$$= rqS_n^{(1)}(0,z){G_1}^*(w){G_2}^*(w){G_3}^*(k)\left[\frac{\left(1-{G_4}^*(w)\right)}{w}\right]. \tag{29}$$

$$\int_0^\infty S_n^{(2)}(x,z)\theta_4(x)dx = rqS_n^{(1)}(0,z){G_1}^*(w){G_2}^*(w){G_3}^*(k)\,{G_4}^*(w). \tag{30}$$

Using (28) and (30) in (18) we get,

$$S_n^{(1)}(0,z) = \frac{\lambda Q(E_k(z)-1)}{z-{G_1}^*(w){G_2}^*(w){G_3}^*(k)q[1+r{G_4}^*(w)]} \ . \tag{31}$$


https://doi.org/10.17993/3ctecno.2021.specialissue8.179-197

To find the probability making limit of the line gauge paying little mind to the state of the structure.

Let $P_q(z)$ be the probability generating function of the Queue size.

Then adding (23), (25), (27) and (29), we get

Hence, $P_q(z) = S_n^{(1)}(z) + D_n(z) + M_n(z) + S_n^{(2)}(z)$

$$= \frac{Q\left\{\begin{matrix}-[1-G_1^*(w)+(1-G_2^*(w))G_1^*(w)+rqG_1^*(w)G_2^*(w)G_3^*(k)(1-G_4^*(w))]+ \\ qG_1^*(w)G_2^*(w)\frac{(1-G_3^*(k))}{k}\lambda(E_k(z)-1)\end{matrix}\right\}}{z-G_1^*(w)G_2^*(w)G_3^*(k)q[1+rG_4^*(w)]}. \quad (32)$$

## 6. RESULTS

The idle time $Q$ is determined by using the normalization condition

$$P_q(1) + Q = 1$$

Using L'Hopital's rule, we get

$$\lim_{z\to 1} P_q(z) = \frac{N'(1)}{D'(1)}$$

Also $Q = \frac{D'(1)}{D'(1)+N'(1)}$

From $Q$, the utilization factor $\rho$ can be determined.

Let $L_q$ a chance to demonstrate the reliable state typical number of customers in the line. By then $L_q = \frac{d}{dz}P_q(z)\big|_{z=1} = \frac{d}{dz}\left\{\frac{N(z)}{D(z)}\right\}\Big|_{z=1}$

Where $N(z)$ and $D(z)$ are the numerator and denominator of (32).

Since $P_q(z) = \frac{0}{0}$ at $z=1$, we utilize two-fold separation and get

$$L_q = \lim_{z\to 1}\frac{d}{dz}P_q(z) = \frac{D'(1)N''(1)-D''(1)N'(1).}{2(D'(1))^2}. \quad (33)$$

Where primes mean subordinates with respect to $z$ and after a course of action of logarithmic enhancement, we get length of the queue $L_q$ in closed frame.


https://doi.org/10.17993/3ctecno.2021.specialissue8.179-197

$$N'(1) = -\{-\lambda E(G_1) - \lambda E(G_2) - rq\lambda E(G_4)\}. \tag{34}$$

$$N''(1) = -\Big\{-\lambda^2\left[E(G_1^{\,2}) + E(G_2^{\,2})\right] + 2\lambda^2 E(G_1)E(G_2) - rq\lambda^2[E(G_4)][E(G_1) + E(G_2)] + rq\{(-\lambda+\gamma)E(G_3)(-\lambda)E(G_4) - E(G_4)\lambda^2[E(G_1) + E(G_2)] + \lambda E(G_4)(-\lambda+\gamma)E(G_3) - \lambda^2 E(G_4^{\,2})\}\Big\} \tag{35}$$

$$D' = 1 - q\left[(1+r)\left[\lambda\left(E(G_1) + E(G_2)\right) + (\lambda-\gamma)E(G_3) + r\lambda E(G_4)\right]\right] \tag{36}$$

$$D'' = -q\left[(1+r)\left[\lambda^2\left(E(G_1^{\,2}) + E(G_2)E(G_1)\right) + \lambda(-\gamma+\lambda)E(G_3)E(G_1)\right] + r\lambda^2 E(G_1)E(G_4) + (1+r)\left[\lambda^2\left(E(G_2^{\,2}) + E(G_1)E(G_2)\right) + \lambda(-\gamma+\lambda)E(G_3)E(G_2)\right] + r\lambda^2 E(G_2)E(G_4) + (1+r)\left[(-\lambda+\gamma)(-\lambda)\left(E(G_1)E(G_3) + E(G_2)E(G_3)\right) + (-\lambda+\gamma)^2 E(G_3^{\,2}) + 2\gamma E(G_3)\right] + rE(G_4)\lambda E(G_3)(\lambda-\gamma) + \lambda r E(G_4)\{\lambda[E(G_1) + E(G_2)] + (\lambda-\gamma)E(G_3)\} + r\lambda^2 E(G_4^{\,2})\right] \tag{37}$$

Substituting for $N'(1)$, $N''(1)$,$D'(1)$, $D''(1)$ from (34) – (37) in (33), we obtain $L_q$ in closed form.

Further the mean waiting time of a customer in the queue as well as in the system and the number of customers waiting in the system can be found using Little's formula $W_q = \frac{L_q}{\lambda}$ , $W = \frac{L}{\lambda}$ , $L = L_q + \rho$

## 7. NUMERICAL JUSTIFICATION OF THE MODEL

Assume that service time follows exponential distribution in particular and based on this condition, the numerical justification is elaborated below:

The values are collected accordingly: $\lambda = 2$, $\theta_1 = 5$, $r = 0.5$, $\gamma = 0.6$

$$E(G_1) = \frac{1}{\theta_1}, \quad E(G_2) = \frac{1}{\theta_2}, \quad E(G_3) = \frac{1}{\theta_3}, \quad E(G_4) = \frac{1}{\theta_4}, \quad E(G_1^{\,2}) = \frac{2}{\theta_1^{\,2}},$$

$$E(G_2^{\,2}) = \frac{2}{\theta_2^{\,2}}, \quad E(G_3^{\,2}) = \frac{2}{\theta_3^{\,2}}, E(G_4^{\,2}) = \frac{2}{\theta_4^{\,2}}$$

**Table 1.** Variation of $\theta_1$=3,5,7,9,11.

| $Q$ | $\rho$ | $Lq$ | $L$ | $W_q$ | $W$ |
|---|---|---|---|---|---|
| 0.2770 | 0.7230 | 4.8008 | 5.5238 | 2.4004 | 2.7619 |
| 0.3817 | 0.6183 | 1.7827 | 2.4010 | 0.8914 | 1.2005 |


https://doi.org/10.17993/3ctecno.2021.specialissue8.179-197

| | | | | | |
|---|---|---|---|---|---|
| 0.4346 | 0.5654 | 1.1901 | 1.7555 | 0.5951 | 0.8778 |
| 0.4667 | 0.5333 | 0.9656 | 1.4989 | 0.4828 | 0.7495 |
| 0.5019 | 0.4981 | 0.7789 | 1.2770 | 0.3895 | 0.6385 |

**Source:** own elaboration.

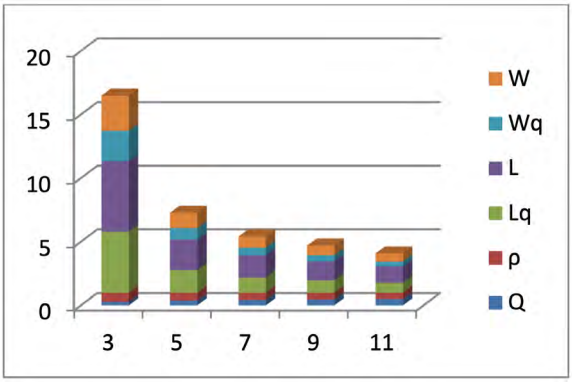


**Graphic 3.** Variation of $\theta_1$.
**Source**: own elaboration.

**Table 2.** Variation of $\theta_2$=5,6,7,8,9.

| $Q$ | $P$ | $Lq$ | $L$ | $W_q$ | $W$ |
|---|---|---|---|---|---|
| 0.2770 | 0.7230 | 4.8008 | 5.5238 | 2.4004 | 2.7619 |
| 0.2850 | 0.7150 | 4.1952 | 4.9102 | 2.0976 | 2.4551 |
| 0.2906 | 0.7094 | 3.9202 | 4.6296 | 1.9601 | 2.3148 |
| 0.2948 | 0.7052 | 3.6871 | 4.3923 | 1.8436 | 2.1962 |
| 0.2980 | 0.7020 | 3.5179 | 4.2199 | 1.7590 | 2.1100 |

**Source:** own elaboration.


https://doi.org/10.17993/3ctecno.2021.specialissue8.179-197

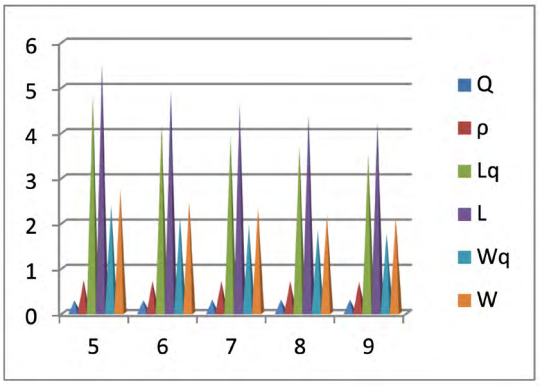


**Graphic 4.** Variation of $\theta_2$.
**Source:** own elaboration.

## 8. NUMERICAL ANALYSIS

From Table1, it is identified that, if the process of completion of work in the first stage increases, it leads to a decrease in the length of the queue and also in the other performance measures. As the work gets completed sooner, the server idle time Q increases. Table 2 gives the fact that, as the probability of completion of vacation increase, it leads to an absence of a long queue in the communication process. It results in the decrease in waiting time of the process to be carried out in the queue as well as in the system. The results are as expected.

## 9. CONCLUSIONS

The Queuing procedure happening in the satellite communication procedure has been well analyzed in this paper. The Queuing problem is solved by means of supplementary variable method. The corresponding Queue execution measures are determined. The numerical illustration and the graphical picture well scrutinized the Queuing problem in satellite communication process. As a future work, obstruction can be brought into various stages. Furthermore, the possibility of Bernoulli move away could be added as it expects an obvious part taking everything together the coating structure. Equivalent examination of execution methods with this model can be appeared by including the parts of kept worthiness, balking in different stages, Priority alliance, set up time and multi move away from strategy. The system of need can be utilized in the above model and as a remarkable


https://doi.org/10.17993/3ctecno.2021.specialissue8.179-197

case this model can be diminished from that as of late arranged model. Retrial cooperation can be considered in this model.

## REFERENCES

**Chang, J.-F., & Lin, S.-H.** (1993). Delay performance of VSAT- based satellite wide area networks. *International Journal of Satellite communications banner, 11*(1), 1-12. https://doi.org/10.1002/sat.4600110102

**Fantacci, R., & Zoppi, L.** (2000). Performance evaluation of polling systems for wireless local communication networks. *IEEE Transactions on vehicular technology, 49*(6), 2148-2157. https://ieeexplore.ieee.org/document/901886

**Giambene, G., & Kota, S.** (2006). Cross-layer protocol optimization for satellite communications networks: a survey. *International Journal of Satellite Communications and networking, 24*(5), 323-341. https://doi.org/10.1002/sat.853

**Hung, A., Montpetit, M., & Kesidis, G.** (1998). ATM via Satellite: A framework and implementation. *Springer wireless networks, 4*(2), 141-153. https://doi.org/10.1023/A:1019191619926

**Lam, S. S.** (1980). A carrier senses multiple access protocol for local networks. *Computer Networks, 4*(1), 21-32. https://doi.org/10.1016/0376-5075(80)90026-4

**Louvros, S., Pylarinos, J., & Kotsopoulos, S.** (2007). Handoff multiple queue model in microcellular networks. *Elsevier computer communications, 30*(2), 396-403. https://doi.org/10.1016/j.comcom.2006.09.008

**Lutz, E.** (1998). Issues in Satellite Personal Communication Systems. *Wireless networks, 4*, 109-124. https://doi.org/10.1023/A:1019187519018

**Maragathasundari, S.** (2015). A Bulk arrival queuing model of three stages of service with different vacation policies service interruption and delay time. *American International Journal of Research in Science and Technology, 11*(1), 52-56. https://citeseerx.ist.psu.edu/viewdoc/download?doi=10.1.1.1043.2705&rep=rep1&type=pdf

**Maragathasundari, S., & Karthikeyan, K.** (2016). A Bulk queuing model of Optional second phase service with short and long vacations. *International Journal of Scientific Research in Science and Technology, 2*(5), 196-201. https://www.researchgate.net/publication/308917899_A_Bulk_Queuing_Model_of_Optional_Second_Phase_Service_with_Short_and_Long_Vacations

**Maragathasundari, S., Anandapriya, B., Gothaiammal, S.B., & Gowri, V.** (2017). M/G/1 Queue with restricted availability during service interruption and compulsory vacation of deterministic time. *International Journal of Mathematics Trends and Technology, 52*(1), 5-9.

**Yeung, R. W., & Zhang, Z.** (1999). Distributed source coding for satellite communications. *IEEE transactions on information theory, 45*(4), 1111-1120. https://ieeexplore.ieee.org/document/761254

**Zaim, A.** (2003). A markov model to calculate new and hand-off call blocking probabilities in LEO satellite networks. *Journal of Research and Practice in Information Technology, 35*(4), 271-283. https://search.informit.org/doi/abs/10.3316/ielapa.145199503050615

**Zhu, J., Rao, Y., Fu, L., Chen, W., & Shao, X.** (2012). Load Balancing Routing Based on Agent for Polar-orbit LEO satellite networks. *Journal of Information and computational science, 9*(5), 1373-1384. https://www.researchgate.net/publication/288271380_Load_balancing_routing_based_on_agent_for_polar-orbit_LEO_satellite_networks


https://doi.org/10.17993/3ctecno.2021.specialissue8.179-197

https://doi.org/10.17993/3ctecno.2021.specialissue8.179-197

/12/


https://doi.org/10.17993/3ctecno.2021.specialissue8

# COMPARISON AND SIMULATION STUDY OF CYLINDRICAL GAA NWMBCFET FOR SUB 35NM

**S. Ashok Kumar**
Research Scholar, Centre for VLSI Design, Department of Electronics and Communication Engineering, Kalasalingam Academy of Research and Education, Virudhunagar, (India).
E-mail: 6691ashok@gmail.com
ORCID: http://orcid.org/0000-0002-0957-6685

**J. Charles Pravin**
Associate Professor, Centre for VLSI Design, Department of Electronics and Communication Engineering, Kalasalingam Academy of Research and Education. Virudhunagar, (India).
E-mail: charles@klu.ac.in
ORCID: http://orcid.org/0000-0002-9009-6274

**Recepción:** 11/11/2019 **Aceptación:** 26/10/2020 **Publicación:** 30/11/2021

**Citación sugerida:**
Kumar, S. A., y Pravin, J. C. (2021). Comparison and Simulation study of Cylindrical GAA NWMBCFET for sub 35nm. *3C Tecnología. Glosas de innovación aplicadas a la pyme, Edición Especial,* (noviembre, 2021), 199-209. https://doi.org/10.17993/3ctecno.2021.specialissue8.199-209

## ABSTRACT

In this paper, a cylindrical Gate All Around Nano Wire Field Effect Transistor (GAA NWFET) is compared with cylindrical Gate All Around Nano Wire Multi Bridge Channel Field Effect Transistor (GAA NWMBCFET) for sub 35nm devices using Technology Computer Aided Design (TCAD) simulation tool. Instead of one channel with equal distance in vertical and horizontal stacking, about 12 thin channels have been created in GAA NWMBCFET. The device performance has been numerically evaluated using coupled Drift-diffusion (DD) method and Shockley-Read-Hall Recombination method (SRH). The compared transfer and output characteristics of GAA NWFET and GAA NWMBCFET has been reported using the TCAD numerical simulation calibrations. The inclusion of multi bridge channel in the device has increased its current drive because of the Ultra-Thin Body (UTB). It has been accounted for that the GAA structure has a decent insusceptibility to short channel impacts.

## KEYWORDS

Cylindrical GAA NWFET, Cylindrical GAA NWMBCFET, TCAD, UTB, MBCFET.


https://doi.org/10.17993/3ctecno.2021.specialissue8.199-209

# 1. INTRODUCTION

Gate All Around structure is a promising candidate for short channel transistors as per ITRS 2015 (ITRS version 2.0., 2015). The idea of Multi Bridge channel originates from stacking channels one over the other. Contingent upon the quantity of channels stacked in the transistor MBCFET ensures high output current. The output current is increased by using Ultra-Thin Body (UTB) in the Si channel and also by reducing the oxide thickness (Lee *et al.*, 2003; Lee *et al.*, 2004a).

GAA NWFET is one of the better alternatives for accomplishing superiority in Nano-level transistors. The GAA NWFET could decrease short channel impacts like Drain Induced Barrier Lowering (DIBL), SS and VTH roll off because of its geometric structure (Singh *et al.*, 2006; Al-Ameri *et al.*, 2017). The GAA NWFET constitutes of various structures like cubical, cylindrical and elliptical (Lin *et al.*, 2018; Nagy *et al.*, 2018; Salmani-Jelodar *et al.*, 2015). An MBCFET of 5 µm channel length was fabricated in the year 2003, and achieved high output current of 4.6 times larger (Lee *et al.*, 2003). In Lee *et al.* (2004a) an MBCFET structure in 2004 with a reduced gate length of 250 nm was manufactured. Multi-channel transistors were fabricated with different materials having gate lengths of 90nm and 30nm as discussed in Lee *et al.* (2004b) and Yoon *et al.* (2004) respectively. All multi bridge channel devices with enlarged width attained high output current as given in Yoon *et al.* (2004); Lee *et al.* (2003); Lee *et al.* (2004b). An n-channel cylindrical structure as like in Nayak *et al.* (2014), has been developed in this paper, 12 thin channels have been made rather than one channel and every channel is encompassed by an oxide layer in TCAD.

# 2. DEVICE STRUCTURE

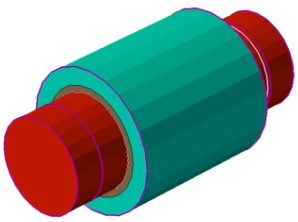

**Figure 1**. Cylindrical Structure formed in TCAD.
**Source:** own elaboration.


https://doi.org/10.17993/3ctecno.2021.specialissue8.199-209

The cylindrical n-channel GAA NWFET (Figure 1) is formed in TCAD by using the details given in Nayak *et al.* (2014), which is detailed in Table 1. The simulation was done utilizing the Drift-Diffusion and Shockley-Read-Hall models.

A. Drift-Diffusion Model

In drift-diffusion model, the electron current density is:

$$\overrightarrow{Jn} = \mu_n(n\nabla E_C - 1.5nkT\nabla lnm_n) + D_n(\nabla_n - n\nabla ln\gamma_n) \quad (1)$$

and the current density of holes is given by:

$$\overrightarrow{J_p} = \mu_p\left(p\nabla E_v - 1.5pkT\nabla lnm_p\right) + D_p(\nabla_p - n\nabla ln\gamma_p) \quad (2)$$

The first term takes into account the contribution due to the spatial variations of the electrostatic potential, the electron affinity, and the band gap. The remaining terms consider the contribution due to the gradient of concentration, and the spatial variation of the effective masses mn and mp. Through the Einstein relation the diffusivities are derived using the mobilities.

$$D_n = kT\mu_n \; and \; D_p = kT\mu_p \quad (3)$$

**Table 1.** Parameters and values.

| Parameters | Values (nm/ $cm^3$) |
|---|---|
| Gate Length | 35 |
| Gate Oxide | 1.5 |
| NW Diameter | 21.45 |
| Drain/Source Doping | 1e20 |
| Channel Doping | 1e15 |

**Source:** own elaboration.


https://doi.org/10.17993/3ctecno.2021.specialissue8.199-209

B. Shockley-Read-Hall Recombination

Recombination through deep defect levels in the gap is usually labeled SRH recombination. In Sentaurus device, the following form is implemented:

$$R_{net}^{SRH} = \frac{np - n_{i,eff}^2}{\tau_p(n+n_1)+\tau_n(p+p_1)} \quad (4)$$

with:

$$n_1 = n_{i,eff}\exp\left(\frac{E_{trap}}{KT}\right) \quad (5)$$

and:

$$p_1 = n_{i,eff}\exp\left(\frac{-E_{trap}}{KT}\right) \quad (6)$$

where $E_{trap}$ is the difference between the defect level and the intrinsic level. The variable $E_{trap}$ is accessible in the parameter file. The default $E_{trap}$ value for Silicon is 0.

The doping dependence of the SRH lifetimes is modeled in Sentaurus device by use of the Scharfetter relation:

$$\tau_{dop}(N_{A,0} + N_{D,0}) = \tau_{dop} + \frac{\tau_{max}-\tau_{min}}{1+\left(\frac{N_{A,0}+N_{D,0}}{N_{ref}}\right)^{\gamma}} \quad (7)$$

After achieving same IV characteristics with (Nayak *et al.*, 2014) 12 channels have been formed in the place of single channel and the IV characteristics are measured using the same models. The primary objective here is to increase the output current drivability of the device without increasing the width of the transistor. The schematic of the Multi Bridge channels in a cylindrical channel have been demonstrated in Figure 2b, 2c. The Figure 2d shows equal distance being given to 12 channels and the electrostatic integrity has also been maintained.

The splitted 12 thin channels are surrounded by an oxide layer. A direct metal contact on oxide layer was given with the work function of 4.461 and a high k dielectric is used as an oxide to control the Ioff value.


https://doi.org/10.17993/3ctecno.2021.specialissue8.199-209

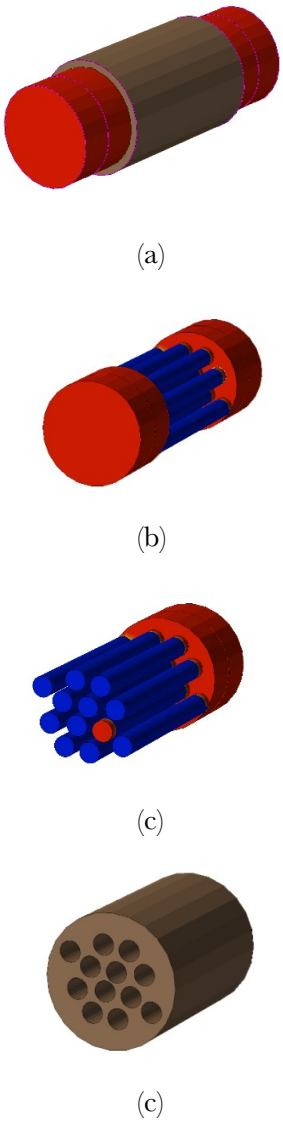


**Figure 2.** a) Cylindrical Structure with oxide layer, b) Multi Bridge Channel, c) 12 Channels, d) Oxide layer surrounding channels.
**Source:** own elaboration.

## 3. RESULTS

Figures 3 and 4 shows the comparison between the transfer and output characteristics of cylindrical GAA NWFET and cylindrical GAA NWMBCFET which clearly indicates that the Multi Bridge increases the current drivability and the short channel effects like Drain


https://doi.org/10.17993/3ctecno.2021.specialissue8.199-209

Induced Barrier Lowering (DIBL) and SS are reduced due to the surrounding oxide layer. The current drive of the device was increased due to the presence of UTB Si channel, without having to increase the width of the transistor. In transfer characteristics the curve has been plotted for $V_D=V_G=$ 1V and $V_G$=50mV, $V_D$=1V for both cylindrical GAA NWFET and cylindrical GAA NWMBCFET. Figure 3 clearly shows an increase in current drive of the GAA NWMBCFET when compared with GAA NWMBCFET. The channel current can be increased further by reducing the oxide layer thickness but there occurs an increase in a short channel effect Threshold voltage rolloff ($V_{TH}$ rolloff).

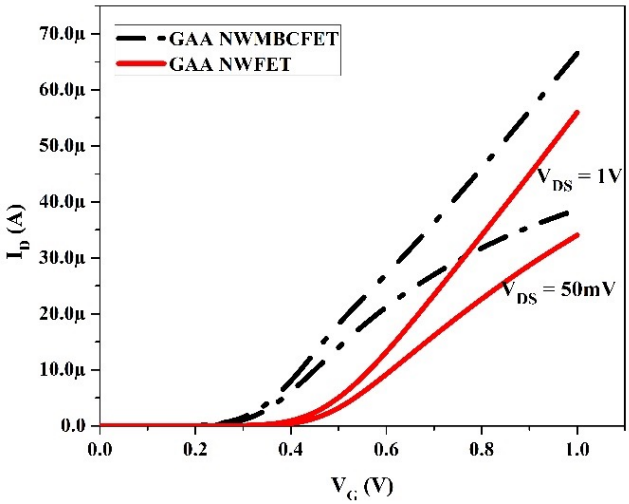


**Figure 3.** Compared Transfer Characteristics between GAA NWMBCFET and GAA NWFET.
**Source:** own elaboration.

The output characteristics are plotted by varying $V_{GS}$ from 0.7 V to 0.9 V for both devices. By comparing the output characteristics with the GAA NWFET, the GAA NWMBCFET clearly indicates more output current. The gate effect has been spread equivalently to all the channels due to the presence of UTB and GAA, but it is still believed that the effect of electro static potential will be more in outer channels than the inner channels. In Basic GAA structure gate controls over the channels so the short channel effects will reduce but in the case 12 channels, the inner channels not directly having contact with metal gate. That may build the short channel impacts.


https://doi.org/10.17993/3ctecno.2021.specialissue8.199-209

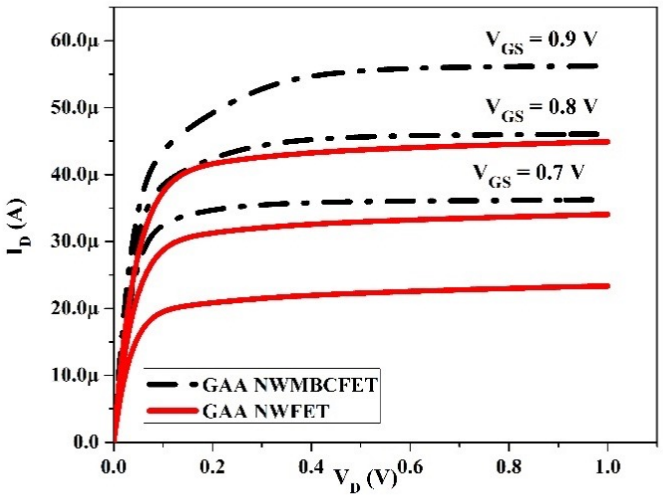


**Figure 4.** Compared Output Characteristics between GAA NWMBCFET and GAA NWFET.
**Source:** own elaboration.

## 4. CONCLUSIONS

A GAA NWFET has been formed in TCAD with a gate length of 35 nm. This device is then developed into a Nanowire Multi-Bridge-Channel FET (GAA NWMBCFET) by splitting 12 different channels from the single channel, and stacking them in vertical and horizontal manner for a gate length of 35 nm. The incorporation of Multi Bridge channels showed an increase in current drive as compared to the normal nanowire structures. Device performance will be varied depending upon the nanowire structure too. The proposed MBC device displayed a maximum current drive of 65 µA, nearly 20% higher than the conventional NWFET. By isolating the channel regions from the metal gate, by using 12 channels, the MBC structure was able to impact and alter short channel effects in such devices. Multi bridge channels are believed to deliver exceptional performances for short channel devices in the future and will be a potential candidate for low power applications.

## 5. ACKNOWLEDGEMENT

The Authors are thankful to the management of Kalasalingam Academy of Research and Education (KARE) for the provision of TCAD laboratory facilities during this research.


https://doi.org/10.17993/3ctecno.2021.specialissue8.199-209

## REFERENCES

**Al-Ameri, T., Georgiev, V.P., Sadi, T., Wang, Y., Adamu-Lema, F., Wang, X., Amoroso, S.M., Towie, E., Brown, A., & Asenov, A.** (2017). Impact of quantum confinement on transport and the electrostatic driven performance of silicon nanowire transistors at the scaling limit. *Solid-State Electronics, 129*, 73-80. https://doi.org/10.1016/j.sse.2016.12.015

**Bangsaruntip, S., Cohen, G.M., Majumdar, A., Zhang, Y., Engelmann, S.U., Fuller, N.C.M., Gignac, L.M., Mittal, S., Newbury, J.S., Guillorn, M., & Barwicz, T.** (2009). High performance and highly uniform gate-all-around silicon nanowire MOSFETs with wire size dependent scaling. *IEEE International Electron Devices Meeting*, 1-4. https://doi.org/10.1109/IEDM.2009.5424364

**ITRS version 2.0.** (2015). http://www.semiconductors.org/main/2015_international_technology_roadmap_for_semiconductors_itrs/

**Lee, S.Y., Kim, S.M., Yoon, E.J., Oh, C.W., Chung, I., Park, D., & Kim, K.** (2003). A novel multibridge-channel MOSFET (MBCFET): fabrication technologies and characteristics. *IEEE Transactions on Nanotechnology, 2*(4), 253-257. https://doi.org/10.1109/TNANO.2003.820777

**Lee, S.Y., Kim, S.M., Yoon, E.J., Oh, C.W., Chung, I., Park, D., & Kim, K.,** (2004a). Three-dimensional MBCFET as an ultimate transistor. *IEEE Electron Device Letters, 25*(4), 217-219. https://doi.org/10.1109/LED.2004.825199

**Lee, S.Y., Yoon, E.J., Kim, S.M., Oh, C.W., Li, M., Kim, D.W., Chung, I., Park, D., & Kim, K.** (2004b). Three-dimensional multi-bridge-channel MOSFET (MBCFET) fabricated on bulk Si-substrate. *Conference Digest [Includes' Late News Papers' volume] Device Research Conference, 2004. 62nd DRC,* 119-120. https://doi.org/10.1109/DRC.2004.1367812

**Lin, Y.R., Yang, Y.Y., Lin, Y.H., Kurniawan, E.D., Yeh, M.S., Chen, L.C., & Wu, Y.C.** (2018). Performance of Stacked Nanosheets Gate-All-Around and Multi-

Gate Thin-Film-Transistors. *IEEE Journal of the Electron Devices Society, 6,* 1187-1191. https://doi.org/10.1109/JEDS.2018.2873008

**Nagy, D., Indalecio, G., García-Loureiro, A.J., Elmessary, M.A., Kalna, K., & Seoane, N.** (2018). FinFET versus gate-all-around nanowire FET: Performance, scaling, and variability. *IEEE Journal of the Electron Devices Society, 6,* 332-340. https://doi.org/10.1109/JEDS.2018.2804383

**Nayak, K., Bajaj, M., Konar, A., Oldiges, P.J., Natori, K., Iwai, H., Murali, K.V., & Rao, V.R**. (2014). CMOS logic device and circuit performance of Si gate all around nanowire MOSFET. *IEEE Transactions on Electron Devices, 61*(9), 3066-3074. https://doi.org/10.1109/TED.2014.2335192

**Salmani-Jelodar, M., Mehrotra, S.R., Ilatikhameneh, H., & Klimeck, G.** (2015). Design guidelines for sub-12 nm nanowire MOSFETs. *IEEE Transactions on Nanotechnology, 14*(2), 210-213. https://doi.org/10.1109/TNANO.2015.2395441

**Singh, N., Agarwal, A., Bera, L.K., Liow, T.Y., Yang, R., Rustagi, S.C., Tung, C.H., Kumar, R., Lo, G.Q., Balasubramanian, N., & Kwong, D.L.** (2006). High-performance fully depleted silicon nanowire (diameter/spl les/5 nm) gate-all-around CMOS devices. *IEEE Electron Device Letters, 27*(5), 383-386. https://doi.org/10.1109/LED.2006.873381

**Yoon, E.J., Lee, S.Y., Kim, S.M., Kim, M.S., Kim, S.H., Ming, L., Suk, S., Yeo, K., Oh, C.W., Choe, J.D., & Choi, D**. (2004). Sub 30 nm multi-bridge-channel MOSFET (MBCFET) with metal gate electrode for ultra high performance application. *IEDM Technical Digest. IEEE International Electron Devices Meeting,* 627-630. https://doi.org/10.1109/IEDM.2004.1419244

https://doi.org/10.17993/3ctecno.2021.specialissue8.199-209

# /13/


https://doi.org/10.17993/3ctecno.2021.specialissue8

# QUEUING ISSUES OF BIG DATA ANALYTICS IN HEALTHCARE FRAME WORK

**S. Maragathasundari**
Assistant Professor, Department of Mathematics,
Kalasalingam Academy of Research and Education, Krishnankovi, (India).
E-mail: maragatham01@gmail.com
ORCID: https://orcid.org/0000-0003-1210-6411

**C. Prabhu**
Associate Professor, , Department of Mathematics,
Kalasalingam Academy of Research and Education, Krishnankovil, (India).
E-mail: cprabhumath@gmail.com
ORCID: https://orcid.org/0000-0003-3879-3299

**K. S. Dhanalakshmi**
Assistant Professor, Department of Electronics and Communication Engineering,
Kalasalingam Academy of Research and Education
Krishnankovil, (India).
E-mail: k.s.dhanalakshmi@klu.ac.in
ORCID: https://orcid.org/0000-0001-6285-3656

**Recepción:** 11/11/2019 **Aceptación:** 03/12/2020 **Publicación:** 30/11/2021

**Citación sugerida:**
Maragathasundari, S., Prabhu, C., y Dhanalakshmi, K. S. (2021). Queuing issues of big data analytics in healthcare frame work. *3C Tecnología. Glosas de innovación aplicadas a la pyme, Edición Especial,* (noviembre, 2021), 211-229. https://doi.org/10.17993/3ctecno.2021.specialissue8.211-229

## ABSTRACT

This paper explores an examination on Network traffic checking, investigation for upgrading system asset and improving client involvement in Healthcare Field. Be that as it may, existing systems accessible in medical clinics, which as a rule, depend on an elite server with expansive capacity limit, are not versatile for itemized examination of a vast volume of traffic information dependent on the patient examination subtleties, infection subtleties, blood bunch subtleties and the treatment given to them in intermittent premise and so on. The advantages of medicinal record trade (MRE), to give some examples, incorporate offering more data for doctor finding, giving better constant consideration to released patients, and dispensing with the misuse of copied examinations. In addition, the above system may be interrupted with all type of arriving patients, emergency cases, diagnosis period, consultation services etc. All the above issues happening inhuman services is drawn closer through Queuing hypothesis in this study. Queuing models are helpful for assessing the framework reaction time and all the execution proportions of the social insurance framework. Numerical delineation and an expand graphical investigation are completed toward the conclusion to approve the model. It gives a reasonable considered the calculated investigation of lining hypothesis in health insurance field.

## KEYWORDS

Setup time, Single stage service, Compulsory Phase I Vacation, Optional Phase II Vacation, Restricted Admissibility.


https://doi.org/10.17993/3ctecno.2021.specialissue8.211-229

# 1. INTRODUCTION

Big data in wellbeing and science to handle the difficulties in new models is getting to be huge. In the period of enormous information, the most troublesome issues that stay to be comprehended are the means by which to proficiently manage large quantities and assortments of information. There are numerous diagnostic speculations and models. In this segment, late revelations in big data stockpiling and examination models are overviewed. The procurement of voluminous information relies upon an assortment of clients and gadgets, just as ground-breaking server farms to store and process the information. Therefore, building up an unrestricted system foundation is desperately required; this framework would make it conceivable to accumulate geographically circulated and quickly produced information and send them to server farms for end clients. In one investigation, members saw the different difficulties in Setting up such a system structure.

Among emergency clinics, Electronic medicinal record trade can give more data to doctor determination and diminish costs from copy examinations. The fast development of data and correspondence innovation has accelerated advancement of clinical data frameworks. An ever-increasing number of patient records, research facility reports, drug store drugs, and budgetary and medical coverage information are currently exchanged through PC systems. As of now, most emergency clinics have built up their very own electronic medicinal record frameworks. In any case, these frameworks just help singular medical clinics and don't give correspondence or offer assets among emergency clinics. Along these lines, it is troublesome for a patient to visit his specialist in one clinic and have his restorative record from another medical clinic accessible. The long-haul care units additionally can't get release data from the medical clinics. Every human services supplier must use much time and exertion to gather quiet data, along these lines causing information excess, and maybe notwithstanding imperiling patient wellbeing.


https://doi.org/10.17993/3ctecno.2021.specialissue8.211-229

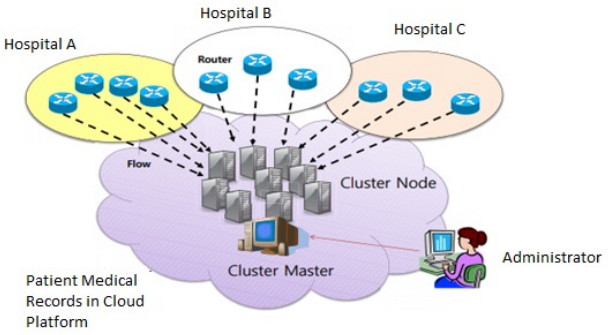


**Graphic 1.** Big Data Model in Healthcare System.
**Source:** own elaboration.

## 1.1. QUEUING PROBLEM IN HEALTH CARE UNIT PROCESS

Diverse applications have distinctive execution prerequisites. We list here seven such necessities:

1) *Batch landing* – Arrival of patients: Assume that the entry time of an outpatient at a clinic. Specifically, expanded asset use does not really suggest longer holding up neither lines nor longer patient stream times.
2) *Set up time* – Nursing Station: It is kept up by the doctor's training to look at the connection between inspecting room limit and patient stream crosswise over center-based execution measures. And furthermore distinguishing a few significant and generalizable parts of outpatient facility tasks
3) *Single Stage Service* - Fixed Normal Service: Traditionally, social insurance has been separated as either inpatient or outpatient. Inpatient care is given when patients are required to stay at a medical clinic or care office for the span of their treatment or disease. With outpatient social insurance, patients are dealt with and discharged that day. An arriving quiet check in and holds on to be called by a nursing room. Given both a nursing room and an inspecting room are accessible; the patient is brought to the nursing room. At the nursing room, the medical caretaker records the patient's indispensable insights and escorts the patient to an accessible looking at room.


https://doi.org/10.17993/3ctecno.2021.specialissue8.211-229

4) *Feedback Service* – "Visit Service": Owing to mechanical advances in diagnostics, prescriptions, and techniques, a greater part of social insurance needs is currently taken care of on an outpatient premise. The patient might be sent to the center research facility or x-beam office through the attendant helper station for doctor produced lab or x-beam work. This was regular amid physical examinations and wandering medical procedure.

5) *Compulsory Phase I Vacation* – Diagnosis period: The patient might be sent to the center lab or x-beam office by means of the attendant helper station for doctor produced lab or x-beam work. This was regular amid physical examinations and wandering medical procedure. During this season of Compulsory Phase I excursion the Server profit get-away (As long as the patient gets the records)

6) *Optional Phase II Vacation*: Final Consultation after conclusion the finish of a patient's "underlying" interview with their doctor was motioned by either the patient leaving the inspecting room (for the nursing station or registration work area) or the doctor leaving the looking at room. In the event that the underlying meeting finished with the doctor leaving the analyzing room, administration proceeded for the patient yet was not really performed in the patient's essence. For the most part, the expansion of administration as an "arrival" meeting included exercises that couldn't be finished inside the inspecting room.

7) *Restricted Admissibility* of Patient to the framework amid Optional get-away: Emergency/Accident Services - During this Optional Phase II get-away there will be a limited suitability of the patient to the framework is conceivable. "Administration" alludes to the period of time a patient went through in meeting with center work force while "stay" alludes to the all-out time spent at some area inside the facility. Pausing and administration times were effectively found as the contrast between the completion and beginning of two continuous administrations. Since the center lab and x-beam office are physically outside the family practice facility, just patient visits at these areas were recorded.


https://doi.org/10.17993/3ctecno.2021.specialissue8.211-229

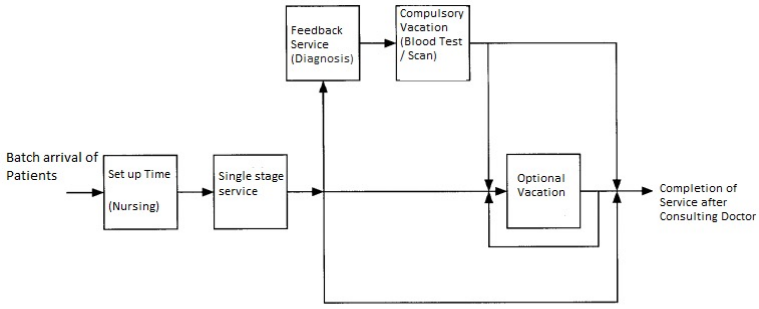


**Graphic 2.** Service Mechanism.
**Source:** own elaboration.

# 2. METHODOLOGY

## 2.1. SOLVING OF HEALTH QUEUING PROBLEM BY VARIABLE SUPPLEMENTRY VARIABLE METHOD OF QUEUING THEORY

The above process carried out in health care unit is a concrete problem which is well analyzed by queuing theory in this suggested current work. The queuing mechanism is developed based on the probability distribution in different range of communication. The above Queuing problem is solved through supplementary variable method of Queuing approach. Hence to start with, we describe the above queuing issue in terms of mathematical study of queuing theory. The above health care unit process is completely transformed to a queuing problem. Governing equations of the queuing problem are framed initially. Then the boundary conditions of the problem are explained. Then by the supplementary variable technique of usage of variable 'z', we derive the probability generating function of the queue size. Then by the tuberin property, length of the queue is found. Finally, the other execution measures of the problem are derived using Little's law. As clarified above in Health care unit process, the procedure comprises of arrival of patients, nurse station, normal fixed service, sojourn service, Diagnosis period, consultation period and emergency, accidental services.


https://doi.org/10.17993/3ctecno.2021.specialissue8.211-229

## 2.2. THE HEALTH CARE UNIT QUEUING PROBLEM IS AS FOLLOWS IN TERMS OF MATHEMATICAL STUDY

Client's arrival follows Poisson distribution. Administration pursues general circulation. To begin with, a set up time technique is presented in this procedure. Single phase of administration is given to all the arriving clients. On the off chance that any of the clients are in need, they are permitted to get an input administration, which gives a total attractive to all the arriving clients. After the fruition of the administration, the server needs to attempt an obligatory excursion, amid which to make the framework run easily to a more prominent degree, a total upkeep work to be done. Toward the finish of mandatory excursion, the server has the alternative to take an all-encompassing get-away if the submitted support work has not been finished amid the past get-away hour.

Restricted admissibility in the arriving customers is considered during the time of optional extended vacation to reduce the length of the queue. The lining issue (Health care unit enormous information issue) is all around explored by strengthening variable technique. For every one of the set-up time, administration process, mandatory get-away and discretionary broadened excursion, beneficial components are distinguished. A determined state line measure assignment and the distinctive execution checks like length of the line, number of clients in the framework, usage factor, latent time of the server, holding up time of the clients in the line likewise as in the structure are inferred. Numerical depiction legitimizes the model and the graphical outline gives a sensible picture about the decisions to be taken before the beginning of the affiliation. To break down the issue in social insurance unit, a verifiable endorsing is rendered close to the end, by strategies for looking numerical results and graphical examination of the model.

Huge information examination has been considered by various creators. In any case, the issue of huge information investigation in medicinal services unit is drawn closer through lining hypothesis is another thought of execution in this examination. McAfee and Brynjolfsson (2012) examined the work on big information the board insurgency. Development of information investigation is totally very much concentrated by Lynch (2008). Big information pathologies are all around assessed by Jacobs (2009).


https://doi.org/10.17993/3ctecno.2021.specialissue8.211-229

Zikopoulos *et al.* (2011) made an analysis on examination for big business class Hadoop and Streaming Data. Manyika, Chui, and Brown (2011) learned about the developments and preparations on Big Data. Celi *et al.* (2013) examined the work on big information in the emergency unit. Sobhy *et al.* (2012) considered the enormous information on human services distributed computing system. Queuing frameworks with expansive scope of excursion arrangements have been planned by various authors. Single get-away strategy is all around examined by Choudhury (2002).

Dhanalakshmi and Maragathasundari (2018) contemplated Mobile ad hoc systems issue through queuing approach. Maragathasundari (2015) inferred the execution measures for a mass entry queuing model of three phases of administration with various excursion policies. Maragathasundari and Srinivasan (2012) made an Analysis on M/G/1 input line. Maragathasundari and Karthikeyan (2016) explored a mass queuing model with short and long get-away.

In this study, we have introduced the big data analytic issue as a batch arrival non-Markovian queuing model with setup time, single service and feedback service. As this is a non markovian queuing model, service time follows a general distribution. A concept of Phase I compulsory vacation and phase II optional vacation are launched in this work which plays a very important role in our study. Here vacation in the sense we mean the maintenance work to be carried out in due course of time which helps the system to run smoothly to a maximum extent. It is expected that during the time of vacation, length of the queue will be maximized. So, to avoid the congestion in the system a phenomenon known to be restricted admissibility is brought in during the time of vacation.

## 2.3. MATHEMATICAL DEPICTION OF THE MODEL

The arithmetical interpretation of the Queuing framework has the capacity to be described by the resulting hypothesis:

Customers cluster arrival follows Poisson procedure Let $\lambda d_i\, dt$ ($i$=1,2,3….) be the first order probability where $0 \leq d_i \leq 1$ and $\sum_{i=1}^{n} d_i = 1$ and $\lambda > 0$ is the mean landing rate of the batches. There is one server giving single sort of administrations of general course. The


https://doi.org/10.17993/3ctecno.2021.specialissue8.211-229

organization time seeks after general (arbitrary) course with first basic distribution function E(x) and density function e(x). Let μ(x)dx be the prohibitive probability of organization finish of the principle period of organization in the midst of the interval (x,x+dx), given that the snuck past time is x, so that $\mu(x) = \frac{e(x)}{1-\bar{E}(x)}$

$$e(x) = \mu(x)e^{-\int_0^x \mu(t)dt} \quad \text{(a)}$$

For the purpose of maintenance work to be carried out, the server takes a compulsory vacation with probability r.

For compulsory vacation, $\gamma_a(x) = \frac{\bar{a}(x)}{1-\bar{A}(a)(x)}$

$$\bar{a}(x) = \gamma_a(x)e^{-\int_0^x \gamma_a(t)dt} \quad \text{(b)}$$

After the completion of compulsory vacation, if in need the server may take an extended vacation with probability k.

For the optional vacation, we have:

$$\gamma_b(x) = \frac{\bar{b}(x)}{1-\bar{S}(b)(x)} \quad , \ \bar{b}(x) = \gamma_b(x)e^{-\int_0^x \gamma_b(t)dt} \quad \text{(c)}$$

After completion of the service, if the client is disappointed with the essential administration, he can quickly join the tail of the first line as a feedback client with likelihood e to rehash the administration until the point when it is fruitful or may leave the framework with likelihood 1- e.

## 2.4 GOVERNING EQUATIONS OF THE MODEL

$S_n$ $(t)$ - This is the probability that at time 't', the server is in setup while there are 'n' customers in the queue. (n ≥1 )

$$\frac{d}{dt}S_n(t) + (\lambda+\gamma)S_n(t) = \lambda\sum_{i=1}^{n} c_i S_{n-i}(t) + \lambda c_n Q(t). \quad (1)$$

$$\frac{d}{dx}P_n(x) + (\lambda+\eta(x))P_n(x) = \lambda\sum_{i=1}^{n} c_i P_{n-i}(x). \quad (2)$$

$$\frac{d}{dx}P_0(x) + (\lambda+\eta(x))P_0(x) = 0. \quad (3)$$

$$\frac{d}{dx}V_n^{(a)}(x) + (\lambda+\gamma_a(x))V_n^{(a)}(x) = \lambda\sum_{i=1}^{n} c_i v_{n-i}^{(a)}(x), n \geq 1. \quad (4)$$


https://doi.org/10.17993/3ctecno.2021.specialissue8.211-229

$$\frac{d}{dx}V_0^{(a)}(x) + (\lambda + \gamma_a(x))V_0^{(a)}(x) = 0. \tag{5}$$

$$\frac{d}{dx}V_n^{(b)}(x) + (\lambda + \gamma_b(x))V_n^{(b)}(x) = \lambda(1-\beta)V_n^{(b)}(x) + \lambda\beta\sum_{i=1}^{n} c_i v_{n-i}^{(b)}(x), n \geq 1 \tag{6}$$

$$\frac{d}{dx}V_0^{(b)}(x) + (\lambda + \gamma_b(x))V_0^{(b)}(x) = \lambda(1-\beta)V_0^{(b)}(x). \tag{7}$$

$$\lambda Q = \int_0^\infty V_0^{(\beta)}(x)\gamma_b(x)dx + (1-k)\int_0^\infty V_0^{(a)}(x)\gamma_a(x)dx + e\int_0^\infty p_0(x)\gamma(x)dx. \tag{8}$$

The accompanying limit conditions are utilized to settle the above conditions.

$$p_n(0) = (1-k)\int_0^\infty V_{n+1}^{(a)}(x)\gamma_a(x)dx + \int_0^\infty V_{n+1}^{(b)}(x)\gamma_b(x)dx + e\int_0^\infty p_n(x)\eta(x)dx + \lambda c_{n+1}Q. \tag{9}$$

$$V_n^{(a)}(0) = r(1-e)\int_0^\infty p_n(x)\eta(x)dx + re\int_0^\infty p_{n-1}(x)\eta(x)dx. \tag{10}$$

$$V_n^{(b)}(0) = k\int_0^\infty V_n^{(a)}(x)\gamma_a(x)dx\,. \tag{11}$$

## 3. DISTRIBUTION OF THE QUEUE LENGTH

To settle conditions (1) to (7) for a shut structure arrangement we pursue the system set out beneath:

We multiply (1) by $z^n$ and sum over $n$ from 1 to $\infty$ add it to (2), we get

$$(\lambda - \lambda c(z) + \gamma)s_q(z) = \lambda Q c(z). \tag{12}$$

$$\frac{d}{dx}p_q(x,z) + \big(\lambda - \lambda c(z) + \eta(x)\big)p_q(x,z) = 0\,. \tag{13}$$

$$\frac{d}{dx}V_q^{(a)}(x,z) + (\lambda - \lambda c(z) + \gamma_a(x))V_q^{(a)}(x,z) = 0. \tag{14}$$

$$\frac{d}{dx}V_q^{(b)}(x,z) + (\lambda\beta - \lambda\beta c(z) + \gamma_b(x))V_q^{(b)}(x,z) = 0. \tag{15}$$

Multiplying (9) by $z^{n+1}$ and summing over $n$ from 0 to $\infty$ results in:

$$zp_q(0,z) = (1-k)\int_0^\infty V_q^{(a)}(x,z)\gamma_a(x)dx + \int_0^\infty V_q^{(b)}(x,z)\gamma_b(x)dx + e\int_0^\infty p_q(x,z)\eta(x)dx + \lambda c(x)Q - [e\int_0^\infty p_0(x,z)\eta(x)dx + (1-k)\int_0^\infty V_0^{(a)}(x,z)\gamma_a(x)dx + \int_0^\infty V_0^{(b)}(x,z)\gamma_b(x)dx]. \tag{16}$$

Using (8) in (16), we get:

$$zp_q(0,z) = (1-k)\int_0^\infty V_q^{(a)}(x,z)\gamma_a(x)dx + \int_0^\infty V_q^{(b)}(x,z)\gamma_b(x)dx + e\int_0^\infty p_q(x,z)\eta(x)dx + \lambda(c(z)-1)Q. \tag{17}$$


https://doi.org/10.17993/3ctecno.2021.specialissue8.211-229

$$V_q^{(a)}(0,z) = r(1-e)\int_0^\infty p_q(x,z)\eta(x)dx + rez\int_0^\infty p_q(x,z)\eta(x)dx. \quad (18)$$

$$V_q^{(b)}(0,z) = k\int_0^\infty V_q^{(a)}(x,z)\gamma_a(x)dx. \quad (19)$$

Now integrating (13) from 0 to $x$ yields,

$$p_q(x,z) = p_q(0,z)e^{-(\lambda-\lambda c(z))-\int_0^x \eta(t)dt}. \quad (20)$$

Integrating (20) by parts with respect to $x$ yields,

$$p_q(z) = p_q(0,z)\left(\frac{1-\bar{E}(a)}{a}\right), a = \lambda - \lambda c(z). \quad (21)$$

Where, $\bar{E}(a) = \int_0^\infty e^{-(\lambda-\lambda c(z))x}\, dE(x)$ is the Laplace stieltjes transform of the service times $E$(x).

Multiply (20) by $\eta$(x) on both the sides, we get

$$\int_0^\infty p_q(x,z)\eta(x)dx = p_q(0,z)\bar{E}(a). \quad (22)$$

Using (20) in (18), we get

$$V_q^{(a)}(0,z) = [r - re(1+z)]p_q(0,z)\bar{E}(a). \quad (23)$$

Similarly,

$$\int_0^\infty V_q^{(a)}(z) = V_q^{(a)}(0,z)\left(\frac{1-\bar{A}(a)}{a}\right)$$

$$= [r - re(1+z)]p_q(0,z)\bar{E}(a)\left[\frac{1-\bar{A}(a)}{a}\right]. \quad (24)$$

$$\int_0^\infty V_q^{(a)}(x,z)\gamma_a(x)dx = [r - re(1+z)]p_q(0,z)\bar{E}(a)\bar{A}(a). \quad (25)$$

Also,

$$V_q^{(b)}(z) = k[r - re(1+z)]p_q(0,z)\bar{E}(a)\bar{A}(a)\left[\frac{1-\bar{S}(b)}{b}\right], b = \lambda b - \lambda bc(z). \quad (26)$$

Hence,

$$\int_0^\infty V_q^{(b)}(x,z)\gamma_b(x)dx = k[r - re(1+z)]p_q(0,z)\bar{E}(a)\bar{A}(a)\bar{S}(b). \quad (27)$$


https://doi.org/10.17993/3ctecno.2021.specialissue8.211-229

Now using (22), (25) and (27) in (17), we get

$$zp_q(0,z) = (1-k)[r-re(1+z)]p_q(0,z)\bar{E}(a)\bar{A}(a) + k[r-re(1+z)]p_q(0,z)\bar{E}(a)\bar{A}(a)\bar{S}(b) + ep_q(0,z)\bar{E}(a) + \lambda(c(z)-1)Q$$

$$\Rightarrow p_q(0,z) = \frac{\lambda(c(z)-1)Q}{z-e\bar{E}(a)-[r-re(1+z)]\bar{E}(a)\bar{A}(a)(1-k+k\bar{S}(b))}. \quad (28)$$

Substituting (28) in (21), (24) and (26), we get

$$p_q(z) = \frac{-(1-\bar{E}(a))Q}{z-e\bar{E}(a)-[r-re(1+z)]\bar{E}(a)\bar{A}(a)(1-k+k\bar{S}(b))}. \quad (29)$$

$$V_q^{(a)}(z) = \frac{-[r-re(1+z)]\bar{E}(a)\bar{A}(a)Q}{z-e\bar{E}(a)-[r-re(1+z)]\bar{E}(a)\bar{A}(a)(1-k+k\bar{S}(b))}. \quad (30)$$

$$V_q^{(b)}(z) = \frac{-[r-re(1+z)]\bar{E}(a)\bar{A}(a)\bar{S}(b)Q}{\beta\left(z-e\bar{E}(a)-[r-re(1+z)]\bar{E}(a)\bar{A}(a)(1-k+k\bar{S}(b))\right)}. \quad (31)$$

Also,

$$S_q(z) = \frac{\lambda Qc(z)}{\lambda-\lambda c(z)+\gamma}. \quad (32)$$

## 4. EXECUTION MEASURES

(i) LIKELIHOOD GENERATING CAPACITY OF THE QUEUE SIZE

Let $D_q^*(z)$ be the probability generating function of the queue size

$$D_q^*(z) = S_q(z) + P_q(z) + V_q^{(a)}(z) + V_q^{(b)}(z).$$

Adding (29) – (31), we get

$$D_q^*(z) = \frac{Q[\beta\lambda C(z)]\left[\beta[z-e\bar{E}(a)-(r-re(1+z))\bar{E}(a)\bar{A}(a)(1-k+k\bar{S}(b))]-(\lambda-\lambda C(z)+\gamma)\left[\left[\beta\left(1-\bar{E}(a)Q+(r-re(1+z))\bar{E}(a)\bar{A}(a)Q(\beta+\bar{S}(b))\right)\right]\right]\right]}{(\lambda-\lambda C(z)+\gamma)\beta\left[[z-e\bar{E}(a)-(r-re(1+z))\bar{E}(a)\bar{A}(a)(1-k+k\bar{S}(b))]\right]}.$$

The idle time $Q$ is determined using the normalization condition $D_q^*(1) + Q=1$ .

From, the utilization factor $\rho$ can be determined.


https://doi.org/10.17993/3ctecno.2021.specialissue8.211-229

(ii) STEADY STATE ARRANGEMENT OF THE QUEUE SIZE

Let $L_q$ a chance to demonstrate the reliable state typical number of customers in the line. By then

$$L_q = \frac{d}{dz} D_q^*(z)|_{z=1} = \frac{d}{dz}\left\{\frac{N(Z)}{D(Z)}\right\}\Big|_{z=1}.$$

Where $N(Z)$ and $D(Z)$ are the numerator and denominator of (27).

Since $D_q^*(z) = \frac{0}{0}$at $=1$ , we utilize two-fold separation and get

$$L_q = \lim_{z\to 1} \frac{d}{dz} D_q^*(z) = \frac{D'(1)N''(1) - D''(1)N'(1)}{2(D'(1))^2}. \quad (33)$$

$$D'(1) = \beta\{-\lambda[1 - e - (r - 2re)] + \gamma[1 - e\lambda E(k) — [-re + (r - 2re)\lambda(E(k) + E(A) + \beta kE(s))]]\}. \quad (34)$$

$$D''(1) = \beta\{-\lambda[-re + (r - 2re)\lambda(E(k) + E(A) + \beta kE(s))]\} + (-\lambda)\left[1 - e\lambda E(k) — \left[-re + (r - 2re)\lambda\lambda\left(E(k) + E(A) + \beta kE(s)\right)\right]\right] + \gamma\left[-e\lambda^2 E(k^2) — re\lambda\left(E(k) + E(A) + \beta kE(s)\right) - re\lambda\left(E(k) + E(A) + \beta kE(s)\right) + (r - 2re)\lambda^2\left[E(k^2) + E(A^2) + k\beta E(s^2) + 2E(k)E(A) + 2k\beta E(s)\left(E(k) + E(A)\right)\right]\right]. \quad (35)$$

$$N''(1) = (\beta\lambda + 1)\{1 - e\lambda E(k) + re - \lambda(r - 2re)(E(k) + E(A) + \beta kE(s))\} + \beta\lambda\{-e\lambda^2 E(k^2) + re\lambda(E(k) + E(A) + \beta kE(s)) + re(E(k) + E(A) + \beta kE(s)) + (r - 2re)[-\lambda E(A^2) - 2\lambda E(k)E(A) - 2E(A)k\beta E(s)\lambda - \lambda E(A^2) - \lambda E(k)k\beta E(s) - \lambda E(A)k\beta E(s) - \lambda E(k)E(s)k\beta - \lambda k\beta^2 E(s^2)]\} - \lambda(r - 2re)\beta - \lambda\left(-\lambda E(A) - re\beta + \beta(r - 2re)(E(k) + E(A) + \beta kE(s))\right) + \gamma[-\lambda^2 E(k^2) - re\lambda\beta(E(k) + E(A) + E(s)) - re\lambda(E(k) + E(A) + \beta E(s)) + (r - 2re)(-\lambda\beta E(k^2) - \lambda\beta E(A^2) - 2\lambda E(k)E(A)\beta - \lambda\beta E(s)[E(k) + E(A)] - \lambda\beta^2 E(s^2))]. \quad (36)$$

$$N' = \beta\lambda[1 - e - (r - 2re)] + \left[1 - e\lambda E(k) - [-re + (r - 2re)(E(k) + E(A) + k\beta E(s))]\right]. \quad (37)$$

Substituting (34) – (37) in (23), we obtain $L_q$ and all the other measures are obtained using Little's formula

(iii)$W_q = \frac{L_q}{\lambda}$ , $W = \frac{L}{\lambda}$, $L = L_q + \rho$.


https://doi.org/10.17993/3ctecno.2021.specialissue8.211-229

# 5. NUMERICAL RESULTS

We depict a numerical perspective with a definitive goal to see the impact and credibility of our consequences of the specific parameters utilized in our model. The estimations of the parameters are collected with a definitive target that the enduring condition is not disturbed.

Assume service time follows an exponential distribution:

$$E(k)=\frac{1}{\eta},E(k^2)=\frac{2}{\eta^2},E(A)=\frac{1}{\gamma_a},E(A^2)=\frac{2}{{\gamma_a}^2},E(s)=\frac{1}{\gamma_b},E(s^2)=\frac{2}{{\gamma_b}^2}\gamma=0.8,\eta=3,\lambda=4,\beta=1.5,\gamma_a=2.5,\gamma_b=3.5,r=0.5,$$

**Table 1.** Effect of change ofe (*e*=6,5.5,5,4.5,4).

| $Q$ | $\rho$ | $Lq$ | $L$ | $W_Q$ | $W$ |
|---|---|---|---|---|---|
| 0.7239 | 0.2761 | 15.551 | 15.827 | 5.184 | 5.184 |
| 0.7512 | 0.2488 | 15.167 | 15.415 | 5.056 | 5.139 |
| 0.7728 | 0.2272 | 14.889 | 15.116 | 4.963 | 5.039 |
| 0.7903 | 0.2097 | 14.679 | 14.889 | 4.893 | 4.963 |
| 0.8049 | 0.1951 | 14.518 | 14.713 | 4.839 | 4.904 |

**Source:** own elaboration.

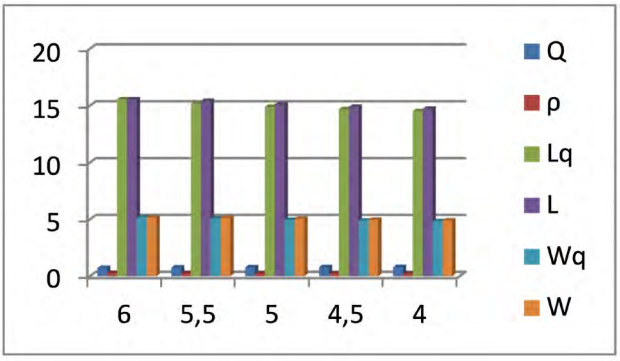


**Graphic 3.** Effect of Variation of *e*.
**Source:** own elaboration.


https://doi.org/10.17993/3ctecno.2021.specialissue8.211-229

**Table 2.** Effect of Variation Of $\gamma$ ($\gamma$=2.1,2.2,2.3,2.4,2.5)

| $Q$ | $\rho$ | $Lq$ | $L$ | $W_Q$ | $W$ |
|---|---|---|---|---|---|
| 0.8751 | 0.1249 | 4.9967 | 5.1216 | 1.2492 | 1.2804 |
| 0.8806 | 0.1194 | 4.3960 | 4.5154 | 1.0990 | 1.1289 |
| 0.8856 | 0.1144 | 3.9666 | 4.0810 | 0.9916 | 1.0202 |
| 0.8902 | 0.1098 | 3.5038 | 3.6136 | 0.8759 | 0.9034 |
| 0.8945 | 0.1055 | 3.0698 | 3.1753 | 0.7674 | 0.7938 |

**Source:** own elaboration.

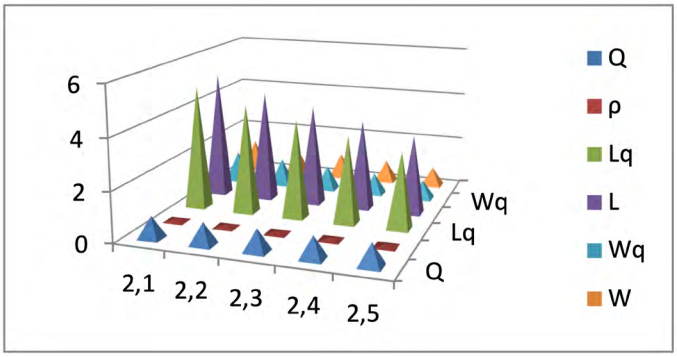


**Graphic 4.** Effect of Variation of $\gamma$.
**Source:** own elaboration.

**Table 3.** Effect of Variation Of $\beta$ ($\beta$=1.6,1.8,2,2.2,2.4)

| $Q$ | $\rho$ | $Lq$ | $L$ | $W_Q$ | $W$ |
|---|---|---|---|---|---|
| 0.6952 | 0.3048 | 20.334 | 20.639 | 5.083 | 5.1596 |
| 0.7077 | 0.2923 | 19.597 | 19.889 | 4.899 | 4.9723 |
| 0.7190 | 0.2810 | 19.047 | 19.328 | 4.762 | 4.8319 |
| 0.7295 | 0.2705 | 18.632 | 18.902 | 4.657 | 4.7255 |
| 0.7391 | 0.2609 | 18.319 | 18.579 | 4.579 | 4.6450 |

**Source:** own elaboration.


https://doi.org/10.17993/3ctecno.2021.specialissue8.211-229

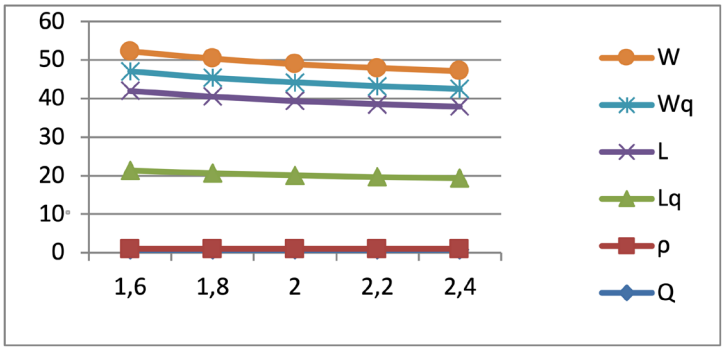


**Graphic 5**. Effect of Variation of $\beta$.
**Source:** own elaboration.

## 6. DISCUSSION

It is evident from Table 1 that lessening the estimation of e, decreases the traffic power, normal length of the line and the normal reaction time while the server inert time increases. From Table 2, the information we collect here is, as the probability of set up time constructs, it prompts a smart presentation of the structure. From now on, the length of the line gets lessens. Also, the other execution measures in like manner get decreased. Furthermore, restricted admissibility yin table3 expect a noteworthy activity in this model. To avoid stop up this thought is exhibited. It means a nice impact in the model. On account of the extension in the confined suitability, the blockage in the structure is avoided. Length of the line gets reduced and moreover the holding up time of the customers in like manner gets diminished. All of the examples showed up by this are true to form. In extension, Graphical examination gives an undeniable picture about the model described in this paper.

## 7. CONCLUSIONS

In this model, we analyzed a Queuing framework with general administration conveyance with various vacation arrangements. Here two kinds of vacations are presented viz. mandatory excursion and discretionary broadened get-away. Also, the idea of feedback administration encourages the clients to get a total fulfillment regarding the administration. Amid the season of both the excursions, a legitimate support work is done which encourages the framework to run easily without intrusion to a greatest dimension. By including another presumption, restricted admissibility in this model, an assorted and a much-created lining


https://doi.org/10.17993/3ctecno.2021.specialissue8.211-229

framework is developed. The relentless state arrangement and the execution proportions of the lining framework are determined. As a future work, building up the above lining model with administration intrusion, postpone time, shut down time, Balking and reneging is proposed

## REFERENCES

**Celi, L. A., Mark, R. G., Stone, D. J., & Montgomery R. A.** (2013). 'Big data' in the intensive care unit: closing the data loop. *American Journal of Respiratory and Critical Care Medicine. 187*(11), 1157–1160. https://doi.org/10.1164/rccm.201212-2311ed

**Choudhury, G.** (2002). A batch arrival queue with a vacation time under single vacation policy. *Computers and Operations Research, 29*(14), 1941-1955. https://doi.org/10.1016/S0305-0548(01)00059-4

**Dhanalakshmi, K. S., & Maragathasundari, S.** (2018). Mobile ad hoc networks problem- A queuing approach. *International journal of communication networks and distributed systems, 21*(4). https://www.inderscience.com/info/inarticle.php?artid=95363

**Jacobs, A.** (2009). The pathologies of big data. *Communications of the ACM, 52*(8), 36–44. https://doi.org/10.1145/1536616.1536632

**Lynch, C.** (2008). Big data: how do your data grow? *Nature. 455*(7209), 28–29. https://doi.org/10.1038/455028a

**Manyika, J., Chui, M., & Brown, B.** (2011). "Big Data" The Next Frontier for Innovation, Competition, and Productivity. *McKinsey Global Institute.*

**Maragathasundari, S.** (2015). A bulk arrival queuing model of three stages of service with different vacation policies, service interruption and delay time. *American International Journal of Research in Science, Technology, Engineering& Mathematics, 11*(1), 52-56. https://www.researchgate.net/publication/295605742_A_bulk_arrival_queueing_model_of_three_stages_of_service_with_different_vacation_policies_service_interruption_and_delay_time


https://doi.org/10.17993/3ctecno.2021.specialissue8.211-229

**Maragathasundari, S., & Karthikeyan, K.** (2016). A bulk queuing model of optional second phase service with short and long vacations. *International Journal of scientific research in science and technology, 2*(5), 196-201. https://www.researchgate.net/publication/308917899_A_Bulk_Queuing_Model_of_Optional_Second_Phase_Service_with_Short_and_Long_Vacations

**Maragathasundari, S., & Srinivasan, S.** (2012). Analysis of M/G/1 feedback queue with three stages and multiple server vacation. *Applied mathematical sciences, 6*(125), 6221-6240. https://www.researchgate.net/publication/259962534_Analysis_of_MG1_Feedback_Queue_with_Three_Stage_and_Multiple_Server_Vacation

**McAfee, A., & Brynjolfsson, E.** (2012). Big data: the management revolution. *Harvard Business Review, 90*(10), 60–68. https://www.researchgate.net/publication/232279314_Big_Data_The_Management_Revolution

**Sobhy, D., El-Sonbaty, Y., AbouElnasr, M., & MedCloud.** (2012). Healthcare cloud computing system. *Proceedings of the International Conference for Internet Technology and Secured Transactions*; London, UK. IEEE (pp. 161–166).

**Zikopoulos, P., Eaton, C., deRoos, D., Deutsch, T., & Lapis, G.** (2011). Understanding Big Data: Analytics for Enterprise Class Hadoop and Streaming Data. *McGraw-Hill Osborne Media.*


https://doi.org/10.17993/3ctecno.2021.specialissue8.211-229

https://doi.org/10.17993/3ctecno.2021.specialissue8.211-229

/14/


https://doi.org/10.17993/3ctecno.2021.specialissue8

# CROSSTALK MEASURE OF THE FM – EDFA IN MDM TRANSMISSION USING PM-QPSK

**T. Senthil**
Ph.D., Kalasalingam University. B.E and M.E degree, M.K university, India.
Associate Professor, department of ECE, Kalasalingam University,
Krishnankoil, Tamilnadu, (India).
E-mail: t.senthil@klu.ac.in
ORCID: https://orcid.org/0000-0002-0044-5371

**Recepción:** 11/11/2019 **Aceptación:** 28/10/2020 **Publicación:** 30/11/2021

**Citación sugerida:**
Senthil, T. (2021). Crosstalk measure of the FM – EDFA in MDM Transmission using PM-QPSK. *3C Tecnología. Glosas de innovación aplicadas a la pyme, Edición Especial,* (noviembre, 2021), 231-241. https://doi.org/10.17993/3ctecno.2021.specialissue8.231-241

## ABSTRACT

In optical fiber communications, Mode –Division Multiplexing in combination with Wavelength Division Multiplexing and advanced modulation formats like QPSK n-QAM are utilized to deliver more amounts of data through a single fiber. For amplifying the signals in the long haul optical fibres link Few –Mode Erbium –Doped Fiber Amplifier is employed to equally and efficiently amplify both modes and respective wavelengths over the telecommunication C-band frequency range. In this paper A Dual-Carrier PM-QPSK transmission system is proposed for enhancing data rate with reduced bit error due to the cross section generated by the optical fibre non-linear properties. The spectrally efficient high bitrate transmission has generated in coherent systems. Using two PM-OPSK carriers, one can reduce transmitter bandwidth requirement to half compared to standard single carrier PM-QPSK while still supporting the same total bitrate. The total bitrate for this layout is given as 40Gbps. The 100-Km of fibre is modelled via a loss element and the fiber dispersion is modelled by an FBG model. Low transmitted power values in coherent systems typically give lower nonlinearity. Each sub-carrier is modulated by 21.4Gbps including FEC overheads. That means each polarization of a carrier is modulated by 10.7Gbps implying the symbol rate of 5.35 GHz. In order to minimize the crosstalk between the two carrier, the separation between them is kept half the symbol rate. As a result, when one carrier is at maximum, the other is at its minimum. The proposed scheme is utilized for both linear and non-linear fiber.

## KEYWORDS

DC-PM- QPSK, Forward Error Correction, Fibre Bragg Grating.


https://doi.org/10.17993/3ctecno.2021.specialissue8.231-241

# 1. INTRODUCTION

In electronics and telecommunication, modulation is the process of varying one or more properties of a periodic waveform, called the carrier signal, with a modulating signalthat typically contains information. The optical communication is one of the fastest communication methods. Afive-mode erbium doped amplifier is described, and the spectral and modal gain distribution is characterized using PDM-QPSK (Askarov & Kahn, 2012). However, the combination of polarization division multiplexing (PDM)or in phase/ quadrature phase modulation formats with (WDM) wavelength division multiplexing in single mode fiber leads to the Shannon limit (Ip, 2012). 41.6 Tbit/s C-band signal is transmitted using 12 spatial & polarization modes over 74.17Km (Genevaux *et al.*, 2016). Multiplexing and De-multiplexing of each spatial mode is needed which causes loss and need several amplifiers, to amplify all the modes at the same time MDM is an economical benefit (Essiambre *et al.*, 2015). General approach to describe and predict the amplifying properties of FM-EDFA – (Few Mode) (Essiambre *et al.*, 2015). The combination of some erbium doped properties with adapted pump has investigated to develop a FM-EDFA model based on the vector modes (Ryf *et al.*, 2012). In this paper we describe the Dual-Carrier transmission using PM-QPSK modulation and describes the need for PM-QPSK in section II. Then the result analysis and tabulation are shown in section III. This paper concludes in section IV.

# 2. MATERIALS AND METHODS

In this paper the Dual-Carrier transmission is generated using coherent system like PM-QPSK. The total bitrate for the layout is 40 Gbps. The system consists of three parts first is the transmission part in which pseudo random bit sequence (PRBS) is used as the data transmission which is modulated using the LASER. Then the modulated data is transmitted through the fiber which the second part is, it consists of the combiner and splitter. The fiber used here is EDFA with 100-Km. Then at the third part receiver is placed which will measure the crosstalk between the two carrier. The process is subjected to both linear and non-linearities of the fiber.


https://doi.org/10.17993/3ctecno.2021.specialissue8.231-241

### A. MODULATION TECHNIQUE

Modulation is the process of combining the information signal with the carrier signal. Here we use PM-QPSK to achieve the spectrally efficient transmission. Using two PM-QPSK the transmitter bandwidth can be reduced half as compared to single carrier. Each subcarrier is modulated by 21.4Gbps. This will improve the bandwidth efficiency of the transmission system effectively. The block diagram of PM-QPSK is given below (Figure 2).

### B. OPTICAL AMPLIFIER

EDFA is an Erbium Doped Fiber Amplifier which amplifies the signal is also called as the optical amplifier. EDFA is used to avoid the repeaters / regenerators in long distance optical fibre transmission. If we use regeneratorsmeans, there will be high noise introduced by them. To avoid this, we go for EDFA system. However, the cost of this fiber will be high. Even though EDFA amplifies the modulated signal, it needs an external laser pump signal. The EDFA amplifier block is given below (Figure 3).

### C. CROSS TALK MINIMIZATION

To minimize the crosstalk between the two carriers the separation between them is kept as half the symbol rate that is when one carrier has the maximum symbol rate means other will be at the minimum. The local frequency is set to the transmitted carrier frequency in single PM-QPSK and so the real and imaginary part of the received electromagnetic is a baseband signal. This drastically reduces the possibility of cross talk occurring by introducing orthogonal property in the modulated signal.

## 3. RESULTS

The separation between the two carrier signals is kept as half the symbol rate. The figure shows the orthogonal nature of the signal so that the maximum point of the one signal coincides with the minimum point of another signal thus reducing the crosstalk nature effectively. The dual polarization itself send the two-information signal thus forming one form of multiplexing.The spectrum of the transmitted dual-carrier PM-QPSK is given below. The bandwidth of the carrier signal is determined by the symbol rate of the baseband signal. Thus, by selecting the appropriate Band Pass Filter in the input section the symbol


https://doi.org/10.17993/3ctecno.2021.specialissue8.231-241

rate can be decided for the required isolation in between two signals thus avoiding the cross talk between the signals.

The BER versus for the various symbol rate data from each carrier is analysed and the equalizer is used in the transmitter part to compensate for all transmission anomalies. The data is received with error free is given below. The BER increases with the increased symbol rate and the crosstalk signal strength i.e. overlapped signal spectrum of the two signals also increases with the symbol rate of the baseband signal. The Mode division multiplexed (MDM) system increases the channel capacity imposed by the non – linear properties of the single mode fibre communication system.

In simulation the dual carrier PM –QPSK is designed and then the fibre is set with the optimized non-linear properties so that the effect of the non – linear nature varying the spectral response of the transmitting fibre. The optical signal and spectrum view is given in the Figure 7. The maximum value of the spectrum coincides with the minimum attenuation windows of the single mode fibre. Then the bit error rate range is given in the Figure 8, for both the modulation end. At the receiver side Fibre Bragg Grating (FBG) is used to compensate the bit error rate. The gain value is calculated which is used to minimize the bit error rate due to the dual carrier nature. The range of gain is 6- 6.5db in our simulation generated. By applying non-linearity of the fibre channel, the resultant bit error rate will be approximately nil for the dual carrier system.

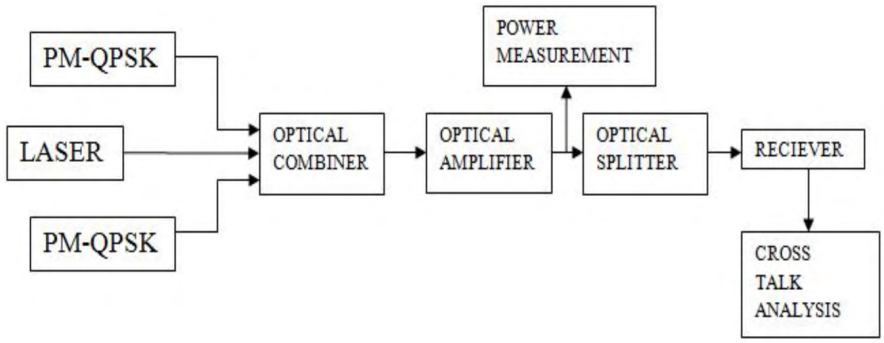


**Figure 1.** Dual Carrier PM-QPSK system.
**Source:** own elaboration.


https://doi.org/10.17993/3ctecno.2021.specialissue8.231-241

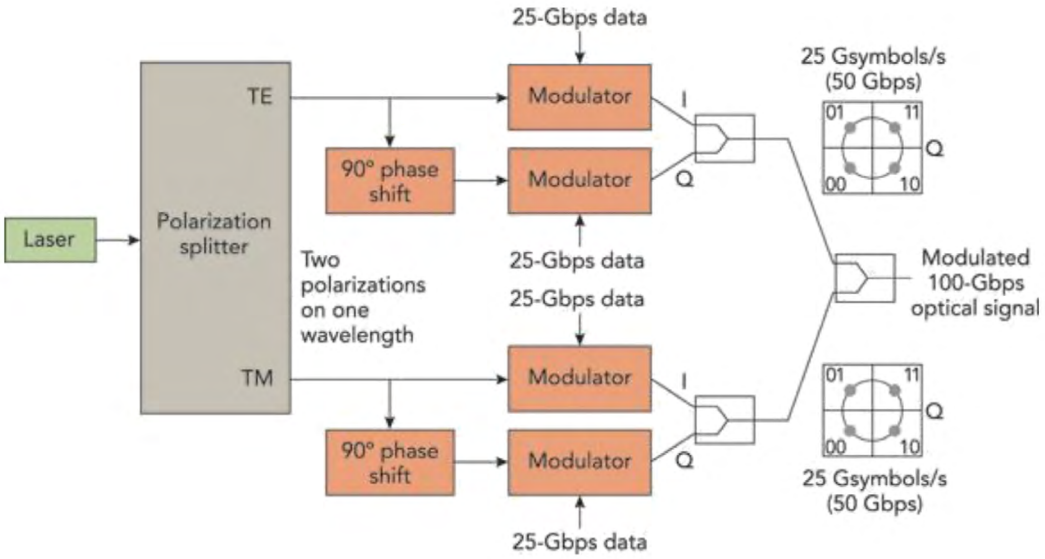


**Figure 2.** Dual Carrier PM-QPSK concept.
**Source:** own elaboration.

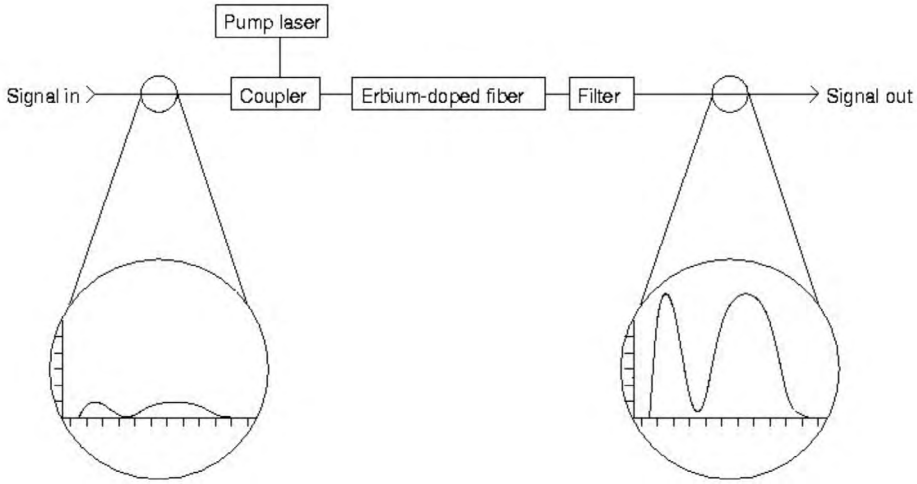


**Figure 3.** EDFA Working.
**Source:** own elaboration.


https://doi.org/10.17993/3ctecno.2021.specialissue8.231-241

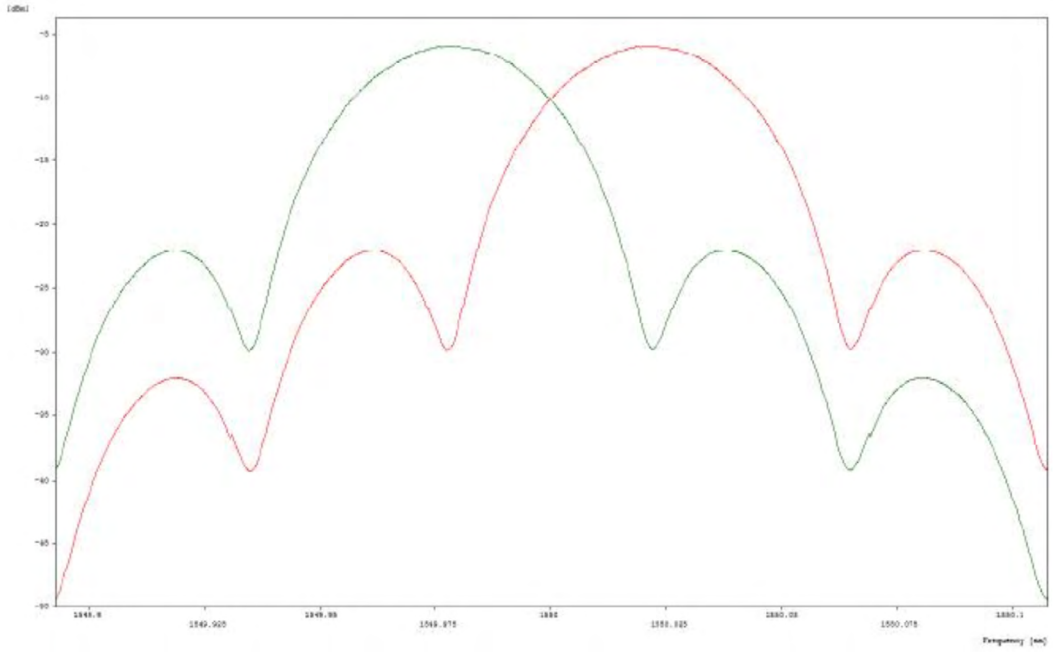

**Figure 4.** Half the symbol EDFA Working.
**Source:** own elaboration.

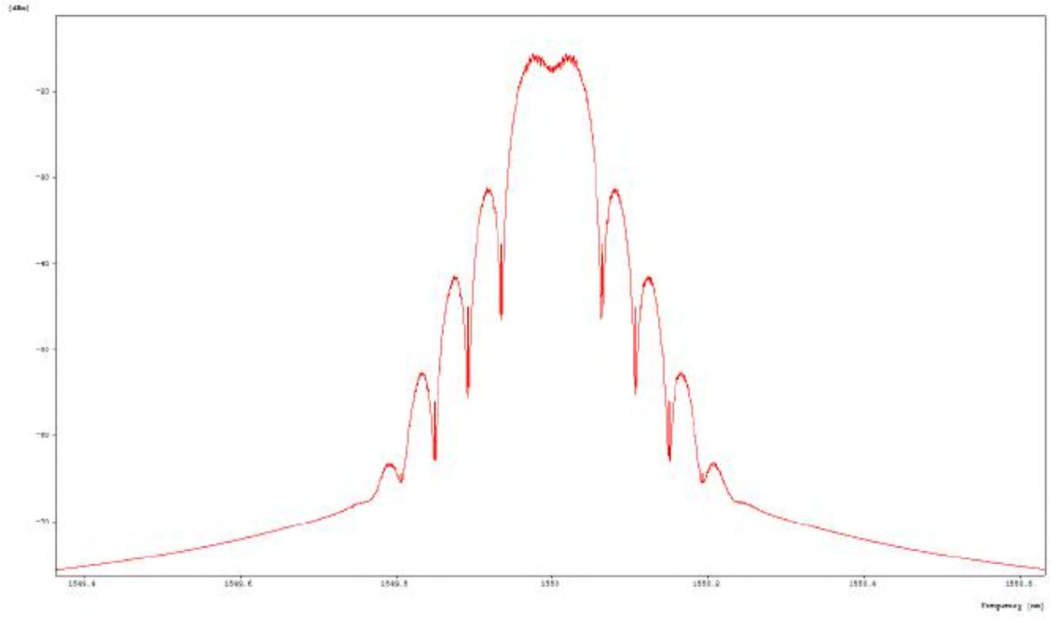

**Figure 5.** DC-PM-QPSK spectrum at the transmitter.
**Source:** own elaboration.


https://doi.org/10.17993/3ctecno.2021.specialissue8.231-241

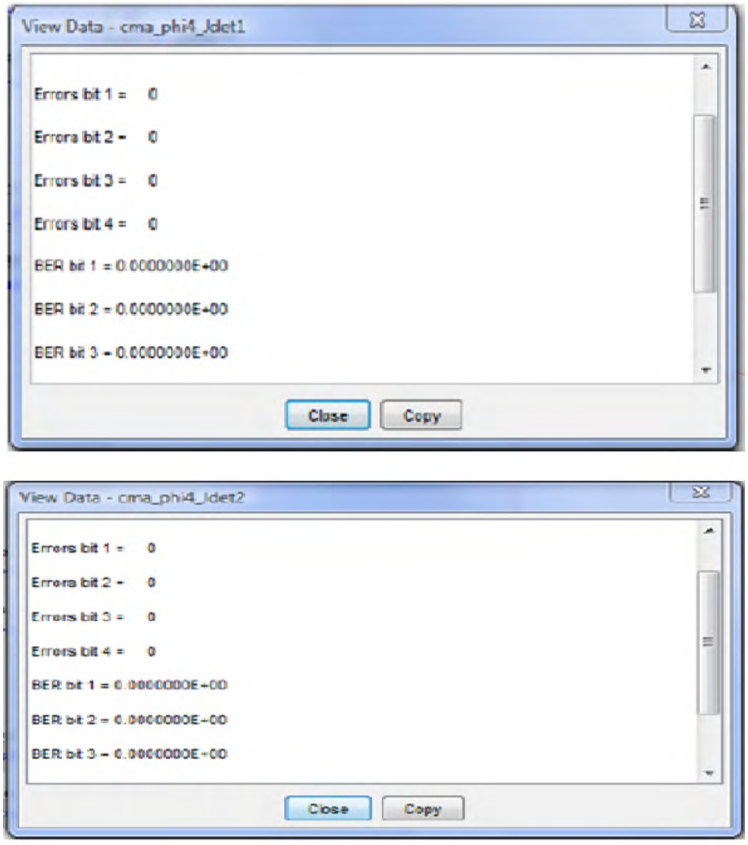


**Figure 6.** BER for each carrier.
**Source:** own elaboration.

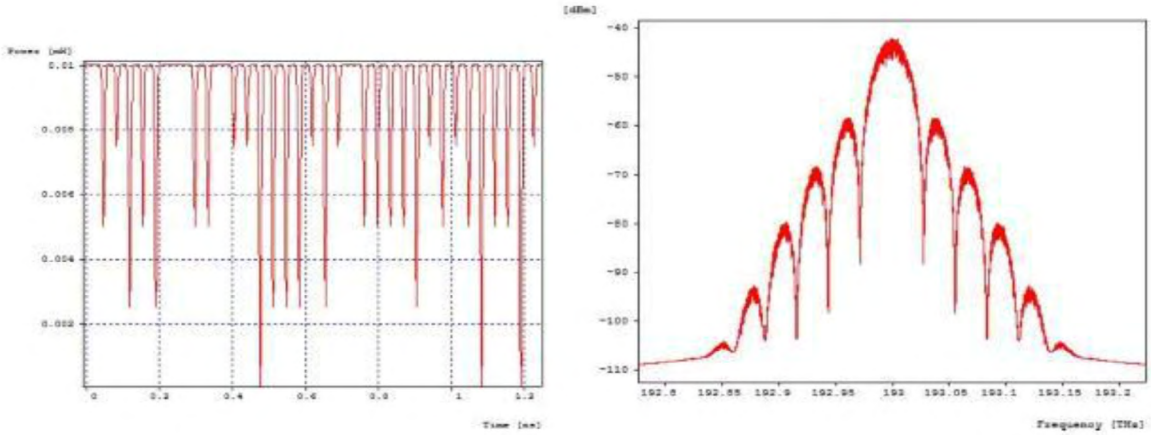

**Figure 7.** Optical signal and spectrum at the transmitted end.
**Source:** own elaboration.


https://doi.org/10.17993/3ctecno.2021.specialissue8.231-241

```
Errors bit 1 = 51
Errors bit 2 = 66
Errors bit 3 = 40
Errors bit 4 = 44

BER bit 1 = 0.7782576E-03
BER bit 2 = 0.1007157E-02
BER bit 3 = 0.6103981E-03
BER bit 4 = 0.6714379E-03

Errors bit 1 = 63
Errors bit 2 = 50
Errors bit 3 = 46
Errors bit 4 = 47
BER bit 1 = 0.9613771E-03
BER bit 2 = 0.7629977E-03
BER bit 3 = 0.7019579E-03
BER bit 4 = 0.7172178E-03
```

**Figure 8.** BER for each carrier while setting the non-linearities.
**Source:** own elaboration.

## 4. CONCLUSIONS

This paper described the dual carrier PM-QPSK in coherent system. In single carrier PM-QPSK, the local frequency is set as the transmitted carrier's frequency. As a result, the real and imaginary part of received electromagnetic field tries to overlap, correspond to the baseband signal. However in DC-PMQPSK, since the carriers are apart by half the symbol rate, the effect of cross talk is minimized by varying the non-linearity of the optical fibre. The various settings for the local oscillator frequency exist in the literature and frequency offsets may appear in the detected signal. For this the two local oscillators – each tuned to corresponding transmitted carrier are used and thus avoiding the frequency offsets at each detected output. In future this idea can also be extended for multichannel (WDM) optical communication systems. Thus, optimizing the distance between two carriers cross talk amount is reduced thus justifying the title.


https://doi.org/10.17993/3ctecno.2021.specialissue8.231-241

## ACKNOWLEDGEMENT

The author thanks the Department of Electronics and Communication Engineering of Kalasalingam University, (Kalasalingam Academy of Research and Education), Tamil Nadu for permitting, to utilize the OptSim software available in the research lab.

## REFERENCES

**Akhtari, S., & Krummrich, P. M.** (2013). Impact of mode beating effects in optical multi-mode amplifiers for space division multiplexing. *IEEE Photonics Technology Letters, 25*(24), 2482–2485. https://ieeexplore.ieee.org/document/6651699

**Askarov, D., & Kahn, J. M.** (2012). Design of transmission fibers and doped fiber amplifiers for mode-division multiplexing. *IEEE Photonics Technology Letters, 24*(21), 1945–1948. https://ieeexplore.ieee.org/document/6316068

**Bigot, L., Le Cocq, G., & Quiquempois, Y.** (2015). Few-mode erbium-doped fiber amplifiers: A review. *Journal of Lightwave Technology, 33*(3), 588–596. https://ieeexplore.ieee.org/document/6983523

**Chen, Y., Lobato, A., Jung, Y., Chen, H.,. Sleiffer, V., Kuschnerov, M., Fontaine, N., Ryf, R., Richardson, D., Lankl, B., & Hanik, N.** (2015). 41.6 Tbit/s C-Band SDM OFDM transmission through 12 Spatial and polarization modes over 74.17 Km few mode fiber. *Journal of Lightwave Technology, 33*(7), 1440–1444. https://www.osapublishing.org/jlt/abstract.cfm?uri=jlt-33-7-1440

**Essiambre, R.-J., Kramer, G., Winzer, P. J., Foschini, G. J., & Goebel, B.** (2015). Capacity limits of optical fiber networks. *Journal of Lightwave Technology, 28*(4), 662–701. https://ieeexplore.ieee.org/document/5420239

**Essiambre, R.-J., Kramer, G., Winzer, P. J., Foschini, G. J., & Goebel, B.** (2015). Capacity limits of optical fiber networks. *Journal of Lightwave Technology, 28*(4), 662–701. https://ieeexplore.ieee.org/document/5420239

**Genevaux, P., Simonneau, C., Le Cocq, G., Quiquempois, Y., Bigot, L., Boutin, A., & Charlet, G.** (2016). A Five Mode Erbium Doped Amplifier For Mode Division


https://doi.org/10.17993/3ctecno.2021.specialissue8.231-241

Multiplexing Transmission. *Journal of Lightwave Technology, 34*(2), 456-462. https://ieeexplore.ieee.org/document/7274319

**Ip, E.** (2012). Gain equalization for few-mode fiber amplifiers beyond two propagating mode groups. *IEEE Photonics Technology Letters, 24*(21), 1933–1936. https://ieeexplore.ieee.org/document/6316074

**Ryf, R., Randel, S., Gnauck, A. H., Bolle, C., Sierra, A., Mumtaz, S., Esmaeelpour, M., Burrows, E. C., Essiambre, E.-J., Winzer, P. J., Peckham, D. W., McCurdy, A. H., & Lingle, R.** (2012). Mode-division multiplexing over 96 km of fewmode fiber using coherent 6 × 6 MIMO processing. *Journal of Lightwave Technology, 30*(4), 521–531. https://ieeexplore.ieee.org/document/6074912

**Spellmeyer, N. W.** (2000). Communications performance of a multimode EDFA. *IEEE Photonics Technology Letters, 12*(10), 1337–1339. https://ieeexplore.ieee.org/document/883822

**Wada, M., Sakamoto, T., Mori, T., Yamamoto, T., Hanzawa, N., Yamamoto, N., & Yamamoto, F.** (2014). Modal gain controllable 2-LP-mode fiber amplifier using PLC type coupler and long-period grating. *Journal of Lightwave Technology, 32*(24), 4694–4700. https://ieeexplore.ieee.org/document/6924757


https://doi.org/10.17993/3ctecno.2021.specialissue8.231-241

# /15/


https://doi.org/10.17993/3ctecno.2021.specialissue8

# EXTERMINATION METHODS OF IMAGE NOISES: A REVIEW

**B. Perumal**
Department of Electronics and Communication Engineering, Kalasalingam Academy of Research and Education, Krishnankoil, Virudhunagar (Dt), (India).
E-mail: palanimet@gmail.com
ORCID: https://orcid.org/0000-0003-4408-9396

**R. Sindhiya Devi**
Department of Electronics and Communication Engineering, Kalasalingam Academy of Research and Education, Krishnankoil, Virudhunagar (Dt), (India).
E-mail: sindhiyadevi14@gmail.com
ORCID: https://orcid.org/0000-0002-7529-6438

**M. Pallikonda Rajasekaran**
Department of Electronics and Communication Engineering, Kalasalingam Academy of Research and Education, Krishnankoil, Virudhunagar (Dt), (India).
E-mail: mpraja80@gmail.com
ORCID: https://orcid.org/0000-0001-6942-4512

**Recepción:** 11/11/2019 **Aceptación:** 05/11/2020 **Publicación:** 30/11/2021

**Citación sugerida:**
Perumal, B., Sindhiya, R., y Pallikonda, M. (2021). Extermination methods of image noises: a review. *3C Tecnología. Glosas de innovación aplicadas a la pyme, Edición Especial,* (noviembre, 2021), 243-259. https://doi.org/10.17993/3ctecno.2021.specialissue8.243-259

## ABSTRACT

To filter an image is necessary in the preprocessing of images for the extermination of noise. Noise is an important factor that affects the information or details in the input image and so it is a need to remove it. Here, we examine a diversified amount of denoising approaches of MRI images by reviewing the positivity and weakness of every method and the well – suited method for the removal of different noises that tend to appear in the MRI images have been discussed. In this paper, we study about different noises of MRI images like Gaussian noise, Rician noise, Speckle noise, Salt and Pepper and the Poisson noise. Also we discuss about some of the basic error metrics like mean squared error, mean absolute error and the peak signal to noise ratio. Furthermore, we have presented a study about the filters like Mean filter, Median filter, Gaussian filter, Wiener filter, Anisotropic Diffusion, Lee and Frost filter, Non Local Means filter and neural network filters in order to eliminate the noises of the MRI images. The advanced technique using neural network tops the list as it follows the training approach. Each of these filters is better in some specific manner and so hybrid filters with the better features of these filters will provide greater accuracy and robustness.

## KEYWORDS

Filter, Noise, positivity, Weakness, MRI Images.


https://doi.org/10.17993/3ctecno.2021.specialissue8.243-259

# 1. INTRODUCTION

Brain is a mind – boggling organ having its size of about only 3 pounds, it is responsible for most of the functions of our human body. Any wreckage to the brain tissue will lead to malfunction of the entire system. One such ravage is the brain tumor, which can be detected with less difficulty with the help of Magnetic Resonant Images.

## 1.1. MAGNETIC RESONANT IMAGE

Medical Resonant Imaging (MRI) is a technique which is non – flamboyant type of investigation either in the exploration or rectification of hindrances in the brain. An efficacious magnetic induction with throbs of extremely high frequency waves are used here in order to beget the embellished outlook of the organs, more precisely the flabby tissues of the human body. This is performed so as to impel the innards of human body to be interpreted easily for the croakers. To explore the organs especially brain, it is the most hyperaware technique.

MRI is more impregnable as it does not adopt emanation and it is quite the contrast of x – ray procedure which is time – honored and the surveying computed tomography (CT). Therefore, no deformation in the chemical reaction occurs in our tissues. We can get diversified standpoints investigated from the images of these scanning processes. Also, we can effortlessly make a distinction of the soft tissues like the gray and white matters and the cerebrospinal fluid (CSF) of the brain by means of MRI images when compared with the CT images.

To perceive the tumefaction in the brain tissues, we can utilize an extensive self – activated process and to make it possible, we should be particularly clear about every minute details of the tissue image. We can get a clear image of the tissues by exiling the discordance in the images.

## 1.2. MRI NOISES

Generally, noise is a signal that randomly appears onto an image and it sometimes affects the entire result. In the medical imaging systems, it is a necessity to obtain clear and undistorted image outputs in order to get a clear cut picture of the affected parts. There exist different


https://doi.org/10.17993/3ctecno.2021.specialissue8.243-259

types of noises in the medical images, especially in the MRI images (Tahir *et al.*, 2016). The major types of noises (Kumar & Nachamai, 2017) that could be seen in the MRI images are Gaussian noise, Rician noise, multiplicative noise and the Speckle noise. Here, we discuss about these noises that affect the quality of Magnetic Resonance Images.

### 1.2.1. GAUSSIAN NOISE

An important and a common type of noise that appears in the MRI images is the Gaussian noise whose probability density function equals the Gaussian distribution (Boyat & Joshi, 2015). This type of noise tends to happen during the image acquisition by some natural causes like poor illumination and high temperature. It is independent of the intensity of the signal caused by thermal noise. Also it does not depend on each pixel of the image.

The Gaussian noise can be also called as the Amplifier Noise as it normally present in the area where high amplification is used rather than the weak amplification areas. This noise is additive in nature (Suryanarayana *et al.*, 2012). It means that this noise, as it is independent of the signal, it simply adds over to the original signal or image to get the distribution. The expectation of the density function of Gaussian noise is determined by the following equation,

$$P(g) = \frac{1}{2\pi\sigma} e^{-(g-\mu)^2/2\sigma^2} \quad \ldots.(1)$$

where, μ denotes the mean and σ2 shows the variance

g specifies the gray level of the image

We know that the Gaussian noise is white. Hence it is clear that it has a flat power spectral density and it is the reason for the auto – correlation of Gaussian noise to be zero.

### 1.2.2. RICIAN NOISE

The Rician Noise is unprejudiced that is almost similar to the Gaussian noise except the fact that the Rician noise depends mainly on the magnitude of the signal at the time of its acquisition every time, whereas the Gaussian noise is independent of the original data.

Generally spoken, Rician noise originates from the complex form of the Gaussian noise but with its original frequency domain measurements. It adheres to Rice propagation (Aja-


https://doi.org/10.17993/3ctecno.2021.specialissue8.243-259

Fernández, Alberola-López, & Westin, 2008) which is also called the Rice – Nakagami distribution as the measurement of the MRI signal can be obtained from the square root of aggregation of the squares of the non – discriminating Gaussian parameters. We can also say this as the Rician noise with high SNR can be considered as the Gaussian noise. Rician probability density function can be given by the following expression,

$$P(r) = \frac{r}{\sigma^2} e^{-\left(\frac{r^2+v^2}{2\sigma^2}\right) I_0\left(\frac{rv}{\sigma^2}\right)} \quad \ldots.(2)$$

where, v is the strength of direct component.

σ shows the noise' orthogonal part.

I0(.) is the propositional mutated Bessel cylindrical function

The noise intensity of the Rician noise is mainly based on the brightest tissue for every acquisition of image. In dark regions which have low intensity, the Rice distribution complies with Rayleigh propagation and in intense zones where the high intensity is available, it tends to Gaussian distribution.

### 1.2.3. SPECKLE NOISE

The Speckle Noise is of course – grained type that is commonly caused by errors during the transmission of data. It also emerges due to ecological impact on the imaging locator during picture procurement. It appears similar to the Gaussian noise with the exception that its probability density function follows gamma distribution. The probability density function of the Speckle noise can be denoted as,

$$P(s) = \frac{s^{\alpha-1} e^{\frac{-s}{a}}}{\alpha-1! a^{\alpha}} \quad \ldots.(3)$$

where, a is the bright region where the gray level is less.

$a^2\alpha$ is its variance.

The Speckle noise is the noise that is obtained in coherent imaging of objects and is multiplicative in nature. These types of noises are commonly seen in case of ultrasound images (Kushwaha & Singh, 2017) but also seen in MRI images.


https://doi.org/10.17993/3ctecno.2021.specialissue8.243-259

### 1.2.4. SALT AND PEPPER NOISE

The Salt-and-Pepper noise is a typical impulse noise as it appears grizzly with canescent pixels. It is said to be Spike noise as it is caused by sharp and sudden disturbances in the signal and it statistically drops the original values. This is the reason for why it is otherwise known as data drop noise.

The Salt and Pepper noise is attributable to the impairment of its constituents in photographic sensors, fallacious memory locale in equipments or the conveyance in a flamboyant medium. It is consistently non − discriminatory and not mutually related to Magnetic Resonance imagery and it is randomly valued (Balamurugan, Sengottuvelan, & Sangeetha, 2013). The density function of the Salt and Pepper noise is given by the following expression,

$$P(sp) = \begin{cases} P_a \; for \; sp = a \\ P_b \; for \; sp = b \\ otherwise \end{cases} \quad \text{....(4) where, a is the bright region}$$

with less gray level

b is the dark region with large gray level

Pa and Pb are the density equations of region 'a' and region 'b' respectively.

We can explain the appearance of the Salt and Pepper noise in the sense of pixels. The salt noise which are the white pixels have high frequency that comes in the range of 255200, whereas the pepper noise which are the dark pixels have low frequency that ranges from 5-0.

## 1.3. ERROR METRICS

The efficiency and accuracy of any filter could be measured by taking the consideration of some error metrics (Nain *et al.*, 2014). These metrics can be used in tracking out the errors. There are a number of error metrics and here we discuss about some of them such as MSE, MAE and PSNR.


https://doi.org/10.17993/3ctecno.2021.specialissue8.243-259

### 1.3.1. MSE

MSE is the Mean Squared Error which can be otherwise referred to as the mean squared deviation. To observe the eminence of the adjudicator, the value of this error is calculated. The MSE is estimated by measuring the mean of squares of the error. When we take the square root of the MSE, we get the error or deviation estimation of the root mean square. This is what we called as Root Mean Square Error which is the RMSE or Root Mean Square Deviation which is RMSD as an alternate. Since the MSE is generally think out as the variance, the RMSE can be called as the Standard Deviation as it is derived by taking the square root of its variance.

The MSE of the filtered image with respect to the original image can be expressed as the summation of the absolute squared erratum in the image which is prorated by the multiplied values of the number of rows and columns in the image.

$$MSE = (abs\ (squared\ error)) / (M*N) \quad ....(14)$$

where M and N are the number of rows and columns of the image respectively.

Squared error is nothing but the absolute value of variation amongst the original and the recreated images.

### 1.3.2. PSNR

PSNR is defined as the proportionality between the original signal or image and the reconstructed signal. It is often used to figure out the eminence of the recreated image. The reconstructed image quality is said to be good, if the PSNR value computed is high.

PSNR is a quality measuring test, which is equivalent in the guesstimate of the humanoid assessment of the excellence of the renovated image. The value of PSNR can be demarcated easily without difficulty by considering the MSE. The PSNR can be mathematically articulated by considering the MSE in the following way:

$$PSNR = 10\ log\_10\ (2552 / MSE) \quad ....(15)$$

Equation (15) represents the calculation of the PSNR from the known MSE values, when each pixel is quantized by 8 bits. The MSE and the PSNR values are related in such a way


https://doi.org/10.17993/3ctecno.2021.specialissue8.243-259

that when the MSE lean towards zero, then the PSNR tends to infinity. It means that if there is no error in the image, then the PSNR is infinite explaining that the renovated image is of high quality.

If the MSE gets lower in its errata, the peak ratio of the reference imagery to the noisy replica increases representing the high portrait quality with exact details.

#### 1.3.3. MAE

The mean absolute error is another term that is responsible for figuring out the quality of the reconstructed image. It is the error detected by calculating the mean of the absolute errata. It is used to estimate the precognition error in its relativity to the reference image. The mean absolute error can be calculated as follows:

$$MAE = (\text{sum } (\text{Reference} - \text{Reconstructed}))/N \quad \ldots. (16)$$

where N is the pair of forecast and observation images. This error should be small to get good quality of images.

## 2. METHODOLOGY

De – noising is quintessential for the maneuvering of images. We can adopt this de – noising functioning as the chief task or as the supplementary of other procedures. There is an existence of several methodologies for the extermination of noise. Yet, it is still bothersome to choose a highly consistent work for a reserved implementation. Here, we discuss some methodologies such as Mean filter, Median filter, Gaussian filter, Wiener filter, Anisotropic Diffusion, Lee and Frost filter and the Non Local Means filter for the noisy imagery acquired from the MRI.

### 2.1. MEAN FILTER

Mean filter is contiguous by speculating the spatial behavior and this can be done with untroublesome implementation of smoothing images. This filter replenishes the halfway point of the kernel by taking the mean of all the other values. Hence it can be also called as the Average filter. It can do the job of a filter that is an LPF (Chandel & Gupta, 2013),


https://doi.org/10.17993/3ctecno.2021.specialissue8.243-259

in which the elements of the image are summed up and then divided by the total number of elements.

The formula for this filter could be denoted as follows,

$$f[x,y] = \frac{1}{mn}\sum_{(s,t)\in S_{xy}} g(s,t) \quad \text{....(5)}$$

where, Sxy is the match of counterparts in a window of size mxn centralized at (x,y).

The working of the mean filter is done by marching throughout the image completely exchanging the value of each dot with the average of neighborhood pixels including it as it is the method of smoothing which is done by lessening the measure of discrepancy of intensity amongst the neighborhood pixels.

The mean filter could be used to remove Gaussian noise and Speckle noise, whereas unsuccessful in Salt and Pepper noise. It is because, when the neighbor of the pixel bestrides a border, then the filter may introduce recently found values for the picture elements on that border which may numb the border.

## 2.2. GAUSSIAN FILTER

The corrosive Gaussian filter does not induce lofty frequency inheritance. It is deliberated to be the exemplary type of filter in time domain (Singh, 2017). It promises its favor to the extent of time on an equal footing with its favor to the extent in frequency. The cutoff may not be sharp at some pass band frequencies. This is due to the fact that this filter has its Fourier transformation as Gaussian.

The Gaussian filter has the formula as given in the expression,

$$g(x,y) = \frac{1}{2\pi\sigma^2} e^{\frac{-(x^2+y^2)}{2\sigma^2}} \quad \text{....(6)}$$

where, x – level stretch from outset

y – erect stretch from outset

σ2 – variance of Gaussian distribution

The kernel coefficients of the Gaussian filter depend on σ where the larger values of σ produce more blurring in the image. These kernels are rotationally symmetric and have no


https://doi.org/10.17993/3ctecno.2021.specialissue8.243-259

directional bias. Gaussian filter is a dynamic, baseband filter whose kernels are separable which results in faster computation.

The Gaussian filters remove the speckle noise which is the spike noise by smoothing the image. Also, Gaussian smoothing could be used in removing the Gaussian noise, a common sort of noise in medical MRI images.

## 2.3. ANISOTROPIC DIFFUSION FILTER

Anisotropic diffusion filter is a mechanism which reduces noise from the imagery by keeping the noteworthy parts of the image untouched. It can be also called as Perona – Malik dispersion as it is presented by Perona and Malik (1990). It is highly space – variant and is locally adaptable.

The Anisotropic Diffusion filter is based on the following equation,

$$\partial_t u = div(g(|\nabla u|^2)\nabla u) \quad \text{....(7)}$$

where, $|\nabla u|2$ measures the larger likelihood of locations to be edges.

The Anisotropic diffusion filter is one of the effective non – linear filters which simultaneously enhances the contrast and also reduces the noise. It depends mainly on the direction of application so that it soothes the homogeneous image regions and retains the edges of the image. Hence, it is one of the well – suited filters for the removal of Rician noise.

## 2.4. WIENER FILTER

Wiener filtering works with the term of the error of squared mean and is determined to be the unsurpassed tradeoff amongst inverse filter and the smoothing filter. It is splendiferous as an endorsement frame. The Wiener filtering provokes the yield by using the rectilinear time invariant filtering of the imagery (Kazubek, 2003). It is a refinement process of rehabilitation.

The approximated formulation for the Wiener filter in the expatriation of noise is specified by,

$$F(x,y) = \left[\frac{1}{H(x,y)}\frac{|H(x,y)|^2}{|H(x,y)|^2+K}\right] G(x,y) \quad \text{....(8)}$$


https://doi.org/10.17993/3ctecno.2021.specialissue8.243-259

where, K is chosen manually to obtain the best visual result.

The Wiener filter is normally a beeline filter which is considered to be stationary. It considers the frequency details instead of the spatial details and it uses the discrete Fourier transform to get the high quality replica. It uses the analytical style of processing. The noise variance can be reduced by the Wiener filter thereby making the blurred images clearly visible. The Wiener filter can be used to find the power spectra of different images and make it useful in other images by taking the average of all the data where a huge set of data exist. This gives a further smoothened imagery.

During rectification purposes, it speculates the province of decadence as well as the noise. It is the process from which we can enumerate the effectiveness of the system by considering various criteria. The image refurbishment with the Wiener filter gives excellent results as it is an outstanding restoration filter. The designing of the Wiener filter is a rectilinear process and is used in removing the Gaussian and the speckle noise, but it is not much better than the median filter.

## 2.5. NON – LOCAL MEANS FILTER

The Non – Local Means filter calculates the neutral value of all the picture elements in the given image, whose weightage is made in such a way that it finds out the level of similarity of these pixels with the intend dot (Wiest-Daesslé *et al.*, 2008). This provides more clarity after filtering with a very little loss percentage of details in contrast to the local means algorithm.

The NL means filter formula is expressed by the following equation,

$$u(x) = \frac{1}{c(x)} \int v(y) f(x,y) dy \quad \text{....(9)}$$

where, u(x) – filtrated estimate of picture at spot 'x'

v(y) – unfiltrated estimate of picture at spot 'y'

f(x,y) – weighing functionate

The level of similarity of the pixels not only depends on the homogeneity of the gray level intensity, but also the geometrical configuration in the neighborhood pixels. The main function of the NL means filter is the dismissal of Rician noise.


https://doi.org/10.17993/3ctecno.2021.specialissue8.243-259

## 2.6. MEDIAN FILTER

The Median filter is probably a spatial filter and is indiscriminate in nature. It is useful for the smoothing of the images. In this filter, the output is obtained from the middle value of the input exemplars in the interface, after the input sampled values are sorted.

The filter formula for the median filter is expressed as follows,

$$v[x,y] = median\{u[m,n], (m,n) \in \omega \quad \text{....(10)}$$

where, ω describes the vicinity established by the user, rested with the location [x,y] of the imagery.

Hence, from the above equation, it is clear that the main principle of the median filter is to restock the value of every single picture element with the middle value of the surrounding pixels, instead of averaging the pixel values (Kazubek, 2003).

Most commonly, the kernel covers odd number of pixels and so the median is the middle value. But, if it is even, then the mean of the duo middle values can be taken as the median. Prior to the start, the voids are inlaid on every margin which makes the squinching to be presented at the borders.

The median filter is mainly used for expatriating the Salt and Pepper noise. In such type of noise, the squinched signal varies from the original and so is its mean value from the true value. Hence Salt and Pepper noise could not be reduced by conventional filters like mean or Gaussian filter successfully, but median filter is well – suited as it removes the drop – out noise effectively and preserves even the small details and edges in a better way. In case of Speckle noise, it is better than the Wiener and the mean filters. It can also be used in removing the Gaussian noise, as it is a spatial filter.

## 2.7. LEE AND FROST FILTER

The Lee filter and the Frost filter are mainly designed to remove the multiplicative noise. The Lee filter was developed by Jong Sen Lee in 1981, whereas the Frost filter was invented by Frost in the year 1982.


https://doi.org/10.17993/3ctecno.2021.specialissue8.243-259

The Lee filter is mainly developed for the generative speckle pattern which utilizes localized enumeration in order to maintain the fine points. It drives in line with the variance. It means that if performs the smoothening operation for the area where the variance is low but not for high variance areas.

The Lee filter formula for the removal of noise is given by the following equation,

$$Y_{xy} = \bar{K} + W(C - \bar{K}) \quad \text{....(11)}$$

where, Yxy is the despeckled image

$\bar{K}$ is the mean of Kernel

C is the central element in the kernel

W is the filter window

The filter window value is given by,

$$W = \frac{\sigma_k^2}{(\sigma_k^2 + \sigma^2)} \quad \text{....(12)}$$

where, $\sigma^2$ is the variance of the reference image

$\sigma_K^2$ is the variance of pixels in kernel of speckled image.

The Frost filter is a linear, convolution filter. This filter is related to the figure of variance i.e., the proportion of localized deviation to the localized mean of corrupted image. Here, the image factor decreases when we abscond from the concerned pixels while increases when near at hand.

$$DN = \sum_{n \times n} K \alpha e^{-\alpha |t|} \quad \text{....(13)}$$

where, $\left(\frac{4}{n\bar{\sigma}^2}\right)\left(\frac{\sigma^2}{\bar{I}^2}\right)$

$|t| = |X - X0| + |Y - Y0|$

K – Normalized coefficient

$\bar{I}$ – Localized mean

Σ – Localized variance

$\bar{\sigma}$ – Image factor of deviation

N – Dimension of roaming kernel


https://doi.org/10.17993/3ctecno.2021.specialissue8.243-259

The Lee filter and the Frost filter are mainly responsible for the removal of Speckle noise (Jaybhay & Shastri, 2015) and they are better in performance than the other filters like Wiener, mean and the median filter.

### 2.8. NEURAL NETWORK FILTER

The image denoising is recently being done by using neural network approaches. The salient point in the depiction of a neural network image filter is to link an image over another with some features that are extracted in order to form a function in a neural network. Bermudez *et al.* (2018) used different degrees of Gaussian noise to test their proposed method which uses a skip connection based autoencoder for denoising and proved that their method towered above the FSL SUSAN software. A combination of deep neural networks with spatio – temporal denoising and bolus injection of contrast agent (CA) has been proposed by Benou *et al.* (2017) for reducing noise. Here, the training of data is performed by adopting a Tofts pharmacokinetic (PK) model and noise realizations. They used concatenated noisy time curves from the surrounding pixels of the frontline for further betterment. Golkov *et al.* (2016) recommended "q-space deep learning" approach, with model-fitting steps to get the scalar properties of voxels directly from the subsampled diffusion weighted images.

## 3. RESULTS

The error metrics MSE and MAE can be compared so as to get a clear pictorial view. The MSE and the MAE are the errors and are to be lower in each and every case (Saladi & Prabha, 2017). With this comparative evaluation of all the filters, we get a vibrant outlook that explains the mediocre values of mean square error and the mean absolute error that are the main distinctive features of an image.

From the review of various filtering methods' positivity and weakness, the basic filters such as mean, Wiener and the Gaussian filters are well and good in the removal of speckle and Gaussian noise, but median filter is better than these by providing clear and sharp edges with details. Lee and Frost are better far from the other local filters. Rician noise could be reduced with Anisotropic diffusion and non local means filter. Comparing to the basic filters, the advanced neural network could be more comfortable in the removal of noises as it adopts the proper training of data. However, hybrid techniques are improving nowadays


https://doi.org/10.17993/3ctecno.2021.specialissue8.243-259

which involve the combination of two or more filters in order to improve the accuracy and robustness.

## 4. CONCLUSIONS

Good quality of images is necessary in every field that involves image processing as its part, especially in medical field. Since brain is a complex organ with soft tissues, expatriation of noise is vital. In this paper, by considering the error metrics, we find that the Gaussian noise could be reduced by using the spatial filters like mean filter, Wiener filter and Median filter. We can also use Gaussian smoothing which can considerably reduce the noise. Salt and Pepper noise can be reduced efficiently by employing median filter. The filters, anisotropic diffusion and NL means are better in removing Rician noise and the Speckle noise reduction can be effectively done by Lee and Frost filters. However, the filter based on neural network is found to be more efficient in filtering noises by mapping of noisy images with the training samples and hybrid methods are far better.

## REFERENCES

**Aja-Fernández, S., Alberola-López, C., & Westin, C.-F.** (2008). Noise and signal estimation in magnitude mri and rician distributed images: a LMMSE approach. *IEEE Transactions On Image Processing, 17*(8), 1383 – 1398. https://doi.org/10.1109/TIP.2008.925382

**Balamurugan, M., Sengottuvelan, P., & Sangeetha, K.** (2013). An empirical evaluation of salt and pepper noise removal for document images using median filter. *International Journal Of Computer Applications, 82*(4), 17-20. https://doi.org/10.5120/14104-2139

**Benou, A., Veksler, R., Friedman, A., & Raviv, T. R.** (2017). Ensemble of expert deep neural networks for spatiotemporal denoising of contrast enhanced MRI sequences. *Medical Image Analysis, 42*, 145–59. https://doi.org/10.1016/j.media.2017.07.006

**Bermudez, C., Plassard, A. J., Davis, T. L., Newton, A. T., Resnick, S. M., & Landman, B. A.** (2018). Learning implicit brain mri manifolds with deep learning. *Proceedings Of SPIE – The International Society For Optical Engineering,* 10574, pii: 105741L. https://doi.org/10.1117/12.2293515

**Boyat, A. K., & Joshi, B. K.** (2015). A review paper: noise models in digital image processing. *Signal & Image Processing: An International Journal (SIPIJ), 6*(2), https://doi.org/10.5121/sipij.2015.6206

**Chandel, R., & Gupta, G.** (2013). Image filtering algorithms and techniques: a review. *International Journal Of Advanced Research In Computer Science And Software Engineering, 3*(10), 198202.

**Golkov, V., Dosovitskiy, A., Sperl, J., Menzel, M., Czisch, M., Sämann, P., Brox, T., & Cremers, D.** (2016). Q-space deep learning: twelve-fold shorter and model-free diffusion mri scans. *IEEE Transactions On Medical Imaging, 35*(5), 1344–51. https://doi.org/10.1109/TMI.2016.2551324

**Jaybhay, J., & Shastri, R.** (2015). A study of speckle noise reduction filters. *Signal & Image Processing: An International Journal (SIPIJ), 6*(3), 71-80. https://doi.org/10.5121/sipij.2015.6306

**Kazubek, M.** (2003). Wavelet domain image de-noising by thresholding and wiener filter. *Signal Processing Letters. IEEE, 10*(11). https://doi.org/10.1109/LSP.2003.818225

**Kumar, N., & Nachamai, M.** (2017). Noise removal and filtering techniques used in medical images. *Oriental Journal Of Computer Science And Technology, 10*(1), 103-113. http://dx.doi.org/10.13005/ojcst/10.01.14

**Kushwaha, S., & Singh, R. K.** (2017). Performance comparison of different despeckled filters for ultrasound images. *Biomedical & Pharmacology Journal, 10*(2), 837-845. http://dx.doi.org/10.13005/bpj/1175

**Nain, A. K., Singhania, S., Gupta, S., & Bhushan, B.** (2014). A comparative study of mixed noise removal techniques. *International Journal Of Signal Processing, Image Processing And Pattern Recognition, 7*(1), 405-414. https://doi.org/10.14257/ijsip.2014.7.1.37

**Perona, P., & Malik, J.** (1990). Scale-space and edge detection using anisotropic diffusion. *IEEE Transactions - Pattern Analysis And Machine Intelligence, 12*, 629-639. https://ieeexplore.ieee.org/document/56205

**Saladi, S., & Prabha, N. A.** (2017). Analysis of denoising filters on mri brain images. *International Journal Of Imaging Systems And Technology, 27*(3), 201-208. https://doi.org/10.1002/ima.22225

**Singh, V.** (2017). Comparative study of algorithms/techniques for denoising of gaussian noise. *International Journal Of Advanced Research In Computer Science, 8*(8), 78-82. http://dx.doi.org/10.26483/ijarcs.v8i8.4614

**Suryanarayana, S., Deekshatulu, B. L., Kishore, K. L., & Kumar, Y. R.** (2012). Estimation and removal of gaussian noise in digital images. *International Journal Of Electronics And Communication Engineering, 5*(1), 23-33.

**Tahir, M., Iqbal, A., & Khan, A. S.** (2016). A review paper of various filters for noise removal in mri brain image. *International Journal Of Innovative Research In Computer And Communication Engineering, 4*(12), 21711-21715.

**Wiest-Daesslé, N., Prima, S., Coupé, P., Morrissey, S. P., & Barillot, C.** (2008). Rician Noise Removal by Non-Local Means Filtering for Low Signal-to-Noise Ratio MRI: Applications to DT-MRI. In Metaxas D., Axel L., Fichtinger G., Székely G. (eds) *Medical Image Computing and Computer-Assisted Intervention – MICCAI 2008*. Lecture Notes in Computer Science, vol 5242. Springer, Berlin, Heidelberg. https://doi.org/10.1007/978-3-540-85990-1_21

/16/


https://doi.org/10.17993/3ctecno.2021.specialissue8

# COMPARATIVE ANALYSIS OF VISU SHRINK AND PMD MODEL ON SAR IMAGES FOR SPECKLE NOISE REDUCTION

**Kalaiyarasi Alagumani**
Department of Electronics and Communication Engineering,
V.S.B. Engineering College, Karur District, Tamil Nadu, (India).
E-mail: mukalaiyarasi@gmail.com
ORCID: https://orcid.org/0000-0001-9306-2654

**Perumal Balasubramani**
Department of Electronics and Communication Engineering, Kalasalingam Academy of Research and Education,Virudhunagar District, Tamil Nadu, (India).
E-mail: palanimet@gmail.com
ORCID: https://orcid.org/0000-0003-4408-9396

**Pallikonda Rajasekaran Murugan**
Department of Electronics and Communication Engineering, Kalasalingam Academy of Research and Education, Virudhunagar District, Tamil Nadu, (India).
E-mail: m.p.raja@klu.ac.in
ORCID: https://orcid.org/0000-0003-4408-9396

**Recepción:** 11/11/2019 **Aceptación:** 09/02/2021 **Publicación:** 30/11/2021

**Citación sugerida:**
Alagumani, K., Balasubramani, P., y Murugan, P. R. (2021). Comparative analysis of VISU shrink and PMD model on SAR images for speckle noise reduction. *3C Tecnología. Glosas de innovación aplicadas a la pyme, Edición Especial,* (noviembre, 2021), 261-277. https://doi.org/10.17993/3ctecno.2021.specialissue8.261-277

## ABSTRACT

Removing noise from original image is often the initial step in image analysis. The best de-noising technique should not be only reducing the noise, but do so without blurring or changing the location of the edges. Many approaches have been proposed for noise reduction. Speckle noise can be easily removed by simple method such as partial Differential Equations method (PDEs). In this paper, Perona-Malik Diffusion (PMD) models have been proposed and compared with VISU Shrinkage (VS) method. Although both the methods are seemed to be comparable with removing speckle noise, speckles are more visible to mages processed by VS method. The experimental results show that the PMD model obtains superior performance with the PSNR value of 61.90%, SSI of 0.40, EPI of 0.51 and SSIM of 69.05%. The PSNR value has been increased by 20.2% when compared with VS de-speckling method.

## KEYWORDS

De-speckling, PDE, Synthetic Aperture Radar, VISU shrink, DWT.


https://doi.org/10.17993/3ctecno.2021.specialissue8.261-277

# 1. INTRODUCTION

Remote sensing images are captured by various sensors. The captured images are often degraded by speckle noise called multiplicative noise. Speckle is predominantly due to the meddling of the requiting wave of the transducer aperture. It is one of the most perilous commotions that amend the quality of Synthetic Aperture Radar (SAR) coherent images (Choi & Jeong, 2019) and decreases the potentiality of the images. Speckle noise in SAR image is broadly severe, precipitating difficulties for image interpretation. It is generated because of the coherent processing of backscattered signals from multiple distributed targets of the earth surface.

The speckle noise reduction is usually the initial step in the analysis of SAR images. There are a several de-noising filters such as average filter, mean filter, median filter, Lee filter, sigma filter, Lee-sigma filter, and wiener filter etc., which are used in the noise removal of SAR images. These filters reduce speckle noise by smoothing and sharpening the original image. Due to which some unavoidable blur has been introduced in the de-noised image, and also the main problem in using adaptive procedure techniques is the empirical choice of thresholds to determine the size of windows. To overcome the above cited drawbacks, PDEs based methods are used for de-speckling SAR images. The PDE algorithm is more efficient for de-speckling the SAR images effectively without blurring the edges of original SAR images.

# 2. RELATED WORKS

Various Second-Order PDE methods including the anisotropic model (Kriti, Virmani, & Agarwal, 2019; Shen Liu *et al.*, 2012) and the total variational model (Rudin & Osher, 1994; Morteza *et al.*, 2019) were developed for suppressing noise. In Kriti *et al.* (2019), Fuzzy Morphological Anisotropic Diffusion method was utilized for SAR image speckle noise reduction. In Shen Liu *et al.* (2012), the anisotropic diffusion filter was used to reduce the speckle noise in ultrasound images. This method produced blur at the edges of the de-speckled image. In Rudin & Osher (1994), total variation with free local constraints method was used for noise reduction. In Morteza *et al.* (2019), Nonlinear total variation-based model was developed for noise removal of the image. This method produced sharp edges at the


https://doi.org/10.17993/3ctecno.2021.specialissue8.261-277

de-noised images. In Ehsan *et al.* (2014), Complex diffusion method for image enhancement was proposed and compared with the second, fourth-order PDE and showed that the complex diffusion method offers better result when the noise is low. The performance of this method is declined when the noise level is high.

In Liu *et al.* (2012a), PDE with Auxiliary images were used to de-speckle the SAR image. Here, the auxiliary images were used as priors. Multispectral and hyperspectral images were used in this experiment. The major drawback of using second-order Partial Differential Equation is the procreation of blocking effect in the de-noised image (Liu, Lai, & Pericleous, 2014, Van Rie *et al.*, 2019). To reduce the block effect, the fourth-order PDE method was developed by replacing the gradient operator by the Laplacian operator and this method gives better results by reducing the block effect (You & Kaveh, 2000). In Didas (2004), and Didas, Weickert and Burgeth (2005), Higher-order PDE based noise removal were performed. The higher-order PDEs are not widely used in de-speckling of SAR images because of its complex numerical implementation and enormous computations.

This paper is further organized as follows. Section III explains the materials and methods used in this paper. Section IV gives the various performance metrics used for comparing the performance of both de-speckling method. Section V provides the results and discussion. Conclusion of this paper is given in Section VI.

## 3. MATERIALS AND METHODS

Speckle noise diminishes the look and quality of SAR images which in turn decreases the performances of SAR image processing and Analysis. Therefore, the noise must be suppressed before processing the SAR images using various image processing techniques like multiple-look processing, adaptive and non-adaptive filters, etc.

### 3.1. VISU SHRINKAGE

De-speckling using wavelet shrinkage method, reduce the speckle noise existing in the noisy image with conserving the textual and edge attributes of the image. VISU Shrinkage (VS) is one the wavelet shrinkage method. In VS, thresholding is performed by applying universal threshold (UT) and it is proposed by Donoho (1994). The block diagram of VS de-speckling


https://doi.org/10.17993/3ctecno.2021.specialissue8.261-277

method is shown in fig 1. In this method, no need to calculate the threshold value at every subband level. Initially, 2D-DWT is applied on the speckled SAR image where the image is separated into four subband regions namely LL LH, HL and HH (Chang, Yu, & Vetterli, 2000). Then UT soft thresholding is performed on the wavelet coefficients. There are two types of thresholding viz. Hard thresholding produce unwanted artifacts in the de-speckled images while soft thresholding yields visually pleasing images. In soft thresholding, the coefficients below UT are set to zero while important coefficients are replaced by UT value. The shrinkage of the wavelet co-efficient is given by (Donoho, 1994):

$$\lambda = \sigma^{Noise}\sqrt{2\log(n)} \tag{1}$$

where, $\sigma^{Noise}$, is the standard deviation of the noise and '$n$' is the number of pixel elements in the image. While UT selection, it is most necessary to evaluate the standard deviation of the noise ($\sigma^{Noise}$) from the wavelet coefficients. It is obtained by using the below formula:

$$\sigma = \frac{MAD}{0.6745} \tag{2}$$

where, *MAD* is the median of the absolute values of the wavelet coefficients (HH band of speckled image). In this experiment, 0.4349 is used as the universal threshold. At last, compute the 2D-IDWT to get the de-speckled SAR image. This technique is simple and effective, it removes speckle noise co-efficient that is insignificant relative to UT. The UT tends to be high for large values of MAD, it over smoothens the speckled SAR image and affects many original images co-efficient along with speckle noise. Also, it has been observed that threshold value should be smaller value for soft thresholding (Bruce & Gao, 1996). For de-speckling of SAR images, VISU shrink does not adapt well to suppress:

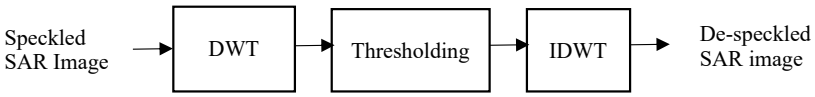


**Figure 1**. VISU Shrinkage (VS) De-speckling method.
**Source:** own elaboration.


https://doi.org/10.17993/3ctecno.2021.specialissue8.261-277

## 3.2. PMD MODEL

SAR images are affected by various noises which include both non-additive and additive noise. The non-additive ie, multiplicative noise in SAR image is otherwise called as speckle noise and it is defined as (Rafati *et al.*, 2016):

$$I(x,y) = f(x,y) * u(x,y) + n(x,y) \tag{3}$$

*Where*, $I\ (x,y)$, is the observed SAR image, $u\ (x,y)$ is the multiplicative component of a speckled image, $n\ (x,y)$ is the additive component of the speckled image. Since, the speckle noise is multiplicative, removing the speckle noise present in the remote sensing images is important. Only the multiplicative component is considered and the additional component is not to be considered. Therefore equation (3) can be rewritten as:

$$I(x,y) = f(x,y) * u(x,y) \tag{4}$$

The process used to de-speckle the SAR image using the PMD model is given in Figure 2. To convert the multiplicative component into the additive component, the log transform has been applied on both the sides of the above equation. Therefore, the above equation becomes,

$$S(x,y) = \log(I(x,y) = \log(f(x,y)) + \log(u(x,y)) \tag{5}$$

PMD model depends on heat diffusion equation which is defined as (Perona & Malik, 1990):

$$\frac{\partial S(x,y,t)}{\partial t} = \nabla.\left(c(x,y,t)\nabla S(x,y,t)\right) \tag{6}$$

*Here*, $S(x,y,t)$ is the log transformed noisy SAR image, $c(x,y,t)$ is the diffusivity, $\nabla$ is the gradient operator, $\nabla$ is the divergence operator. This equation was developed by Perona and Malik (1990). It can be expanded as:

$$\frac{\partial S(x,y,t)}{\partial t} = \nabla.\left(c(x,y,t)\nabla(\log(f(x,y)) + \log(u(x,y))\right) \tag{7}$$

This equation is more effective for suppressing the speckle noise while preserving the edge characteristics of the image. In this case, initially the gradient of the SAR image grad *x, grad y* is calculated in both x and y directions respectively. Then diffusivity is computed by using the below equation which is stated in (Khristenko *et al.*, 2019).


https://doi.org/10.17993/3ctecno.2021.specialissue8.261-277

$$c(x,y,t) = \frac{1}{1+\frac{|\nabla S|^2}{k^2}} \tag{8}$$

Here, $k$ is a small constant used to control the diffusivity. It must be chosen between 5 to 100. The value of diffusivity:

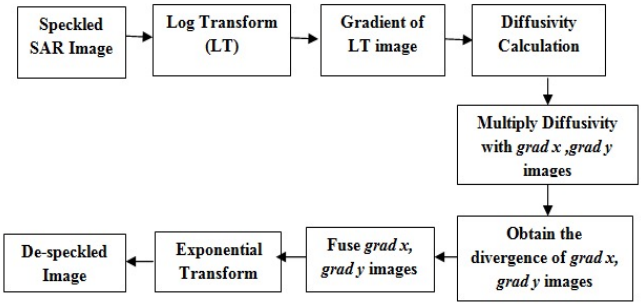


**Figure 2.** Work flow of PMD Model.
**Source:** own elaboration.

'*c*' changes at different regions of the image. The gradient of the image is high during the edges of the images, this leads to diffusivity has a small value. This consequently preserves the edges from smoothing. After that, the diffusivity is multiplied with the gradient image *grad x* and *grad* y images respectively. Thereafter, the divergence of *grad x* and *grad y* images are computed and both the images are fused to get the resultant divergence image. At last, take the exponential transform to get the de-speckled SAR image.

## 4. PERFORMANCE METRICS

To evaluate the performance improvement four different performance measures such as PSNR, SSI, EPI, and SSIM are enumerated based on the speckled SAR image and the de-speckled SAR image.

### 4.1 PEAK SIGNAL TO NOISE RATIO (PSNR)

PSNR is most widely used as a performance analyzing parameter. The higher value of PSNR gives a better quality of the de-speckled image. PSNR is defined as (Kalaiyarasi, Saravanan, & Perumal, 2016):


https://doi.org/10.17993/3ctecno.2021.specialissue8.261-277

$$PSNR = 10\log_{10}\frac{MAX_I^2}{MSE} \tag{9}$$

*Where*, $MAX_I^2$ is the maximum possible value of the original image. MSE is the mean square error, which must be lower value.

## 4.2 SPECKLE SUPPRESSION INDEX (SSI)

SSI is used to find the efficiency of the de-speckling algorithm, which is defined as (Dellepiane & Angiati, 2014):

$$SSI = \frac{\sqrt{Var(F)}}{Mean(F)} \cdot \frac{Mean(I)}{\sqrt{Var(I)}} \tag{10}$$

SSI should be the lowest value and the range lies between [0,1].

## 4.3 EDGE PRESERVATION INDEX (EPI)

Another parameter EPI can be computed by comparing the edges of the de-speckled image and the noisy SAR image. An efficient de-speckling method must have higher in Edge Preservation Index EPI (Ji & Zhang, 2017).

$$EPI = \frac{Gradient\ \ of\ \ the\ \ Filtered\ \ \text{Im}age\ \ Edges}{Gradient\ \ of\ \ the\ \ Noisy\ \ \text{Im}age\ \ Edges} \tag{11}$$

## 4.4 STRUCTURAL SIMILARITY INDEX MEASURE (SSIM)

When suppressing the speckle noise in SAR image processing, preserving edges is the most challenging one. Therefore, the additional parameters like EPI and SSIM have been evaluated here. SSIM is utilized to quantify the closeness amid the original SAR and the de-speckled SAR image. SSIM is define as (Nadernejad, Koohi, & Hassanpour, 2008):

$$SSIM = \frac{4\sigma_{xy}\overline{X}\overline{Y}}{\left(\sigma_x^2 + \sigma_y^2\right)\left[\left(\overline{X}\right)^2 + \left(\overline{Y}\right)^2\right]} \tag{12}$$

Where,


https://doi.org/10.17993/3ctecno.2021.specialissue8.261-277

$$\bar{X} = \frac{1}{N}\sum_{i=1}^{N} x_i \quad , \quad \bar{Y} = \frac{1}{N}\sum_{i=1}^{N} y_i$$

$$\sigma_x^2 = \frac{1}{N-1}\sum_{i=1}^{N}\left(x_i - \bar{X}\right)^2 \quad , \quad \sigma_y^2 = \frac{1}{N-1}\sum_{i=1}^{N}\left(y_i - \bar{Y}\right)^2$$

$$\sigma_{xy} = \frac{1}{N-1}\sum_{i=1}^{N}\left(x_i - \bar{X}\right)\left(y_i - \bar{Y}\right)$$

## 5. RESULTS AND DISCUSSION

Different SAR images have been used for this experiment which is shown in Figure 3.

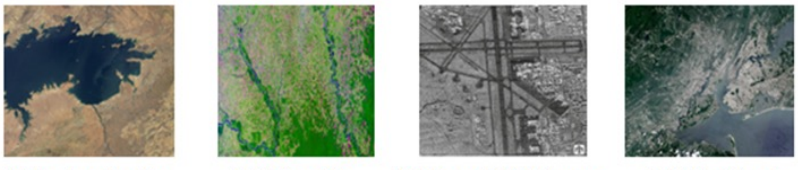


**Figure 3.** SAR images in different location. (a) Eastem Kariba, (b) Colombia Deforestation, (c) Airport SAR Image, (d) Ellis Island.
**Source:** own elaboration.

The de-speckled image using VS method is shown in Figure 4. In this method, noise reduction mainly depends on the UT value. The range of UT lies between 0 to 1. Here 0.4349 has been used as UT for thresholding the SAR image.

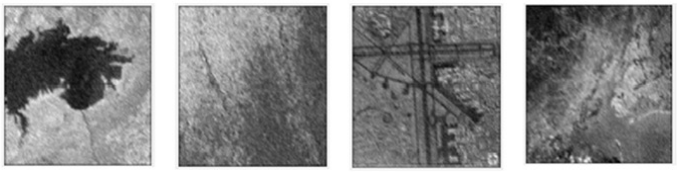


**Figure 4.** De-speckled SAR images using VS method. (a) Eastem Kariba, (b) Colombia Deforestation, (c) Airport SAR Image, (d) Ellis Island.
**Source:** own elaboration.

The de-speckled image using PMD model is shown in Figure 5. The VS method provides poor edge preservation. To overcome that, in PMD model the diffusivity plays an important role in preserving the edges of the images. The value of diffusivity co-efficient must be low for preserving the edges of the images. The obtained minimum and maximum value of


https://doi.org/10.17993/3ctecno.2021.specialissue8.261-277

diffusivity for different SAR images have been listed in Table 1. The gradient value will be high during the edges of the image. From equation (8), it can be noticed that diffusivity will be low when the gradient has a larger value. This technique is used to preserve the edges of the SAR images in the PMD model. The de-speckled image after the PMD model looks more cheerful, by eliminating the noise without affecting the edges and at the same time, it also reduces the block effect.

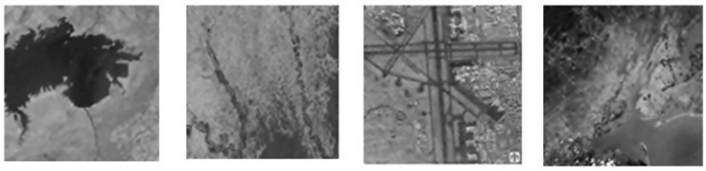


**Figure 5.** De-speckled SAR images using PMD model. (a) Eastem Kariba, (b) Colombia Deforestation, (c) Airport SAR Image, (d) Ellis Island.
**Source:** own elaboration.

From the above ocular results shown in Figures 4-5, it can be deduced that almost all speckle noise is removed, and the de-speckled image looks more comfortable without blocky effect. It is concluded that the PMD model has produced better visual images than the VS method.

**Table 1.** The minimum and maximum value of Diffusivity for SAR images.

| Images | Minimum | Maximum |
|---|---|---|
| Eastem Kariba | 0.0201 | 0.9997 |
| Colombia Deforestation | 0.0202 | 0.9952 |
| Airport SAR Image | 0.0108 | 0.9981 |
| Ellis Island | 0.0131 | 0.9972 |

**Source:** own elaboration.


https://doi.org/10.17993/3ctecno.2021.specialissue8.261-277

**Table 2**. Comparison of performance parameters of VS and PMD model.

| S.No | Images | PSNR | | SSI | | EPI | | SSIM | |
|---|---|---|---|---|---|---|---|---|---|
| | | PMD | VS | PMD | VS | PMD | VS | PMD | VS |
| 1 | Eastem Kariba | 62.17 | 42.36 | 0.39 | 0.23 | 0.56 | 0.37 | 66.84 | 53.29 |
| 2 | Colombia Deforestation | 61.88 | 39.96 | 0.36 | 0.28 | 0.68 | 0.60 | 61.44 | 55.18 |
| 3 | Airport Image | 59.93 | 40.63 | 0.36 | 0.26 | 0.46 | 0.36 | 62.21 | 50.28 |
| 4 | Ellis Island | 62.99 | 43.15 | 0.44 | 0.16 | 0.42 | 0.31 | 75.13 | 67.20 |
| 5 | Wetland | 64.64 | 42.80 | 0.43 | 0.10 | 0.50 | 0.34 | 74.70 | 67.73 |
| 6 | Airborne SAR Image | 63.16 | 40.81 | 0.41 | 0.16 | 0.50 | 0.53 | 70.22 | 50.54 |
| 7 | Sea Ice | 63.20 | 40.79 | 0.41 | 0.16 | 0.49 | 0.44 | 70.11 | 57.77 |
| 8 | Barents Sea Ice Image | 59.53 | 41.53 | 0.38 | 0.12 | 0.40 | 0.45 | 65.54 | 60.40 |
| 9 | Arctic Sea Ice | 60.91 | 39.51 | 0.44 | 0.11 | 0.47 | 0.42 | 75.58 | 63.34 |
| 10 | Sea Ice MEASURES | 62.62 | 42.13 | 0.37 | 0.15 | 0.38 | 0.39 | 63.28 | 57.59 |
| 11 | Amazon_2010 | 56.92 | 42.54 | 0.40 | 0.28 | 0.50 | 0.36 | 68.67 | 59.29 |
| 12 | Amazon_2020 | 64.03 | 44.57 | 0.45 | 0.27 | 0.67 | 0.22 | 77.11 | 53.22 |
| 13 | Amazon_2030 | 63.95 | 42.63 | 0.43 | 0.25 | 0.55 | 0.35 | 74.09 | 62.17 |
| 14 | Amazon_2040 | 61.62 | 42.27 | 0.41 | 0.19 | 0.67 | 0.38 | 69.74 | 55.54 |
| 15 | Amazon_2050 | 60.96 | 39.84 | 0.35 | 0.24 | 0.50 | 0.47 | 61.16 | 52.45 |
| | Average | 61.90 | 41.70 | 0.40 | 0.19 | 0.51 | 0.39 | 69.05 | 57.73 |

**Source:** own elaboration


https://doi.org/10.17993/3ctecno.2021.specialissue8.261-277

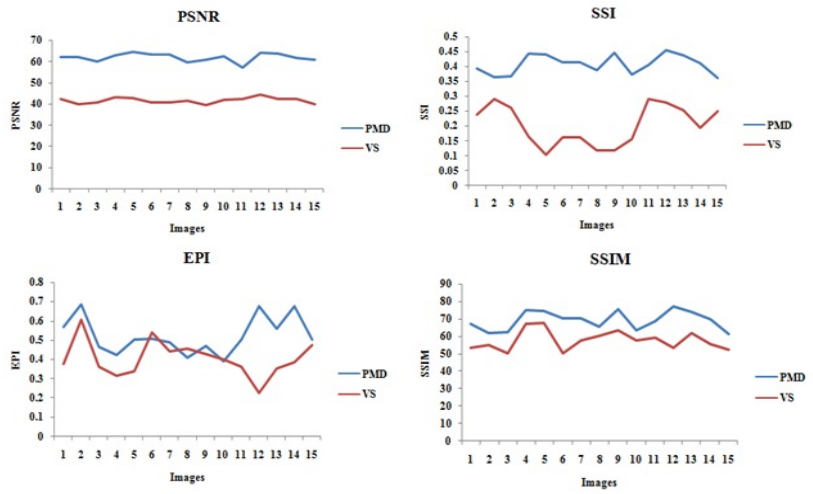


**Figure 6.** Graphical representation of PSNR, SSI, EPI and SSIM for VS method and PMD model.
**Source:** own elaboration.

Table 2 gives the comparison of performance parameters of VISU shrinkage and NSO-PDEs method on different SAR images respectively. From both the methods, VISU Shrink has the least performance as theoretically it uses a universal threshold for all sub-bands which is not optimal (Dixit *et al.*, 204). Figure 6 shows the comparison of PSNR, SSI, EPI, and SSIM for the two methods. From the four charts, it is inferred that the PMD model provides better PSNR, EPI, SSI and SSIM than VS method.

**Table 3.** Average Values of Performance Metrics.

| Parameters | Methods | |
|---|---|---|
| | PMD | VS |
| PSNR | 61.90 | 41.70 |
| SSI | 0.40 | 0.19 |
| EPI | 0.51 | 0.39 |
| SSIM | 69.05 | 57.73 |

**Source:** own elaboration.

The average values of performance metrics are given in Table 3. The average values have been calculated by taking the mean average values of total images used for this experiment. The graphical illustration of comparative analysis has been presented in Figure 7. From the graphical illustration analysis, it is noticed that the PMD de-speckling method produces


https://doi.org/10.17993/3ctecno.2021.specialissue8.261-277

better outcomes in terms of various performance metrics which includes PSNR of 61.90%, SSI of 0.40, EPI of 0.51 and SSIM of 69.05%.


**Figure 7.** Comparative analysis of Performance metrics of PMD and VS de-speckling methods. a) PSNR and SSIM, b) SSI and EPI.

**Source:** own elaboration.

## 6. CONCLUSIONS

PDE method has been most broadly used in SAR image processing particularly in suppressing speckle noise. In this paper, the PMD model has been proposed for speckle noise reduction. The performance of the PMD model is compared with the VISU shrinkage method. VS method follows the universal threshold scheme. This method does not minimize the mean


https://doi.org/10.17993/3ctecno.2021.specialissue8.261-277

squared error and it does not remove the speckle noise effectively. The experimental results show that the PMD model of speckle noise reduction yields a better result when compared to the VISU Shrinkage method. Additionally, the quality of the de-speckled image is better enhanced using the PMD model in terms of PSNR of 61.90%, SSI of 0.40, EPI of 0.51 and SSIM of 69.05%. The PSNR value has been increased by 20.2% when compared with the VS de-speckling method

## ACKNOWLEDGMENT

We thank the Department of ECE of Kalasalingam Academy of Research and Education (Deemed to be University), Tamil Nadu, India for the computational facilities made available in Centre for Signal Processing Laboratory (Supported by Department of Science and Technology (DST), New Delhi under FIST Programme). (Reference No: SR/FST/ETI-336/2013 dated November 2013).

## REFERENCES

**Bruce, G., & Gao, H.** (1996). Understanding Wave Shrink: Variance and bias estimation. *Biometrika, 83*, 727-745. https://doi.org/10.1.1.135.913

**Chang, S. G., Yu, B., & Vetterli, M.** (2000). Adaptive wavelet Thresholding for image denoising and compression. *IEEE Transactions on Image Processing, 9*(9), 1532-1546. https://ieeexplore.ieee.org/document/862633

**Choi, H., & Jeong, J.** (2019). Speckle Noise Reduction Technique for SAR images using Statistical Characteristics of Speckle Noise and Discrete Wavelet Transform. *Remote Sensing, 11*, 1-27. https://doi.org/10.3390/rs11101184

**Dellepiane, S. G., & Angiati, E.** (2014). Quality Assessment of Despeckled SAR Images. *IEEE Journal of Selected Topics in Applied Earth Observations and Remote Sensing, 7*(2), 691-707. https://ieeexplore.ieee.org/document/6595646

**Didas, S.** (2004). *Higher order variational methods for noise removal in signals and images* (Diploma thesis). Department of Mathematics, Saarland University, 2004. https://www.mia.uni-saarland.de/Theses/didas-dipl04.pdf

**Didas, S., Weickert, J., & Burgeth, B.** (2005). Stability and Local Feature Enhancement of Higher Order Nonlinear Diffusion Filtering. In Kropatsch W.G., Sablatnig R., Hanbury A. (eds) *Pattern Recognition. DAGM 2005*. Lecture Notes in Computer Science, vol 3663. Springer, Berlin, Heidelberg. https://doi.org/10.1007/11550518_56

**Dixit, A., & Sharma, P.** (2014). A Comparative Study of Wavelet Thresholding for Image Denoising. *International Journal of Image Graphics and Signal Processing, 12*, 39-46. http://www.mecs-press.org/ijigsp/ijigsp-v6-n12/IJIGSP-V6-N12-6.pdf

**Donoho, D. L.** (1994). Ideal spatial adaptation by wavelet shrinkage. *Biometrika, 81*(3), 425–455. https://doi.org/10.1093/biomet/81.3.425

**Ji, X., & Zhang, G.** (2017). Contourlet domain SAR image de-speckling via self-snake diffusion and sparse representation. *Multimedia Tools and Applications, 76*(4), 5873-5887. https://doi.org/10.1007/s11042-015-2560-2

**Kalaiyarasi, M., Saravanan, S., & Perumal, B.** (2016). A survey on: De-speckling Methods of SAR image. *Proceedings of International Conference on Control, Instrumentation, Communication and Computational Technologies (ICCICCT)*.

**Khristenko, U., Scarabosio, L., Swierczynski, P., Ullmann, E., & Wohlmuth, B.** (2019). Analysis of Boundary Effects on PDE-Based Sampling of Whittle--Matérn Random Fields. *SIAM/ASA Journal on Uncertainty Quantification, 7*(3), 948-974. https://doi.org/10.1137/18M1215700

**Kriti, Virmani, J., & Agarwal, R.** (2019). Effect of de-speckle filtering on classification of breast tumors using ultrasound images. *Biocybernetics and Biomedical Engineering, 39*(2), 536-560. https://doi.org/10.1016/j.bbe.2019.02.004

**Liu, P., Huang, F., Li, G., & Liu, Z.** (2012a). Remote-Sensing Image Denoising Using Partial Differential Equations and Auxiliary Images as Priors. *IEEE Geoscience and Remote Sensing Letters, 9*(3), 358-362. https://ieeexplore.ieee.org/abstract/document/6061940

**Liu, S., Wei, J., Feng, B., Lu, W., Denby, B., Fang, Q., & Dang, J.** (2012b). An anisotropic diffusion filter for reducing speckle noise of ultrasound images based on separability.

*Proceedings of the 2012 Asia Pacific Signal and Information Processing Association Annual Summit and Conference (APSIPA ASC).* https://ieeexplore.ieee.org/document/6411801

**Liu, X. Y., Lai, C.-H., & Pericleous, K. A.** (2014). A fourth-order partial differential equation denoising model with an adaptive relaxation method. *International Journal of Computer Mathematics, 92*(3). https://doi.org/10.1080/00207160.2014.904854

**Nadernejad, E., Koohi, H., & Hassanpour, H.** (2008). PDEs-Based Method for Image Enhancement. *Applied Mathematical Sciences, 2*(20), 981-993. https://www.researchgate.net/profile/Hamidreza-Koohi/publication/228653972_PDEs-Based_Method_for_Image_Enhancement/links/0c9605260d3508cda6000000/PDEs-Based-Method-for-Image-Enhancement.pdf

**Perona, P., & Malik, J.** (1990). Scale-space and edge detection using anisotropic diffusion. *IEEE Transactions on Pattern Analysis and Machine Intelligence, 12*(7), 629–639. https://ieeexplore.ieee.org/document/56205

**Rafati, M., Arabfard, M., Zadeh, M. R. R., & Maghsoudloo, M.** (2016). Assessment of noise reduction in ultrasound images of common carotid and brachial arteries. *IET Computer Vision, 10*(1), 1-8. https://doi.org/10.1049/iet-cvi.2014.0151

**Rudin, L. I. & Osher, S.** (1994). Total variation based image restoration with free local constraints. *IEEE International Conference on Image Processing, 1*, 31–35. https://ieeexplore.ieee.org/document/413269

**Salehjahromi, M., Wang, Q., Gjesteby, L. A., Harison, D., Wang, G., & Yu, H.** (2019). A directional TV based ring artifact reduction method. *Proceedings of SPIE 10948, Medical Imaging 2019, Physics of Medical Imaging, 109482C, 9,* https://doi.org/10.1117/12.2513037

**Van Rie, J., Schütz, C., Gençer, A., Lombardo, S., Gasser, U., Kumar, S., Salazar-Alvarez, G., Kang, K., & Thielemans, W.** (2019). Anisotropic Diffusion and Phase Behavior of Cellulose Nanocrystal Suspensions. *Langmuir, 35*(6), 2289-2302. https://doi.org/10.1021/acs.langmuir.8b03792

**You, Y.-L., & Kaveh, M.** (2000). Fourth-order partial differential equations for noise removal. *IEEE Transaction on Image Processing, 9*(10), 1723–1730. https://ieeexplore.ieee.org/document/869184


https://doi.org/10.17993/3ctecno.2021.specialissue8.261-277

/17/


https://doi.org/10.17993/3ctecno.2021.specialissue8

# SELF - ACTIVATED SEGMENTATION PRACTICES OF BRAIN TUMEFACTION IN MR SCAN IMAGES: A STUDY

**B. Perumal**
Department of Electronics and Communication Engineering, Kalasalingam Academy of Research and Education, Krishnankoil, Virudhunagar (Dt), (India).
E-mail: palanimet@gmail.com
ORCID: https://orcid.org/0000-0003-4408-9396

**R. Sindhiya Devi**
Department of Electronics and Communication Engineering, Kalasalingam Academy of Research and Education, Krishnankoil, Virudhunagar (Dt), (India).
E-mail: sindhiyadevi14@gmail.com
ORCID: https://orcid.org/0000-0002-7529-6438

**M. Pallikonda Rajasekaran**
Department of Electronics and Communication Engineering, Kalasalingam Academy of Research and Education, Krishnankoil, Virudhunagar (Dt), (India).
E-mail: mpraja80@gmail.com
ORCID: https://orcid.org/0000-0001-6942-4512

**Recepción:** 11/11/2019 **Aceptación:** 26/10/2020 **Publicación:** 30/11/2021

**Citación sugerida:**
Perumal, B., Devi, R. S., y Rajasekaran, M. P. (2021). Self – activated segmentation practices of brain tumefaction in mr scan images: a study. *3C Tecnología. Glosas de innovación aplicadas a la pyme, Edición Especial,* (noviembre, 2021), 279-291. https://doi.org/10.17993/3ctecno.2021.specialissue8.279-291

## ABSTRACT

To segment a tumefaction of brain images obtained from any of the imaging modalities is a lofty goal owing to the varied shape, locality and measure of tumor. This segmentation process can be done manually by a Doctor or otherwise can be done automatically using computer aided diagnosis. Self – Activated segmentation of brain tumor is nothing but the separation of the tissues that are not related with the tissues within the brain case akin to the regions with myelinated nerve fibers without dendrites, portions of nerve fibers with dendrites and the cerebrum area along with the cerebrospinal fluid (CSF). The various imaging modalities are the scans from the radioscopy with emitting positrons (PET), multiple X – rays (CT) and through Magnetic Resonance (MRI). In this paper, an overview of recent automatic brain tumor segmentation techniques of MRI and the advantages of multimodal imaging techniques has been explained. The segmentation techniques such as thresholding, edge based, morphology based, watershed, k means and markov random method are the conventional tactics of segmentation that are addressed. Also, the advanced segmentation methods such as region growing, genetic method, fuzzy clustering, deformation, atlas method and artificial neural network are also discussed. Moreover, the hybrid methods that have different combination of genetic algorithm, artificial neural networks and SVM are also considered. Among all the methods, the hybrid methods are found to be better as they provide the beneficiary factors of every method involved. But one should be aware about the algorithm's robustness and accuracy.

## KEYWORDS

Tumor, Segmentation, Automatic, Multimodal Imaging, MRI Images.


https://doi.org/10.17993/3ctecno.2021.specialissue8.279-291

# 1. INTRODUCTION

Tumor arises when the cells of certain portions of our body starts growing abnormally. Detecting tumor in the early stage is of the greatest significance for the survival of life. Also, the size and shape of the brain tumor decides the treatment modality. Over 120 different types of brain tumor are in existence and are possibly graded as primordial and metastatic brain tumor. The primary tumors do not spread to another part of the body and stay within the brain. Statistically, it is found that primary tumor is found to be developed more in older adults and children. The meta-static tumor taints the extant organs of the body from the region of its origination. It is more prevalent in fully – grown people in comparison with offspring.

Based on the characteristics, tumors can be categorized as benignant and virulent. The benignant tumors are leisurely developing and are destructive to a lesser extent. The malignant tumor is rapid growing and life threatening.

The ways and means of dissociating an image into multitudinal portions are said to be segmentation. And it is seen that the pixels within the region have same characteristics. During the preprocessing stage like segmentation separation of different tumor tissues from normal tissues is done. In practical life, segmentation of brain tumor is performed laboriously. But this laborious technique of splitting the tumor yields extended time span and may sometimes create impreciseness in its results. With the intension of doing a favor for medicos in the diagnosis and treatment of tumor the research in automatic segmentation techniques of brain tumor is getting more important.

# 2. MATERIALS AND METHODS

## 2.1. COVENTIONAL SEGMENTATION TECHNIQUES

MRI is a noninvasive diagnosing imaging modality. It affords certain benevolent lineaments like multi – planar capabilities. Separation methodologies are abundant in the assessment surveys. A few among the prevailing conventional tactics for segmenting brain tumor are addressed henceforth.


https://doi.org/10.17993/3ctecno.2021.specialissue8.279-291

### 2.1.1. THRESHOLDING METHOD

Thresholding is one of the segmentation techniques which correlate the brightness of the pixels with the thresholds which may be one or many. The local and global thresholding (Lin *et al.*, 2012) are their prominent categories.

We can distinguish the tumor region from its backdrop by considering the selected threshold and we can utilize this bifurcation for segmentation. The object portion with tumor is allocated the binary value 1 so that those picture elements satisfy the selected threshold value. Others that are insufficient when compared with the threshold value are allocated with the binary value 0 and they are the background pixels (Khan & Ravi, 2013).

If an image possesses homogeneity in its intensity levels, then splitting up with the global thresholding paves a better way. Over segmentation and under segmentation are possible with thresholding means of separation, which may be a major drawback. The global thresholding may cause brighter and darker patches on the grounds of inhomogeneous intensity levels.

### 2.1.2. EDGE – BASED METHOD

Edge based approaches are many in number that includes Canny, Sobel and Prewit. Canny method (1987) is obtained by simply adding up some alteration in the Sobel method. Canny edge detector implements Gaussian in its criteria so that the consequence of noise could be reduced. It indulges enhanced sharp edges in comparison with other methodologies.

In the segmentation of medicating imagery, we have an alternative which is the Chan and Vese Active contour model (2001). We can call it in other words as Active contour model. The interior contours and the undefined boundary objects are competently recognized by this methodology.

The steepness of edge of the image is detected by the snake model, which is a customary edge indicator. The images with inhomogeneous intensity that need the betterment results use this model. Generally, the edge – based segmentation approach is uncomplicated. The edge-based segmentation produces open contour and also the edges are sensitive to the threshold values.


https://doi.org/10.17993/3ctecno.2021.specialissue8.279-291

### 2.1.3. MORPHOLOGICAL BASED METHOD

The process in which the anatomical features of the image are employed is the morphology-based methodology. The utilization of this method is to extract the data from the image centered on their shape presentation. The most basic morphological operations used are erosion and dilatation. They are contrast to each other. It means that the resultant pixels of these processes are least possible and the uttermost values of the total pixels that appears nearby the input picture element. In other words, we can say that, in a binary image, if any pixel is allotted the value 1, then the dilation makes the resultant to be '1' and it is '0' in case of erosion.

The manipulation of the erosion algorithm is for shrinking while dilation is for developing the image size. The morphological based technique has the tendency to segment tumor even in images with lesser intensity. This process incorporates some steps that include image enrichment, generating new samples, extrication of color plane and morphological methodology to get the Region of Interest (RoI) from the image (Sudharania, Sarma, & Prasad, 2016). These are employed in order to eliminate picture elements of reduced frequency and border portions.

### 2.1.4. WATERSHED METHOD

The working of the watershed algorithm is similar to the action of water on the landscape. We know that the partitioned landscape is of separated portions by dams and reservoirs. The water flows from various troughs at a centered region where the dam is present. The flow of water stops at once when the water touches the tip of the landscape. Therefore, every portion of landscape has a dam and resembles the watershed technique. So, an exhaustive silhouette is formed which needs no jointure.

Over – segmentation is the principal drawback of this method. In order to subjugate this confinement, images should be processed both at the pre – stage and the post – stage of segmentation to get satisfactory results. Pandav (2014), in her paper, propose Marker – Controlled Watershed Segmentation which utilize floods and image gradient initiated from the notches instead of localized least for its dissection which brings about superior outcome


https://doi.org/10.17993/3ctecno.2021.specialissue8.279-291

from heterogeneous zones simultaneously. It generates the entire lineament of the segments and hence it needs no jointure which is an added advantage.

#### 2.1.5. K – MEANS CLUSTERING

The clustering technique which is the simplest and the merest mean of segmenting image is the K-means clustering algorithm (Kamble & Rathod, 2015). In this process of clustering, k bands are initialized first and then for each band, we develop a barycenter or centroid in a random manner. The centroid values are changed depending on the values of the neighborhood bands until the stability is reached. The new centroid is assigned in such a way that it is taken from the mean of every object in every barycenter.

#### 2.1.6. MARKOV RANDOM FIELD METHOD

The model which converts the structural data into the procedure of crowding is the Markov random field (MRF) model. In this model, the overhanging of split – up and the impact of noise are diminished. Hence, it is a user – friendly technique in segmenting medical images.

A novel method that utilizes the conjoint spatial features to extricate the configuration with Gabor decomposition, for the fragmentation of tumor from the backdrop is explored in Zhang, Brady, and Smith (2001). After this, the outcomes were additionally purified with this methodology as it categorizes every sub – class of the image. But it is a perplexing procedure. Despite that, it is an effectual method to work with images having inhomogeneous intensity.

### 2.2. ADVANCED SEGMENTATION APPROACHES

There are some advanced methods of segmentation. Some of those advanced techniques are discussed in the following section.

#### 2.2.1. REGION GROWING METHOD

The process which involves the grouping of regions according to the similarity of the pixels until each pixel is allocated to a group is called the Region growing method. We start this operation by electing a seed point. The seed selection is done either automatic or manual. Similar neighbors of the chosen seed are added to the region. We repeat this growing of regions each seed is allocated to a region. The region growing when used along with


https://doi.org/10.17993/3ctecno.2021.specialissue8.279-291

fuzzy logic to get a knowledge – based region growing is always profitable (Lin *et al.*, 2012). Here, different objects are grouped with the geographical data and equivalence from the multimodal images, fuzzy logic and homogeneity of the images are employed in finding out the initial seed.

The region growing methodology on the basis of its image texture is explained in Charutha and Jayashree (2014). We can consider the threshold value of both the intensity and texture for the extraction of brain tumor in medical images. As in every method, it also has its own merits and drawbacks. Its merit is that the similarity of pixels could be easily measured and tracked, while it has a demerit that it is more complex in selecting initial seed point and is susceptible to noise.

### 2.2.2. GENETIC METHOD

The method used for solving both the guarded and unguarded problems for finding optimization and it is a selection process gleaned from the natural transformation (Fan, Jiang, & Evans, 2002). We use chromatins in the genetic algorithm with the purpose of expressing the population. We can rejuvenate the population of individuals repetitiously by the usage of terms like alteration and crossover with a selection operator. The function that is meant for assessing population in the genetic method for the optimization is called fitness function. We use this genetically dependable algorithm for effective optimization of the segmenting portions of MRI images (Chandra & Rao, 2016).

In the methodology described in Chandra and Rao (2016), they used K – means to get the bands for the population at the initial stage. The barycenter or the centroid is estimated by a specific fitness function. The exchange of healthy chromosomes with the weaker ones is done by using crossover and mutation. If the problem is of more difficulty, then the genetic algorithm provides a better solution.

### 2.2.3. FUZZY CLUSTERING

Fuzzy clustering is one of the advanced clustering techniques in which the grouping is mainly based on the membership function (Oliveira & Pedrycz, 2007). The membership function in the fuzzy logic owns a value within the bounds of 0 to 1. This value of the factor shows the homogeneity amongst the picture element and its barycenter. The process of fuzzy


https://doi.org/10.17993/3ctecno.2021.specialissue8.279-291

clustering allots a membership function for each and every picture element determined by its characteristics. The pixel is said to be located near the barycenter if it possesses the value 1. The vicinage fascination with reference to the locale and the pixel's connection to adjacency pixels surge the potential of Fuzzy C Means (Selvakumar, Lakshmi, & Arivoli, 2012).

The extent of the most appropriate value along with the scope of connection between the pixels are established by making use of the combined Genetic algorithm ad Particle Swarm algorithm. Normally, there are two main stages in the system that includes the analysis and evocation. The main disadvantage of the fuzzy based clustering is that the non – usage of geometrical data for segmenting tumors (Ain, Jaffar, & SunChoi, 2014).

### 2.2.4. DEFORMATION MODEL

The deformation model better suits for locally changing environment since it befalls in the variable image object. This model resembles a closed curve in 2D while a closed surface in 3D images. This model is of two major types. They are the parametric deformation where the model is snakes which are the active outliers and the geometric deformation.

A method that uses Chan Vese Active contour model also called as Active contour model is specified in Chan and Vese (2001). It recognizes the innards and the other objects without gradient undefined boundaries. A traditional snake model edge which depends on the gradient value of the image is further improved by Chan Vese model. This model gives better yield for images with similar inhomogeneity.

### 2.2.5. ATLAS METHOD

An atlas is nothing but a reference image that is previously segmented by an expert for the tumor extraction in unobserved images. In the atlas dependable method, we first register both the atlas model and the goal image to be segmented. Then we have to map the model with the target image for effective segmentation. A novel technique without any mesh to design the atlas for well – conditioned brain imagery along with a reformed atlas for a diseased or morbid brain image has been projected in Bauer *et al.* (2010).


https://doi.org/10.17993/3ctecno.2021.specialissue8.279-291

In order to embellish its accuracy, the tumor's locale along with the reason that provokes the tumor growth should be equipped with the atlas. In case of segmentation in multiple regions, (Al-Shaikhli, Yang, & Rosenhahn, 2014) used an adapted multileveled set of articulation with the atlas data of the statistical provost graph. Diaz and Boulanger (2015) used Total Lagrangian Explicit Dynamic (TLED) method to tackle a massive disfiguration devoid of giving up. The atlases for the deformed brain image employ the genuine pattern of the tumor rather than employing erratic pattern (Dia & Boulanger, 2015). The initial seed point need not be initialized in this technique which in turn multiplies the vibrancy. Also, the processing time is diminished because of the parallel processing system. Its performance shows the merit while its demerit is that more time span will be taken for the construction of atlas models.

### 2.2.6. ARTIFICIAL NEURAL NETWORK

The main idea of the artificial neural network (ANN) classifier is machine learning. They are the brain – stimulated systems in such a way that it resembles the same way by which the human beings learn. It comprises various nodes including the insertion node, transitional nodes and the unexposed nodes.

We need to train the machine to determine the worth of the parameter factors. The region of interest (RoI) is systematized by employing the modified probabilistic neural network (PNN) with linear vector quantization (LVQ) modeling process as shown in Song *et al.* (2007). Every RoI is designated with a combo of countenance and a counterweight which are meant for deriving an interconnected structure with reference to LVQ. It also has its own restriction that the size of the network holds the difficulty criteria. It means that the complexity increases with the loftiness in its size, since it requires surplus tutoring.

### 2.2.7. HYBRID METHOD

The best characteristics of different methodologies are combined together to get the hybridized method. Those hybrid methods are faster with greater accuracy. The pulse-coded neural network (PCNN) if enhances, it will improve its reality feature of simulation. The primary firing involves the selection of neurons as its seed points for region growing and the secondary firing grows the region by summing up the seeds with feed forward back


https://doi.org/10.17993/3ctecno.2021.specialissue8.279-291

neural network (FFBNN). The feed forward process is done to reach the uniformity in its input. Stationary wavelet transform (SWT) is exercised for getting the sub images with the data of multiple resolutions (Ortiz *et al.*, 2013).

Spatial filtering along with LVQ is done with the purpose of extracting numerical features and regulating of the resultant image. Here, the segmentation is performed with Content – Based active contour model (Sachdeva *et al.*, 2012). Genetic Algorithm helps in reducing parameters with higher dimensions. While comparing the hybrid process of GA and SVM with GA and ANN, the prior is good in speed while the latter is better in its accuracy. The hybrid method slips in the step that it possesses higher computative expenses.

## 3. DISCUSSION

Segmentation methods are becoming more growing day by day and gaining importance in clinical research. In spite of the numerous contradictions in the process of segmentation over MRI imagery, they are blooming nowadays. One such contradiction is the need of transpicuousness. Another question is about its accountability to understand the need. Some other conflicts include laboring antiquity and movement antiquity. The impact of sectional measure and the inhomogeneous intensity are also the pervasive problems in the splitting up of the brain tumor. The deviation in its structure such as shape, size and the locale of tumor also affects segmentation results. The value of Signal to Noise Ratio should be low so that the resolution will be elevated. So, the relics must be eliminated by using the appliances with higher resolution and worthier filtrating which causes no loss in its anatomy. The tumor has its impact not only in the affected area but also the surrounding portions. This shows the fact that the segmentation of every affected region is necessary. Hence, further awareness should be paid on the robustness and accurateness of the algorithm. The algorithm's effectiveness can be validated by utilizing ground truth images.

## REFERENCES

**Ain, Q., Jaffar, A., & SunChoi, T.** (2014). Fuzzy anisotropic diffusion based segmentation and texture based ensemble classification of brain tumor. *Applied Soft Computing, 21*, 330–340. https://doi.org/10.1016/j.asoc.2014.03.019


https://doi.org/10.17993/3ctecno.2021.specialissue8.279-291

**Al-Shaikhli, S., Yang, M., & Rosenhahn, B.** (2014). Multi region labelling and segmentation using a graph topology prior and atlas information in brain images. *Computerized Medical Imaging And Graphics, 38*(8), 725–734. https://doi.org/10.1016/j.compmedimag.2014.06.008

**Bauer, S., Seiler, C., Bardyn, T., Buechler, P., & Reyes, M.** (2010). Atlas-based segmentation of brain tumor images using a Markov Random Field-based tumor growth model and non-rigid registration. In *Annual International Conference of the IEEE Engineering in Medicine and Biology,* 4080-4083. https://doi.org/10.1109/IEMBS.2010.5627302

**Canny, J.** (1987). A computational approach to edge detection. *Readings In Computer Vision,* 184-203. https://doi.org/10.1109/TPAMI.1986.4767851

**Chan, T. F., & Vese, L. A.** (2001). Active contours without edges. *IEEE Transactions On Image Processing, 10*(2), 266-277. https://doi.org/10.1109/83.902291

**Chandra, R., & Rao, K. R. H.** (2016). Tumor detection in brain using genetic algorithm. *Procedia Computer Science, 79,* 449-457. https://doi.org/10.1016/j.procs.2016.03.058

**Charutha, S., & Jayashree, M. J.** (2014). An efficient brain tumor detection by integrating modified texture based region growing and cellular automata edge detection. *International Conference On Control, Instrumentation, Communication And Computational Technologies (ICCICCT),* 1193-1199. https://doi.org/10.1109/iccicct.2014.6993142

**Diaz, I., & Boulanger, P.** (2015). Atlas to patient registration with brain tumor based on a mesh – free method. In 37th *Annual International Conference Of The IEEE Engineering In Medicine And Biological Society,* 2924-2927. https://doi.org/10.1109/EMBC.2015.7319004

**Fan, Y., Jiang, T., & Evans, D. J.** (2002). Volumetric segmentation of brain images using parallel genetic algorithms. *IEEE Transactions On Medical Imaging, 21*(8), 904-909. https://doi.org/10.1109/TMI.2002.803126

**Kamble, S. T., & Rathod, M. R.** (2015). Brain tumor segmentation using k-means clustering algorithm. *International Journal of Current Engineering and Technology, 5*(3),

1521–1524. https://inpressco.com/brain-tumor-segmentation-using-k-means-clustering-algorithm/

**Khan, A. M., & Ravi, S.** (2013). Image segmentation methods: a comparative study. *International Journal Of Soft Computing And Engineering (IJSCE), 3*(4). D1760093413/2013©BEIESP

**Lin, G. C., Wang, W. J., Kang, C. C., & Wang, C. M.** (2012). Multispectral MR images segmentation based on fuzzy knowledge and modified seeded region growing. *Magnetic Resonance Imaging, 30*(2), 230–246. https://doi.org/10.1016/j.mri.2011.09.008

**Oliveira, J. V. D., & Pedrycz, W.** (2007). *Advances in fuzzy clustering and its applications.* John Wiley And Sons Ltd.

**Ortiz, A., Górriz, J. M., Ramírez, J., Salas-Gonzalez, D., & Llamas-Elvira, J. M.** (2013). Two fully – unsupervised methods for mr brain image segmentation using som based strategies. *Applied Soft Computing, 13*(5), 2668-2682. https://doi.org/10.1016/j.asoc.2012.11.020

**Pandav, S.** (2014). Brain tumor extraction using marker controlled watershed segmentation. *International Journal Of Engineering Research & Technology (IJERT), 3*(6), 2020-2022. https://www.ijert.org/brain-tumor-extraction-using-marker-controlled-watershed-segmentation

**Sachdeva, J., Kumar, V., Gupta, I., Khandelwal, N., & Ahuja, C. K.** (2012). A novel content based active contour model for brain tumor segmentation. *Magnetic Resonance Imaging, 30*(5), 694-715. https://doi.org/10.1016/j.mri.2012.01.006

**Selvakumar, J., Lakshmi, A., & Arivoli, T.** (2012). Brain tumor segmentation and its area calculation in brain mr images using k-mean clustering and fuzzy c-mean algorithm. *IEEE-International Conference On Advances In Engineering, Science And Management*, 186-190. Corpus ID: 9928458

**Song, T., Jamshidi, M. M., Lee, R. R., & Huang, M.** (2007). A modified probabilistic neural network for partial volume segmentation in brain mr image. *IEEE Transactions On Neural Networks, 18*(5), 1424-1432. https://doi.org/10.1109/TNN.2007.891635

**Sudharania, K., Sarma, T. C., & Prasad, K. S.** (2016). Advanced morphological technique for automatic brain tumor detection and evaluation of statistical parameters. *Procedia Technology, 24,* 1374–1387. https://doi.org/10.1016/j.protcy.2016.05.153

**Zhang, Y., Brady, M., & Smith, S.** (2001). Segmentation of brain mr images through a hidden markov random field model and the expectation-maximization algorithm. *IEEE Transactions On Medical Imaging, 20*(1), 45-57. https://doi.org/10.1109/42.906424

/18/


https://doi.org/10.17993/3ctecno.2021.specialissue8

# INTELLIGENT TRANSPORTATION SYSTEM OF SOLAR POWERED HYBRID ELECTRIC VEHICLES USING PATTERN MATCHING TECHNIQUES IN LABVIEW ENVIRONMENT

**M. Pallikonda Rajasekaran**
Professor, Dept. of ECE, Kalasalingam Academy of Research and Education, Anand Nagar, Krishnankoil, (India).
E-mail: mpraja80@gmail.com
ORCID: https://orcid.org/0000-0001-6942-4512

**N. Pothirasan**
Research Scholar, Dept. of ECE, Kalasalingam Academy of Research and Education, Anand Nagar, Krishnankoil, (India).
E-mail: gofire9988@gmail.com
ORCID: https://orcid.org/0000-0002-1254-0421

**V. Muneeswaran**
Assistant Professor, Dept. of ECE, Kalasalingam Academy of Research and Education, Anand Nagar, Krishnankoil, (India).
E-mail: munees.klu@gmail.com
ORCID: https://orcid.org/0000-0001-8061-8529

**Recepción:** 11/11/2019 **Aceptación:** 08/01/2021 **Publicación:** 30/11/2021

**Citación sugerida:**
Rajasekaran, M. P., Pothirasan, N., y Muneeswaran, V. (2021). Intelligent transportation system of solar powered hybrid electric vehicles using pattern matching techniques in labview environment. *3C Tecnología. Glosas de innovación aplicadas a la pyme, Edición Especial,* (noviembre, 2021), 293-311. https://doi.org/10.17993/3ctecno.2021.specialissue8.293-311

## ABSTRACT

While people driving a vehicle due to the distraction of drivers many persons suffer in accidents. The main reason behind these accidents is breaking the rules and not concentrates on the road signals. The main objective of this work is to build an IoT enabled intelligent transportation system. In this paper presented by utilizing a function there we make some links between the car and the signals present on the roads. The proposed system identifies the road sign with 98% accuracy. By doing this we can minimize the accident that will happen. Additionally, by defining MPPT control algorithm we can control the BLDC motor inside the E-vehicle to consume less amount of power. And, by using color detection algorithm and shape algorithm, we can capture the road signal and we will save ourselves from accidents. In calculating the census of the death rate in 2017, we came to know that most of the people die in road accidents. They suffered to a condition that they cannot be able to lead their daily lives like normal persons. This work improvises the current infrastructure of autonomous vehicle and removes the hurdles that people facing by imparting automated algorithms.

## KEYWORDS

Computer Vision, Road Vehicles, Transportation, Artificial Vision, Intelligent Transportation Systems, Lane Detection, Obstacle Detection.


https://doi.org/10.17993/3ctecno.2021.specialissue8.293-311

# 1. INTRODUCTION

By the survey of 2017, we came to know that most of the people died in the road accidents. These types of accidents make them have heavier wounds and lost their organs and even lead to death. People travel faster in road-side and are not just thinking about the effects of the accidents and spoil their whole future and people are not following the rules and drivers are not concentrating on the signals, these could made them lead to accidents. And, on the other-side, we noticed that because of using vehicles that run-in petrol and diesel, air pollution will happen and it creates pollution the environment. And people will suffer because of inhaling these polluted gases. While we are travelling in car, we could not easily identify the signals in the road-side. So, because of this, many accidents will happen and the people cannot be able to drive their own cars and they fixed their own cars and they fixed a driver to drive it.

Now-a-days, the cost of fuel is very high and there is no possible in using the cars which run in petrol/diesel. So, we can use E-vehicle instead of using fuel cars. By using E-vehicle, we can avoid the supply of the external battery. E-vehicles are good because we can avoid pollution by utilizing it. And, we can avoid the diseases caused by the environmental pollution. We can have a safe and simple journey in E-vehicle. By using vehicle, we must not spot on car repairs and damages because it was made by using small electronic devices. E-vehicle made our driving safe and secured. E-vehicle can be used by any person of old-age people, children and also by differently-abled people. Because it was designed with that much comfort ability. The amount of breakdown happens in E-vehicle is very low. It is designed as there we can take external sources like battery-operator, light and horns from the E-vehicle.

# 2. RELATED WORKS

This section gives a detailed description about the few notable works in the field of power electronics and hybrid vehicle design. The usage of computer vision is greatly emphasized by Bertozzi *et al.* (2002). Bertozzi *et al.* (2002) detected the application of pattern detection is being used in vital transport applications such as the detection of lanes, monitoring the mobility, etc. In his work, Emadi, Lee, and Rajashekara (2008), provided a brief review on


https://doi.org/10.17993/3ctecno.2021.specialissue8.293-311

the working characteristics of the circuit system and the involvement of power electronics systems in the construction of alternative vehicles. This conceptual analysis is helpful for analysing the effects of intrinsic behaviour of the lithium-ion batteries. The authors analysed the importance of parameters including the losses in the feeder, variance in load and the load factor for a PHEV charging in coordinated system.

Based the relativeness of the above three parameters a charging algorithm which in-turn will reduce the unwanted charging behaviour in connected system of PHEV's was developed. The importance of image processing was discussed in very recent works (Li *et al.*, 2019; Muneeswaran & Rajasekaran, 2019). Pothirasan et.al. described the logical way interaction of Electric vehicles with the roadside signals through an efficient V-V and V-I communication interfaces (Pothirasan & Rajasekaran, 2016, 2019). The usage of IoT in real time environment is depicted in Ramakala *et al.* (2017). Hadley and Tsvetkova (2009) described the statistical analysis of the market demand of PHEV as it provides alternative to the fuel system. Sun, Bebis, and Miller (2006) introduced an intelligent vehicular system by adding a pattern recognition technique that aids in detection of nearby vehicles and their speed range in iterative manner. Based on the knowledge gathered from these works the authors attempt to construct an intelligent transportation system with the support of LabVIEW environment.

## 3. BLOCK DIAGRAM OF INTELLIGENT TRANSPORTATION SYSTEM

We can run the BLDC Motor through the three phase inverter by means of converting DC (lead acid) into AC source. There are three methods available to charge the battery. 1. Solar Panel, 2. Regenerative braking system, 3. Using Grid. The power gained from solar panel and the power stored in the battery is given as input through MPPT Technique. Three phase inverter is working in double direction and the boost converter working in single phase. The overall block diagram of the proposed prototype explains the whole process.


https://doi.org/10.17993/3ctecno.2021.specialissue8.293-311

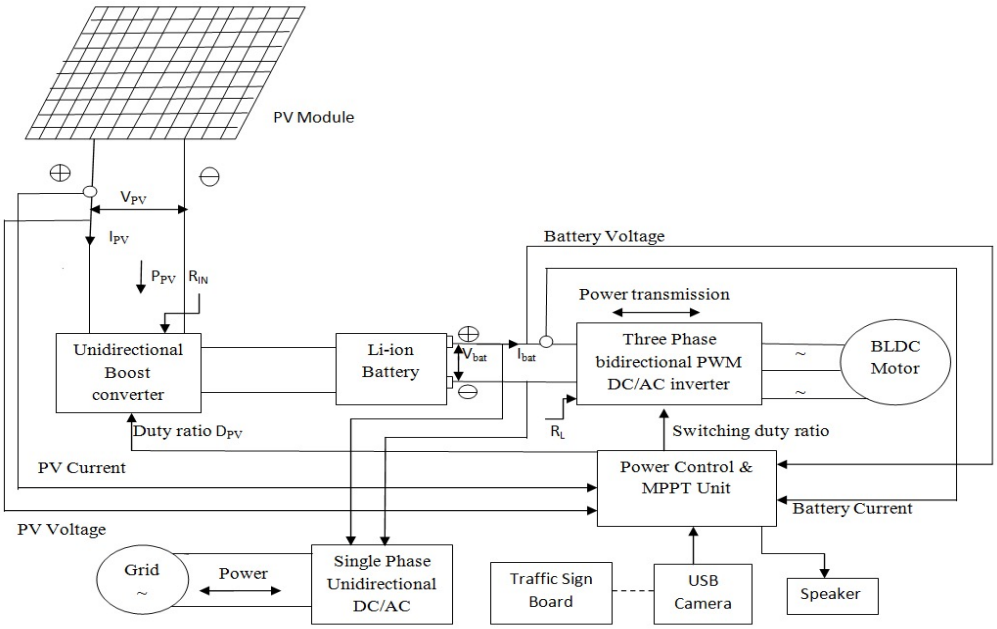


**Figure 1.** Block Diagram of Intelligent Transportation System.
**Source:** own elaboration.

The road side sign boards and traffic signals are captured by means of a camera fixed in the vehicles and it is displayed in the monitor to create awareness to the user. When the user failed to control the vehicle manually, the controller system itself will automatically control the vehicle after some period.

# 4. MATERIALS AND METHODS

## 4.1. WORKING PRINCIPLE OF SOLAR PANEL

There is an increment of shortage of electricity. It we use solar energy by all houses we can reduce the scarcity of electricity. The working of solar panel (photon) or particles of light to knock electrons force from atoms. By using this solar panel can generate power. The combination of two or more solar cells is Calles solar panel. In photo voltaic cell two silicones of semi-conducting material, usually by using silicon they using in microelectronics.

Generating current from photo voltaic cell is more required. Much like that magnetic field which occurs in conductors due to opposite poles of an electric occurs when opposite


https://doi.org/10.17993/3ctecno.2021.specialissue8.293-311

charges are separated. To get this field manufactures "dopc" silicon with other materials giving each silicon of sandwich positive or negative electrical charge. They include in to layer of silicon seed phosphorus and add extra electrons to negative charge layer. In the bottom layer boron and least amount of electrons are included to the positive charge. When sunlight's fall on photon the electron force is pushed through the electric field and electrons released through junction. The other components of the cell turn these electrons on couple to make usable power and gives to us. On the side of the cell a metal conductive plate was fixed and electrons are getting and sent through wires.

The electron flow that is taken from the point is called as sources of electricity. Recent researches told that while the manufacturing of ultrathin flexible solar cells 1.3 microns thicked 1/100th it is width of human hair, and having 20 times lesser amount of office sheet paper solar panel will made. In fact, the cells are so light that they can sit on top of a soup bubble and yet they produce energy with about as much efficiency as glass based solar cells. By using this kind of flexible solar cell, we can use it as aerospace technology or in wearable electronic. By using many types of solar panel solar power technology was presented.

Solar Thermal and concentrated solar power [CSP] were designed, with different fashion than photo voltaic solar panel. The energy produced from solar panel is generated through sunlight, heat water and air. In sunlight there is a natural nuclear reactor. The tiny particles released from these are called photons. The photons we are getting 93 million miles away from the sun and it reaches earth in 8.3 minutes. Currently, Photovoltaic power is lesser amount consumed in India solar energy is increasing and cost is dropping rapidly. On coming years, solar energy becomes the required energy to lead a normal life.

## 4.2. BOOST CONVERTER DESIGN

A Boost converter is a DC-DC power converter. It is a step-up voltage from its solar panel to battery. Diode and transistor acts as semiconductor devices in the boost conductor. On the other hand, capacitor and inductor acts as energy storage element and kept as two in combination. To reduce the voltage ripple inside and outside DC, A filter made of DC is fixed. Batteries, solar panels, rectifiers and DC generator are kept as the source of boost converter. In boost converter battery voltage is greater than solar panel voltage and in case of current battery current is lower than the source current. Since (P=VI) must be conserved.


https://doi.org/10.17993/3ctecno.2021.specialissue8.293-311

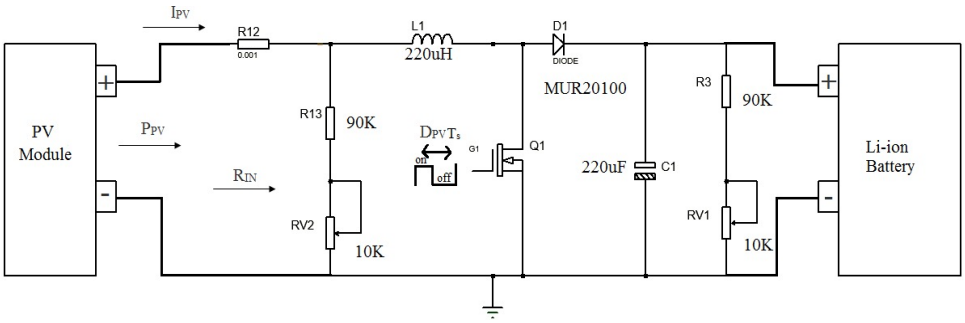


**Figure 2.** Boost Converter Design.
**Source:** own elaboration.

## 4.3. CALCULATING THE DUTY CYCLE

$$D = 1 - \left[\frac{V_{IN(min)} * \eta}{V_{OUT}}\right]$$

Where D = Duty Cycle

$V_{IN\,(min)}$ = minimum input voltage (this will lead to the maximum switch current)

$V_{OUT}$ = desired output voltage

## 4.4. CHOOSING THE INDUCTOR

$$\mathrm{L} = \frac{\mathrm{V_{IN}} * (\mathrm{V_{OUT}} - \mathrm{V_{IN}})}{\Delta \mathrm{I_L} * \mathrm{f_s} * \mathrm{V_{OUT}}}$$

Where L = Inductance in Henry

$V_{IN}$ = Typical input voltage, here, 0.9V

$f_s$= minimum switching frequency of the converter. here, 960 kHz (from datasheet)

$\Delta I_L$= estimated inductor ripple current as discussed


https://doi.org/10.17993/3ctecno.2021.specialissue8.293-311

## 4.5. OUTPUT CAPACITOR SELECTION

$$C_{OUT(min)} = \frac{I_{OUT(max)} * D}{f_s * \Delta V_{OUT}}$$

$C_{OUT\,(min)}$ = minimum output capacitance needed

$I_{OUT\,(max)}$ = maximum output current of the desired application

$D$ = Duty Cycle of the converter

$f_s$ = minimum switching frequency of the converter,960kHz

$\Delta V_{OUT}$ = desired output voltage ripple. here, 10mV

$\Delta V_{OUT\,(ESR)}$ =ESR*$I_{SW(max)}$

Where, $\Delta V_{OUT\,(ESR)}$ = additional output voltage ripple due to ESR.

## 4.6. BRUSHLESS DC MOTOR

The traditional DC motor has a mechanical commutated. A commutates is a suitable (mechanical or electrical) used to change the path of the current through two or more routes or (current through the windings) but BLDC motor seeks an external computation. This is realized by six IGBT power semiconductor switches to rout the path of the current through three winding in 6 directions.

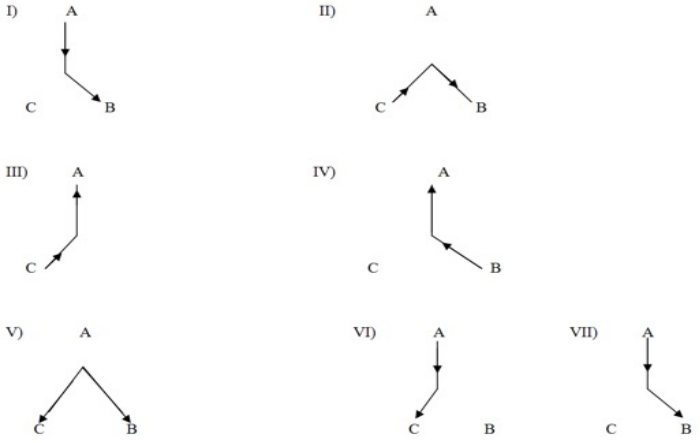


**Figure 3.** Winding Directions.
**Source:** own elaboration.


https://doi.org/10.17993/3ctecno.2021.specialissue8.293-311

In Figure 3, Figures I and VII are one and the same. Figure VII is the start of the second cycle and Figure 1 is the start of the first cycle. To change this sequence path of current (stator called as commutation). 6 IGBT switches are sequentially fixed in synchronization with the position of the poles of the permanent magnet of the rotor. The BLDC motor has a smaller size (lighter) in comparison with traditional DC motor because of the absence of the mechanical commutator and the electromagnetic (temporary magnets) field windings. Now a day's BLDC motor used in the domestic ceiling Fans.

## 4.7. BATTERY CHARGING STATUS IDENTIFICATION

In this project lead-acid batteries are used. The lead-acid battery consists of a small metal by which we can store the power through chemical reactions. Four numbers of 12V, 100 Ampere hour lead acid batteries connected in series (12V x 4=48V). BLDC main motor has the voltage rating of 48V so, four numbers of 12V batteries are used. The capacitor of this motor is chosen as 750Watts that is 15A at fuel rated load. If the efficiency of battery is considered as 80% than 100Ah x 0.8=80Ah. The duration of travel at fuel load will be 1.4 hours of fuel load. In this process positively charged particles are called as ion and negatively charged particles are called as electrons. In both cases of charging and discharging electrons flow in the opposite direction to the ions. The lab view software is used to identify the range of charging and discharging process of the battery. This can be monitored in a tablet computer is operated by 5V Power supply which is another buck converter is to be used. This tablet will have 5000mAh [5Ah] battery. This can be charged by 1A current rating at 5 Level. During charging process of any battery, that battery must be charged slowly (8 Hours) as per the charging time duration given by the supplier.

## 4.8. CONSTRUCTION OF E-VEHICLE CONTROLLER DESIGN

The myRIO controller plays a vital role in PHEV design. To safeguard the myRIO controller from reverse power effect, a driver board (IR2110) is designed. Driver boards are mostly used in the regulation of current flowing through a circuit or controls other factors such as the other devices or components in the circuit. The IR2110 Driver board is used to protect the myRIO (low power) from the High power IGBT circuit. This IR2110 also separates the gate signals of the upper IGBT from the lower IGBT signals, since the


https://doi.org/10.17993/3ctecno.2021.specialissue8.293-311

upper IGBT needs separate grounding for its gate signal with respectively emitter terminal. With the help of Hall Effect sensor, using myRIO controller we can identify the position of motor. Also running process of motor live forward/Reverse/Brake can be controlled by means of embedded "c" programming. It also consists of manual speed control device. To run BLDC motor, a three phase inverter and a power circuit can be used. It is explained in terms of graphical diagram in given above Figure 4.

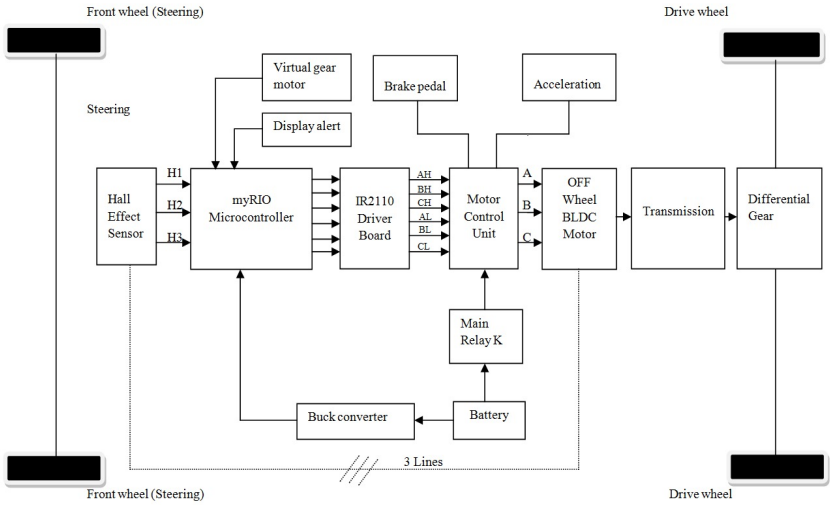


**Figure 4.** PHEV Design.
**Source:** own elaboration.

## 5. CONSTRUCTIONAL DETAILS OF SOLAR POWERED E-VEHICLE

To bring the traffic sign board signals to vehicle vision sensor is required. Also are wanted to come across image pre-processing. Board captured by vision sensor are all not in a same quantity. In image pre-processing the original image brightness, contrast, pixel of image and set in constant quantity. By using LabVIEW icons like geometry, lookup table we can set. Using geometry icon IV, we can propose of Re sampling technique. Also, by using lookup table we can make pixel intensity to good quality. Because of this image can be set in same quality and same quantity. There are four major works in intelligent transportation system of PHEV they are Detection, Recognition, BLDC motor controlling and voice output. Here we proposed is, by using old method of classification we detect the traffic sign board. After the recognition process, we started controlling the BLDC motor. For the unidentified


https://doi.org/10.17993/3ctecno.2021.specialissue8.293-311

things we used voice output. In our intelligent transportation system, the processes we proposed are follows:

1. Traffic sign board of Detection, Extraction, Recognition.
2. To recognition of some Traffic sign board to control the BLDC motor.
3. Traffic sign board of to deliver the voice output.

In the case, if it not been identified it makes human to deliver the voice output. In my paper to recognize the traffic sign board, I have used two techniques, one is deep learning of the sample pattern and the other is object pattern and I approached two process one is OCR (Object Character Recognition) and other is geometric pattern matching. The modifying Hough transform of circular by doing detection process. Shape detection plays important role in detecting the sign boards. We can filter the unwanted substance came inside by utilizing colour thresholding. We, detect the sign board s are in circular and triangular shape and in red, black and white in colour of background. So, this detection process is classified into shape detection, colour thresholding detection.

## 5.1. SHAPE DETECTION

By utilizing shape detection algorithm, we can detect the circular board. In sign board the circular diameter is 15cm-30 cm measure and it was designed by range. But some sign boards are not detected. So, it unfortunately stopped the detection process so the undetected sign board are detected by using colour thresholding technique triangular sign boards are by geometric algorithm matched by changed into template create by detected. This colour thresholding design set at a local range. This range reference is done by online image. Segment was settled according to only red outline was designed. By using filter, we make better quality of segmentation and equalized. After colour thresholding by shape detection we detected to triangular shape board we applied thresholding we attained segmentation segmented boards triangular shape was by geometric algorithm. we template created and matched and finally detected.

## 5.2. EXTRACTION OF SIGN BOARDS

We set co-ordinate the detected sign board and extract sign board from over all image and using detected boards mask location was settled and extracted.


https://doi.org/10.17993/3ctecno.2021.specialissue8.293-311

### 5.3. RECOGNITION OF SIGN BOARDS

Inside the extracted sign boards to recognize the information three types are utilized.

1. Threshold segmentation.
2. Canny edge filtering.
3. Geometric algorithm.

Using a local threshold algorithm called NI back threshold and using dark object technique are done segment. Dark object range is locally set by the NI block algorithm. By Canny edge filtering the applied NI block image edges are filtered and equalization is by edge based geometric algorithm template created and by matching the edges we can recognize.

## 6. CONSTRUCTION OF INTELLIGENT TRANSPORTATION SYSTEM AND HARDWARE EXPERIMENTAL VERIFICATIONS:

In the proposed PHEV vehicle, we can charge the battery, using the variable voltage and current obtained from the solar panels with the help of boost converter. By converting a three phase inverter, we can run the BLDC motor. MPPT control algorithm can be used for closed loop control system. It consists of input 48V, 26Ah battery, solar panel and camera. The purpose of the camera is to capture the roadside signals. The proposed intelligent transportation system of PHEV is considered a battery bank of 48V; 100A/h and the solar panel of 150W are taken place.

Power revealed from the solar panel changes according to level of sunlight passes on it. The variable current and variable voltage derived from the PV module and the same derivation from variable battery voltage and variable battery current both given as an input for power control & MPPT control. By doing this, we can adjust the PWM duty ratio and we will receive a constant voltage and constant current. To charge 100Ah lead acid battery we need maximum 10 hours. But for charging we require 10Ampere per hour. (10Ampere x 10hour = 100Ah).

If the current receiving by the battery exceeds 10Ampere the battery get blast or its size become enlarged. Also, if the battery gets fully charged it was denoted in the LCD display. In some case, if we do identify it buzzers every 30 minutes. For this identification a program


https://doi.org/10.17993/3ctecno.2021.specialissue8.293-311

is set. By these proper handling methods, we can increase the battery's life. In PHEV, myRIO controller has a unique position. PWM ratio revealed from the myRIO Controller with the help of MPPT controller it provides constant current and constant voltage to the battery. By this activity, battery will charge in the efficient manner.

To measure the voltage, drop in the solar panel and boost converter a potential divider circuit is used. By utilizing this, a loop voltage is sent as an analog input for myRIO converter. In other hand, to measure the current shunt present inside the solar panel and boost converter 1NA168 integrated circuit is used. By utilizing this current is send as closed loop for the myRIO controller. By giving voltage loop and current loop as input we can receive a constant voltage & constant current. By processing this we can perfectly charge the battery. By presenting battery power as an input to the three phase inverter we can run the BLDC motor. Information in traffic sign board changes into the way inside PHEV vehicle is called as vehicle to infrastructure. By using of myRIO controller keeping Vision mission inside the NI labview and using the process of image acquisition we can identify the traffic sign board and the information inside this can be captured by camera.

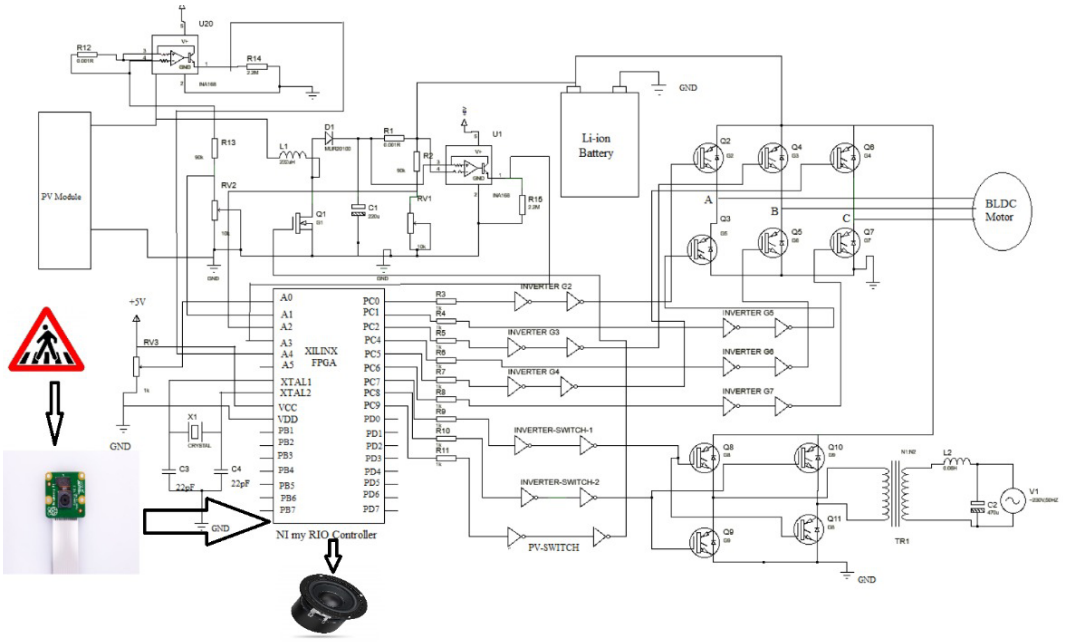


**Figure 5.** Integration of PHEV Design and V2R Communication.
**Source:** own elaboration.


https://doi.org/10.17993/3ctecno.2021.specialissue8.293-311

Lastly in PHEV by utilizing display and motor control we can prevent from accidents because of using LabVIEW software image acquisition process is held rapidly. Information denoted on traffic sign board gives a voice alert inside the warning. A buzzer strikes loudly. If he/she drives by not knowing this BLDC motor would be control automatically. By displaying road signals on the laptop and driver can easily identify the signals. To bring the traffic board signals to vehicle vision mission is required. This type of intelligent PHEV vehicle and designed of using this only on smart cities.

## 7. RESULTS

The front panel design for effective recognition of road sign is implemented using LabVIEW. It recognizes the character earlier and the time taken is also reduced and it is shown in Table 1.

**Table 1.** Time taken for Sign Board Recognition.

| S.No | Pattern | Time taken (in Secs) |
|---|---|---|
| 1 | Road Sign for One way | 2.031 |
| 2 | Road Sign for 20 Km | 1.033 |
| 3 | Road Sign for U turn | 2.421 |
| 4 | Road Sign for Speed Braker | 2.228 |

**Source:** own elaboration.


https://doi.org/10.17993/3ctecno.2021.specialissue8.293-311

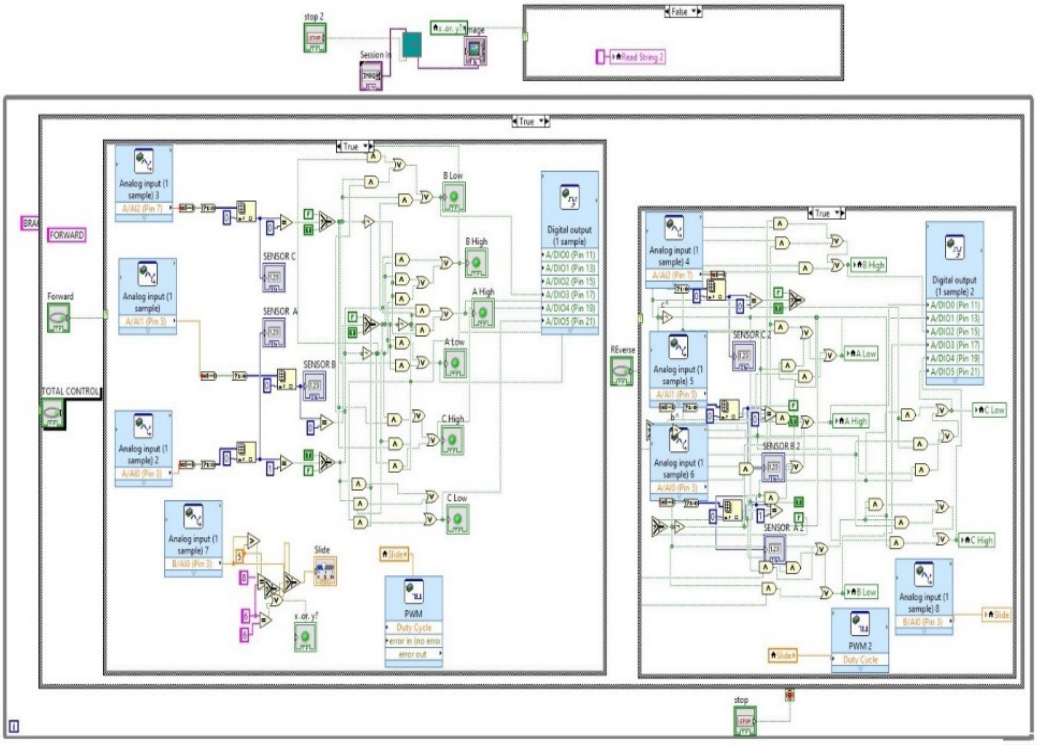


**Figure 6**. Simulation experiment done in LabVIEW Environment (Block Diagram).
**Source:** own elaboration.

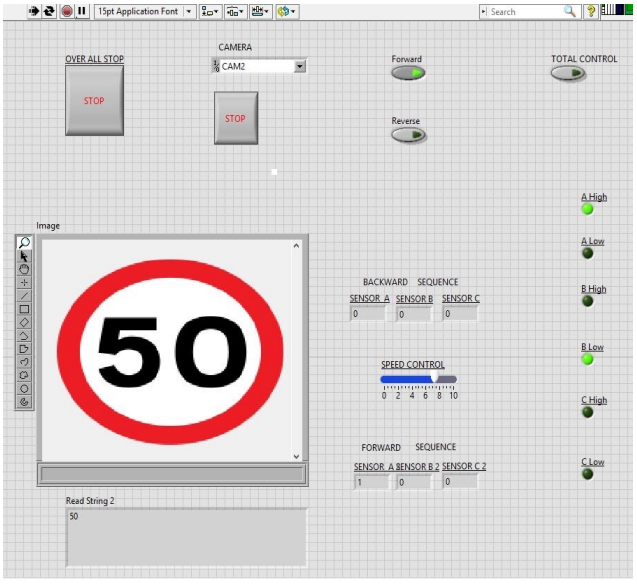


**Figure 7.** Simulation experiment done in LabVIEW Environment (Front Panel).
**Source:** own elaboration.


https://doi.org/10.17993/3ctecno.2021.specialissue8.293-311

## 8. CONCLUSIONS

In this paper, a brief solution to a rising societal problem in designing intelligent transportation system was discussed. The proposed recognition system efficiently recognizes the road sign accurately with the help of thresholding and edge detection algorithm. The defined comprehensive and integrated system approach, referred to as intelligent transportation systems (ITS), links the vehicle, the infrastructure, and the driver to make it possible to achieve more mobile and safer traffic conditions by using state-of-the-art electronic communication and computer-controlled technology. This work will be helpful for automated vehicular transportation. The future work of this system includes building automated decision making based on the detected and recognized sign boards.

## ACKNOWLEDGEMENT

The authors thank the Department of ECE, Kalasalingam Academy of Research and Education, for permitting them to use the computational facilities available in the Centre for Research in Signal Processing and VLSI Design which was established with the support of the Department of Science and Technology (DST), New Delhi under FIST Program in 2013 (Reference No: SR/FST/ETI-336/2013 dated November 2013).

## REFERENCES

**Bertozzi, M., Broggi, A., Cellario, M., Fascioli, A., Lombardi, P., & Porta, M.** (2002). Artificial vision in road vehicles. *Proceedings of the IEEE, 90*(7), 1258-1271. https://ieeexplore.ieee.org/document/1032807

**Emadi, A., Lee, Y. J., & Rajashekara, K.** (2008). Power electronics and motor drives in electric, hybrid electric, and plug-in hybrid electric vehicles. *IEEE Transactions on industrial electronics, 55*(6), 2237-2245. https://ieeexplore.ieee.org/document/4493430

**Hadley, S. W., & Tsvetkova, A. A.** (2009). Potential impacts of plug-in hybrid electric vehicles on regional power generation. *The Electricity Journal, 22*(10), 56-68. https://doi.org/10.1016/j.tej.2009.10.011

**Li, L., Muneeswaran, V., Ramkumar, S., Emayavaramban, G., & Gonzalez, G. R.** (2019). Metaheuristic FIR filter with game theory based compression technique-A reliable medical image compression technique for online applications. *Pattern Recognition Letters, 125*, 7-12. https://doi.org/10.1016/j.patrec.2019.03.023

**Muneeswaran, V., & Rajasekaran, M. P.** (2019). Automatic segmentation of gallbladder using intuitionistic fuzzy based active contour model. In *Microelectronics, Electromagnetics and Telecommunications* (pp. 651-658). Springer, Singapore.

**Muneeswaran, V., & Rajasekaran, M. P.** (2019). Local contrast regularized contrast limited adaptive histogram equalization using tree seed algorithm—an aid for mammogram images enhancement. In *Smart intelligent computing and applications* (pp. 693-701). Springer, Singapore.

**Pothirasan, N., & Rajasekaran, M. P.** (2016). Automatic vehicle to vehicle communication and vehicle to infrastructure communication using NRF24L01 module. In *2016 International Conference on Control, Instrumentation, Communication and Computational Technologies (ICCICCT)* (pp. 400-405). IEEE.

**Pothirasan, N., & Rajasekaran, M. P.** (2019). Retrofitting of Sensors in BLDC Motor Based e-Vehicle—A Step Towards Intelligent Transportation System. In *Smart Intelligent Computing and Applications* (pp. 61-69). Springer, Singapore.

**Pothirasan, N., Rajasekaran, M. P., & Muneeswaran, V.** (2018). Real time reactive power compensation for battery/photovoltaic hybrid power source for internet of hybrid electric vehicle system. *Cognitive Systems Research, 52*, 473-488. https://doi.org/10.1016/j.cogsys.2018.07.030

**Ramakala, R., Thayammal, S., Ramprakash, A., & Muneeswaran, V.** (2017). Impact of ICT and IOT Strategies for Water Sustainability: A Case study in Rajapalayam-India. In *2017 IEEE International Conference on Computational Intelligence and Computing Research (ICCIC)* (pp. 1-4). IEEE.

**Sun, Z., Bebis, G., & Miller, R.** (2006). On-road vehicle detection: A review. *IEEE transactions on pattern analysis and machine intelligence, 28*(5), 694-711. https://ieeexplore.ieee.org/document/1608034


https://doi.org/10.17993/3ctecno.2021.specialissue8.293-311

https://doi.org/10.17993/3ctecno.2021.specialissue8.293-311

/19/


https://doi.org/10.17993/3ctecno.2021.specialissue8

# THERMAL AND CONGESTION AWARE ALGORITHM FOR 3D INTEGRATED CIRCUITS

**Pandiaraj Kadarkarai**
Department of ECE, Kalasalingam Academy of Research and Education, Tamil Nadu, (India).
E-mail: pandiaraj@klu.ac.in
ORCID: https://orcid.org/0000-0001-9610-2172

**Sivakumar Pothiraj**
Department of ECE, Kalasalingam Academy of Research and Education, Tamil Nadu, (India).
E-mail: siva@klu.ac.in
ORCID: https://orcid.org/0000-0003-1328-8093

**Recepción:** 11/11/2019 **Aceptación:** 05/03/2021 **Publicación:** 30/11/2021

**Citación sugerida:**
Kadarkarai, P., y Pothiraj, S. (2021). Thermal and congestion aware algorithm for 3D integrated circuits. *3C Tecnología. Glosas de innovación aplicadas a la pyme, Edición Especial*, (noviembre, 2021), 313-331. https://doi.org/10.17993/3ctecno.2021.specialissue8.313-331

## ABSTRACT

In VLSI physical Design methodology, Routing has been a most important in VLSI design, because the routing results are like circuit delay, power consumption, chip responsibility and manufacturability etc. With the advancements in 3D ICs, this issue has turned out to be substantially more complex. With the size of present-day plans at a huge number of nets, global routing has turned into a noteworthy computational test. The main purpose of the global routing is to reduce the wire length. In this work, a thermal and congestion aware formula is projected to attenuate the mixture wire length and to beat the congestion by systematically diffusive the nets within the routing region. The investigational output of the planned global router utilizes less wirelength and keeps far from congestion by ripping up and re-routing the nets. In future planned to use machine learning algorithm to reduce temperature between the layers in an integrated circuit.

## KEYWORDS

Global Routing, NP completeness, 3D ICs, Wire Length Minimization, Congestion.


https://doi.org/10.17993/3ctecno.2021.specialissue8.313-331

# 1. INTRODUCTION

VLSI physical outline is the way toward deciding the physical area of dynamic gadgets and interconnecting them inside the limit of a VLSI chip. Physical configuration of a circuit is the stage that goes before the manufacture of a circuit. For the most part, it alludes to all union strides succeeding rationale plan and going before manufacture. The physical outline systems intend to create designs with a little region, high flag respectability, diminished postponement, decreased force utilization and higher yield. Physical design phases include partitioning, floor planning, placement, clock-tree synthesis and routing as shown in Figure 1.

Execution of VLSI circuits is in effect to a great extent overwhelmed by the between interfaces because of diminishing wire pitch and expanding bite the die size. Issue is additionally testing a 3D IC due to the distance of elements. It in the end builds the significance of global routing issue which makes it all the more difficult. Advanced methods are utilized for global routing frequently. The most recent looks into on global routing is meant to upgrade diverse multi-target capacities related with execution and blockage, warm issues (Goplen & Sapatnekar, 2005), obstruction (Minz, Wong, & Lim, 2005), impediment mindful steering (Pandiaraj *et al.*, 2017a; Ghosal, Das, & Das, 2012b) and so forth.

3D Integration offers an assortment of points of interest for future VLSI configuration, similar to 1) higher packing thickness and littler footprint; 2) negligible global interconnect on account of the insignificant length of through-silicon vias (TSVs) and furthermore the flexibleness vertical routing, results in advanced execution and diminished power utilization of the interconnects; 3) furthermore of heterogeneous structure: each and every single die can have completely new innovations and collected interconnectivity is considered as the primary advantage in developing execution by contributing the huge data transfer capacity and low-latency TSV structures (Pandiaraj, Sivakumar, & Geetharamani, 2017b). TSV is significant in executing interconnectivity over the layer.


https://doi.org/10.17993/3ctecno.2021.specialissue8.313-331

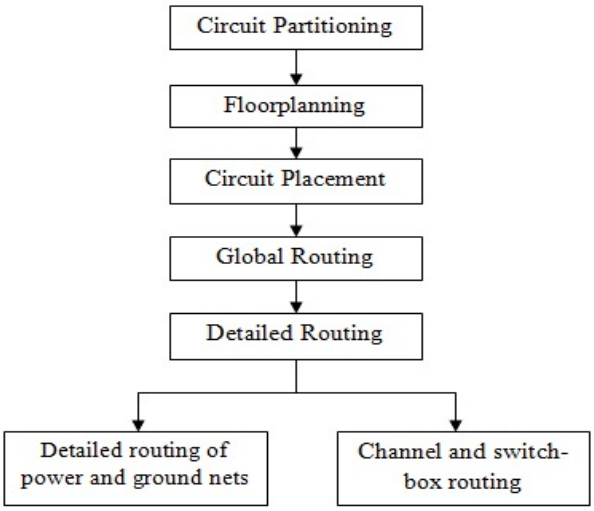


**Figure 1.** VLSI Physical Design phases.
**Source:** own elaboration.

With the improvement in innovation and developing interest for system on a chip (SOC) coordinated circuit had turned out to be increasingly muddled. This makes a major test in IC plan. Among ventures in the outline procedure the routing which is required as the last stride in physical configuration has particularly turned out to be imperative. A better routing will reduce number of interconnections among sub-circuits and result in better routing area of layout (Sivakumar, Pandiaraj, & Prakash, 2019). The main objective of routing includes minimization of wirelength between the modules.

# 2. MATERIALS AND METHODS

## 3D GLOBAL ROUTING

The main purpose of a global router is to break down an enormous routing issue into very little and smart sub-issues (detailed routing). This deterioration is done by finding an unpleasant way for every net to remember the final output to reduce the chip size, shorten wire length and uniformly convey the blockage over the routing region. Amid global routing, pins with identical voltage are associated utilizing wire segments. A net is a rendezvous of 2 or additional sticks that have an equivalent potential. within the last chip set up, they need to be associated. A standard p-pin net interfaces one yield stick of a gate


https://doi.org/10.17993/3ctecno.2021.specialissue8.313-331

and p − 1 information pins of different entryways; its fan out resembles p − 1. The term netlist insinuates everything contemplated to all or any nets.

In global routing, the wire parts used by net topologies are no doubt embedded in the chip group. The chip an area is delineated by an unpleasant directing matrix, and available materials are portrayed by edges with specific parameters during a grid graph. Nets are then conveyed to those routing assets. The consequent terms are applicable to global routing by and large.

- A routing way (segment) is accessible there as flat and vertical wiring way. Now and then the net uses a grouping of wavering flat tracks and vertical segments, any place adjoining tracks and sections are associated by between layer vias.
- A routing area could be a locale it ought to contain routing tracks as well as sections.
- The similarly dispersed level and vertical grid lines that produce a standard network over the chip space is making a uniform routing region. This grid is typically referenced as a ggrid (global grid); it's made out of unit gcells (global cells). Grid lines are for the most part dispersed 7 to 40 directing tracks separated to balance out the complexities of the chip-scale global routing and gcell-scale point by point routing issues.
- The horizontal and vertical limits that are adjusted to outer stick associations are making the non-uniform routing region. This coordinates to channels and switchboxes − routing region that have varying sizes. all through global routing, nets are allocated to those directing areas. In detailed routing, every one of the nets are appointed to explicit wiring ways.
- Every one of the pins are situated on the more extended sides of the routing region and there are no pins on the shorter side of the routing region. There are two distinct sorts of channels are accessible - horizontal and vertical.
- A horizontal channel has the pins on the top and base limits of the routing area.
- A vertical channel has the pins on the left and right limits of the routing area.


https://doi.org/10.17993/3ctecno.2021.specialissue8.313-331

- The pins of a net are related with the routing channel by segments, which are related with totally various segments by tracks. Because of the developed scope of driving layers in present-day designs, this standard channel model must a decent degree lost its pertinence. Or maybe, over-the-cell (OTC) directing is utilized.

The channel limit is communicated by the quantity of realistic routing tracks or segments. For single-layer routing, the capacity is determined by the tallness h of the channel isolated by the pitch dpitch, any place dpitch is that the base separation between the significant (vertical or even) bearing. For multilayer routing, the capacity(σ) is that the aggregate of the limits all things considered.

$$\sigma(\text{layers}) = \sum_{\text{layer}\in\text{layers}} [h/\text{dpitch(layer)}]$$

Layers is representing to the arrangement everything being equal, and dpitch (layer) is represents to the directing pitch for the layers.

Objectives and goals of Global routing:

The main aim of global routing is to provide complete information to the detailed router on where to route every interconnection. The objectives of global routing are one or more of the following:

- Total wire length minimization.
- Distribution of congestion over the routing region in an even manner.
- Minimization the critical path delay.
- Probability maximization that the detailed router can complete the routing.

## III. THE GLOBAL ROUTING FLOW

A grid graph is illustrated as ggrid = (V, E), any place the nodes v € V represents the routing framework cells (gcells) and thusly the edges represent to associations of lattice cell sets (vi,vj). the global routing network diagram is two-dimensional, be that as it may, ought to represent to k directing layers. Thus, k unmistakable limits ought to be kept up at each node of the matrix chart. for example, for a two-layer routing network (k = 2), an ability pair (3,1)


https://doi.org/10.17993/3ctecno.2021.specialissue8.313-331

for a directing matrix cell will represent to 3 even areas and one vertical section still open. Elective ability portrayals are achievable.

Step 1: Forming the regions of routing area:

In this movement, the design region is detached into routing territories. On occasion, nets will be routed over standard cells (OTC directing). The routing territory units are encircled as 2 Dimensional or 3 Dimensional channels, switch boxes and diverse district types. These different types of routing methodologies are then depicted with a diagram as appeared in Figure 2.

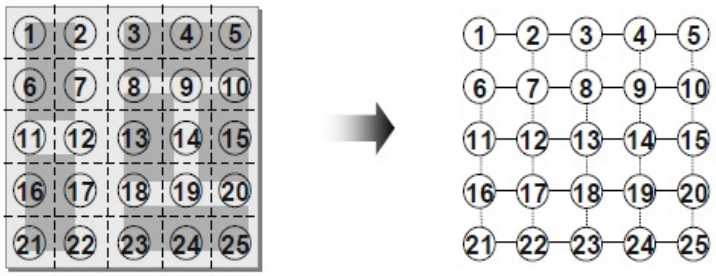


**Figure 2.** A layout and its corresponding connectivity graph.
**Source:** own elaboration.

Step 2: Nets are mapping with routing regions:

During this movement, each net of the design is presumably going consigned toward 1 or many routing zones identify with the pins of the routing regions. The routing furthest reaches of each routing area is determined by the quantity of nets crossing the specific locale.

Step 3: Assigning crosspoints:

During movement, also called halfway routing, routes are allocated to adjusted zones or crosspoints. Crosspoint assignment enables scaling of global and detailed routing to traces with a colossal assortment of cells and conjointly disseminated and parallel calculations, since the routing areas will be dealt with self-rulingly in detailed routing. Finding an ideal Crosspoint assignment needs learning of net affiliation conditions and channel requesting. A heuristic for global directing in partner degree network chart has showed up in Figure 3. Connectivity graph for a global routing.


https://doi.org/10.17993/3ctecno.2021.specialissue8.313-331

```
Input: netlist Netlist, layout LA
Output: routing topologies for each net in Netlist
1. RR = DEFINE_ROUTING_REGIONS(LA)          // define routing regions
2. CG = DEFINE_CONNECTIVITY_GRAPH(RR) // define connectivity graph
3. nets = NET_ORDERING(Netlist)             // determine net ordering
4. ASSIGN_TRACKS(RR,Netlist)                // assign tracks for all pin
// connections in Netlist
5. for (i = 1 to |nets|)                    // consider each net
6. net = nets[i]
7. FREE_TRACKS(net)                         // free corresponding tracks
// for net's pins
8. snets = SUBNETS(net)                     // decompose net into
                                            // two-pin subnets
9. for (j = 1 to |snets|)
10. snet = snets[j]
11. spath = SHORTEST_PATH(snet,CG)          // find shortest path for snet
                                            // in connectivity graph CG
12. if (spath == Ø)                         // if no shortest path exists,
13. continue                                // do not route
14. else                                    // otherwise, assign snet to
15. ROUTE(snet,spath,CG)                    // the nodes of spath and
                                            // update routing capacities
```

**Figure 3.** Connectivity graph for a global routing.
**Source:** own elaboration.

## PROBLEM STATEMENT

The routing problem is described as a three-dimensional grid graph. The 3D graph is regenerate into a 2D grid graph to first get the 2D routing result. Lastly, layer assignment is very difficult to assign every net to the corresponding metal layer to get a 3D routing result (Ghosal, Das, & Das, 2012b; Ghosal *et al.*, 2012d). Let pins of a net distributed across n (n≥1) layers of a tool be P= {p1, p2…pn}. Let the set of all nets be N= {n1, n2, …nm}. Let the set of modules be M={m1, m2….mk} contact the routing space, wherever every mi has its coordinates (xi, yi). The wirelength and congestion are determined in line with the algorithm. The difficulty target is to create an entire routing Tree (T) covering the total set (N) utilizing the projected congestion routing strategy. Using this proposed algorithm all the routing regions are resolved with minimum wire-length for all nets. The routing layer are described as a grid structure (Roy & Markov, 2008).

The quality factors which will be employed in global routing to evaluate the standard of the routing result are: i) Wire-length ii) Total overflow.


https://doi.org/10.17993/3ctecno.2021.specialissue8.313-331

## IV. PROPOSED ALGORITHM AND RELATED WORK

### I. NET DECOMPOSITION:

Multi-pin nets – nets with more than 2 pins – are regularly spoiled into two-pin subnets, trailed by each subnet in venture with certain requests. Such net decay is performed toward the beginning of global routing and may affect the standard of the last routing goals.

### II. RECTILINEAR ROUTING:

The rectilinear Steiner Minimal Tree (RSMT) (Sivakumar *et al.*, 2019) and rectilinear Minimum Spanning Tree (RMST) built by utilizing a calculation to decay multi-pin nets into two-pin subnets before routing stages. Be that as it may, the RSMT is mind boggling than RMST as it utilizes the idea of Steiner focuses and is less adaptable than that of RMSTs (Ghosal *et al.*, 2012a). Then again, the RMST creates the blockage mindful routing way of each subnet by utilizing an example or monotonic routing. A heuristic for consecutive Steiner tree is as appeared in Figure 4.

### III. RECTILINEAR SPANNING TREE:

All terminals (pins) are associated by a rectilinear Spanning Tree utilizing pin-to-pin associations that are made by vertical and even portions. pin to- pin associations will meet exclusively at a pin, i.e., "crossing" edges don't keep running into, and no further intersections (Steiner focuses) are permitted. The traversing tree isn't delivered if the entire length of fragments is stripped, at that point the tree might be a rectilinear least crossing tree (RMST). Partner RMST is regularly figured in O(p2) time, any place p is that the scope of terminals inside the net utilizing techniques like Prim's calculation (Müller, 2006). This calculation assembles partner mst by starting with one terminal and voraciously adding least-cost edges to the halfway built tree until all terminals are associated. Progressed computational-geometric procedures slice back the runtime to O(p log p).

### IV. RECTILINEAR STEINER TREE (RST):

A rectilinear Steiner Tree (RST):


https://doi.org/10.17993/3ctecno.2021.specialissue8.313-331

will associate all p pin areas and probably some further areas (Steiner focuses). While any rectilinear spreading over tree for a p-pin net is moreover a rectilinear Steiner tree, the general net length is decreased by including the Steiner focuses. Partner RST could be a rectilinear Steiner least tree (RSMT) if the general length of net portions acclimated interface all p pins is negligible (Roy, Ghosal, & Das, 2014). F∫or instance, in an exceptionally uniform routing grid, let a unit net stage be a position that interfaces 2 adjoining gcells; partner RST is partner RSMT if it's the base assortment of unit web fragments. The accompanying certainties are recognized with respect to RSMTs. A RSMT for a p-pin net has among 0 and p − 2 (comprehensive) Steiner focuses.

- Any routing area pin will have a degree as 1, 2, 3 or 4. A Steiner point has degree either 3 or 4.
- A rectilinear Steiner insignificant Tree is frequently gulped inside the MBB (Minimum Bounding Box) of the net.
- The complete edge length LRSMT of the rectilinear Steiner negligible Tree is at least a large portion of the border of the base-jumping box of the net: LRSMT ≥ (LMBB/2).

Building RSMTs inside the general case is NP-hard; practically speaking, heuristic ways are utilized. One brisk philosophy, FLUTE (Chang *et al.*, 2010; Chu & Wong, 2007), discovers ideal RSMTs for up to 9 sticks and creates close insignificant RSTs, typically at interims one hundred forty-five of the base length, for bigger nets. Be that as it may, RSMTs are appropriate for wire length minimization and ill-advised for web topology by and by.


https://doi.org/10.17993/3ctecno.2021.specialissue8.313-331

## V. SEQUENTIAL STEINER TREE HEURISTIC:

**Input:** set of all pins *P*
**Output:** heuristic Steiner minimum tree *T*(*V*,*E*)
1. *P'* = *P*
2. (*pA*,*pB*) = CLOSEST_PAIR(*P'*) // closest pin pair
3. ADD(*V*,*pA*) // add *pA* to *T*
4. ADD (*V*,*pB*) // add *pB* to *T*
5. REMOVE(*P'*,*pA*) // remove *pA* from *P'*
6. REMOVE(*P'*,*pB*) // remove *pB* from *P'*
7. **if** (*P'* == Ø) // shortest path connecting
8. ADD(*E*,*L*-shape connecting *pA* and *pB*) // *pA* and *pB* is any *L*-shape
9. **else**
10. *curr_MBB* = MBB(*pA*,*pB*) // MBB of *pA* and *pB*
11. **while** (*P'* || Ø)
12. (*pMBB*,*pC*) = CLOSEST_PAIR(*curr_MBB*,*P'*) // closest point pair, one from
// *curr_MBB*, one from *P'*
13. ADD(*V*,*pMBB*) // add *pMBB* to *T*
14. ADD(*V*,*pC*) // add *pC* to *T*
15. REMOVE(*P'*,*pC*) // remove *pC* from *P'*
16. **if** (*pMBB* || *P*) // if *pMBB* is a pin, either
17. ADD(*L*-shape connecting *pMBB* and *pC*) // *L*-shape is shortest path
18. **else** // if *pMBB* is not a pin, add
19. ADD(*E*,*L*-shape that includes *pMBB*) // *L*-shape that *pMBB* is on
20. *curr_MBB* = MBB(*pMBB*,*pC*) // MBB of *pMBB* and *pC*
21. ADD(*V*,*pC*) // connect *T* to remaining pin
22. ADD(*E*,*L*-shape connecting *pMBB* and *pC*) // with *L*-shape

**Figure 4.** Sequential Steiner Tree Heuristic.
**Source:** own elaboration.

## VI. HANAN GRID:

The wire length of the net is diminished by adding Steiner focuses to relate degree RMST. In 1966, Hanan (Dai, Liu, & Li, 2012) prove that to discover a RSMT, it does the trick to consider exclusively Steiner focuses put at the crossing points of vertical and horizontal lines that get together with terminal pins. A lot of officially, the Hanan framework (as appeared in Figure 5) comprises of the lines x = xp, y = yp that get together with each stick area (xp, yp). The Hanan framework contains at the most p2 competitor Steiner focuses, along these lines enormously lessening the territory for finding a best RSMT.

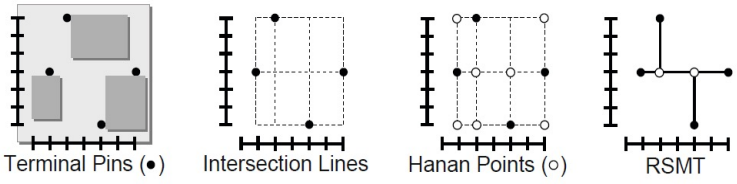


**Figure 5.** Getting the Hanan grid and subsequently the Steiner points of an RSMT.
**Source:** own elaboration.


https://doi.org/10.17993/3ctecno.2021.specialissue8.313-331

## VII. RIP-UP AND RE-ROUTE:

In stylish global routing, to maintain a strategic distance from floods, Rip-up and re-routing system especially that depends on exchange strategy are generally utilized that spotlights on expanding the punishment of a network edge to stay away from way watching out on aforesaid flooded framework edges. numerous exchange-based cost capacities are anticipated in (Dai *et al.*, 2012; Liu *et al.*, 2010; Roy *et al.*, 2014). McMurchie and Ebeling (1995) detail the exchange based steering cost work of matrix edges e as pursues:

$$\text{cost}(e) = (be + he) \times pe \ldots\ldots\ldots\ldots\ldots\ldots (1)$$

where cost(e), be, he, and pe are the cost of routing, the bottom cost, the history cost, and also the congestion penalty of e, severally. As overflow happens the history cost, he will increase.

Also, FGR (Xu, Zhang, & Chu, 2009) formulates another cost perform formula as follows:

$$\text{cost}(e) = be + he \times pe \ldots\ldots\ldots\ldots\ldots\ldots (2)$$

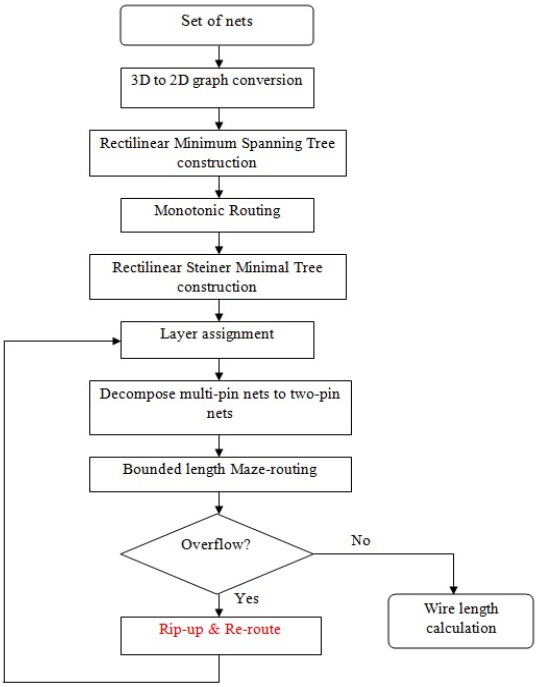


**Figure 6.** Flow chart for proposed algorithm.
**Source:** own elaboration.


https://doi.org/10.17993/3ctecno.2021.specialissue8.313-331

### VIII. BOUNDED LENGTH MAZE ROUTING:

To reduce the looking through area of maze routing and to quicken maze routing, different global routers will receive a bounding box (Ghosal *et al.*, 2012d) technique and well-ordered loosen up the bounding box if a flood free directing answer can't be found. In any case, maze routing could make a few reroutes or neglect to search out a concise way among the bounding box. Hence, this article creates limited Length Maze Routing (Ghosal *et al.*, 2012d) to accelerate maze routing by lessening the pursuit area comparatively on well improve routing asset usage by change repetitive wirelength. A stream graph for the anticipated recipe is appeared in Figure 6.

### IX. WIRELENGTH MINIMIZATION:

The objective of the wire length minimization [19] is so outlined as follows:

The trivial edge on the number of tracks is larger than the peak of a particular vertex vi (corresponding to net ni) in vct i. e.

Max (dtmax, vtmax)>htvi

Then we are able to prorogue the present assignment of ni wherever dmax= channel density, VC= (V, A) is built to represent the vertical constraints h= height of the vertex. wherever tvi= chosen vertex.

## 3. RESULTS

The proposed algorithms were implemented in C/C++ language. ISPD 2007 (Nam, 2007) and ISPD 2008 (Sze, 2008) benchmark circuits were employed in our experiments. The wirelength is in small units and therefore the overflow altogether cases are zero. The results were compared with NCTU-GR (Chang, Lee, & Wang, 2008) and NTHU-GR (McMurchie & Ebeling, 1995; Liu *et al.*, 2013).


https://doi.org/10.17993/3ctecno.2021.specialissue8.313-331

**Table 1.** Comparison of wire lengths of planned global router with NCTU-GR and NTHU-GR on overflow free cases.

| Comparison of wirelength (in micro units) of various global routers with the Planned Global router | | | |
|---|---|---|---|
| **Benchmark** | **Proposed Global Router** | **NCTU-GR** | **NTHU-GR** |
| Adaptec 1 | 5304K | 5350K | 5349K |
| Adaptec 2 | 5151K | 5197K | 5230K |
| Adaptec 3 | 12924K | 13008K | 13111K |
| Adaptec 4 | 12053K | 12062K | 12172K |
| Adaptec 5 | 15401K | 15501K | 15555K |

**Source:** own elaboration.

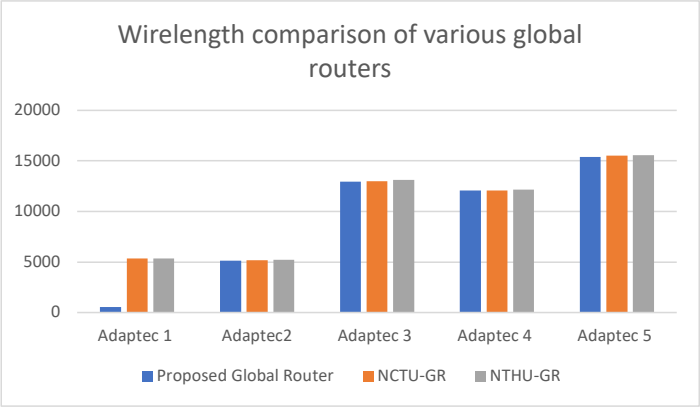


**Figure 7.** Results.
**Source:** own elaboration.

The Figure 7 provided here shows the Wire-length results on the ISPD2008 benchmarks. The test problem varies from adaptec1 to adaptec5. The proposed global router is compared with the existing techniques.

## 4. CONCLUSIONS AND FUTURE WORK

This work presents a novel global routing scheme by using RSMT and RSMT algorithms for net decomposition, monotonic routing for routing all the nets, bounded length maze routing to find the shortest paths for wire length minimization. Negotiation primarily based rip-up and re-routing theme is employed to avoid the congestion. Congestion is represented in terms of overflow. If overflow occurs the nets are ripped-up and re-routed by redefining


https://doi.org/10.17993/3ctecno.2021.specialissue8.313-331

the layers, decomposing the multi-pin nets and then bounded length maze routing is applied again and this process is repeated until the overflow is zero. In future using machine learning methodology the temperature has been reduced between the layers.

## ACKNOWLEDGEMENT

We thank the Department of Electronics and Communication Engineering of Kalasalingam University, (Kalasalingam Academy of Research and Education), Tamil Nadu, India for permitting to use the computational facilities available in Centre for Research in Signal Processing and VLSI Design which was setup with the support of the Department of Science and Technology (DST), New Delhi under FIST Program.

## REFERENCES

**Chang, Y.-J., Lee, T.-H., & Wang, T.-C.** (2010). GLADE: A modern global router considering layer directives. In *2010 IEEE/ACM International Conference on Computer-Aided Design (ICCAD)*, 319–323. https://doi.org/10.1109/ICCAD.2010.5654094

**Chang, Y.-J., Lee, Y.-T., & Wang, T.-C.** (2008). NTHU-route 2.0: A fast and stable global router. In *2008 IEEE/ACM International Conference on Computer-Aided Design*, pp. 338–343.2008. https://doi.org/10.1109/ICCAD.2008.4681595

**Chen, H.-Y., Hsu, C.-H., & Chang, Y.-W.** (2009). High-performance global routing with fast overflow reduction. In *2009 Asia and South Pacific Design Automation Conference*, pp. 582–587. https://doi.org/10.1109/ASPDAC.2009.4796543

**Chu, C., & Wong, Y.-C.** (2007). FLUTE: Fast Lookup Table Based Rectilinear Steiner Minimal Tree Algorithm for VLSI Design. *IEEE Transactions On Computer-Aided Design, 27*(1), 70-83. https://doi.org/10.1109/TCAD.2007.907068

**Dai, K.-R., Liu, W.-H., & Li, Y.-L.** (2012). NCTU-GR: Efficient simulated evolution-based rerouting and congestion-relaxed layer assignment on 3-D global routing. *IEEE TVLSI, 20*(3), 459–472. https://doi.org/10.1109/TVLSI.2010.2102780

**Ghosal, P., Das, A., & Das, S.** (2012a). Obstacle Aware RMST Generation Using Non-Manhattan Routing for 3D ICs. *ACITY,* (3), 657–666. https://doi.org/10.1007/978-3-642-31600-5_64

**Ghosal, P., Das, S., & Das, A.** (2012b). A Novel Algorithm for Obstacle Aware RMST Construction during Routing in 3D ICs. *ACITY,* (2), 649–658. https://doi.org/10.1007/978-3-642-31552-7_65

**Ghosal, P., Das, S., & Das, A.** (2012c). A New Class of Obstacle Aware Steiner Routing in 3D Integrated Circuits. *ACITY,* (3), 697–706. https://doi.org/10.1007/978-3-642-31600-5_68

**Ghosal, P., Rahaman, H., Das, S., Das, A., & Dasgupta, P.** (2012d). Obstacle Aware Routing in 3D Integrated Circuits. In Thilagam, P. S., Pais, A. R., Chandrasekaran, K., & Balakrishnan, N. (eds.) *Advanced Computing, Networking and Security.* ADCONS 2011. Lecture Notes in Computer Science, vol. 7135. Springer, Berlin, Heidelberg. https://doi.org/10.1007/978-3-642-29280-4_53

**Goplen, B., & Sapatnekar, S.** (2005). Thermal Via Placement in 3D ICs. In *Proceedings of the International Symposium on Physical Design,* pp. 167–174. https://doi.org/10.1145/1055137.1055171

**Kahng, A. B., Lienig, J., Markov, I. L., & Hu, J.** (2011). *VLSI Physical Design_ From Graph Partitioning to Timing Closure*. Springer. https://doi.org/10.1007/978-90-481-9591-6

**Liu, W.-H., Kao, W.-C., Li, Y.-L., & Chao, K.-Y.** (2010). Multi-threaded collision-aware global routing with bounded-length maze routing. In *Proceedings of the 47th Design Automation Conference (DAC),* pp. 200–205. https://doi.org/10.1145/1837274.1837324

**Liu, W.-H., Kao, W.-C., Li, Y.-L., & Chao, K.-Y.** (2010). Multi-Threaded Collision-Aware Global Routing with Bounded-Length Maze Routing. In *Proceedings of Design Automation Conference (DAC),* pp. 200-205. https://doi.org/10.1145/1837274.1837324

**Liu, W.-H., Kao, W.-C., Li, Y.-L., & Chao, K.-Y.** (2013). NCTU-GR 2.0: Multithreaded Collision-Aware Global Routing with Bounded-Length Maze Routing. *IEEE*

*Transactions On Computer-Aided Design Of Integrated Circuits And Systems, 32*(5), 709-722. https://doi.org/10.1109/TCAD.2012.2235124

**McMurchie, L., & Ebeling, C.** (1995). Pathfinder: A negotiation-based performance-driven router for FPGAs. In *3rd International ACM Symposium on Field-Programmable Gate Arrays,* pp. 111–117. https://doi.org/10.1109/FPGA.1995.242049

**Minz, J., Wong, E., & Lim, S. K.** (2005). Thermal and Crosstalk-Aware Physical Design for 3D System-On-Package. In *Proceedings of Electronic Components and Technology Conference,* pp. 824–831. https://doi.org/10.1109/ECTC.2005.1441368

**Müller, D.** (2006). Optimizing yield in global routing. In *2006 IEEE/ACM International Conference on Computer Aided Design,* pp. 480–486. https://doi.org/10.1109/ICCAD.2006.320161

**Nam, G.-J.** (2007). *ISPD 2007 Contest.* http://archive.sigda.org/ispd2007/contest.html

**Ozdal, M. M., & Wong., M. D. F.** (2007). ARCHER: A history-driven global routing algorithm. In *2007 IEEE/ACM International Conference on Computer-Aided Design*, pp. 488–495. https://doi.org/10.1109/ICCAD.2007.4397312

**Pandiaraj, K., Sivakumar, P., & Geetharamani, N.** (2017b). Reduction of temperature rise in 3D IC routing. In *2017 IEEE International Conference on Electrical, Instrumentation and Communication Engineering (ICEICE)*, pp. 1-5. https://doi.org/10.1109/ICEICE.2017.8191907

**Pandiaraj, K., Sivakumar, P., & Sridevi, R.** (2017a). Minimization of wirelength in 3d IC routing by using differential evolution algorithm. In *2017 IEEE International Conference on Electrical, Instrumentation and Communication Engineering (ICEICE)*, pp. 1-5. https://doi.org/10.1109/ICEICE.2017.8191950

**Roy, D., Ghosal, P., & Das, N.** (2014). A Thermal and Congestion Driven Global Router For 3D Integrated Circuits. *Proceeding of the 2014 IEEE Students' Technology Symposium*, pp. 303-308. https://doi.org/10.1109/TechSym.2014.6808065

**Roy, D., Ghosal, P., & Das, N.** (2014). A Thermal And Congestion Driven Global Router For 3D integrated Circuits. *Proceedings of the 2014 IEEE Students' Technology Symposium*, pp. 303-308. https://doi.org/10.1109/TechSym.2014.6808065

**Roy, J. A., & Markov, I. L.** (2008). High-performance routing at the nanometer scale. *IEEE TCAD, 27*(6), 1066–1077. https://doi.org/10.1109/TCAD.2008.923255

**Sivakumar, P., Pandiaraj, K., & Prakash, K. J.** (2019). Optimization of Thermal Aware Multilevel Routing For 3D IC. *International journal of analog integrated circuits and signal processing, 103*(1), 131-142. https://doi.org/10.1007/s10470-019-01513-y

**Sze, C.** (2008). ISPD 2008 *Contest*. http://archive.sigda.org/ispd2008/contests/ispd08rc.html

**Xu, Y., & Chu, C.** (2011). MGR: Multi-level global router. In *2011 IEEE/ACM International Conference on Computer-Aided Design (ICCAD)*, pp. 250–255. https://doi.org/10.1109/ICCAD.2011.6105336

**Xu, Y., Zhang, Y., & Chu, C.** (2009). FastRoute 4.0: Global router with efficient via minimization. In *2009 Asia and South Pacific Design Automation Conference*, pp. 576–581. https://doi.org/10.1109/ASPDAC.2009.4796542


https://doi.org/10.17993/3ctecno.2021.specialissue8.313-331

https://doi.org/10.17993/3ctecno.2021.specialissue8.313-331

/20/


https://doi.org/10.17993/3ctecno.2021.specialissue8

# AUTOMATIC KNEE SEGMENTATION USING EAGLE ALGORITHM WITH MULTI STOCHASTIC OBJECTIVE PROCESS

**C. Rini**
Research Scholar, Department of ECE, Kalasalingam Academy of Research and Education.
Krishnankoil, Virudhunagar (Dt), (India).
E-mail: rinidass2002@yahoo.co.in
ORCID: https://orcid.org/0000-0002-4413-5850

**B. Perumal**
Associate Professor, Department of ECE, Kalasalingam Academy of Research and Education.
Krishnankoil, Virudhunagar (Dt), (India).
E-mail: palanimet@gmail.com
ORCID: https://orcid.org/0000-0003-4408-9396

**M. Pallikonda Rajasekaran**
Professor, Department of ECE, Kalasalingam Academy of Research and Education.
Krishnankoil, Virudhunagar (Dt), (India).
E-mail: mpraja80@gmail.com
ORCID: https://orcid.org/0000-0001-6942-4512

**V. Muneeswaran**
Assistant Professor, Department of ECE, Kalasalingam Academy of Research and Education.
Krishnankoil, Virudhunagar (Dt), (India).
E-mail: munees.klu@gmail.com
ORCID: https://orcid.org/0000-0001-8061-8529

**Recepción:** 11/11/2019 **Aceptación:** 21/12/2020 **Publicación:** 30/11/2021

**Citación sugerida:**
Rini, C., Perumal, B., Rajasekaran, M. P., y Muneeswaran, V. (2021). Automatic knee segmentation using eagle algorithm with multi stochastic objective process. *3C Tecnología. Glosas de innovación aplicadas a la pyme, Edición Especial,* (noviembre, 2021), 333-353. https://doi.org/10.17993/3ctecno.2021.specialissue8.333-353

## ABSTRACT

In our living world, Osteoarthritis (OA) is known to be foremost sicknesses which affect the knee region especially affect hoarier people. The reason for OA in a person may be due to ageing, malformed joints, rough cartilage, genetics effects or continuous repetitive stress towards the joint. Magnetic Resonance Imaging (MRI) enacts a vigorous role in the medical field for detecting issues regarding bone structure, cartilage, and meniscus region and tibia bone. Though it provides the details about the bone, it is not useful to detect clearly about the faults in the bone due to many unfavorable conditions like poor segmentation, broken pixels or some other natural issues including the shakes while clicking the image, blurring, etc. Besides, manual calculations have some unexceptional error with partial accuracy. Hence automated segmentation should be implemented for achieving perfection in accuracy and the bone segmentation. In our work, we proposed eagle algorithm as the segmentation method which provides an improved accuracy in contrast with other traditional methods. The performance is measured by the metrics such as thickness, mean and Standard Deviation (SD).

## KEYWORDS

Pre-Processing, Contrast Enhancement, Stochastic Multi-Objective Process, Levy Walk Random Process, Eagle Algorithm.


https://doi.org/10.17993/3ctecno.2021.specialissue8.333-353

# 1. INTRODUCTION

Generally, 3-D Magnetic Resonance (MR) imaging delegates the therapies regarding noninvasive, high-resolution as well as isotropic voxels. On behalf of quantitative studies including dimensional (3-D) reconstruction and dimension of the cartilage, truthful segmentation of the images is obligatory. The main objective of our work is to improve and authenticate software for automated segmentation and thickness representing of articular cartilage from three-dimensional (3-D) gradient-echo MR images of the knee. Inelegantly, random noise occurs throughout the MR image processing and hence the quality of the image is vitiated. Besides, the medical diagnostic tasks and noise damage many image processing and investigation charges like registration, segmentation, super resolution and visualization, etc. Hence the suppression of noise is essential to recover the image quality. Many methods and algorithms are being introduced for attaining clear segmentations are discussed in the next section.

Classically, joints are the regions where two bones meet in our body. Habitually, 360 joints are there in our human body which include 86 skull joints, six throat joints, 66 thorax joints and 76 in the spine and pelvis region. In case of limbs, 32 joints found in each upper limb and 31 joints in each lower limb. Among that, knee joint is solitary and it connect the leg and thigh of our human body. The knee joint is a hinge type synovial joint provide the flexion and extension of the leg. Knee joint is formed by articulations among patella bone, femur bone (thigh bone) and tibia bone (leg bone). There are two articulations in the knee joint. One of them is located between the femur and tibia bone and the latter is built between the patella and femur (Peterfy *et al.*, 2008); Eckstein, Burstein, & Link, 2006).

On the other hand, Condyle is defined as the round prominence at the end of a bone, a part of the joint which articulate with another bone. It is also said to be one of the markings or features of bones. In the femur bone of the knee joint, condyles are two types of condyles namely medial condyle and lateral condyle. The joints are shaped by means of the condyles of femur bone and tibia bone. The interior structure of knee joint comprise of synovial cavity covering synovial fluid, articular cartilage, meniscus region (semi-lunar cartilages), cruciate ligaments and burse. Articular cartilage is a silky, white tissue that wrap the ends of bones together with bones to form joints. In the mechanism of joints,


https://doi.org/10.17993/3ctecno.2021.specialissue8.333-353

if the cartilage is fine, it is easier to move. It certifies the bones to glide over each other with a very slight friction.

Articular cartilage which covers patella bone, tibia bone and femur bone are frequently injured by wounds or normal wear and tear. When the thickness of the cartilage is diminished, the growth of Osteoarthritis (OA) begins. Osteoarthritis (OA) is the most common form of arthritis, affect millions of people in worldwide. It occurs when the protective cartilage on the ends of the bones wears down over time. Osteoarthritis symptoms can be effectively managed, although the underlying process cannot be reversed. Maintenance of vigorous weight and other treatments may leads for slow progression of the disease and help recover pain and joint function. The cartilage joint is completely vanished whoever suffering from severe OA.

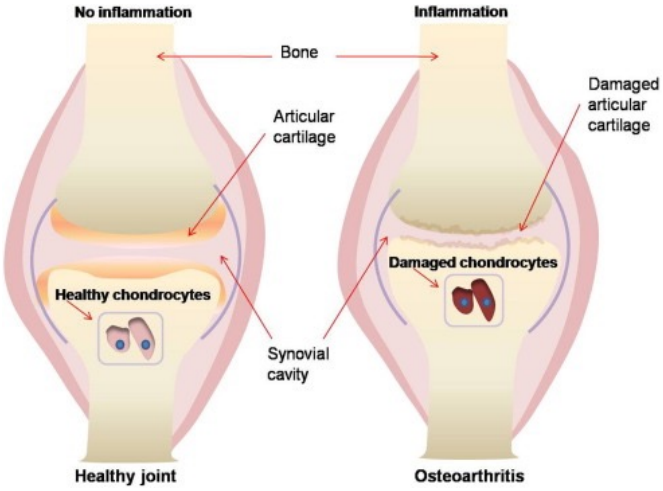


**Figure 1.** Knee joint for healthy and affected people.
**Source:** own elaboration.

During the cartilage joint reduction, the synovial fluid drops its lubrication ability which results in pain, inflammation and eased movement of the joint. The bones get scratch while gliding without fluid and new tiny bones called spurs start to develop. Therefore, the cartilage function (shock absorber) is constrained due to the stress on joint result in severe influence. The growth of Osteoarthritis (OA) may be stopped or diminished by introducing a vigorous biomarkers to resolve the issue. An organization named Osteoarthritis Initiative (OAI) has the main objective to detect and analyze the risk factors of Osteoarthritis which


https://doi.org/10.17993/3ctecno.2021.specialissue8.333-353

are performing by several private health organizations. According to their survey, 50.2% of the people among the age 65 and 74 years and 97.7% of people of age eighty-four and above, are being affected by this disease.

Body mass Index (BMI) should be maintained for reduction of Osteoarthritis (OA). People with high BMI rage falls under the respected disease and leads to give heavy burden at the joint. The normal value of BMI range for both male and female is 18.5 - 25. People having BMI beyond this range is considered to be overweight and they have the chances to suffer from Osteoarthritis (OA). It was 51.36% for the people with a BMI below 25 and 100% for the people with a BMI above 40. The cartilage damage in the joints of knee can be observed by means of Magnetic Resonance Images (MRI). MRI scan is used to scrutinize the in-vivo and in-vitro structures of the human body meanwhile it is non-invasive and has great resolution soft tissue contrast. Sagittal, coronal and axial planes are three different planes where MRI scan the joints. The knee joint MRI images without Osteoarthritis (OA) as publicized in Figure 2(a). At the same time, Figure 2(b) shows the MRI images regarding knee joint of an OA affected person. With numerous time series of MR images, the physicians detect femur, tibia and cartilage of knee bones and observe the influences of OA.

Magnetic Resonance Imaging (MRI) create the magnetic properties of assured atomic nuclei. The human body is mostly covered by water. The hydrogen nuclei present in the water act as compass needles which are incompletely aligned by a strong magnetic field in the scanner. Radio waves rotates the nuclei and oscillate in the magnetic field while returning to equilibrium successively. For examining the tissues, the waves concurrently emit radio signals which are detected by antennas. MRI does not have process like radioactivity or ionization comparing to the traditional methods. The range of Radio Frequency (RF) for the operation is normal and won't affect the body. The signal of MRI is sensitive to a wide range of effects like nuclear mobility, molecular structure, flow and diffusion.


https://doi.org/10.17993/3ctecno.2021.specialissue8.333-353

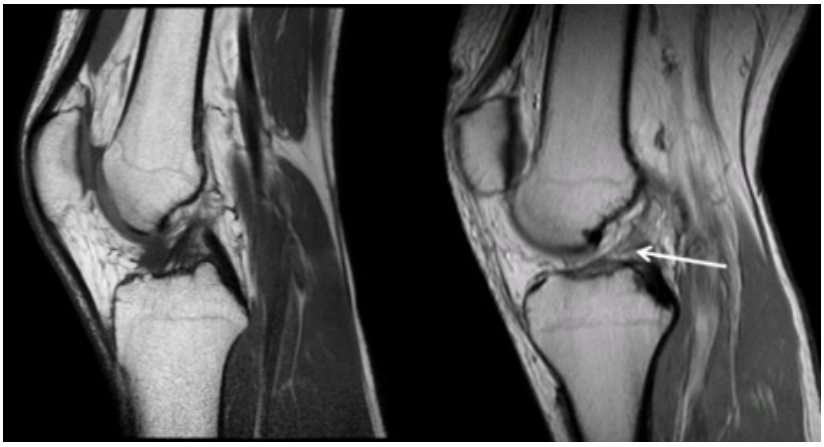

**Figure 2.** a) MRI of normal knee, b) MRI of OA knee.
**Source:** own elaboration.

As a consequence, MRI is a very flexible technique that provides the interior results of both structure and function. Initially, the output image of MRI is processed with quantization. In case of knee joints, MRI images are captured for detecting obvious output regarding meniscal lesions, cartilage thickness, reshaping the bones, osteophytes, bone marrow lesions and synovitis (Pelletier *et al.*, 2008). The image segmentation is required to observe the exact issue happened on the knee whereas the manual calculations have partial accuracy. Hence, some auto segmentation methods are introduced for detecting and computing the structure of the bone clearly. In our work, we proposed eagle algorithm (Yang & Deb, 2010) for segmentation process which executes accurate image quality and reduced pixel breakdown. When compare with the existing method, the accuracy is greatly enhanced and the thickness can be measured obviously.

## 2. RELATED WORKS

Early quantitative MRI studies assured promising morphological cartilage metrics for describing the status of disease and perhaps to screen its progression (Norman, Pedoia, & Majumdar, 2018). Nonetheless, the recent studies utilize larger OA cohorts by means of demonstrating MRI articular cartilage biomarkers may have limited approachability to disease progression. On other hand, the study has sustained to grow novel and better image segmentation tools (Kubassova, Boyle, & Pyatnizkiy, 2005; Yin *et al.*, 2010). In the present


https://doi.org/10.17993/3ctecno.2021.specialissue8.333-353

decades, most quantitative analysis methods require uninterrupted human involvement and also should be proficient for accurate cartilage segmentation (Kauffmann *et al.*, 2003). Image acquisition and denoising are the two techniques used to reduce the noise from the images. Average of number of the similar samples that obtained is the result of image acquisition technique. Conventionally, the image is denoised by denoising techniques which acquire less time for computation (Liu *et al.*, 2010).

Novel segmentation algorithm (Peterfy, Schneider, & Nevitt, 2008) presented knee cartilages with level-based segmentation method and new template data. It gives consequence of three cartilage tissues such as tibia, femur and fibula bone. The segmentation of cartilage is grim in atlas-based segmentation (Pelletier *et al.*, 2008), since cartilage intensity varies by thin or fat and the boundary of the cartilages are girdled by the muscle tissues. A main shortcoming of atlas-based approach is the large inconsistency of the articular cartilage. The potential for preference is equivalent to the target delay in accuracy (Raynauld *et al.*, 2004).

The multi-atlas based algorithm (Pavlyukevich, 2007) overcome atlas based algorithm with promising results where it combine simple label fusion approach but not utilize any other correction methods to report abnormalities like osteophytes produced besides the joint margins. Alternatively, Local Weighted Vote (LWV) algorithm is built where the multi atlas data merges and provide the result (Rini *et al.*, 2020). The segmentation structure grips three procedures including multiple-atlas building, applying a locally weighted vote (LWV) and adjusting the region. In case of atlas building process, every training cases are recorded to a target image - a non-rigid registration method and the finest coordinated atlases are designated. However, LWV algorithm was usually applied for integrating the data from these atlases and produce the initial segmentation outcome. At last, in the region adjustment procedure, the statistical data of bone, cartilage, and surrounding regions is calculated from the preliminary segmentation result. The statistical data absorbed the automated determination of the seed points in all regions of bone intended for the graph-cut based method.

The locus-correlated background by voxel subsampling technique is preferred than uniform or Gaussian subsampling to distinguish the objects of interest from supplementary


https://doi.org/10.17993/3ctecno.2021.specialissue8.333-353

objects. These supplementary objects have similar and close structures that frequently knock into MR images, particularly for objects focusing on highly curved and complex shapes (Stammberger *et al.*, 1999). In this approach, cartilage compartments are segmented underprivileged of prior segmentation of bones or determination of Bone Cartilage Interface (BCI) demanding multiple MR images of a participant. Recently, a novel method is introduced called U-net model whose results show longitudinal precision proves the heftiness of algorithm, free of the ground truth definition (Norman *et al.*, 2018).

The recent convolutional neural networks produce fast, accurate, and precise automatic segmentations in cartilage and meniscus compartments which are invariant across patients with OA. This approach also have continuous compensation of computational speed and established efficacy in extracting relaxation times and morphologic features which used in the prediction and intensive care of joint degeneration in OA. Local Coordinate System (LCS) is a method used to segment the femoral and tibia cartilage regions based on 2-D active contour algorithm (Kauffmann *et al.*, 2003). This method obtains a uniform sketch of cartilage dimensions. Cartilage regions were usually segmented in the 3D-MRI scan and developed into offset maps with certain gaps acquired from an inter-slice distance. The offset maps were expressed by Local Coordinate System (LCS).

The gaps are filled with bi-cubic interpolation process. Several segmentation methods of knee joints are performed on semi-automatic segmentation such as B-spline snakes (Stammberger *et al.*, 1999), active contours (Lynch *et al.*, 2000; Raynauld *et al.*, 2004), directional gradient vector flow snakes (Tang *et al.*, 2006), region-growing scheme (Stammberger *et al.*, 1999) and extended watershed algorithm, where others are achieved habitually akin to voxel classification algorithm (Stammberger *et al.*, 1999) and statistical shape model (Fripp *et al.*, 2007). These approaches explain cartilage boundaries in two- or three-dimensional image spaces. Owing to the curved and thin structure of cartilage in core, the cartilage segmentation job are quite complex in stimulation. In the work of Grau *et al.* (2004), it does not permit informal control of segmentation outflow or objective tessellation but suffer with lack of stability and excessive sensitivity to noise.

The reported techniques used basic signal analysis such as directional edge filters (Wolf, Weierich, & Niemann, 1997), mathematical morphology (Dogdas, Shattuck, & Leahy,


https://doi.org/10.17993/3ctecno.2021.specialissue8.333-353

2002), gray-level classification (Folkesson *et al.*, 2005), histogram analysis (Kubassova, Boyle, & Pyatnizkiy, 2005), and other techniques including the hybrid signal and model, e.g., texture level-set (Lorigo *et al.*, 1998) and model fitting. Nonetheless, these solutions needed a specific tuning which is responsible for the mutable image quality or the signal corrosion owing to disease. This tuning trusts on initial manual contribution, additional signal data or cooperating tuning by making the independent use of these methods difficult in the context of a large scale process. Alternatively, an algebraic strategy called Douglas-Rachford Splitting method is presented in the work of Rini, Perumal, and Rajasekaran (2020) which is segmented by means of proximal splitting method. Various applications of image processing have been demonstrated in the literature (Muneeswaran & Rajasekaran, 2016, 2017, 2019c).

## 3. MATERIALS AND METHODS

The block diagram of the proposed Eagle Algorithm (EA) method is shown in Figure 3. The input image is the MRI images of the Osteoarthritis (OA) affected knee image. In case of image processing, image acquisition is mandatory to transform the analogous image into a digitalized form. It is done by the process of sampling and quantization. The spatial resolution of the digitalized image is determined by the sampling rate, whereas the quantization level controls the number of gray levels in the digitized image. An acquisitioned image is send as input to the preprocessing where the contrast and the illumination of the image is completely adjusted. Eagle algorithm extract the thickness of the cartilage region from the femur, tibia or patella bone and segment the portion. The image is then quantized for desired number of outputs. The output image is the noiseless and hassle free MRI image which can detect the thickness of the cartilage precisely.

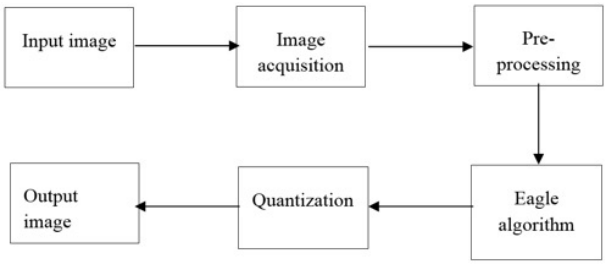


**Figure 3.** Block diagram of the proposed method.
**Source:** own elaboration.


https://doi.org/10.17993/3ctecno.2021.specialissue8.333-353

## 3.1. PRE-PROCESSING

The purpose of preprocessing is to convert the RGB image into gray image. The image cannot be processed under the RGB image. Hence it is converted into the binary image (grey scale image). The gray scale image suffer with the issues like contrast, illumination and blur. In our proposed method, these problems are resolved by using Contrast Enhancement Method (CHE). CHE provides perfect lightning effect regarding the background and the Anisotropic Filter (AF) eradicate the noise in image. The Anisotropic Filter (AF) alters the image to concentrate on the extracted portion where the edges are turned to be blurred. This filter is non-linear type that permit dispersion in the consistent area and obstructs at the boundaries. The partial differential equation (PDE) of anisotropic filter is given by Equation (1).

$$\begin{cases} \frac{\partial A}{\partial t} \\ A(t=0) = A_o \end{cases} = div[c(|\nabla A|)\nabla A\} \tag{1}$$

Where $\nabla$- gradient operator, $div$ - divergence operator, $A_0$- Initial image and $c(|\nabla A|)$- diffusion coefficient, which is represented as

$$c(x,y) = e\left(-\left[\frac{\nabla A(x,y)}{k}\right]^2\right) \tag{2}$$

The input image (A) is a gray level 3-D image from MRI scanning, where the gray value of a pixel at a point (a′, b′, c′) is specified by x = (a′, b′, c′). Thus, the slices of the 3-D image are signified as 2-D images, $A$a′.

$$A_{a'=h} \equiv \{A(a',b',c')/(a'=h)\}$$
$$A_{b'=j} \equiv \{A(a',b',c')/(b'=j)\}$$
$$A_{c'=t} \equiv \{A(a',b',c')/(c'=t)\}$$

The 2D images are outlined as 3D image limits having gray levels. The image space S is the collection of all points of (a′, b′, c′) and the slices for the groups are $\Omega$a′=$h$= {(b′, c′)/ $A$a′=$h$> 0}, *idemfor* $\Omega$b′=j, $\Omega$c′=$t$ and these spaces are called as axial, coronal and sagittal slices respectively. The 3-D image $A$ can be defined as a discrete function of the Euclidian 3-D space and their measurements are represented as,

$$(a', b', c') = (a', b', c') \in Z^3$$


https://doi.org/10.17993/3ctecno.2021.specialissue8.333-353

For the given bone region (ϕ), the femur region or tibia region are in the same MR image $A$, then the region is defined by two factors (u,v) as given in equation (4),

$$(a', b', c') = (u, v)\,(a', b', c') \in R^3$$

The bone region (ϕ) is a reference region which have a volume of interest in the whole cartilage. The values of $a'$, $b'$ and $c'$ indices are integer values, since the values of the 3-D image are digital. Similarly a set $D$ is computed by implicating the equation through intensity level $l$ which is discrete.

$$V = \{(a', b', c') / (a', b', c') = l\}$$

The voxels is a set of unit cubes in $R^3$ which is similar to the coordinate axes and midpoints are located in $Z^3$.

## 3.2. STOCHASTIC MULTI OBJECTIVE OPTIMIZATION

Generally, a regular optimization problem without including any noise or uncertainty, can be given by

$$\min_{x \in R^d} f_i(s), i(1,2,\ldots.,N)$$

$$\emptyset_j(S) = 0, (j = 1,2,3,\ldots.,N)$$

$$\psi_k(S) = 0, (k = 1,2,3,\ldots.,K)$$

Where s = (s1, s2... sd)$^T$ is the vector of design variables.

Monte Carlo method is a sampling technique to determine μf. After the samples drawn randomly, we have

$$\mu_{f_i} \approx \frac{1}{M_i} \sum_{p=1}^{M_i} f_i\left(X, \xi^{(p)}\right) \quad (6)$$

Where $M_i$ denotes the number of samples.

## 3.3. EAGLE ALGORITHM

The scavenging behavior of eagles especially the behavior of golden eagle is motivating. Generally, an eagle feeds in its own region by flying freely in a random manner similar to the Levy flights. When the prey is found by eagle, automatically it will alter its search strategy to a concentrated chasing strategies to catch the prey as efficiently as possible. Thus,


https://doi.org/10.17993/3ctecno.2021.specialissue8.333-353

two important mechanisms are involved in an eagle's hunting strategy: random search by Levy flight (or walk) and intensive chase by fastening its aim on the objective. The work of Reynolds and Frye works with fruit flies, see the sights at their landscape by means of a series of straight flight paths interrupted by an unexpected 900 turn, prominent to a Levy-flight-style sporadic scale-free search pattern. However, light also can be connected to Levy flights (Barthelemy, Bertolotti, & Wiersma, 2008). Consequently, this kind of behavior has been utilized in the process of optimization and optimal search, and preliminary results depicted with its enhanced capability (Pavlyukevich, 2007).

In our proposed work, let us fetishize the two-stage approach of an eagle's foraging behavior. At first, assumption is made that an eagle has to do the Levy walk in the entire domain. After the detection of prey, it alters to a chase strategy. Next, the chase strategy can be measured as an intensive local search using any optimization techniques. Likewise, the output image of the Anisotropic Filter (AF) is scanned randomly for the segmentation process. When it detects the area of region where have to be segment, then the area is intensely chased and segmented. Since the area of the region is chasing intensely without considering any other region, the pixel is broken in reduced number. In the initial step, EA is a two-stage strategy rather than a simple iterative method which going to conglomerate a better randomization technique of global search with an intensive and well-organized local search method. Additionally, EA applies Levy walk rather than simple randomization, which resource that the global search space can be reconnoitered proficiently. In fact, the studies show that Levy walk is more efficient than simple random-walk exploration. The Levy walk has a random step length being drawn from a Levy distribution which is given by

$$EA \sim v = T^{-\lambda}, (1 < \lambda \leq 3) \quad (7)$$

Where v represents the infinite variance with infinite mean. Here the steps of the eagle motion is fundamentally a random walk process by means of a power-law step-length distribution with a substantial tail. The special case ($\lambda = 3$) corresponds to Brownian motion, whereas the case ($\lambda = 1$) has a physical appearance of stochastic excavating, which may be more resourceful to escape being surrounded in local optima. In our proposed work, we use the eagle algorithm to do the local search, since the eagle algorithm was designed to crack multimodal global optimization problems.


https://doi.org/10.17993/3ctecno.2021.specialissue8.333-353

# 4. RESULTS

For our proposed work, we have taken an input set with three regions of knee bone namely femur, tibia and patella region. These three samples are tested with every process of Eagle Algorithm (EA) as follows. Initially, the input images of the knee bone region are the gray scale or RGB image which covers the cartilage region as revealed in Figure 4. The input image is converted to gray scale image under the process of preprocessing. Anisotropic Filter (AF) filters the brightness whereas the Contrast Enhancement Method (CHE) adjust the brightness of the image.

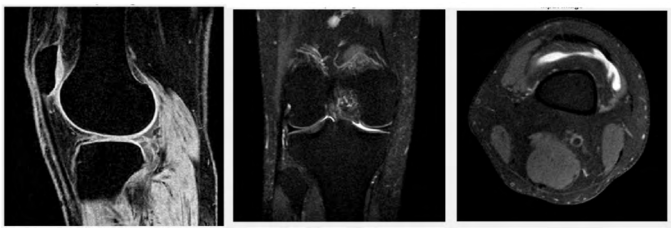

**Figure 4.** The input images of femur, tibia and patella of knee bone region.
**Source:** own elaboration.

In case of the binary images, the thresholding process is mandatory. Our technique works with the Otsu method for binarization which further provide contrast enhancement in the binary images. Otsu method produce best results in contrast with the other threshold filters and also ensures the clear view about the thickness of the images as shown in Figure 6.

**Figure 5.** Otsu method output images.
**Source:** own elaboration.

The contrast enhancement for altering the effect of the color images at the cartilage region as shown in Figure 6. It shown clearly about the cartilage region at where we can obviously view the cartilage region. Comparing the Figure 5 and Figure 6, it is obvious about the optimal differences in the region differentiation.


https://doi.org/10.17993/3ctecno.2021.specialissue8.333-353

**Figure 6.** Contrast enhancement.
**Source:** own elaboration.

The Anisotropic Filter (AF) is included with the process to remove the noise and region of interest (ROI) of the image as shown in Figure 7. From this depicted figure, we can observe the removal of noise at the segmenting region.

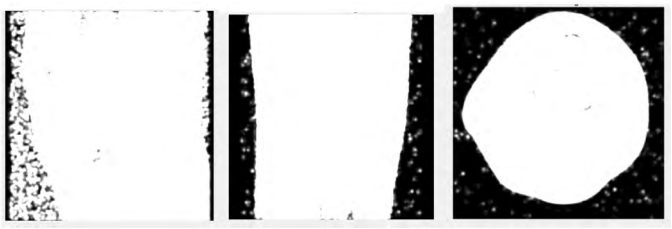

**Figure 7.** Anisotropic Filter (AF) image.
**Source:** own elaboration.

As we discussed above, the Eagle Algorithm (EA) is categorized under levy walk process for extracting the area pattern and intensive chasing for identifying the thickness of the pattern. The stochastic multi objective process deliberates the random search to extract that where the thickness has to be determined. After it founds the region, it concentrates on the desired pattern whereas another surround with blur as shown in Figure 8.


https://doi.org/10.17993/3ctecno.2021.specialissue8.333-353

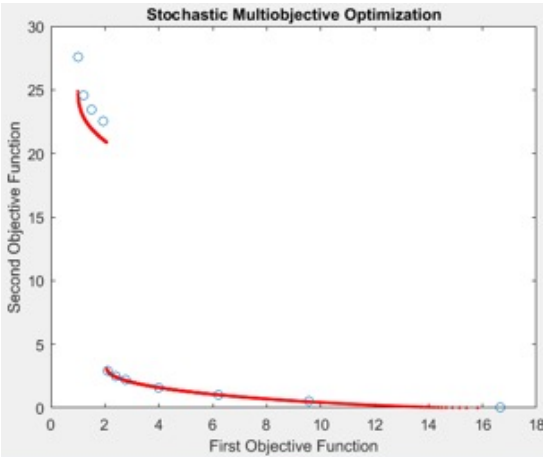


**Figure 8**. Stochastic multi objective process.
**Source:** own elaboration.

The above figure illustrates the probability of achieving maximum thickness for several input set images. The objective function of the scale measures the value of the accuracy in the images. It is found that the images are steadily removed by the noise and after the completion of the search. In contrast with the traditional method, less computation time is required in this process. The power law regression of the set of data sets of MRI images are depicted in Figure 9.

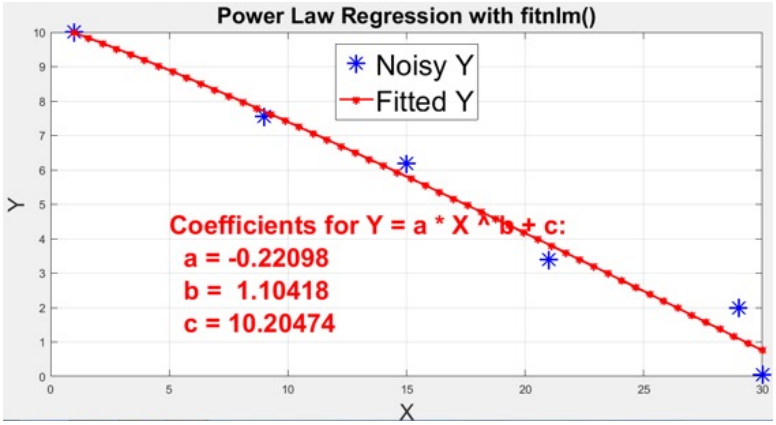


**Figure 9.** Power law regression.
**Source:** own elaboration.


https://doi.org/10.17993/3ctecno.2021.specialissue8.333-353

## 4.1. PERFORMANCE METRICS

The quality measurement of the output image is dignified by means of the thickness, mean and the standard deviation as publicized in Table 1. The proposed work greatly enhanced accuracy of the image when compare with the existing method.

**Table 1.** Performance metrics of input images using eagle algorithm.

| Inputs | Thickness | Mean | Standard Deviation |
|---|---|---|---|
| 1 | 0.35503 | 0.04237 | 0.016560 |
| 2 | 0.45060 | 0.04183 | 0.015588 |
| 3 | 0.24184 | 0.04351 | 0.015193 |
| 4 | 0.19432 | 0.04329 | 0.013595 |
| 5 | 0.30043 | 0.04190 | 0.015678 |
| 6 | 0.53720 | 0.04266 | 0.014890 |
| 7 | 0.39266 | 0.04251 | 0.015023 |
| 8 | 0.40385 | 0.04414 | 0.013999 |
| 9 | 0.39356 | 0.04380 | 0.013750 |
| 10 | 0.27988 | 0.04380 | 0.013653 |

**Source:** own elaboration.

Thus, the eagle algorithm extracts the specific pattern to segment and concentrate on that pattern by clear segmentation with multi stochastic process and the better accuracy is achieved.

# 5. CONCLUSIONS

Our work, we proposed Eagle Algorithm (EA) for the enhancement of the segmentation process of knee images. The pre-processed image is a binary image with heavy noise. The noise is reduced by using Anisotropic Filter (AF). The brightness of the image is controlled and stabilized by Contrast Enhancement Method (CHE). The segmentation is done with two steps namely levy walk and intensive chasing. After the random search, the area is extracted accurately with intensive chasing. The algorithm fixes the cartilage part of the bone and segment with better clarity. The performance of the algorithm is analyzed using mat lab simulations. The thickness, mean and standard deviation result shows that the proposed method has developed result in contrast with the traditional methods.


https://doi.org/10.17993/3ctecno.2021.specialissue8.333-353

## REFERENCES

**Barthelemy, P., Bertolotti, J., & Wiersma, D. S.** (2008). A Lévy flight for light. *Nature, 453*(7194), 495-498. https://www.nature.com/articles/nature06948

**Dogdas, B., Shattuck, D. W., & Leahy, R. M.** (2002). Segmentation of the skull in 3D human MR images using mathematical morphology. In *Medical Imaging 2002: Image Processing* (Vol. 4684, pp. 1553-1562). International Society for Optics and Photonics. https://ui.adsabs.harvard.edu/abs/2002SPIE.4684.1553D/abstract

**Eckstein, F., Burstein, D., & Link, T. M.** (2006). Quantitative MRI of cartilage and bone: degenerative changes in osteoarthritis. *NMR in Biomedicine: An International Journal Devoted to the Development and Application of Magnetic Resonance In vivo, 19*(7), 822-854. https://www.researchgate.net/publication/6720453_Quantitative_MRI_of_cartilage_and_bone_Degenerative_changes_in_osteoarthritis

**Folkesson, J., Dam, E., Olsen, O. F., Pettersen, P., & Christiansen, C.** (2005). Automatic Segmentation of the Articular Cartilage in Knee MRI Using a Hierarchical Multi-class Classification Scheme. In Duncan, J.S., & Gerig, G. (eds.) *Medical Image Computing and Computer-Assisted Intervention – MICCAI 2005*. Lecture Notes in Computer Science, vol 3749. Springer, Berlin, Heidelberg. https://doi.org/10.1007/11566465_41

**Fripp, J., Crozier, S., Warfield, S. K., & Ourselin, S.** (2007). Automatic segmentation of the bone and extraction of the bone–cartilage interface from magnetic resonance images of the knee. *Physics in Medicine & Biology, 52*(6), 1617. https://pubmed.ncbi.nlm.nih.gov/17327652/

**Grau, V., Mewes, A. U. J., Alcaniz, M., Kikinis, R., & Warfield, S. K.** (2004). Improved watershed transform for medical image segmentation using prior information. *IEEE transactions on medical imaging, 23*(4), 447-458. https://ieeexplore.ieee.org/document/1281998

**Kauffmann, C., Gravel, P., Godbout, B., Gravel, A., Beaudoin, G., Raynauld, J. P., ... & de Guise, J. A.** (2003). Computer-aided method for quantification of


https://doi.org/10.17993/3ctecno.2021.specialissue8.333-353

cartilage thickness and volume changes using MRI: validation study using a synthetic model. *IEEE transactions on Biomedical Engineering, 50*(8), 978-988. https://ieeexplore.ieee.org/document/1213850

**Kubassova, O., Boyle, R. D., & Pyatnizkiy, M.** (2005). Bone segmentation in metacarpophalangeal MR data. In *International Conference on Pattern Recognition and Image Analysis* (pp. 726-735). Springer, Berlin, Heidelberg.

**Li, L., Muneeswaran, V., Ramkumar, S., Emayavaramban, G., & Gonzalez, G. R.** (2019). Metaheuristic FIR filter with game theory based compression technique-A reliable medical image compression technique for online applications. *Pattern Recognition Letters, 125*, 7-12. https://doi.org/10.1016/j.patrec.2019.03.023

**Liu, H., Yang, C., Pan, N., Song, E., & Green, R.** (2010). Denoising 3D MR images by the enhanced non-local means filter for Rician noise. *Magnetic resonance imaging, 28*(10), 1485-1496. https://doi.org/10.1016/j.mri.2010.06.023

**Lorigo, L. M., Faugeras, O., Grimson, W. E. L., Keriven, R., & Kikinis, R.** (1998). Segmentation of bone in clinical knee MRI using texture-based geodesic active contours. In Wells W.M., Colchester, A., Delp, S. (eds.) *Medical Image Computing and Computer-Assisted Intervention* — MICCAI'98. Lecture Notes in Computer Science, vol 1496. Springer, Berlin, Heidelberg. https://doi.org/10.1007/BFb0056309

**Lynch, J. A., Zaim, S., Zhao, J., Stork, A., Peterfy, C. G., & Genant, H. K.** (2000). Cartilage segmentation of 3D MRI scans of the osteoarthritic knee combining user knowledge and active contours. In *Medical Imaging 2000: Image Processing* (Vol. 3979, pp. 925-935). International Society for Optics and Photonics.

**Muneeswaran, V., & Rajasekaran, M. P.** (2016). Analysis of particle swarm optimization based 2D FIR filter for reduction of additive and multiplicative noise in images. In *International Conference on Theoretical Computer Science and Discrete Mathematics* (pp. 165-174). Springer, Cham.

**Muneeswaran, V., & Rajasekaran, M. P.** (2016). Performance evaluation of radial basis function networks based on tree seed algorithm. In *2016 International Conference on*


https://doi.org/10.17993/3ctecno.2021.specialissue8.333-353

*Circuit, Power and Computing Technologies (ICCPCT)* (pp. 1-4). IEEE. https://ieeexplore.ieee.org/document/7530267

**Muneeswaran, V., & Rajasekaran, M. P.** (2017). Beltrami-Regularized Denoising Filter Based on Tree Seed Optimization Algorithm: An Ultrasound Image Application. In Satapathy, S., Joshi, A. (eds.) *Information and Communication Technology for Intelligent Systems (ICTIS 2017)* - Volume 1. ICTIS 2017. Smart Innovation, Systems and Technologies, vol 83. Springer, Cham. https://doi.org/10.1007/978-3-319-63673-3_54

**Muneeswaran, V., & Rajasekaran, M. P.** (2018). Gallbladder shape estimation using tree-seed optimization tuned radial basis function network for assessment of acute cholecystitis. In *Intelligent Engineering Informatics* (pp. 229-239). Springer, Singapore.

**Muneeswaran, V., & Rajasekaran, M. P.** (2019a). Automatic segmentation of gallbladder using bio-inspired algorithm based on a spider web construction model. *The Journal of Supercomputing, 75*(6), 3158-3183. https://doi.org/10.1007/s11227-017-2230-4

**Muneeswaran, V., & Rajasekaran, M. P.** (2019b). Automatic segmentation of gallbladder using intuitionistic fuzzy based active contour model. In *Microelectronics, Electromagnetics and Telecommunications* (pp. 651-658). Springer, Singapore.

**Muneeswaran, V., & Rajasekaran, M. P.** (2019c). Local contrast regularized contrast limited adaptive histogram equalization using tree seed algorithm—an aid for mammogram images enhancement. In *Smart intelligent computing and applications* (pp. 693-701). Springer, Singapore.

**Norman, B., Pedoia, V., & Majumdar, S.** (2018). Use of 2D U-Net convolutional neural networks for automated cartilage and meniscus segmentation of knee MR imaging data to determine relaxometry and morphometry. *Radiology, 288*(1), 177-185. https://pubmed.ncbi.nlm.nih.gov/29584598/

**Pavlyukevich, I.** (2007). Lévy flights, non-local search and simulated annealing. *Journal of Computational Physics, 226*(2), 1830-1844. https://doi.org/10.1016/j.jcp.2007.06.008

**Pelletier, J. P., Raynauld, J. P., Abram, F., Haraoui, B., Choquette, D., & Martel-Pelletier, J.** (2008). A new non-invasive method to assess synovitis severity in relation to symptoms and cartilage volume loss in knee osteoarthritis patients using MRI. *Osteoarthritis and cartilage, 16,* S8-S13. https://pubmed.ncbi.nlm.nih.gov/18672386/

**Peterfy, C. G., Schneider, E., & Nevitt, M.** (2008). The osteoarthritis initiative: report on the design rationale for the magnetic resonance imaging protocol for the knee. *Osteoarthritis and cartilage, 16*(12), 1433-1441. https://www.ncbi.nlm.nih.gov/pmc/articles/PMC3048821/

**Raynauld, J. P., Martel-Pelletier, J., Berthiaume, M. J., Labonté, F., Beaudoin, G., De Guise, J. A., ... & Hochberg, M. C.** (2004). Quantitative magnetic resonance imaging evaluation of knee osteoarthritis progression over two years and correlation with clinical symptoms and radiologic changes. *Arthritis & Rheumatism: Official Journal of the American College of Rheumatology, 50*(2), 476-487. https://pubmed.ncbi.nlm.nih.gov/14872490/

**Rini, C., Perumal, B., & Rajasekaran, M. P.** (2020). Automatic knee joint segmentation using Douglas-Rachford splitting method. *Multimedia Tools and Applications, 79*(9), 6599-6621. https://doi.org/10.1007/s11042-019-08303-8

**Schmid, J., & Magnenat-Thalmann, N.** (2008). MRI bone segmentation using deformable models and shape priors. In *International conference on medical image computing and computer-assisted intervention* (pp. 119-126). Springer, Berlin, Heidelberg.

**Stammberger, T., Eckstein, F., Michaelis, M., Englmeier, K. H., & Reiser, M.** (1999). Interobserver reproducibility of quantitative cartilage measurements: comparison of B-spline snakes and manual segmentation. *Magnetic resonance imaging, 17*(7), 1033-1042. https://pubmed.ncbi.nlm.nih.gov/10463654/

**Tang, J., Millington, S., Acton, S. T., Crandall, J., & Hurwitz, S.** (2006). Surface extraction and thickness measurement of the articular cartilage from MR images using directional gradient vector flow snakes. *IEEE Transactions on Biomedical Engineering, 53*(5), 896-907. https://ieeexplore.ieee.org/document/1621141


https://doi.org/10.17993/3ctecno.2021.specialissue8.333-353

**Wolf, M., Weierich, P., & Niemann, H.** (1997). Automatic Segmentation and 3D-Registration of a femoral bone in MR images of the knee. *Pattern Recognition and Image Analysis (Advances in Mathematical Theory and Applications), 7*(1), 152-165.

**Yang, X. S., & Deb, S.** (2010). Eagle strategy using Lévy walk and firefly algorithms for stochastic optimization. In *Nature Inspired Cooperative Strategies for Optimization (NICSO 2010)* (pp. 101-111). Springer, Berlin, Heidelberg.

**Yin, Y., Zhang, X., Williams, R., Wu, X., Anderson, D. D., & Sonka, M.** (2010). LOGISMOS—layered optimal graph image segmentation of multiple objects and surfaces: cartilage segmentation in the knee joint. *IEEE transactions on medical imaging, 29*(12), 2023-2037. https://pubmed.ncbi.nlm.nih.gov/20643602/


https://doi.org/10.17993/3ctecno.2021.specialissue8.333-353